Determining the Combustion Kinetics of vegetable oil based fuels

MAYURESH ARUN SAHASRABUDHE

Thesis submitted for the degree of

Doctor of Philosophy in Chemical and Process Engineering

to Heriot-Watt University, Edinburgh, UK

July 2014

ABSTRACT

In last few years' interest in application of Bio Diesel as an alternative fuel in commercial diesel engines has been increased. However, combustion kinetics is required to predict and model combustion performance of a fuel. The chemical kinetic mechanisms are available for hydrocarbon (C_4 to C_{16}) combustion, but not for commercial Biofuel's combustion. The aim of this research work is to investigate combustion kinetics of Rapeseed oil Methyl Ester (RME) by experimentally in Jet Stirred Reactor and modeling using CHEMKIN a software package at 1 and 10 bar for different fuel conditions. Rapeseed Oil (RSO) combustion kinetics will also be predicted using related theory and chemistry difference between RME and RSO.

RME oxidation experiments and comparison with commercial Diesel showed that RME oxidation performance was better at fuel-lean conditions and higher temperatures in terms of profile trends of pollutants, especially at higher pressure suggesting higher Air/Fuel ratio is more suitable for RME combustion. RME oxidation was simulated taking unique approach of using surrogate fuels (n-hexadecane, Methyl Acetate) as a model fuel, and RME as a model fuel. The surrogate fuel model results showed that oxidation of commercial biodiesel like RME can be simulated using surrogate model-fuels, but with some limitations and less accuracy. The modeling with RME as model fuel gives good agreement between the model and experimental data in terms of profile trends of key oxidation components. However model needs improvement at high pressure (10 bar). The RME reaction mechanism consists of 496 species and 2652 reversible reactions. The chemical kinetic mechanism for RSO oxidation is represented by Oleic acid ($C_{18}H_{34}O_2$) oxidation. The reaction mechanism consists of 485 species and 2531 reversible reactions. The model is validated against RME oxidation data. The model is able to produce to reproduce profile trends of key oxidation components with some discrepancy.

To my wife Bharati, Baba, Aai, late. Pethe kaka, my in-laws, My Sisters, my late Aajji, nana and Mai Aajji, Ojus, Swara and My friends for their love and support

ACKNOWLEDGEMENTS

I would like to sincerely thank my supervisors, Prof. Graeme White, Dr. Turgay Pekdemir and Dr. Philippe Dagaut for their immense support, guidance and encouragement during my three years of PhD study. Special thanks to Dr Iskander Gökalp, for his moral and financial support, guidance and encouragement. I would like to thank also Professor Ken Brizenski and Professor Janusz Kozinski, Dr. Pascale Gillon for their support, encouragement and guidance on scientific work. I would like to thank specially Chemical Engineering Department, Heriot-Watt University and ICARE-CNRS for providing me the Research Scholarship during my stay in Orleans and Edinburgh.

I would also like to thank Dr Sandro.Gail and Dr Guillaume.Dayma for their advice and help on chemical kinetics mechanism. Sincere thanks to Ms Murielle Chevrier, Ms Alex Campbelle, Ms Ann Blyth, Ms Claude Fougere, and Ms Nadege Oriol for their support and help regarding administrative work and my visa. Special thanks to my friend and officemate Fabien Jouot for his continuous support and help during my stay in ICARE. I would like to thank all my friends Tushar, Adwait, Srinivas, Nikhil, Kanchan, Pablo, Marc, Caroline, Nicolas, Ludivine, Fred, Angelique, Joel, Fouzi, Homan, Pascal, Marie, Antoine, Astrid, Thomas 1&2 and all other friends from ICARE-CNRS, Orleans and India for their support and encouragement.

Finally, I would like to thank my parents, my wife, Pethe kaka, my sisters, and my in-laws for their love and support during my PhD project.

DECLARATION

This is to declare that the thesis is an account of the author's work carried out at Heriot-Watt University, Edinburgh, UK and ICARE-CNRS, Orleans, France except where acknowledgement is made, and has not been submitted for any other degrees.

MAYURESH ARUN SAHASRABUDHE (Candidate)

PROF. GRAEME WHITE (Supervisor)

DR. PHILIPPE DAGAUT (Supervisor)

TABLE OF CONTENTS

LIST OF TABLES

LIST OF FIGURES

GLOSSARY

$C^0_{P_k}$ Standard state molar heat capacity at constant pressure for k^{th} species (cal/mole K)

H^0_k Standard state molar enthalpy of k^{th} species (ergs/mole)

S^0_k Standard state molar entropy of k^{th} species (ergs/mole K)

G^0 Standard state molar Gibbs free energy (ergs/mole)

H^0 Standard state molar enthalpy (ergs/mole)

S^0 Standard state molar entropy (ergs/mole K)

Gi^{θ} Standard state molar Gibbs free energy for i^{th} species (ergs/mole)

K_{Pi} Equilibrium constant for the i^{th} reaction in pressure units

K_{r_i} Reverse rate constant for i^{th} reaction

K_{f_i} Forward rate constant for i^{th} reaction

K_{c_i} Equilibrium constant for the i^{th} reaction in concentration units

υ_{ki} Stoichiometric coefficient of the k^{th} species in i^{th} reaction

υ'_{ki} Stoichiometric coefficient of the k^{th} reactant species in i^{th} reaction

υ''_{ki} Stoichiometric coefficient of the k^{th} product species in i^{th} reaction

P_T, P_r Total and Reduced pressure (dynes/cm^2)

X_k Mole fraction of k species

$\acute{\omega}_k$ Chemical production rate of kth species (mole/cm^3.sec)

q_i Rate of progress of i^{th} reaction (moles/cm^3.sec)

E_i Activation energy in the rate constant of the i^{th} reaction (cal/mole K)

R_c Universal Gas constant (cal/mole K)

F Blending function

PUBLICATION BY AUTHOR

CONFERENCE PROCEEDING PAPERS

1. Philippe Dagaut, Sandro Gaïl, **Mayuresh Sahasrabudhe**, 2007, "Rapeseed oil methyl ester oxidation over extended ranges of pressure, temperature, and equivalence ratio: Experimental and modeling kinetic study", Proceedings of Combustion Institute, Vol.31, Issue 2, 2955,2961

2. **M. Sahasrabudhe**, P. Dagaut, S. Gaïl, T. Pekdemir, "Kinetics of rapeseed oil methyl ester oxidation over extended ranges of pressure, temperature, and equivalence ratio: Experimental and modeling study", Proceedings of 19th International Symposium on Gas Kinetics, Orleans, France, July 22-27, 2006 (Poster Presentation).

3. **M. Sahasrabudhe**, P. Dagaut, S. Gaïl, T. Pekdemir, "An experimental and modeling kinetic study of rapeseed oil methyl ester (RME) oxidation", Proceedings of 14th European Biomass Conference, Paris, 17-21 October 2005 (Poster Presentation).

CONFERENCE PRESENTATIONS

1. P. Dagaut, S. Gaïl, T. Pekdemir, **M. Sahasrabudhe**, **"**Bio-diesel fuel chemistry: An Experimental and Modeling Kinetic Study of rapeseed oil methyl ester oxidation". 230th ACS National Meeting, Washington D.C., August 28-September 1, 2005.

STRUCTURE OF THESIS

Chapter 1 Thesis begins with the introduction, which will give general idea about object of this thesis and kind of work will be done.

Chapter 2 reviews the current literature regarding pollution and energy scenario, need of alternative fuels, types of Renewable/Biofuels, vegetable oils as fuels and its limitations, what is Biodiesel, need of Biodiesel, Biodiesel as fuel and ts environmental effects and economics. Finally chapter covers Rapeseed oil methyl ester as a diesel engine fuel.

Chapter 3 describes the experimental set up (Jet Stirred Reactor) used for oxidation of Rapeseed oil methyl ester (RME), experimental procedure, the composition of RME and experimental conditions. It will also describe the different types of analytical techniques used for analysis of experimental results.

Chapter 4 will describe the results obtained from RME oxidation experiments. The results are presented in graphical format in terms of mole fractions against working temperature. This chapter will also cover the effect of pressure and temperature on RME oxidation and esters compounds obtained from GC-MS, GC/FID.

Chapter 5 deals with comparison of RME oxidation with commercial diesel fuel oxidation on experimental basis. This chapter also describes the simulation of RME oxidation results using n-hexadecane ($C_{16}H_{34}$) and Methyl Acetate (CH_3COOCH_3) as surrogate model-fuels. It also covers the importance of surrogate model fuel approach for simulation of commercial diesel engine fuels.

Chapter 6 will define the chemical reaction mechanism and it will describe the modeling tools used in this study to identify the correct kinetics; CHEMKIN simulation package and Perfectly Stirred Reactor (PSR) code. It also covers the literature survey on chemical kinetic modeling study of Biodiesel combustion and structure of typical high temperature chemical kinetic mechanism. The last part of chapter explains the development of chemical kinetics mechanism for oxidation of RME.

Chapter 7 describes the simulation results for RME oxidation at 1 bar and 10 bar using RME as model fuel. This chapter explains and compares experimental results with simulation results. It also includes analysis of modeling results using tools like Rate of Production and Sensitivity Analysis.

Chapter 8 deals with development of reaction mechanism for oxidation of Rapeseed oil (RSO) and modeling results. As there is no experimental data available for Rapeseed oil oxidation in Jet Stirred Reactor (JSR), Rapeseed oil methyl ester (RME) oxidation experimental data is used for modeling work.

Chapter 9 Thesis will be concluded with conclusion about experimental results, results obtained from modeling work done for simulating RME as well as Rapeseed oil (RSO) combustion. It ends with general conclusion about thesis overall work done and scope for future work. It will be followed by list of reference used.

List of all references and publications by author will be followed by annex, which covers combustion kinetics mechanism developed for RME and RSO oxidation, thermochemistry of all species used in mechanism and nomenclature.

CHAPTER 1

INTRODUCTION

The increasing energy crisis, rapid depletion of petroleum resources and increasing environmental problems lead the world to search for alternative resources. The sectors consuming energy resources and increasing the pollution are mainly Power generation and Transport. The transport sector including all modes of transports (rail, air and road) is dominant in petroleum products consumption, consuming 50% of petroleum products compared to other sectors like Power, Chemical, Agricultural and heating industry [1.1]. The transport sector is expected to represent 54% of total oil demand by 2030, where the total energy demand will reach 3.2 Gtoe [1.1]. The transport sector is also responsible for 25% world's energy related green house gas emissions and 21 % world's CO_2 emissions [1.1]. In the UK the rise in energy consumption by transport sector alone is 67% over 1980 to 2005. It was predicted that by 2010, mode of transports like rail including metro and tram, air, and road will account for 36% of UK's energy demand [1.2].

Amongst all transport routes (rail, air, road), road transport is responsible for a higher percentage of energy consumption. It represents 81% of transport related total energy demand [1.5]. The road transport sector is dominated by personal cars and heavy duty vehicles using petroleum based fuels like diesel and petrol. For solving emission problems, to avoid rapid depletion of conventional energy resources and concern for long time supply of petroleum based fuels, it is necessary to develop alternative or renewable fuels which are environment friendly, sustainable, technically acceptable, easily available and also compatible with conventional fuels.

Renewable fuels or Bio fuels are available in liquid form as bio-alcohols, vegetable oils, biodiesel and in gaseous form as biogas, syngas, and synthetic fuels. Biodiesel and bio oils processed from biological material such as vegetable oils, recycled cooking oils, animal fats, plant and forest waste products can be blended with non renewable petroleum fuels to use in transport engines, boilers, space heating and industrial processes. Biofuels blended with commercially

available fossil fuels promote energy efficiency and reduce pollutant emission. These fuels also reduce dependency on conventional fuels and fluctuating energy prices [1.4]. The commercially available renewable fuels in Europe and UK are Biodiesel, Ethanol and different vegetable oils. Ethanol is widely used as an alternative for petrol; where as vegetable oils and vegetable oil based Biodiesel are used as an alternative to conventional diesel. As rapeseed is a traditional growing crop in the UK and Europe; Rapeseed Oil Methyl Ester (RME) has been used in oxidation experiments and chemical kinetic modeling study.

The vegetable oils such as Rapeseed oil, Palm oil, Soybean oil, Sunflower oil, Peanut oil and Olive oil have been used for nine decades as diesel fuels [1.4]. They have good heating power, low sulphur contents and cause less environmental damage than diesel [1.3]. However, the properties like low volatility, very high viscosity, low mass heating value, high cloud and pour points make them less competitive. The higher molecular weight and viscosity of vegetable oils causes the inefficient mixing of oil with air leading to incomplete combustion, more deposit formation, carbonization of injector tips, poor cold engine start up, piston ring sticking and misfire [1.7] [1.8]. Therefore the concept of using alkyl (methyl/ethyl) esters of vegetable oils, i.e. Biodiesel came up.

The different types of vegetable oil based long carbon chain (C_{14} to C_{22}) alkyl (methyl/ethyl) esters are used as Biodiesel. Biodiesel has almost $1/3^{rd}$ molecular weight than that of pure vegetable oil [1.4]. Biodiesel has better combustion characteristics which lead to less CO_2, PAH and hydrocarbon emissions. Biodiesel also has almost zero sulphur content and low viscosity than pure vegetable oils [1.8]. These vegetable oil based alkyl esters are tested in conventional diesel engines, current CDI and Turbo engines either directly as fuel or in blends with commercial diesel [1.9]. The application of Biodiesel is commercially restricted due to high cost, scarcity of resources, engine modification requirement and lack of combustion kinetics knowledge. However, to predict accurate combustion performance & emission characteristics of fuel it is important to study the reaction path of fuel combustion. In order to simulate engines and model combustion of particular fuel, it is necessary to know the combustion kinetics of the fuel. The diesel engine study of biodiesel is limited to emission profile and combustion performance. Also the chemical kinetic

mechanisms available are only for hydrocarbons ranging from methane (CH_4) to n-hexadecane ($C_{16}H_{34}$), which is used as surrogate fuel for commercial diesel, but not much information is available for combustion kinetics of Biodiesel or vegetable oils.

The past research work (either experimental or modelling) done on combustion kinetics of Biodiesel was limited to small methyl esters (typically C_4). The largest simulated Biodiesel fuel molecule is Methyl Decanoate i.e. C_{10} carbon chain. To understand combustion path of Biodiesel or vegetable oils practically in detail, it is highly important to develop chemical kinetics for long carbon chain (C_{10+}) alkyl esters or oils. The chemical kinetic mechanism developed by modeling work also helps to find out the main reactions responsible for intermediate pollutant production. It also helps to understand the effect of temperature, pressure (1- 40 bar), and varying fuel/air ratio on combustion performance and to validate the experimental database. Following are the objectives of this research work.

1.1 The objective of research project

1. To investigate the combustion kinetics of vegetable oil esters (Biodiesel) experimentally. The oxidation of Rapeseed oil Methyl ester (RME) will be carried out at 1 bar and higher pressure (10 bar) for fuel lean to rich conditions in a Jet Stirred Reactor i.e. well stirred reactor which offers non catalytic homogenous oxidation. The experimental database for Biodiesel (RME) combustion is not available.

2. To develop a complete chemical kinetics model for combustion of Biodiesel i.e. RME and validate it with experimental results. The chemical kinetics reaction mechanisms are not available for complex fuel like RME, so detailed chemical kinetics study is needed to understand the combustion of Biodiesel (RME) compared to commercial diesel. It will also help to understand the impact of application of Biodiesel (RME) as B100 fuel in commercial diesel engines. The simulation package ChemKin and PSR code will be used to develop the model.

3. To study the effect of pressure (atmospheric and high) and temperature on combustion kinetics of Biodiesel (RME). As commercial diesel engines run at very high pressure and temperature, this study is important to understand the changes in combustion kinetics of fuel with increasing temperature and pressure.

4. To predict the combustion kinetics of straight vegetable oils like pure Rapeseed oil (RSO) by developing chemical kinetics model based on related theory and the chemistry difference between the vegetable oil and their esters. Due to lack of experimental database for Rapeseed oil combustion in Jet Stirred Reactor, the chemical kinetic model developed for RSO combustion will be validated against Rapeseed oil methyl ester (RME) combustion.

References

1.1 Plouchart.G, 2005, *Energy Consumption in the Transport Sector*, Panorama Technical Reports , Panorama-2005 http://www.ifp.com/information-publications/publications

1.2 Meeting the Energy Challenge, A White Paper on Energy, May 2007, http://www.berr.gov.uk/files/file39387.pdf

1.3 Barnwal.B.K, Sharma.M.P, 2004, *Prospects of Biodiesel production from vegetable oil in India*, Renewable and Sustainable Energy Reviews, 9 (4), 363-378

1.4 Srivastava.A, Ram Prasad, 2000, *Triglycerides-based diesel fuels*, Renewable and Sustainable Energy Reviews, 4,111-113

1.5 Bensaid.B, 2005, *Road Transport Fuels in Europe: the Explosion of Demand For Diesel Fuel*, Panorama Technical Reports, www.ifp.com

1.6 Peterson.C.L, Hystrulid.T, 1998, *Carbon Cycle for Rapeseed oil Biodiesel Fuels*, Biomass and Bio energy, 14 (2), 91-101

1.7 Ramadhas.A.S, Jayaraj.D, Maraleedharan.C, 2005, *Use of Vegetable oils as I.C engine fuels-A Review*, Renewable Energy, 29, 727-742

1.8 Guibet.J-C, Faure-Birchem.E, 1999, Fuels and Engines, Technip Editions 2

1.9 Labeckas.G, Slavinskas.S, 2006, *The effect of rapeseed oil methyl ester on direct injection Diesel engine performance and exhaust emissions*, Energy Conversion and Management, 47, Issue 13-14, 1954-1967

CHAPTER 2

LITERATURE REVIEW

This chapter reviews the current literature regarding the types of Renewable/Bio fuels, the use of vegetable oils and Biodiesel as fuel. This chapter is divided into three parts; first part (section 2.1, 2.2 and 2.3) deals with energy resource consumption and greenhouse gas emissions in EU from the transport sector. It also covers different types of Biofuels and European/UK Biofuel targets. The section 2.4 describes different types of vegetable oils, their properties and work done using vegetable oils as fuel in diesel engines. The last part of the chapter i.e. section 2.5 gives a review of Biodiesel, its properties and use as fuel. It also covers the discussion on the economic feasibility of Biodiesel.

The world is facing energy crisis and it is increasing day by day. The problems like scarcity of petroleum resources, increasing atmospheric pollution, and Global warming are generating interest in alternative fuels like renewable fuels or biofuels. Biofuels are defined as fuels derived from renewable biological resources like agricultural crops; animal waste, municipal waste and lignocellulosic based material. Green house gas emission from conventional resources is another serious concern. The areas accountable for these emissions are transport, power generation, chemical industries and domestic household operations. Amongst these sectors, transport sector is dominant in consuming petroleum products. Figure 2.1 shows the world petroleum product consumption in 2002. The transport sector consumed almost 50% of petroleum products. [2.1].

In the transport sector, road transport accounts for highest percentage of energy consumption. Road transport is responsible for 84% of total CO_2 emissions coming from the transport sector. The rapid increase in air pollution by increasing usage of heavy-duty road-trains, agricultural machines, tractors and personal cars needs to be addressed. Amongst the commercially available fuels in Europe, diesel is common in commercially available transport vehicles like personal cars and heavy-duty motors. The diesel engines like IC engines, CRDI, Turbo dominate the European automobile industry. It is estimated that transport energy demand should reach 3.2 Gtoe (Giga ton oil equivalent) by 2030 with oil

accounting for 95%, where as in the UK by 2010 transport will account for 36% energy demand [2.2]. Although total green house gas emission is increasing all over the world, it fell in the UK by 14.5 between years 1990 to 2005 mainly due to fall in CO2 emissions [2.3]. Figure 2.2 shows the UK CO_2 green house gas emissions from 1990-2005. It can be seen that green house gas and CO_2 emission is reduced from 1990 to 2005.

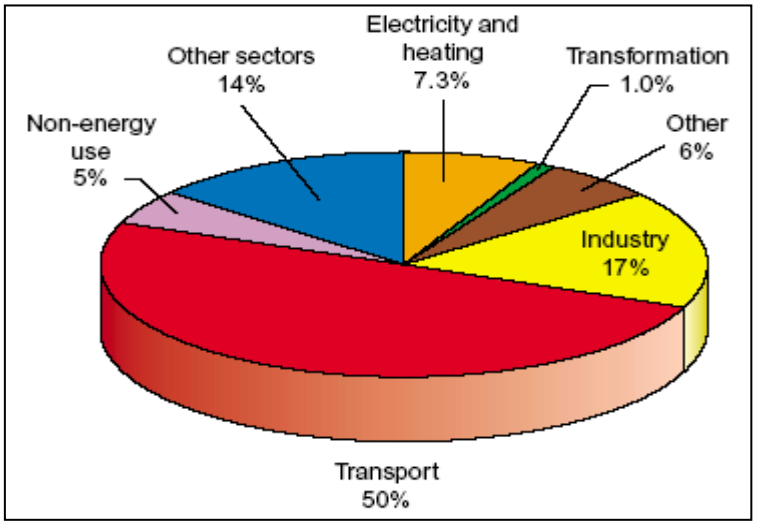

Figure 2.1: World petroleum product consumptions in 2002 [2.1]

In response to international pressure, governments are set to reduce greenhouse gas emissions. The European Union has set a target to reduce green house gas emissions by 20% from 1990 levels by 2020 or by 30% in conjunction with other countries [2.2]. UK has set a target under Kyoto protocol to reduce green house gas (GHG) emission by 12.5% from 1990 levels by 2008-2012. The UK carbon emissions are projected to be 119.2-128.9 MtC in 2020, equating to a 20-26% reduction on 1990 levels [2.4]. In the Climate Change Bill, the UK has set a target of 26 to 32% reduction in emissions on 1990 levels by 2020. Figure 2.3 gives the UK CO_2 projection values with Kyoto target up to year 2020.

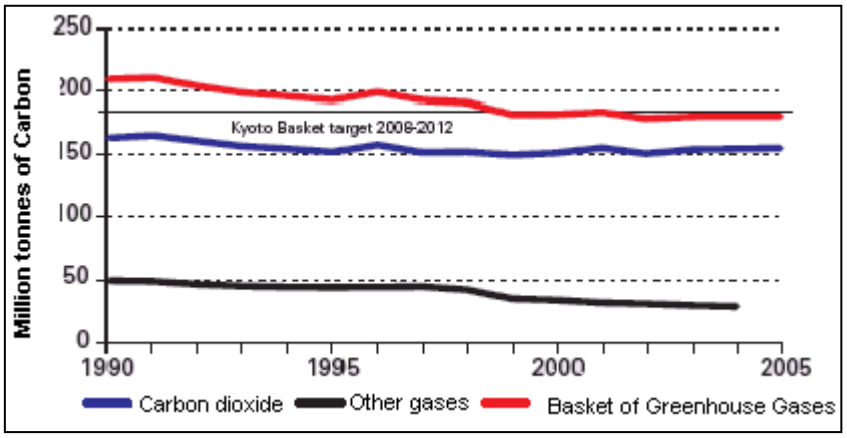

Figure 2.2: U.K CO_2 and greenhouse gas emissions from 1990 to 2005 [2.3]

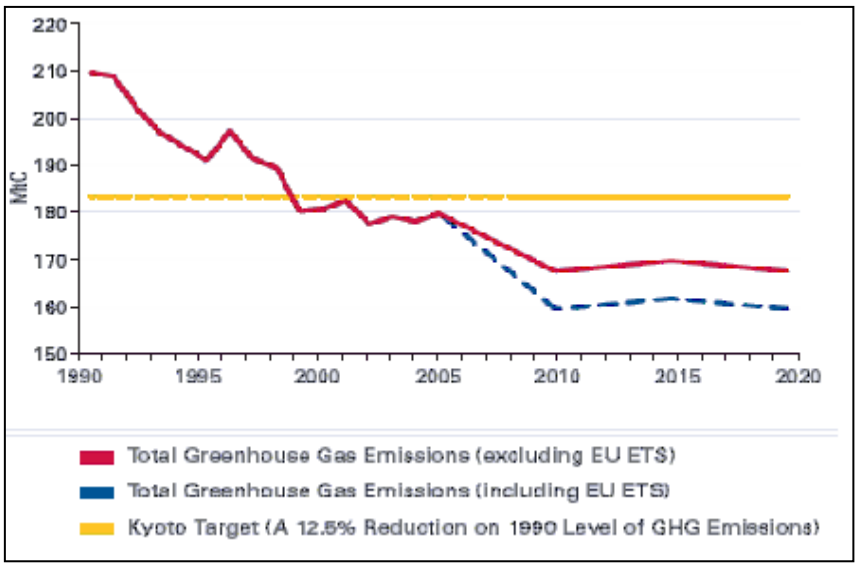

Figure 2.3: UK CO2 emission projections up to 2020 [2.4]

2.1 European Emission Standards

To achieve GHG reduction targets and to control pollution from new vehicles, the European Commission set emission standards or acceptable limits for exhaust emissions of petrol/diesel vehicles in 1992 in EURO1. EURO 1 to 6 are acceptable limits for exhaust emissions of new vehicles sold in EU states. The standards are set for main pollutants like Carbon monoxide, Hydrocarbons, Particulate Matter and NOx. These standards are applicable to new vehicles and not to vehicles already on road. There are no limits set for CO_2 emissions now but EC has drafted legislation to limit CO_2 average emissions from passenger cars to 120g/km by 2012. Apart from these standards, European Commission (EC) has set motor fuel standards for sulfur content up to 50 ppm by 2005 and 10 ppm

2009. Table 2.1 gives European emission standards from Euro 1 to 6 for passenger cars [2.5]. The values mentioned in table are grams (g) of individual pollutant emitted per 1 kilometer (km) run of vehicle or engine.

Standards (g/km)	CO		HC	NOx		HC + NOx			PM	
	P	D	P	P	D	P	D		D	
		DI/IDI			DI/IDI		DI	IDI	DI	IDI
EURO 1 (92-93)	2.72		-	-		0.97			0.14	
EURO 2 (96-97)	2.2	1.0	-	-		0.5	0.7	0.9	0.08	0.1
EURO 3 (2000)	2.3	0.64	0.2	0.15	0.5	-	0.56		0.05	
EURO 4 (2005)	1.0	0.5	0.1	0.08	0.25	-	0.3		0.025	
EURO 5 (2008/09)	1.0	0.5	0.1	0.06	0.18	-	0.23		0.005[b]	
EURO 6 (Proposed)	1.0	0.50	0.10	0.06	0.08	-	0.17		0.005[b]	

P = Petrol D = Diesel DI = Direct Injection IDI = Indirect Injection

b = Particulate Matter (PM) values are same for Petrol & Diesel in EURO 5, 6

Table 2.1: European Emission Standards for passenger cars [2.5]

For solving emission problems, to improve energy security, to reduce oil dependency, to achieve emission reduction targets and concern for long time supplies of diesel, it is necessary to develop sustainable alternative fuels compatible with conventional diesel. The compatibility with conventional diesel will ensure that there is no need of engine design modifications. Though new technologies like electric cars, hybrid engines will solve the transport emission issue in future, conventional liquid fuel engines will be in use for some time so we need to improve efficiency of current diesel engines.

The requirements of alternative fuels/ Biofuels:

- It should have applicability in commonly marketed engines/ fuel-injection systems.
- Oxidation and storage resistance should be comparable to that of mineral oil-based fuels.

- It should be economically sustainable (CO_2 and energy balance) and should maintain emission declarations made for conventional fuels.
- It should be available easily and at acceptable price.

2.2 Biofuels in European Union (EU)

The EU agreed to use 2% of Biofuels by 2005, 5.75% by 2010 and 10% by 2020. EU Bio fuels Directive required that 5.75% of all transport fossil fuels should be replaced by Biofuels by December 31 2010. UK had set up its own level of obligation mentioned in table 2.2 for financial years of 2008-2011 to achieve bio fuel targets. The targets were set on volume basis.

Financial Year	Level of obligation
2008/09	2.5%
2009/10	3.75%
2010/11	5%

Table 2.2: UK Renewable Transport Fuel Obligation [2.7]

The EU directive decided to create market demand of 10.5 billion litres (9.5 million tonnes) of Biodiesel by 2010. The Biodiesel production statistics of EU showed that overall Biodiesel production of EU-25 was 1.9 million tonnes in 2004 to 3.3 millions tonnes in 2005[2.6]. However this increased to 4.9 million tonnes, by year 2006. The EU-25 Bio ethanol production in 2006 was 1.2 million tonnes; this indicating that at Biodiesel production in 2005-2006 made up around 80% of EU Biofuel production. In 2006, EU produced 77% of total Biodiesel produced in world. This represented 65% growth in 2005 and 54% growth in 2006 [2.6]. In US, production of Biodiesel was around 75 million gallons (250,000 tonnes) in 2005; where as in the UK total Biodiesel sale was 33 million litres (29000 tonnes) accounting for 0.07% of total fuel sales [2.7]. In 2005, global Vegetable Oil Methyl Ester (VOME) output was 4 Mt. It was expected that by 2007 EU Biodiesel production capacity would have reached 10 million tonnes. Table 2.3 shows EU action plan for 2005 and 2010. It was estimated that total 12.72 Million hectares cultivation land will be required in 2010 to achieve biofuel targets.

	2005	2010
Target Proportion	2%	5.75%
Total Diesel consumption	158.6 Mio.t	165.0 Mio.t
Total Biodiesel requirement	3.69 Mio.t	11.0 Mio.t
Cultivation area required for Biodiesel	2.63 Mio.ha	7.88 Mio.ha
Total Petrol consumption	124.8 Mio.t	113.6 Mio.t
Total Ethanol requirement	3.7 Mio.t	9.7 Mio.t
Cultivation area required for Ethanol	1.85 Mio.ha	4.84 Mio.ha
Total cultivation area required	4.48 Mio.ha	12.72 Mio.ha

Mio.t = Million Tonnes, Mio.ha = Million Hectares

Table 2.3: Details of EU's biofuel target [2.8]

2.3 Biofuels

As defined in chapter 1 Biofuels are fuels obtained from renewable feedstock and available in liquid as well as gaseous form. The different types of Biofuels feed stock and their production methods are shown in Figure 2.4.

1st generation biofuels were produced from fermentation of grains, cereals, sugar, starch, crops such as sugar cane, sugar beet, wheat, corn and vegetable oil based biofuels such as pure vegetable oils and Biodiesel produced from oil seed crops such as rapeseed, soybean, palm, tallow oils, waste cooking oil and animal fats. The 2nd generation Biofuels are fuels produced from lignocellulosic material such as plant stalks, leaves, wood, tall grasses, crop residues, Ethanol produced by using enzymes, Synthetic diesel via gasification/ Fischer Tropsch process, liquid fuels from agricultural waste and switch grass. The major difference between 1st and 2nd generation biofuels is in the resources used in production and methods of production.

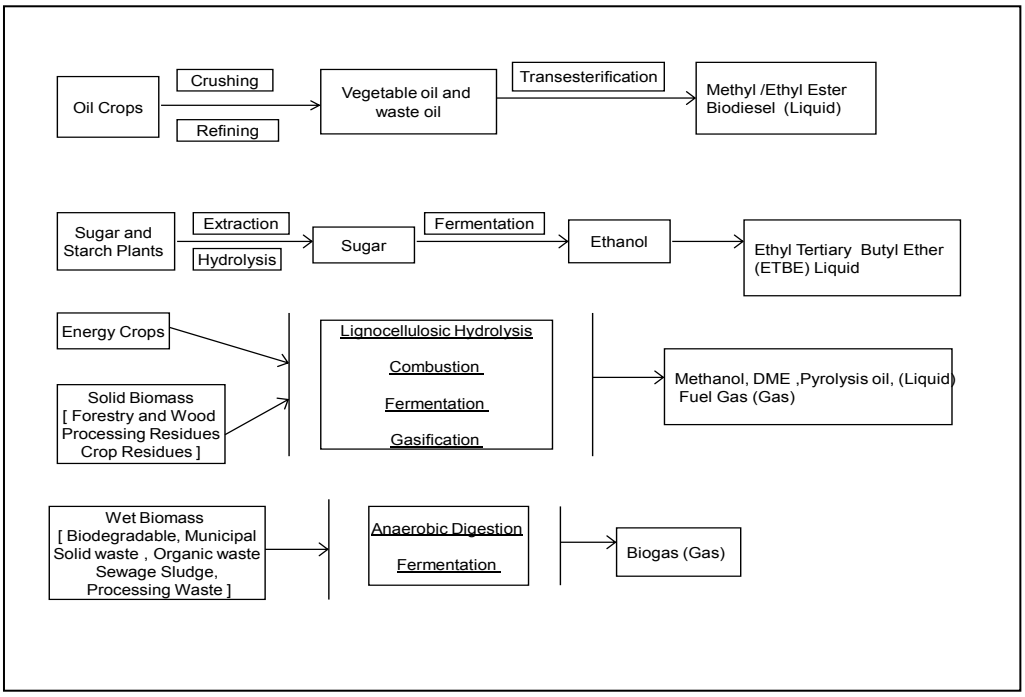

Figure 2.4: The different types of biofuels feedstock [2.9] [2.10]

The commercial biofuels can be listed as follows [2.11]:

1. Bio-Ethanol (Bio-ETOH): This is a refined product which is a stable transport fuel for gasoline and diesel fuel blends. Energy content of Bio-ethanol is 30% lower than that of gasoline (petrol). It can be produced from sugar, starch, lignocellulosic biomass and sludge solid residue.

2. Bio-ETBE: It is produced by reacting mixture of bio-ethanol (48% in volume) and tertiary butanol or isobutylene with heat over a catalyst. It can be used in existing gasoline engines without any modification thus offering environmental benefits like reducing emissions of aromatic compounds like Benzene.

3. Biodiesel: It is defined as mono-alkyl (Ethyl/Methyl) ester of long chain fatty acids obtained from transesterification of triglyceride with alcohol. They have properties closed to conventional diesel. They can be used directly (100%) or in blends with diesel in existing diesel engines.

4. Bio-Methanol (Bio-MEOH): It can be produced from bio-syngas mixtures of H_2 and CO derived from biomass via oxygen/thermal gasification process, by steam reforming of charcoal followed by catalytic synthesis of

CO_2 and H_2. It has potential to substitute methanol derived from natural gas.

5. Bio-MTBE: It is like Bio-ETBE, obtained by reacting mixture bio methanol (36% in volume) and tertiary butanol with heat over a catalyst.

6. Bio Gas: It is a mixture of 60% methane and 40% CO_2, which is produced by anaerobic fermentation of very humid biomass (live stock, liquid manure, sludge, waste etc).

7. Bio-Dimethyl ether: It is similar to LPG and can be used as substitute for LPG or as oxygenated additive in gasoline for diesel blending. Due to its combustion properties, it can be used as fuel in diesel engines.

8. Bio-synthetic fuels: They can be obtained from bio-syngas derived from biomass through Fisher-Tropsch process. This process can produce fuels like Bio-diesel oil, Bio-Middle Distillate, Bio-Naphtha or Bio-Methane.

9. Bio-Hydrogen: It can be defined as hydrogen derived from biomass resources. It is a clean fuel, highly energetic and does not emit CO_2. It can be obtained by water electrolysis, by catalytic shifting of bio-syngas, by membrane separation from bio-syngas and from bio methanol by steam reforming.

10. Bio-Butanol: It is produced from same agricultural feed stock used for ethanol like sugar cane, corn, sugar beet, wheat and sorghum. In future it can be produced from lignocellulosic feedstock. As it has low vapor pressure than gasoline, it is easily blended with gasoline. It has higher energy content compared to other existing biofuels.

The benefits of using Biofuels:

- Reduction in oil demand: Biofuels can be applicable in vehicles as direct fuel or can be blended with conventional fuels. Fuels like Biodiesel, Ethanol, and Bioethanol can be used as direct fuel (on 100% basis) or can be blended with different volume % in conventional diesel/gasoline

engines. Also fuels like Bio-diethyl ether, Biogas, Bio-synthetic fuels, Bio-hydrogen can help to reduce oil dependency in future.

- Environmental Benefits: Renewable fuels show significant reduction in greenhouse gases compared to conventional fuels. In many studies it was observed Biodiesel/Ethanol can reduce the higher quantity of emission of pollutants like carbon monoxide, particulate matter, sulphates and overall hydrocarbons [2.15] [2.21]. However application of these fuels increases nitrogen oxide emissions. Figure 2.5 shows estimated reduction in greenhouse gases by application of Biodiesel and Ethanol. Overall these fuels can help to tackle environmental problems thus preserving nature and protecting people's health.

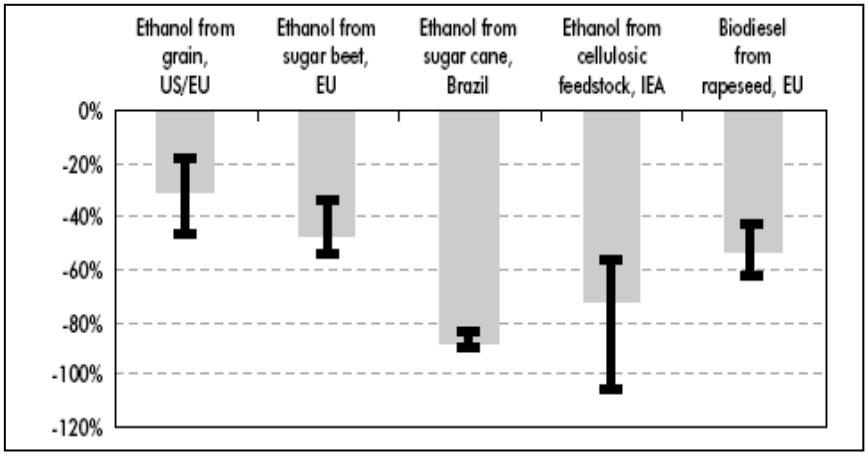

Figure 2.5: Estimated greenhouse gas reductions from biofuels [2.11]

- Agricultural Benefits: Biofuels reduce agricultural wastes from cropland, waste oils, grease and waste through recycling. They also protect ecosystem and soils. The production of energy or biofuel crops such as corn, rapeseed and wheat provides additional product market for farmers, enhancing the rural economic development, though there is threat to food production by increasing consumption of vegetable oils in transport fuel sector.

- Other benefits: These fuels also smoothens the engine operations. Ethanol has high octane number (around 110) so can be used as additive to

increase octane number of gasoline, where as Biodiesel can improve diesel lubricity and increase the cetane number.

2.4 Vegetable Oils

More than 100 years ago Dr Rudolf Diesel ran compressed ignition engine on 100% peanut oil in the World Exhibition at Paris in1900. Since then the vegetable oils are considered as good alternative fuels for diesel engines. The vegetable oils such as palm oil, soybean oil, sunflower oil, peanut oil and olive oil have been used as diesel fuels. The vegetable oils being renewable are widely available from variety of sources and have low sulphur contents [2.12].

The basic constituent of vegetable oils is triglyceride (Figure 2.6). The vegetable oils comprise 90 to 98% triglycerides and small amounts of mono- and diglycerides. Triglycerides are esters of three fatty acids and one glycerol. They contain substantial amounts of oxygen in their structure. Fatty acids vary in their carbon chain length and in the number of double bonds. The chemical composition of different vegetable oils is given in Table 2.4. The vegetable oils contain free fatty acids (1 to 5%), phospholipids, phosphatides, cartenes, tocopherols, sulphur compounds and traces of water [2.13].

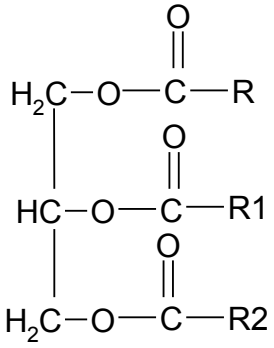

Where R, R1 and R2 represent hydrocarbon chain of fatty acids

Figure 2.6: Structure of a typical triglyceride molecule

The basic families of vegetable oils are [2.14]:

- **Lauric Oils:** They are high in saturated C_{12} & C_{14} groups. Examples are Copra, Palm-Kernel.
- **Palmitic Oils:** They include significant numbers of C_{16} groups. Examples are Palm, Lord and Tallow.

- **Oleic Oils:** These have only one unsaturation per molecule. Examples are Olive, Peanut and Rapeseed.

  C- C---……C = C-…….. - C

  1 2 9 10 18

- **Linoleic Oils:** They are characterised by high level of Linoleic groups (two double bonds). They have low resistance to oxidation. Examples are Sunflower, Cotton, Soya and Corn.

  C- C- C = C- C – C = C – C – C……C

  1 2 3 4 5 6 7 8 9 18

- **Linolenic Oils:** They have high levels of tri-unsaturated C_{18} groups. Example is Linseed Oil.

  C- C- C = C- C – C = C – C – C = C…… C

  1 2 3 4 5 6 7 8 9 10 18

Vegetable oil	Fatty Acid Compositoon (wt %)									
	14:0	16:0	18:0	20:0	22:0	24:0	18:1	22:1	18:2	18:3
Corn	0	12	2	Tr	0	0	25	0	6	Tr
Cottonseed	0	28	1	0	0	0	13	0	58	0
Peanut	0	11	2	1	2	1	48	0	32	1
Rapeseed	0	3	1	0	0	0	64	0	22	8
Safflower	0	9	2	0	0	0	12	0	78	0
Soybean	0	12	3	0	0	0	23	0	55	6
Sunflower	0	6	3	0	0	0	17	0	74	0

Tr = traces

Table 2.4: Chemical composition of vegetable oils [2.13]

2.4.1 Characteristics of vegetable oil

The properties of different vegetable oils are given in Table 2.5. The following are the characteristics that vegetable oil should possess as a substitute to diesel fuel:

Cetane Number:

It is a measure of ignition quality of the fuel and it should be as high as possible. The high cetane number represents short ignition delay; a long ignition delay leads to engine knock. The ideal range of cetane number for vegetable oil

substituting diesel fuel should be 40-60. The cetane rating for vegetable oil varies from 30 to 40 depending on type of oil and its purity [2.15].

Viscosity:

Viscosity is one of the most important properties of fuels in combustion in engines. The appropriate value of viscosity is required for smooth operation of engine; too high viscosity can cause incomplete combustion whereas, too low viscosity can increase system pressure at an unacceptable level and can affect the injection. An important issue for vegetable oils is their very high viscosity. Ramadhas et.al reports that viscosity of vegetable oils is five times higher than that of diesel [2.15]. For example viscosity of diesel fuel is 4.3 mm^2/s at 27^0C, sunflower oil is 58.5 mm^2/s and sunflower oil methyl ester (biodiesel) is 10.3 mm^2/s [2.15].

Heating Value:

Heating value of the fuel should be high, so it can help to reduce quantity of fuel handled and to maximize the equipment operating range. Vegetable oils have heating values closed to 80% that of diesel [2.15].

Important Temperatures:

Pour point and cloud point are important temperatures which indicate performance of fuel under cold weather conditions and they should be below freezing point of the oil. Flash point is another important temperature which shows tendency of fuel to form flammable mixture with air. The value for Flash point should be as high as possible. The values of all above temperatures for vegetable oils are higher than that of diesel [2.15]. As like viscosity, flash point, cloud point and pour point of vegetable oil is higher than that of diesel; making diesel fuel unsuited to low temperature engine operations. For example cloud point and pour point of Rapeseed oil is -3.9 ^0C and -31.7 ^0C respectively [2.13].

Other Properties:

The sulphur content, carbon residue and ash cause corrosion, wear and tear in engines. They also increase environmental pollution so their values should be as low as possible. The typical values for vegetable oils are 0.5% sulphur, 0.27% carbon residue and 0.01% ash [2.15].

Properties	Cotton-seed	Peanut	Rapeseed	Safflower	Soybean	Sunflower
Kinematic Viscosity (mm^2/s)	33.5	39.6	37	31.3	32.6	33.9
Cetane no	41.8	41.8	37.6	41.3	37.9	37.1
Heating Value (MJ/kg)	39.5	49.8	39.7	39.5	39.6	39.6
Cloud Point (^0C)	1.7	12.8	-3.9	18.3	-3.9	7.2
Pour point (^0C)	-15.0	-6.7	-31.7	-6.7	-12.2	-15.0
Flash point (^0C)	234	271	246	260	254	274
Density (Kg/L)	0.9148	0.9026	0.9115	0.9144	0.9138	0.9161
Carbon residue (wt %)	0.24	0.24	0.30	0.25	0.27	0.23
Ash (wt %)	0.010	0.005	0.054	0.006	<0.01	<0.01
Sulfur (wt %)	0.01	0.01	0.01	0.01	0.01	0.01

Table 2.5: Properties of different vegetable oils [2.12]

2.4.2 Vegetable oils as fuels

The performance of vegetable oils as fuels in diesel engines depends on their physical and chemical properties, their combustion characteristics, type of engine and conditions of operation. Following are the processes that can be used for application of vegetable oil as a combustible fuel:

- Pyrolysis
- Micro-emulsions
- Transesterification
- Direct use and blending

Pyrolysis:

The pyrolysis can be defined as a chemical change cause by application of thermal energy in the presence of catalyst. Pyrolysed material can be vegetable oils, hydrocarbons, animal fats, natural fatty acids or methyl esters of fatty acids. Thermal decomposition of triglycerides produces the intermediate fuel compounds like alkanes, alkenes, alkadienes, aromatics and carboxylic acids. The pyrolyzed products have low viscosity and high cetane numbers compared to pure vegetable oils [2.9] [2.13].

Micro-emulsions:

This is a colloidal equilibrium dispersion of optically isotropic fluid microstructures with dimensions generally in the range of 1-150nm formed two immiscible liquids. A micro-emulsion of vegetable oils with esters is possible by using solvents such as methanol, ethanol and butanol to reduce the viscosity of the vegetable oil blends. Due to the presence of alcohol, micro-emulsions have high latent heat of vaporization and tend to cool the combustion chamber which reduces injection nozzle coking [2.13]. A micro emulsion of methanol with vegetable oils can perform as well as diesel fuels [2.9] [2.13].

Transesterification:

It is a process in which the reaction of fat or oil with an alcohol to form alkyl esters (Biodiesel) and glycerine. The biodiesel formed is quite similar to conventional diesel in characteristics and performance. The transesterification process is used to reduce viscosity of triglycerides like vegetable oil. A catalyst is used to increase the reaction rate and yield. The typical reaction with methanol in this process is

Fat or oil + 3 Methanol = Glycerol + 3 Methyl ester

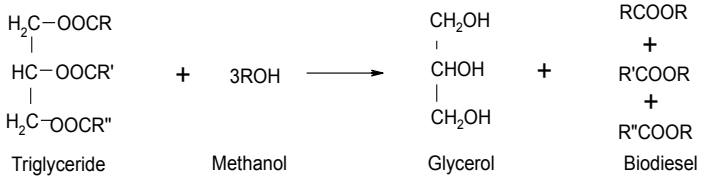

The molar ratio of alcohol (methanol) to triglyceride ratio in above reaction is 3:1 but in industrial processes a 6:1 molar ratio is often used to obtain yield of alkyl

ester more than 98% [2.9]. Amongst all the alcohols, methanol and ethanol are used commercially because of their low cost & physical and chemical properties.

Direct use and blending:

The vegetable oils can be used in conventional diesel engines directly without any modification or in blends with diesel fuel to reduce viscosity and give better performance. The different types of vegetable oils have been tested in diesel engines and experimental set up. Details of vegetable oil combustion work done are summarized in Table 2.6 and a few of them is explained below [2.9].

Pangavane [2.17] conducted experiments on soybean oil in diesel engine. The reduction in CO and HC emission by 21 and 47% respectively was reported whereas, NOx emission was found to increase with increasing engine load. Jacobus et al. [2.18] conducted trials on sunflower oil, cottonseed oil, soybean oil and peanut oil blend with diesel. It was observed that these oils provided almost similar characteristics based on comparison of engine performance and emission characteristics. Senthil Kumar [2.19] found by blending jatropha with diesel fuel that exhaust gas and temperature, smoke HC and CO emissions were higher compared to diesel. Abbas et al. [2.20] used Sunflower oil and reported high values of particulate matter, CO, NOx and HC as compared to that of the diesel due to shorter ignition delay and higher diffusive burning. In diffusive burning or diffusion flame oxidizer or oxidant for example O_2 combines with the fuel by diffusion, whereas in premixed flame oxidizer is mixed with fuel before it reaches the flame front.

Author	Fuel Used	Experimental Set-up/Engine	Experimental Analyses
G.Vicente et.al.(2005)	Sunflower and rapeseed oil, alternate seed oils, genetically modified vegetable oils	Three necked batch reactor	Study of oils for biodiesel production
D.San Jose Alonso (2005)	Rapeseed oil and Diesel oil mixtures	Generator Group Boiler	Production of heat energy and yield of combustion
K.Nishi (2004)	Rapeseed oil	Robin YD-4l Diesel engine	CO, CO_2, HC emission
D.L.Lance and J.Anderson (2004)	Virgin vegetable oil	1.9 L D.I engine 1.5L IDI engine	Emission Performance

K.Pramanik (2002)	Jatropha Curcas oil and diesel fuel blends	I C engine	Engine Performance, Analysis for blends,
Y.He, Y.D.Bao (2002)	Rapeseed oil	Single cylinder diesel engine	Emission Performance
D.R.Pangavane, P.B.Kushare (2002)	Soybean oil	Diesel engine	Exhaust emissions
C.A.Silvico et. al (2002)	Palm oil	Diesel Generator	Performance of diesel generator
S.Saka, D.Kusdiana (2001)	Rapeseed oil	Reaction vessel made of Imonel-625	Kinetics of Transesterification
S.Cetinkaya and others (2000)	Vegetable oil	Single cylinder Direct Injection Diesel engine	Engine performance and exhaust emission
S.Dhinagar (1999)	Neem oil, Rice bran oil, Karanji oil	Low heat rejection diesel engine	Fuel Efficiency
N.Bakhshi et. al (1996)	Canola oil	Fixed bed stainless steel micro reactor	Thermal cracking products
M.V.Kok, M.Reha Pamir (1995)	Turkish oil shale samples	Du Pont 9900 thermal analysis system	Pyrolysis and combustion kinetics
Z.Mariusz (1992)	Sunflower oil	Diesel engine	Engine operation at low and high speed
M.H.Hassan, S.Mat (1991)	25,50 and 75% blends of palm oil and diesel oil	Diesel engine	Engine Performance
M.L.Schick et al. (1988)	Soybean oil and sunflower oil	Diesel engine	Engine Performance
A.W.Schwab et al. (1988)	Soybean oil	ASTM std Distillation equipment (AE 133-78)	Thermal decomposition products
H.J.Goettler, H.J.Klosterman (1986)	Plant oil (Sunflower, corn , olive and safflower oils)	Air Heater	Formation of Residues
M. Ziejewski (1986)	Blend of 25/75% high oleic safflower oil and diesel oil , Blend of 25/75% alkali refined sunflower oil and diesel oil, a non-ionic sunflower oil-aqueous ethanol micro emulsion	Turbocharged, 4Cylinder Allis-Chalmers Diesel engine	Performance of diesel engine

T.J.German et al. and K.R.Kaufman et al. (1985)	Blends of 25/75% and 50/50% alkali refined winterized sunflower oil	Tractors with turbo-charged diesel engines.	Engine Performance
H.J.Goettler et.al (1985)	Blend of diesel oil and crude sunflower oil	Diesel engine	Performance of diesel engine
M.A.Mazed et al. (1985)	10 and 25% blends of pure Cottonseed oil and diesel oil 10/90% blend of Cottonseed oil and diesel fuel	Lister and Deutz Diesel Engine	Power output and Fuel efficiency
M.A.Mazed et al. (1985)	10% Soybean oil and diesel oil , Peanut, Soybean and cottonseed oil	Indirect Injection Diesel engine	Injector and Nozzle performance, Smoke emission
M.A.Mazed et al. (1985)	25/75% blend of Cottonseed oil and diesel oil	Diesel Engine with pre-combustion chamber	Power output and Fuel efficiency
T.Murayama et al. (1984)	Rapeseed oil , RME, Rapeseed oil blended with Diesel oil , Ethanol	Direct injection naturally aspirated diesel engine	Engine Performance
N.J.Schlautman et al. (1984)	75/25% Soybean oil and diesel oil blend	Direct injection diesel engine	Lubricant contamination and Carbon deposits
C.S.Hawkins et.al (1983)	Pure Sunflower oil, 25/75% alkali refined sunflower oil and diesel oil	Direct injection diesel engine	
T.L.Peterson et al. (1983)	Oleic and linoleic Safflower oils	Diesel engine with pre-combustion chamber	Engine Performance
B.S. Samaga (1983)	Sunflower oil and groundnut oil	Single cylinder water-cooled duel fuel IC engine	Engine Performance
M.J.Jacobous (1983)	Cottonseed oil with diesel oil , Sunflower oil, Soybean oil and Peanut oil	Single cylinder diesel engine	Engine performance and emission characteristics
M.C.Ziemke et al. (1983)	Soybean oil , Saponified Soybean oil distillate and aqueous ethanol solutions	Turbocharged diesel engine	Exhaust emission

C.L.Peterson et al. (1983)	70/30% Rapeseed oil and Diesel oil blend	Single cylinder swirl chamber diesel engine	Engine Performance
R.A. Baranescu and J.J Lusco (1982)	Alkali Refined Sunflower oil	D1 Turbo charged Diesel engine	Sunflower oil as fuel extender
R.W.Pryor et al. (1982)	Crude soybean oil Crude degummed Soya bean oil and Soya bean Ethyl Ester	Small direct direction diesel engine	Use of Soybean oil in diesel engine
P.N.Blumberg et al. (1982)	Pure Cotton seed oil , Cotton seed oil methyl ester with diesel oil	Turbocharged open chamber diesel engine	Engine performance and emissions
Du Plesis (1981)	Sunflower oil	Air-cooled, pre-combustion chamber engine	Sunflower oil as tractor fuel
N.J.Barsic, H.Humke et al (1981)	100% sunflower oil 100% Peanut oil 50% Sunflower oil with diesel 50% Peanut oil with diesel	Naturally Aspirated Diesel engine	Engine Performance
G.R.Quick (1980)	20/80% blend of sunflower oil and diesel oil	Diesel engine	Engine performance
B.Bansal, B.Junja and Dhinagar et al. (1980)	Neem oil and diesel oil blends of 10, 20, 30% blends	Diesel engine	Neem oil as diesel fuel

Table 2.6: Summary of combustion work done using vegetable oil

Yasufumi et al. [2.21] did experiments with stable emulsified fuel including frying oil composed of vegetable oil discarded from restaurants and households. A reduction in NOx emission and smoke density was observed compared to that obtained from diesel. Yu et al [2.22] combusted waste cooking oil collected from the noodle industry. The combustion characteristics observed were similar to diesel fuel, however emission of CO, NOx and SOx were higher than the diesel fuel. At high temperatures, tar like substances was found to be deposited in combustion chamber. Silvico et al. [2.23] used heated palm oil as fuel in diesel generator; exhaust gas temperature, specific fuel consumption, carbon

monoxide emission were increased, while NOx emissions were lower than that of diesel fuel.

Souligny et al. [2.24] observed the emission performances of pure virgin vegetable oil in 2 Euro II compliant diesel vehicles and measured CO, PAH emissions. The virgin vegetable oil (vvo110) was tested in 1.51 Direct Injection (DI) and 1.91 Indirect Injection (IDI) vehicles and compared with Ultra Low Sulphur (ULSD) diesel fuel. CO emissions were approximately 2.7 times higher whereas lower PM emissions were observed compared that obtained from ULSD. For 1.91 IDI vehicles, the increase in HC emissions by 250%, and CO emissions by 420% was observed, whereas in 1.51 DI engines HC emissions increased by 170% HC, and CO emissions increased by 60% compared to ULSD. NOx emission was decreased by 8% for both vehicles [2.24].

Samaga [2.25] operated single cylinder duel fuel engine using sunflower oil and ground nut oil. The performance characteristics were compared with that obtained from diesel fuel. He suggested periodic cleaning of the nozzle tip to ensure adequate spray characteristics. Barsic [2.26] conducted experiments using 100% Sunflower oil, 100% Peanut oil, 50% Sunflower oil with diesel and 50% Peanut oil with diesel. Increase in power and emission was observed.

The combustion of vegetable oil in diesel engine shows that vegetable oil in pure form or as a blend with diesel increases Hydrocabons, Particulate Matter (PM) and CO emission. It also increases NO_x and SO_x emission. The exhaust temperature and smoke density is also observed to be increased. Even in some combustion work tar like substances and carbon particles were found to be deposited in combustion chamber. Overall vegetable oil as a fuel increases intermediate hydrocarbons, pollutants emissions and form engine deposits. So alkyl esters of these vegetable oils i.e. Biodiesel need to be evaluated as diesel engine fuel.

2.4.3 Rapeseed and Rapeseed oil

Amongst the vegetable oils or vegetable oil seeds, Rapeseed is widely grown in Europe, India and China. Rapeseed is the 3rd most important source of vegetable oil in the world after Soybean and Palm oil. Currently 20% of total

rapeseed grown in EU is used for biodiesel production. It is widely used as cooking oil, salad oil and making margarine. It is also used for non-edible purposes providing lubricants and hydraulic fluids. High erucic rapeseed oil is used in lubricants especially where high heat stability is required. Typical Rapeseed oil molecule consists of oleic acid (C18:1), Linoleic acid (C18:2) and Linolenic acid (C18:3) and few traces of saturated acid [2.16]. Table 2.4 from section 2.4 'Vegetable Oils,' shows typical composition of Rapeseed oil. The well developed rapeseed seed contains 40 to 44% oil and Rapeseed oil contains 60 to 65% of mono-saturated fats and 30 to 35% of polyunsaturated fats.

Figure 2.7: Rapeseed plant

Rapeseed, also known as Rape, Rapa, Oil seed Rape, Rapaseed and Canola, is a bright yellow flowering member of the brassicaceae family group. Its scientific name is Brassica napus where as other name 'Rape' is derived through old English from a term for turnip, rapum. It is also grown as winter-cover crop. The process of oil extraction from rapeseed provides high-protein animal feed. Rapeseed meal contains approximately 40% of protein which rates among the nutritionally best plant proteins. Figure 2.8 shows all end uses of Rapeseed. Rapeseed is very sensitive to high temperature at blooming time even when mole moisture is available. The growth of Rapeseed is most vigorous in temperature between 10 ^{0}C and 30 ^{0}C with optimum around 20 ^{0}C [2.16]. Long periods of over 30 ^{0}C can result in severe sterility and high yield loss. The oil seed content is highest when seed mature under low temperature (10 ^{0}C to 15 ^{0}C).

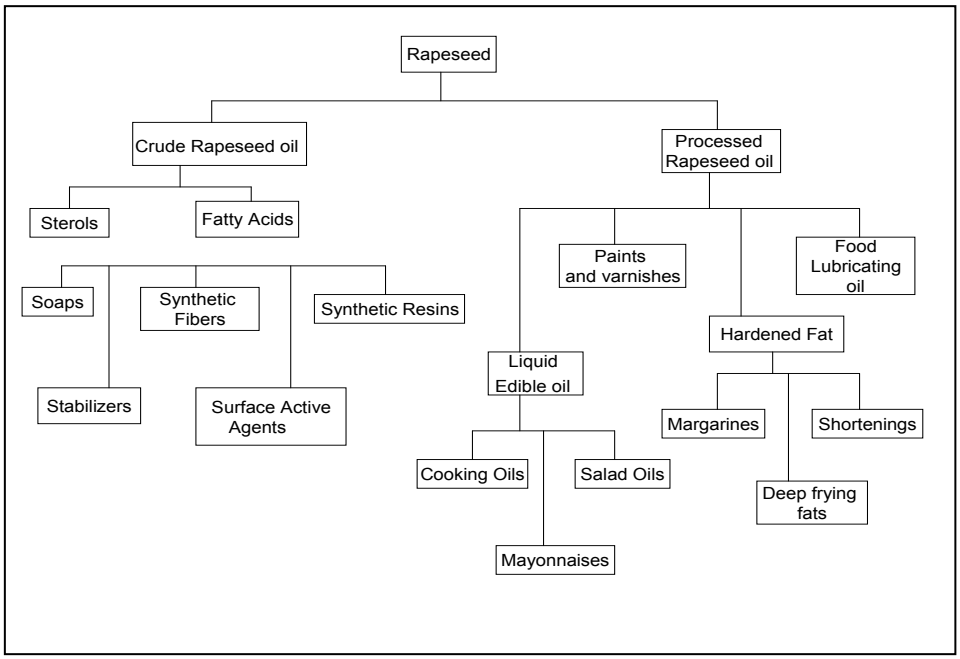

Figure 2.8: End uses from Rapeseed [2.16]

2.4.4 Rapeseed oil as fuel

K.Nishi and others tested refined rapeseed oil in a direct injection and natural aspirated diesel engine (Robin YD-41). They observed that total hydrocarbon emission was improved and low NOx values were observed for refined Rapeseed oil compared to diesel. However when the engine was operated for long periods of time, deposits were built-up implying problems in long term running of the engine with rapeseed oil [2.27]. Montagne [2.28] also conducted experiments with rapeseed oil in diesel engines. An increase in NOx emission and decrease in HC emission was observed. An increase in noise and smoke level were noted at cold start of engine. Hemmerlein et al. [2.29] conducted experiments on naturally aspired exhaust gas turbo charged air cooled and water cooled engines using Rapeseed oil. The brake power, mechanical stress, torque of engine and combustion noise was lower for rapeseed oil compared to that for diesel. The emission of CO and HC were higher where as NOx and Particulate emission was lower compared as diesel.

Todashi et al. [2.30] tested the feasibility of using palm oil and rapeseed oil in naturally aspirated direct injection diesel engine. The performance of oils was evaluated in terms of short term and long term engine operation. The engine performance and exhaust emissions were at acceptable levels for short term

operation. The carbon deposits build ups and sticking of piston rings were observed for extended operation.

J.O.Olsson [2.31] oxidized small samples of Rapeseed oil and superior quality of diesel oil in reactor. The oxidation products were analyzed using gas chromatographic (GC/MS) method. It was observed that Rapeseed oil produced high amounts of acrolein and other aldehydes. High amounts of reactive organic intermediates like 1-alkenes, dienes, aldehydes and aromatics were formed using Rapeseed oil. It was observed Rapeseed oil produced a factor of 10 more intermediates than diesel oil.

D.Lance and J.D.Andersson [2.32] combusted 100 % vegetable oil (VVO100) with Ultra Low Sulphur (ULSD) in 1.9l Direct Injection(DI) and 1.5l Indirect Injection (IDI) diesel vehicles. The vegetable oil was rapeseed origin and of food grade standard. Two types of engines (DI and IDI) were selected to represent current UK diesel vehicles. It was observed VVO100 increased HC emission by ~250% and CO emission by ~420% in 1.9l DI vehicle and HC emission by 170% and CO by 60% in 1.5l IDI vehicle compared to ULSD. The vegetable oil also increased Particulate Matter (PM) emission by ~100%, whereas NOx emission was reduced by 8% compared to ULSD in the 1.9l DI vehicle. These effects were not observed in the 1.5l IDI vehicle combustion [2.32]. High erucic acid rapeseed (winter rape) and low erucic acid rape seed (spring rape) were tested for short and long-term engine test. The performance of winter rape blends was closer to diesel oil. The problems like gumming, lubricating oil thickening were absent when engine ran with winter rape.

J.San.Jose Alonso and co-workers [2.33] studied mixtures of rapeseed oil and diesel oil for producing heat in a conventional diesel installation. The heat emitted per kg for different rapeseed oil and diesel mixtures was higher than that emitted per kg of diesel. Apart from reduction in sulphur oxide and CO_2 emissions, increase in combustion efficiency was also observed.

N.Bakhshi and others [2.34] studied thermal cracking of Canola oil in a fixed-bed reactor in presence and absence of steam. It was observed that Canola oil conversions increase with an increasing cracking temperature and decrease in

Canola oil space velocity and steam/Canola oil ratio. Space velocity is inverse of residence time. Thus higher the spacer velocity indicates shorter the residence time. The products obtained were C_4 and C_5 hydrocarbons, aromatics and C_6+ aliphatic hydrocarbons and C_2-C_4 olefins and hydrogen. The selectivity for C_2-C_4 olefins in the gas phase product was increased with an increase in both temperature and steam/canola oil ratio.

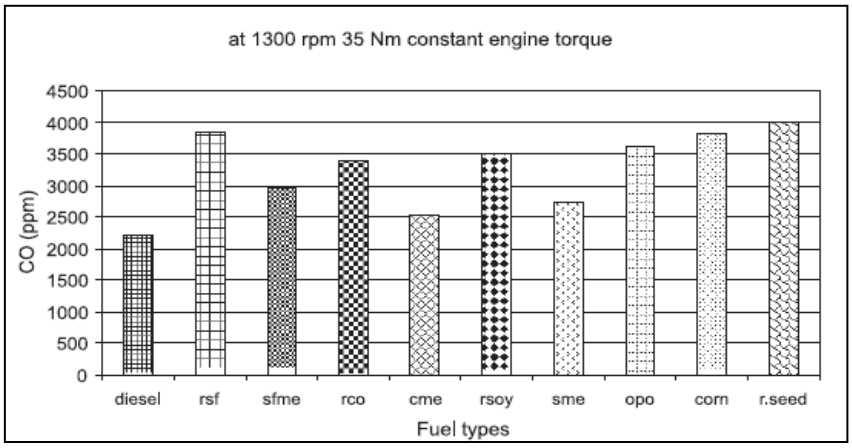

Figure 2.9: The emission of CO in relation with the fuel types [2.35]

Recep.A et al. [2.35] combusted different vegetable oil fuels like raw sunflower oil (rsf), raw cottonseed oil (rco), raw soybean oil (rsoy), refined corn oil, distilled opium poppy oil (opo), refined rapeseed oil (r.seed) and their methyl esters in direct injection single cylinder diesel engine. It can be seen from figure 2.9, the CO emission from diesel oil is 2225 ppm; whereas CO emission from rapeseed oil is 4000 ppm. The smoke opacity observed with diesel fuel was 29.3% and 49% with rapeseed oil. Particulate emissions of vegetable fuels were higher than that of diesel fuel. Power loss with vegetable oil fuel operation was lower compared to diesel fuel. He observed that vegetable oils can be used as fuel in diesel engines with some modification.

Overall Rapeseed oil as fuel increases emission of total Hydrocarbons and Particulate Matter. It also increases emission of oxygenated compounds like Carbon Monoxide, Acrolein and Aldehydes. However it reduces NO_x, CO_2 emission brake power and mechanical stress of diesel engine. The long run engine operation with Rapeseed oil shows engine deposits including carbon deposits.

2.4.5 Advantages & Disadvantages of Vegetable oils as fuels

The different types of vegetable oils are applicable in diesel engines as fuels, but due their chemical and physical properties they have limitations. This section summarizes advantages and disadvantages of vegetable oils as fuels.

Advantages:

- Vegetable oils are biodegradable, non-toxic renewable fuels, which are readily available and have liquid natural portability.
- They have low aromatic contents compare to diesel fuels, almost zero emission of sulfates, low carbon monoxide and carbon dioxide emissions.
- Vegetable oils take away more carbon dioxide from the atmosphere during their production than carbon dioxide added to the atmosphere by their combustion.
- They can replace diesel oil in boilers, internal combustion engines without any modification.
- Vegetable oils show less knocking tendency in diesel engines.
- Extraction and processing of vegetable oils are simple low energy processes.
- Vegetable oils have good heating power with 80 % heating value compared to that of diesel.
- They are good friction-reducing agents.
- The vegetable oil like Rapeseed oil contains considerable fraction on antioxidants (β-carotene). It has also low level of contamination.

Disadvantages:

- They have high molecular weights in the range of 600 to 900, which are three to four times higher than diesel fuel. Also volatility is very poor.
- They have higher cloud and pour point temperatures also flash point is much higher than diesel.
- Due to its high molecular mass and chemical structure it has very high viscosity almost 10 to 20 times more than that of diesel fuel.
- Poor combustion and fuel atomization, cold engine start up and misfire.
- The mass heating values are lower than conventional diesel.
- Lower stoichiometric mixture ration and specific enthalpy of combustion than diesel fuel.

- It creates problems like forming carbon deposits, injector coking, piston ring sticking, lubricating oil thickening and oil degradation and wear in combustion chamber.
- Some oils (rapeseed, cotton, peanut, and soya) remain fluid at slightly negative temperatures (0 to -10^0C). For example Rapeseed oil has pour point of -31.7^0C)

2.5 Biodiesel

Bio diesel is defined as monoalkyl esters (RCOOR) of long chain fatty acids derived from renewable lipid sources like vegetable oils or animal fats. They are obtained by transesterification of triglycerides with alcohol mainly with methanol and ethanol giving alkyl ester and glycerol. The resulting Biodiesel is quite similar to conventional diesel fuel in characteristics. Biodiesel is biodegradable, non toxic in nature and possesses low emission profiles. It is compatible with conventional diesel engines and can be blended in any proportion. The conversion of triglycerides into methyl or ethyl esters through transesterification process reduces the molecular weight to one-third that of the triglyceride, viscosity by factor of eight and marginally increases volatility. Bio diesel has viscosity close to diesel fuels and cetane number around 50. These esters contain 10 to 11% oxygen by weight, which may encourage more combustion than hydrocarbon- based diesel fuels in the engine [2.49].

Different types of oil esters are used as Biodiesel. In the USA the majorly are from Soybean, in Asia from Palm and in Europe from Rapeseed oil for blends of biodiesel. The blends of biodiesel and diesel are defined in terms of biodiesel % quantity in blends. The product is known as B100 when biodiesel is used directly or BX when used in blends with diesel, (where x = 5 to 95%). These blends consist of fatty acid methyl esters obtained from isomers of glycerides ranging from C_{14} to C_{24}. In European countries blends of Biodiesel (Rapeseed oil methyl ester) and Diesel fuel up to B25 or B30 are commercially available. The international standard for application of Biodiesel as a fuel is EN14214. This standard is based on EN590 (standard for diesel fuel) and DIN 51606(German standard for biodiesel) [2.16] [2.36]. The standard EN14214 describes the minimum requirements for Biodiesel, produced from rapeseed, soya, jatropha or

other virgin oils, used-cooking oil, municipal solid waste or any other feed stock. Table 2.7 gives details of all above mentioned standards for biodiesel fuel quality.

Criteria	Derv (EN590)	Biodiesel (DIN51606)	Biodiesel (EN14214)
Density @ 15°C (g/cm)	0.82-0.86	0.875-0.9	0.86-0.9
Viscosity @ 40°C (mm /s)	2.0-4.5	3.5-5.0	3.5-5.0
Flashpoint (°C)	>55	>110	>101
Sulphur (% mass)	0.20	<0.01	<0.01
Sulphated Ash (% mass)	0.01	<0.03	0.02
Water (mg/kg)	200	<300	<500
Carbon Residue (% weight)	0.30	<0.03	<0.03
Total Contamination (mg/kg)	Not Specified	<20	<24
Copper Corrosion 3h/50°C	Class 1	Class 1	Class 1
Cetane Number	>45	>49	>51
Methanol (% mass)	Not Specified	<0.3	<0.2
Ester Content (% mass)	Not Specified	>96.5	>96.5
Monoglycerides (% mass)	Not Specified	<0.8	<0.8
Diglycerides (% mass)	Not Specified	<0.4	<0.2
Triglyceride (% mass)	Not Specified	<0.4	<0.4
Free Glycerol (% mass)	Not Specified	<0.02	<0.02
Total Glycerol (% mass)	Not Specified	<0.25	<0.25
Iodine Number	Not Specified	<115	120
Phosphor (mg/kg)	Not Specified	<10	<10
Alcaline Metals Na. K (mg/kg)	Not Specified	<5	

Table 2.7: International standards for Biodiesel Fuel Quality [2.36]

2.5.1 Method of producing Bio diesel

As mentioned in section 2.4:2 ‘vegetable oils as fuels’; transesterification is the reaction of fat or oil with an alcohol to form esters and glycerol. Figure 2.10 shows the typical transesterification reaction. The chemical composition of transesterification product i.e. Biodiesel, is depend on the length and degree of unsaturation (double or triple bond) of the fatty acid alkyl chain present in triglyceride. Transesterification reaction is carried out by two methods; catalytic and non catalytic. Typical catalysts used are Enzymes, Alkali (NaOH), Acids (sulphuric acid) respectively. The alcohols that can be used are methanol, ethanol, propanol, butanol and amyl alcohol. Different processes like Novamont, Ballestra, and process from IFP, Henkel, and ATT [2.13] are commercially available for production of Bio diesel.

2.5.2 Chemistry of Trans-esterification Reaction

The overall chemical reaction of a transesterification process is given as

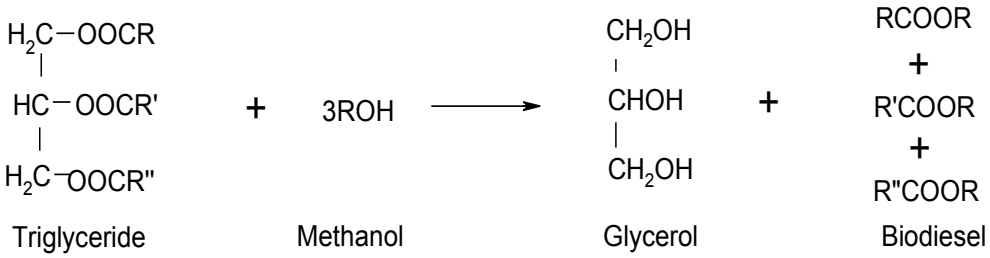

Where R, R', R" are long alkyl chains

Figure 2.10: Transesterification Reaction [2.12]

Transesterification is a typical steady state reaction and takes place easily at atmospheric pressure and a temperature of about 60 to 70^0C. The typical products of transesterification reaction are alkyl ester, glycerol, alcohol, and unreacted tri-, di- and monoglycerides. The molar ratio of alcohol needed to complete the transesterification process is 3:1 whereas, excess alcohol (molar ratio of 6:1) is required to shift equilibrium to the product side. The conversion rates are very high (over 98%) however, consumption of alcohol can be reduced by conducting the reaction in steps, where part of alcohol and a catalyst are added at the start of each step and glycerol is removed at the end of each step. Typical reaction time of 4-5 hours is required to achieve this conversion when reaction is carried out in Continuously stirred tank reactor (CSTR). The detailed flow diagram of transesterification reaction is given in Figure 2.11. Alkali-catalysed transesterification is much faster than acid-catalyzed transesterification. The conversion rates are over 98% [2.37]. The other method of carrying out transesterification is by using low frequency ultrasound. C.Stavarache [2.38] carried out transesterification of the vegetable oil with short-chain alcohols in the presence base- catalyst by using low frequency ultrasound (28 and 40 kHz). He observed that by using ultra-sounds the reaction time is much shorter (10-40mins) than simple mechanical stirring with yield of 98 to 99%.

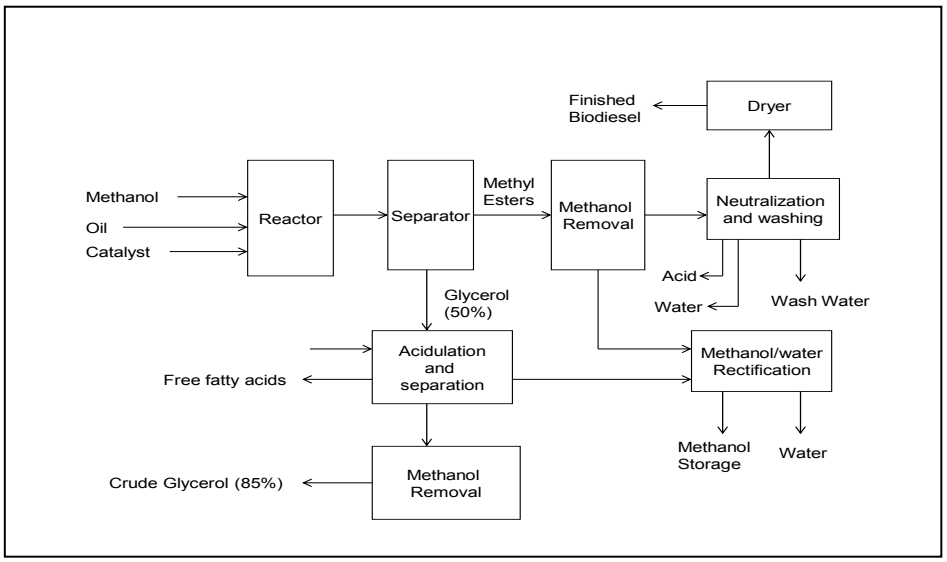

Figure 2.11: Flow diagram of Transesterification Process [2.37]

2.5.3 The properties of Bio diesel

The transesterification reaction reduces the molecular weight of triglycerides by 1/3rd. It also decreases viscosity by a factor of about 8 and marginally increases volatility. The cetane number of vegetable oil based biodiesel (46-52) is about the same that of diesel. The cetane number is a measure of ignition quality of the fuel and it should be as high as possible. They have lower volumetric heating values (by 10%) compared to diesel, but have higher flash point. The presence of 10 to 11% Oxygen by weight also boosts up their combustion performance [2.11]. Table 2.8 summarizes values for different properties of vegetable oil (Rapeseed oil), Biodiesel (Rapeseed oil methyl and ethyl ester, Soy ester) and low sulfur diesel.

Test	Low Sulfur Content Diesel	Rapeseed Methyl Ester (RME)	Neat Rapeseed Oil (RSO)	Rapeseed Ethyl Ester	Hydro-Genated Soy Ethyl Ester
Cetane Number	46	61.2	42.6	59.7	61
Flash Point, °C	67	180	270	185	144
Cloud Point, °C	-12	-2	-11	-2	7
Pour Point, °C	-16	-10	-31.7	-20	7
Boiling Point, °C	191	347	311	273	142
Viscosity, (cs) @ 40° C	2.98	5.65	47.6	6.1	5.78
SULFUR (%,wt)	0.036	0.012	0.022	0.012	0.023
Nitrogen, ppm	0	6	4	7	12
Heat of Combustion- BTUs/lb. (gross)	19,500	17.500	17,370	17,500	17,113
- KJ/Kg (gross)	46,420	40,600	40,400	40,510	39,800
Specific Gravity	0.8495	0.8802	0.906	0.876	0.872

Table 2.8: Properties of Biodiesel, vegetable oil and diesel [2.40]

2.5.4 Energy balance of Biodiesel

The main features affecting vehicle's fuel economy are type of engine, the efficiency of engine, and the fuel's volumetric energy content or heating value. The energy content of fuel is its heat of combustion; the heat released when known quantity of fuel is burned under specific conditions. Table 2.9 shows average net heating value for diesel, biodiesel and biodiesel blends. The energy content of Biodiesel is depend on feedstock used in manufacturing process and is less variable than that of diesel. The efficiency of diesel engines does not vary with type of fuel used. So the difference in fuel economy, or torque generated in engine is due to energy content of that individual fuel.

Fuel	Density g/cm^3	Net Heating Value Avg. Btu/gal	%Difference Vs. No. 2 Diesel Avg.
No.2 Diesel	0.850	129,500	
Biodiesel (B100)	0.880	118,296	8.65 %
B20 Blend (B20)	0.856*	127,259*	1.73 %*
B2 Blend (B2)	0.851*	129,276*	0.17 %*

* Calculated Values from those of No.2 Diesel and Biodiesel (B100)

Table 2.9: Average net heating value for Biodiesel and Diesel [2.47]

Table 2.9 shows that average net heating value of Biodiesel is almost 90% of that of diesel value. As Biodiesel has oxygen present in its structure, it has higher burning efficiency and better lubricity. This helps to yield similar effective energy content as that of diesel [2.54]. Table 2.10 shows the energy content in all products of transesterification processes for producing 1 ton of ester (for RME and REE) [2.54]. The U.S Department of Energy and U.S Department of Agriculture showed that total energy efficiency ratio (i.e. total fuel energy/total energy used in production, manufacture, transportation and distribution) for diesel fuel and biodiesel are 83.28% for diesel vs. 80.55% for biodiesel indicating both have similar energy efficiency [2.47]. It was also observed that Biodiesel is four times as efficient as diesel fuel in utilizing fossil energy.

Product	Energy content of RME (MJ/t)	Energy content of REE (MJ/t)
Ester	37,699.8	41,514.0
Glycerol	1659.8	1581.0
Straw	88,220.0	83,700.0
Cake	36,428.5	34,562.5

Table 2.10: Energy content of the products from ester production [2.54]

Biodiesel has positive energy balance in terms of the quantity of energy obtained from biodiesel compared to the quantity of energy used in its production. It also has possible energy saving effect of ca. 0.85 kg mineral oil saved per 1 kg of Bio diesel. Thus in RME fuel life cycle if rapeseed oil is used to produce RME, energy use in production is about 30% lower than that for diesel when fossil fuels are used to process and 60% lower if rape straw is used to produce RME [2.54].

2.5.5 Economic Feasibility of Biodiesel

The cost of biodiesel can be divided into: cost of raw material and cost of processing. The cost of raw material accounts for 60 to 80% of the total cost of biodiesel fuel [2.55], making them 2-3 times more expensive than hydrocarbon based diesel fuels. Reducing the raw material cost can be 1st step in reducing total production cost. The cost of edible vegetable oils is 2-3 times more than that of non-edible oils, used cooking/frying oils and other waste oils. Though now days used cooking or waste vegetable oil is used on larger scale, fluctuating cost of this type of oil makes biodiesel expensive. This indicates that use of edible vegetable oils increase the manufacturing cost of biodiesel. The continuous transesterification is another option to lower production cost. It is based on shorter reaction time and greater production capacity. The Biodiesel produced from waste cooking oil by using Acid-catalyzed process had lower total manufacturing cost than that of alkali-catalyzed process [2.55].

Another important factor is the yield in the biodiesel production process i.e. to what degree trans-esterificable triglycerides and free fatty acids are turned into high value methyl-esters. This should not be lower than 99.7%. Furthermore, recovery of high quality of glycerine and price fluctuations for glycerine can change the price of methyl ester. Figure 2.12 shows current and future biodiesel production cost for US and EU. The cost can be less in developing countries in future due to abundant availability of biomass feed stock. The cost can be reduced by applying improved technology but again it can vary as per the price of feed stock used [2.11].

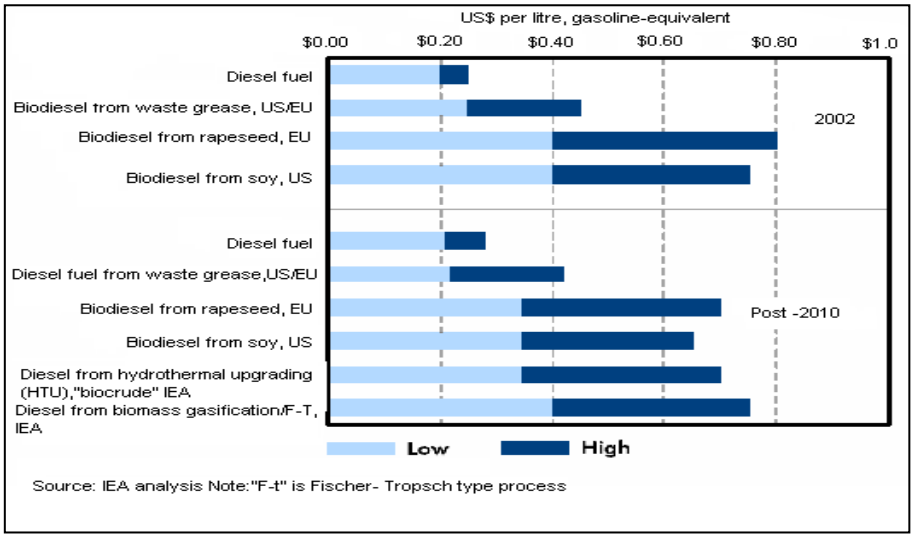

Figure 2.12: Cost ranges for current & future biodiesel production [2.11]

The another added economic advantage by achieving EU biofuels targets is 212,000 and 354,000 jobs that can be created in rural areas in 2010 & 2020 respectively.

2.5.6 Biodiesel as a fuel

Bio diesel from different sources/oils has been combusted and their performances have been studied in different types of engines and reactors. Table 2.9 summarizes work on combustion of biodiesel in different engines. The Cummins diesel test engines (with mechanical fuel injection/ electric fuel injection) were operated on 500ppm sulphur diesel fuel and blends of Biodiesel (5% and 20%) from vegetable oil, animal fat and used cooking oil in the Biobus project [2.24]. It was observed that Biodiesel blends reduced hydrocarbon emissions by 11 to 30%. However no improvement was observed for used cooking oil blends. The significant reduction in Particulate Matter (PM) emissions was observed, whereas CO_2 emissions were not affected by addition of esters to base diesel fuel. Carbon monoxide emissions were reduced by 9 to 31% [2.24].

R. McCormick et al [2.41] tested seven Biodiesel produced from different feedstocks and pure fatty acids in a heavy duty-truck engine using US heavy-duty federal test procedure. The emission of NOx was higher while that of PM was lower than certification diesel. They observed highly saturated fuels, those with no double bond in fatty acid chain, appear to have the lowest NOx. Also longer chain esters had lower NOx emissions.

When combustion of biodiesel produced from hazel nut soap stock /waste sunflower oil mixture was carried out in diesel engine, reduction in CO emission was obtained but CO_2 emission was high in blends of diesel and biodiesel [2.42]. There was significant reduction in SO_2 emissions and an increase in NOx emission was observed. Mahua oil (Madhuca Indica seed oil) methyl ester was tested and it was observed that 11% reduction in smoke number produced compared with diesel. CO emission was reduced by 30% compared to diesel and reduction of 35% in HC emission was observed. Even 4% reduction in NOx emission was observed [2.43].

Author	Fuel Used	Experimental Set-up/Engine	Experimental Analyses
G.Knothe, C.Sharp and T.W.Ryan III (2006)	Methyl Laurate, neat Methyl Palmitate, technical grade Methyl Oleate, commercial Biodiesel, Hexadecane , low sulfur petrodiesel	Heavy duty 6 cylinder 14L Diesel engine	Exhaust (NOx, PM, CO and HC) emission
V.Makareviciene, P.Janulis, E.Sendezikiene (2006)	Rapeseed oil Methyl Ester, Diesel, Ethanol	D1 Cylinder AVL Test engine Type 502.019	Effect of fuel oxygen content on exhaust emissions
A.Munack and others (2006)	Shell Middle Distillate, Premium Diesel Fuel, Fossil Diesel Fuel, Rapeseed oil methyl ester	Mercedez-Benz DM 906 LA	HC, CO, NOx and particle emissions
A.K.Bhatnagar, etc. (2006)	Methyl esters of non-edible oils	High Frequency Reciprocating rig	Effect of biodiesel on lubrication , properties of diesel
A.K.Agarwal (2006)	Alcohol and Biodiesel	Combustion engine(SI and CI engines)	Review – Biofuels as combustion engine fuels
S.Fernando, C.Hall, S.Jha (2006)	Biodiesel	Diesel Engines	NOx emission Reduction
Md.Narun.Nabi and others (2006)	Diesel, Diesel-Neem oil Methyl Ester blends	Single cylinder DI engine	CO_2 , NOx and smoke emission
K.A.Subramanian, S.K.Singal, M.Saxena et al. (2005)	Ethanol, Soy Biodiesel-Diesel Blends	Automotive Diesel Engines	Review about policy and planning about utilization of Biofuels
R.Subramanian, L.D.Schmidt (2005)	Biodiesel from Soy oil	Autothermal reactors	Renewable olefin formation
G.Labeckas, S.Slavinskas, et al. (2005)	RME, RME with diesel blends (5 to 35%)	Direct Injection Diesel Engine	Emission Composition Changes, Smoke Opacity

F.Karaosmanoglu and M.Cetinkaya (2005)	Used cooking oil, Originated Biodiesel and diesel blends	Generators, 9-KW 3LD 510 coded diesel engine	Engine and Generator peformance
S.WinLee, T.Herage, B.Young (2004)	Blend of 20% Soybean Methyl Ester and No.2 fuel	Residential-scale hot water boiler	PM, SO_2 and green house gas emission
N.Usta and et. al (2004)	Diesel, Hazelnut Soapstock/ waster Sunflower oil blends.	Turbocharged Indirect injection Diesel Engine	Effect of biodiesel on performance and emission
D.L.Lance and J.Anderson (2004)	Blend of 5% RME with Ultra low sulfur diesel	1.9 L D.I engine 1.5L IDI engine	Emission Performance
N.Vedaraman and et.(2004)	Mahua oil Methyl Ester	DI Compression ignition diesel engine	Performance and emissions of CO, HC, NOx
R.Quigley and H.Barbour (2004)	Rapeseed oil methyl ester (RME)	Standard XUD-9 test	Effect of RME on injector fouling and corrosion
M.Souligny, L.Graham, G.Rideout, and P.Hosatte (2004)	Blends of sulphur diesel fuel and Biodiesel (Blend of originates from vegetable oil, animal fat and used cooking oil, 5and 20% Blend	Four stroke, 250HP Cummins Diesel Engine	All exhaust emissions
H.Raheman, A.G.Phadatare (2004)	20 to 80% Blends of diesel and Karanja Methyl Ester	Single cylinder DI water cooled diesel engine	CO_2 , NOx emission, smoke density, Engine performance
C. Morin et.al (2004)	Rapeseed oil Methyl Ester and Sunflower oil Methyl Ester	Jet-Stirred Reactor	Oxidation Results
O.M.I.Nwafor (2003)	Rapeseed oil Methyl Ester and blends with diesel	Petter model AC/single cylinder energy cell diesel engine	CO_2 and Hydrocarbon emission
G.Knothe, A.C.Matheaus and T.W.Ryan III (2003)	Straight-chain and branched C1-C4 Esters and 2-ethylhexyl esters	Ignition quality tester (IQT)	Determination of cetane numbers
M.Haas and etc.(2001)	Biodiesel from Soybean Soapstock	Heavy Duty DDC series 60 Engine	Engine performance CO, NOx, HC emission

S.Sidhu, J.Graham and R.Striebich (2001)	CNG, DME, Biodiesel and Diesel	A single pulse reflected shock tube	Particle formation analysis
R,McCormick, M.Graboski et al (2001)	Fatty acid methyl and ethyl esters from real-world feedstock	Heavy-duty truck engine	Effect of structure of biodiesel on PM and Nox emission
E.M.Fisher, W.J.Pitz, H.J.Curran, C.K.Westbrook (2000)	Methyl Butanoate, Methyl Formate	Static Reactor	Chemical kinetic mechanism
O.Schroder, J.Krahl et. al (1999)	Rapeseed oil Methyl Ester	Farymann engine, Fendt tractors	Environmental and Health Effects
F.Billaud and D.Archambault (1999)	Methyl Oleate	Tubular Flow Reactor	Experimental and Modeling study of Pyrolysis
J.R.Pederson, J.O.Olsson , A.Ingemarsson (1999)	Rapeseed oil Methyl Ester , Rapeseed oil , Diesel Fuel	Thermo stated Stainless steel tube reactor	Oxidation Results GC-MS Analysis
H.Prankl and M.Worgetter, J.Rathbauer (1999)	RME, SME and Camelina oil methyl ester with high iodine number	Single cylinder, DI, 1D41 Z engine	Analysis of chemical and physical properties of biodiesel and effect on engine parts
M.Graboski, R.McCormick (1998)	Vegetable oil, Biodiesel	Diesel engine	Engine performance and emission
C.Peterson and T.Hustrulid (1998)	Rapeseed oil Methyl and Ethyl ester	----	Carbon Cycle
X.Montagne (1996)	Rapeseed oil Methyl Ester and diesel blend	Euro2 and Euro1 620-45 engine, MIDR 602-2 engine, Truck and Car engine	Effect of RME addition on engine emissions
J.Krahl and others (1996)	Rapeseed oil Methyl Ester, Rapeseed oil, Diesel Fuel	Diesel Engine Vehicle	Exhaust emissions(HC, CO, Nox,) Environmental Effects
L.G.Schumacher et.al (1996)	10 to 40% Soyabean Methyl Ester- diesel blend	6V92TA Diesel engine	Exhaust emission

C.Peterson and others (1996)	Rapeseed oil Ethyl Ester	Dodge 2500 turbo charged diesel vehicle	Engine emissions, vehicle performance
O.M.I.Nwafor and G.Rice (1995)	Rapeseed oil Methyl Ester	Petter model AC/single cylinder energy cell diesel engine	Engine Performance and HC emission
M.Z.M.Yosof (1987)	Palm oil Mehtyl Ester	Diesel Engine	Performance of ester

Table 2.11: Summary of combustion work done using Biodiesel

Md.N.Nabi et al [2.44] combusted Neem oil methyl ester in a four stroke naturally aspirated (NA) direct injection (DI) diesel engine. Nabi observed the reduction in smoke by 15 % and carbon monoxide emission was reduced by 4%. NOx emission was increased by 5%. However the concentration of CO_2, H_2O was higher for Neem oil methyl ester compared to diesel. Karanja Methyl Ester (Bio diesel B100) and its blends (B20, B40, B60 and B80) were tested in single cylinder, four stroke DI and water cooled diesel engine. It was observed that minimum and maximum CO concentration was produced with values of 0.004 and 0.016% resulting in reduction of 94% and 73%, respectively, compared to diesel. NOx emission concentration varied between 4 and 12 ppm for B20 and B100 as compared to 12 and 13 ppm for diesel. On an average 26% reduction in NOx was obtained for Biodiesel and its blends as compared to diesel. Similar trends for smoke density were observed [2.45].

S.Win Lee et al [2.46] combusted blend of 20% Soybean methyl ester with No.2 diesel fuel in a residential-scale hot water boiler. He observed that SO_2 emission was lower than No.2 diesel fuel by 19.7+/- 2.5%, whereas NOx emissions were similar. PM emissions were lower by 15.7+/- 7.5 % than No.2 fuel and particulate bounded sulphates were lowered by 14.1+/- 6.1%. U.S Department of Energy and Agriculture published results of study on Biodiesel, Petroleum Diesel lifecycles and effect of Biodiesel on tailpipe emissions [2.47]. Table 2.12 shows the effect of Biodiesel on tailpipe emissions. The study determined that carbon dioxide life cycle emissions were 78% lower than overall CO_2 emissions from diesel. The emissions for CO were 35% lower than overall carbon monoxide from diesel. The PM emissions were reduced by 32% compared to that from diesel where as sulphur oxides emissions were found 8% lower than diesel. The

NOx emissions were greater than 13% diesel and for methane they were lower by 3%.

Emission in PPM	Diesel fuel Baseline	20% Biodiesel blend	100% Neat Biodiesel
Carbon Dioxide	633.28	534.10	136.45
Carbon Monoxide	1.2	1.089	0.6452
Hydrocarbons	0.1	0.09265	0.06327
Particulate Matter (PM100)	0.08	0.0691	0.02554
Nitrogen Oxides (NO_2)	4.8	4.885	5.227

Table 2.12: Effect of Biodiesel on Tailpipe Emissions [2.47]

It can be seen from table 2.12 and biodiesel combustion work explained above that biodiesel reduces hydrocarbon and particulate matter emissions irrespective of feed stock material. NO_x emission also found to be higher for biodiesel compared to that from diesel. CO emission is also reduced in biodiesel combustion work; however there are discrepancies in CO emission results for biodiesel-diesel blends. As CO_2 emission results are varying especially for biodiesel blends, no concrete conclusion can be made for CO_2 emission. Higher CO_2 formation is an indication of a complete combustion. Overall biodiesel as a fuel has a positive impact on intermediate's emission. However biodiesel combustion work only talks about increase or decrease in combustion products and pollutant emission. It does not explain intermediate pollutant formation routes, effect of Fuel/Air ratio on pollutant formation.

2.5.7 RME as diesel engine fuel:

Rapeseed oil methyl ester (RME) is produced from transesterification of rapeseed oil with methanol. RME is commercially available biodiesel in Europe. The formula of RMR is $C_{18}H_{34}O_2$ with unsaturation at C_9 position. Figure 2.13 shows typical structure of Rapeseed oil methyl ester (RME).

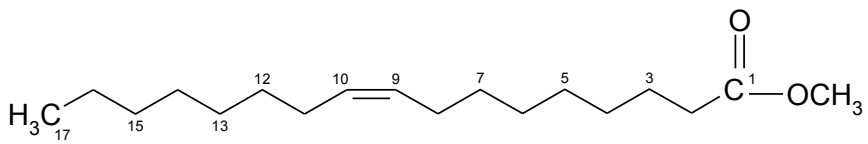

Figure 2.13: The structure of Rapeseed oil methyl ester (RME)

As Rapeseed is the 3rd most important source of vegetable oil in the world, Biodiesel (Rapeseed Methyl/Ethyl Ester) produced from Rapeseed oil is combusted and its performance is studied in different types of diesel engines and reactors. RME can be used directly in conventional diesel engine or in blends with diesel fuel. Though table 2.9 in section 2.5.6 summarizes work on combustion of biodiesel in different experimental set up and engines, this section will summarize combustion work of RME as a fuel.

C.Morin [2.48] studied the oxidation of Rapeseed oil methyl ester (RME) in a Jet Stirred Reactor at pressure of 0.1 and 1 MPa. She compared vegetable oil methyl ester (VOME) oxidation results with diesel fuel. Results showed that maximum mole fractions of oxygenated compounds were lower for VOME than diesel fuel and maximum CO mole fraction for diesel fuel was twice as high. Further, that the aldehydes formation was favoured by presence of unsaturated chains in VOME and acrolein was favoured by presence of glycerol & glycerides [2.48]. It was observed that the nature of the main species was not changed with increasing pressure but their level of formation in terms of concentration in ppm was decreased. C.Morin [2.48] observed that the vegetable oil methyl esters were degraded and oxidised like n-paraffin solvents and synthetic diesel fuel.

G.Labeckas et al. [2.49] operated a four stroke, four cylinders, direct injection naturally aspirated diesel engine on neat Rapeseed oil methyl ester (RME) and blends with diesel fuel. It was observed that NOx level increased proportionally with mass % of oxygen in biofuels and engine speed. The CO emission was lowered by up to 51.6% for all loads and speed. The CO_2 emissions were slightly higher for B20/B35 blends and neat RME. The emission for unburned hydrocarbons (HC) for all fuels was low ranging 5-21 ppm. Peterson et al. [2.50] ran a 1994 Dodge 2500 turbocharged and intercooled diesel pick up truck with 100% Rapeseed oil Ethyl Ester. It was driven from Idaho, Moscow to different cities in America and then back to Moscow covering distance of 14,069 km (8742 miles). The fuel used for this trip was processed at University of Idaho and was carried on-board. The emission test with vehicle showed reduction in HC (55.6%), CO (50.6%) and NOx (11.8%) and increase in CO_2 (1.1%) and PM (10.3%). Labeckas [2.49] observed that the vehicle performance was extremely good without any problem.

The emissions from a bus fuelled with RME rich fuel (100%) were studied for two cycles; 13-mode cycle (ECE 49) and AQA F21 urban cycle. The emission values for these cycles with Diesel and RME as fuel are given in Table 2.13 and Table 2.14. It was observed that particulates emission; CO & HC emission was lower than diesel fuel for both cycles [2.14].

Regulated emission (g/kWh)	Diesel fuel	100% RME
CO	2.5	1.9
HC	0.6	0.5
NOx	17.9	19.6
Particulates	0.8	0.5

Table 2.13: 13-mode cycle (ECE 49) [2.14]

Regulated emission (g/kWh)	Diesel fuel	100% RME
CO	5.9	5.3
HC	2.2	1.9
NOx	21.8	20.4
Particulates	1.2	1.1

Table 2.14: AQA F21 urban cycle [2.14]

Nwafor [2.51] [2.52] tested RME and its blends in diesel engine. He observed a significant reduction in Hydrocarbon (HC) emissions for RME and its blends. The CO emissions were similar to that from diesel fuel, where as CO_2 emissions were slightly higher for RME and its blends. Hohl [2.53] conducted experiments using rapeseed methyl ester and cooking oil. It was observed that the performance, the emissions, oil changing intervals, engine wear and knocking characteristics remained unchanged when compared with diesel fuel. The exhaust emissions were also lower than that of diesel fuel.

RME combustion results are in agreement with overall biodiesel performance in diesel engine. RME reduces intermediate hydrocarbon, particulate matter (PM) and CO emissions similar to other vegetable oil based biodiesel combustion performance. RME also has positive impact on pollutant emission and CO_2 production. The effect of pressure, temperature and Fuel/Air ratio or fuel conditions on RME combustion needs to be evaluated in detail.

2.5.8 Advantages & Disadvantages of Bio diesel as fuel

The work done on the application of biodiesel as fuel in diesel engine is mentioned in detailed in previous section. This section summarises the advantages and disadvantages of biodiesel as fuel when compared to diesel fuel.

Advantages [2.11] [2.12] [2.37]

- It is a renewable, biodegradable, non toxic fuel coming from agriculture crops and their feed stocks. It can help to reduce oil dependence.
- It can be used in existing engines and fuel injection equipment with little impact on operating performance.
- Bio diesel has lower pour point temperatures than petroleum fuels which, reduces cold flow problems due to fuel gelling.
- As RME has lower ratio (6.5) of carbon to hydrogen mass proportion than that of diesel (6.9), it leads to more complete combustion and higher engine performance.
- It improves engine lubricity, also its solvent properties can be used to keep engine clean and well running. 1% of biodiesel can provide up to 65% increase in lubricity.
- It reduces energy use in extracting, transporting and refining crude oil.
- Biodiesel reduces levels of CO CO_2, HC & particulates. It also reduces PAH, unburned hydrocarbons and smoke capacity. Also it is sulfurless fuel.
- Biodiesel reduces overall CO_2 emissions by 78% compared to that from petroleum based fuels.
- Shorter ignition delays, longer combustion duration resulting in minimum carbon deposition on injector nozzles.

Disadvantages

- Production cost of Bio diesel is very high compared to diesel fuel.
- NOx emission is not reduced, infact it is bit more than convention diesel.
- The biodiesel fuel can create problems in winter conditions in diesel engines.
- Bio diesel is less useful at lower temperature because of higher viscosity compare to conventional diesel.
- The increased usage of fertilisers and pesticides to increase oil seed production for use in biodiesel production can create serious environmental impact.
- The feedstock production for biodiesel has to compete with other applications such as crop production for food and electricity generation.
- It is not compatible with certain types of elastomer and natural rubber compounds and can degrade them.
- A high content of unsaturated acids in the esters increases the risk of polymerization in engine oil.

The literature survey on diesel engine combustion showed that vegetable oil as a fuel increases intermediate hydrocarbons, carbon monoxide, particulate matter and pollutants emissions and form engine deposits. Though it reduces NO_x, CO_2 emission brake power, it is not suitable as fuel for diesel engine combustion. Biodiesel as a fuel reduces NO_x, CO, hydrocarbon and particulate matter emissions irrespective of feed stock material. This indicated that biodiesel as a fuel has a positive impact on intermediate's emission. However biodiesel combustion work only talks about increase or decrease in concentration combustion products and pollutant emission. It does not explain intermediate pollutant formation routes, effect of temperature, pressure Fuel/Air ratio on pollutant formation and combustion performance. Effect of unsaturation (double and triple bond), carboxyl and ester group present in vegetable oil and biodiesel structure on fuel combustion performance is also not explained in diesel engine combustion work. So a detailed chemical kinetic model has to be developed to understand combustion chemistry of biodiesel and vegetable oil. Also experimental database has to be generated for biodiesel combustion, which will be used to evaluate chemical kinetic model.

References

2.1 Plouchart.G, 2005, *Energy Consumption in the Transport Sector*, Panorama Technical Reports , Panorama-2005 http://www.ifp.com/information-publications/publications

2.2 Meeting the Energy Challenge, A White Paper on Energy, May 2007, http://www.berr.gov.uk/files/file39387.pdf

2.3 UK Energy in Brief, July 2006, http://www.berr.gov.uk/files/file32387.pdf

2.4 UK Energy and CO2 Emission Projections, July 2006, http://www.berr.gov.uk/files/file31861.pdf

2.5 http://en.wikipedia.org/wiki/European_emission_standards

2.6 European Biodiesel Board, EBB Press Release: 2006, 2007 production and capacity statistics

2.7 UK Report to European Commission on Biofuels, 2006, http://www.dft.gov.uk/pgr/roads/environment/

2.8 Bockey.D, 2006, *Current situation and prospects for biodiesel and vegetable oils as fuels: From niche products to market players*, Union Zur Forderung Von (www.ufop.de)

2.9 Agarwal.A.K, 2007, *Biofuels (alcohols and biodiesel) applications as fuels for internal combustion engines*, Progress in Energy and Combustion Science, 33, 233-271

2.10 Demirbas.A, 2006, *Progress and recent trends in biofuels*, Progress in Energy and Combustion Science, 33, Issue 1, 1-18

2.11 Biofuels for Transport *An International Perspective 2004*, IEA Publications

2.12 Barnwal.B.K, Sharma.M.P, 2004, *Prospects of Biodiesel production from vegetable oil in India*, Renewable and Sustainable Energy Reviews, 9, 4, 363-378

2.13 Srivastava.A, Ram Prasad, 2000, *Triglycerides-based diesel fuels*, Renewable and Sustainable Energy Reviews, 4,111-113

2.14 Guibet.J-C, Faure-Birchem.E, 1999, *Fuels and Engines: Technology, Energy, Environment*, 2, Technip Editions

2.15 Ramadhas.A.S, Jayaraj.D, Maraleedharan.C, 2004, *Use of Vegetable oils as I.C engine fuels-A Review*, Renewable Energy, 29, 727-742

2.16 www.svlele.com/rapeseed.html

2.17 Pangavane.DR, Kushare.PB, 2002, *Bio-diesel need of India*, Proceedings of Recent Trends in Automotive Fuels, Nagpur, India

2.18 Jacobus.MJ, Geyer.SM, 1983, *Single cylinder diesel engine study on four vegetable oils*, SAE Paper no: 831783

2.19 Senthil Kumar.M, Ramesh.A, Nagalingam.B, 2001, *Experimental investigation on Jatropha oil-Methanol duel fuel engines*, SAE Paper No: 2001-01-0153

2.20 Abbas.MK, Davis.IL, 1990, *The composition of organic fraction of particulate emissions of a diesel engine operated on vegetable oil*, SAE Paper No: 901563

2.21 Yasufumi.Y, Masayuki.O and Hiroya.T, 1999, *Reduction of NOx, smoke, B S F C in a diesel fueled bio-diesel emulsion used frying oil*, SAE Paper No: 1999-01-3598

2.22 Yu.CW, Bari.S, Ameen.A, 2002, *A comparison of combustion characteristics of waste cooking oils as fuels in a D.I engines*, I.Mech.E, Part E, 216D3

2.23 Silvico.CA, Carlos.R, Marious.VG, Leonarodos SR, Guilherme.F, 2002, *Performance of diesel generator fueled with palm oil*, Journal of Fuels, 81, 2097-102

2.24 Souligny.M, Graham.L, Rideout.G, Hosatte.P, 2004, *Heavy-Duty Diesel Engine Performance and Comparative Emission Measurements for Different Biodiesel Blends used in the Montreal BIOBUS Project* , Society of Automotive Engineers International, 2004-01-1861,1-14

2.25 Samaga.BS, 1983, *Vegetable oil as alternative fuels for I.C Engines*, 8th National Conference on I.C Engines, Trivandrum, India

2.26 Barsic.NJ, Humke.H, 1981, *Performance and emission characteristics of a naturally aspirated diesel engine with vegetable oil*, SAE Paper No: 810262

2.27 Nishi.K, Matsu.K.K and Tanaka.J, 2004, *Potential of Rapeseed Oil as Diesel Engine Fuel*, SAE Paper No: 2004-01-1858

2.28 Montagne.X, 1996, *Introduction of Rapeseed Methyl Ester in Diesel Fuel-The French National Program*, SAE Technical Paper Series Paper no: 962065

2.29 Hemmerlein.N, Korte.V and Richter.H, 1991, *Performance, exhaust emission and durability of modern diesel engines running on rapeseed oil*, SAE Paper no: 910848

2.30 Todashi.Y, 1984, *Low carbon build up, low smoke and efficient diesel operation with vegetable oil by conversation to monoesters and blending with diesel oil or alcohols*, SAE Paper no:841161

2.31 Pedersen.R.J, Ingemarsson.A and Olsson.O.J, 1999, *Oxidation of Rapeseed oil, Rapeseed Methyl Ester (RME) and diesel fuel studied with GC/MS*, Chemosphere, 38, 11, 2467-2474

2.32 Lance.D.L and Anderson.J.D, 2004, *Emissions Performance of Pure Vegetable Oil in Two European, Light Duty Vehicles*, SAEngineers Paper No: 2005-01-1881

2.33 Alonso Jose.San.J, Lopez.Sastre.A.J, Romero-Avila.C, Lopez.Romero.J.E, 2006, *Combustion of rapeseed oil and diesel oil mixtures for use in the production of heat energy*, Fuel Processing Technology, 87, 97-102

2.34 Bakhshi.N.Narendra , Katikaneni.R.P.Sai and Idem.O Raphael, 1996, *Thermal cracking of Canola oil: Reaction products in the presence and absence of Steam*, Energy & Fuels, 10, 1150-1162

2.35 Altn.R, Cetinkaya.S, Yucesu.H.S, 2001, *The potential of using vegetable oil fuels as fuel for diesel engines*, Energy Conversion and Management, 42,529-538.

2.36 http://www.biodieselfillingstations.co.uk/approvals.htm

2.37 Gerpen.Jon.Van, 2005, *Biodiesel Processing and Production*, Fuel Processing Technology, 86, Issue10, 1097-1107

2.38 Stavarache.C, Vinatoru.M, Nishimura.R, Maeda.Y, 2005, *Fatty acids methyl esters from vegetable oil by means of ultrasonic energy*, Ultrasonic Sonochemistry, 12, 367-372

2.39 Saka.S and Kusdiana.D, 2001, *Kinetics of transesterification in rapeseed oil to biodiesel fuel as treated in supercritical methanol*, Fuel, 80, 693-698

2.40 www.biodiesel.org

2.41 McCormick.R.L, Graboski.M.S, Allman.T.L and Herring.A.M, 2001, *impact of Biodiesel Source Material and Chemical Structure on Emissions of Criteria Pollutants from a Heavy-Duty Engine*, Enviorn.Sci.Technol, 35, 1742-1747

2.42 Usta.N, Ozturk.E, Can.O, Conkur.E.S, Nas.S, Con.A.H, Can.A.C, Topcu.M, 2004, *Combustion of Biodiesel fuel produced from Hazelnut Soapstock/waster Sunflower oil mixture in a Diesel Engine*, Energy Conversion and Management, 46, 741-755

2.43 Pushan.S, Vedaraman.N, Boppana.V.B.Ram, Sankarnarayanan.G, Jeychandran.K, 2004, *Mahua Oil (Madhuca Indica Seed Oil) Methyl Ester as Biodiesel- preparation and emission characteristics*, Biomass and Bio Energy, 4, 77-86

2.44 Nabi.Md.N, Akhter.Md.S, Shahadat.Mhia.Md.Z, 2006, *Improvement of engine emissions with conventional diesel fuel and diesel-biodiesel blends*, Bioresource Technology, 97, 372-378

2.45 Raheman.H, Phadatare.A.G, 2004, *Diesel engine emissions and performance from blends of Karanja Methyl Ester and Diesel*, Biomass and Bio Energy, 27, 393-397

2.46 Win.Lee.S, Herge.T, Young.B, 2004, *Emission reduction potential from the combustion of Soy Methyl Ester fuel blended with petroleum distillate fuel*, 83, 1607-1613

2.47 Sheehan. J and others, 1998, *An Overview of Biodiesel and Petroleum Diesel Life Cycles, National Renewable Energy Laboratory*, U.S. Department of Energy and U.S. Department of Agriculture

2.48 Morin.C, Chauveau.C, Dagaut.P, Gokalp.I and Cathonnet.M, 2004, *Vaporization & Oxidation of liquid fuel droplets at high temperature and high pressure: Application to n-alkanes and vegetable oil methyl esters*, Combustion Science and Technology, 176, 499-529

2.49 Labeckas.G, Slavinskas.S, 2006, *The effect of rapeseed oil methyl ester on direct injection Diesel engine performance and exhaust emissions*, Energy Conversion and Management, 47, Issue 13-14, 1954-1967

2.50 Peterson.C.L, Reece.L.D, Thompson.C.J, Beck.M.S and Chase.C, 1996, *Ethyl ester of Rapeseed used as a biodiesel fuel- a case study*, Biomass and Bioenergy, 10, 331-336

2.51 Nwafor.O.M.I, 2004, *Emission characteristics of diesel engine operating on rapeseed methyl ester*, Renewable Energy, 29, 119-129

2.52 Nwafor.O.M.I, Rice.G, 1995, *Performance of Rapeseed Methyl Ester in diesel engine*, Renewable Energy, 6, No3, 335-342

2.53 Hohl.G.H, 1995, *Rape oil methyl ester and used cooking oil methyl ester as alternative fuels*, SAE 952755

2.54 Janulis.P, 2004, *Reduction of energy consumption in biodiesel fuel life cycle*, Renewable Energy, 29, 861-871

2.55 Hanna.A.M, Fangrui.Ma, 1999, *Biodiesel production: a review*, Bioresource Technology, 70, 1-15

CHAPTER 3

EXPERIMENTAL SET- UP AND ANALYTICAL TECHNIQUES

Chapter 2 described the current pollution and energy scenario, need of alternative fuels, 1st and 2nd generation biofuels, vegetable oils as fuels and its limitations, biodiesel, need of biodiesel, work done on combustion of biodiesel, its environmental effects and economics. The literature survey showed that vegetable oil as a fuel increases emission of intermediate compounds and pollutants. Its higher viscosity and lower volatility makes it unsuitable for diesel engine combustion. Biodiesel as a fuel reduces CO, intermediate hydrocarbon and particulate matter emissions irrespective of feed stock material, indicating that it has a positive impact on diesel engine combustion. However diesel engine combustion work does not explain intermediate pollutant formation routes, effect of temperature, pressure, Fuel/Air ratio, unsaturation (double & triple bond), and ester group present in biodiesel structure on pollutant formation and combustion performance. So a detailed chemical kinetic model has to be developed to understand combustion chemistry of biodiesel i.e. RME in this research work. To validate chemical kinetic model an experimental database has to be generated for biodiesel (RME) combustion. This chapter will describe the experimental set-up used for combustion of RME, the composition of RME, experimental conditions and calculations. It will also describe different analytical techniques used for the analysis of experimental results. The oxidation experiments on RME were carried out at 1 bar and 10 bar in a Jet Stirred Reactor.

3.1 Jet Stirred Reactor (JSR)

The Jet Stirred Reactor used here is based on guide lines established by David and others [3.5]. This continuous flow stirred tank reactor (FSTR) was first conceived for residence time around 1 s [3.1] [3.5]. Such reactors have been built are commonly used to study combustion reactions of hydrocarbons [3.1]

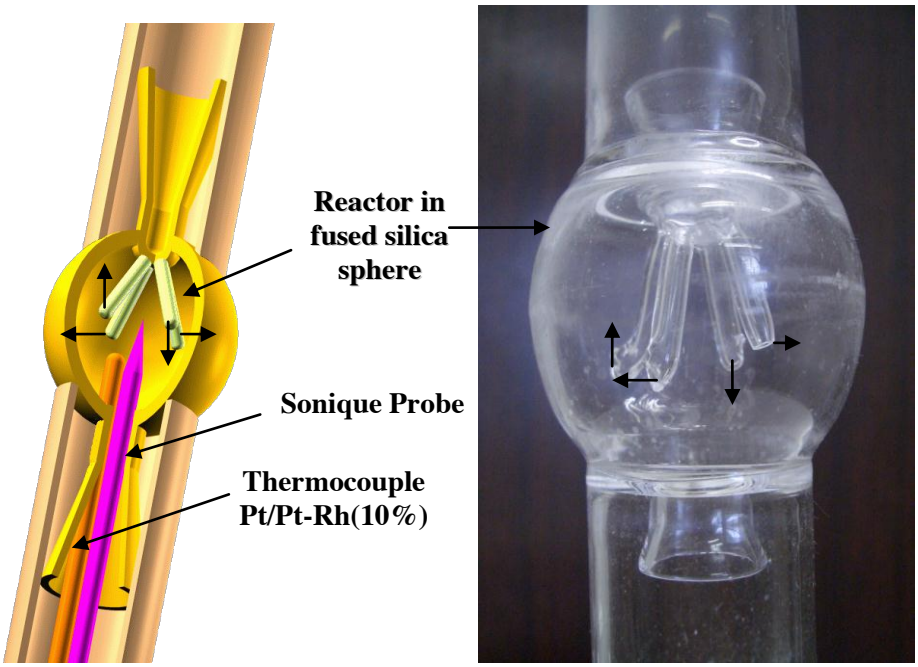

Figure 3.1: Jet Stirred Reactor (Sphere and nozzles)

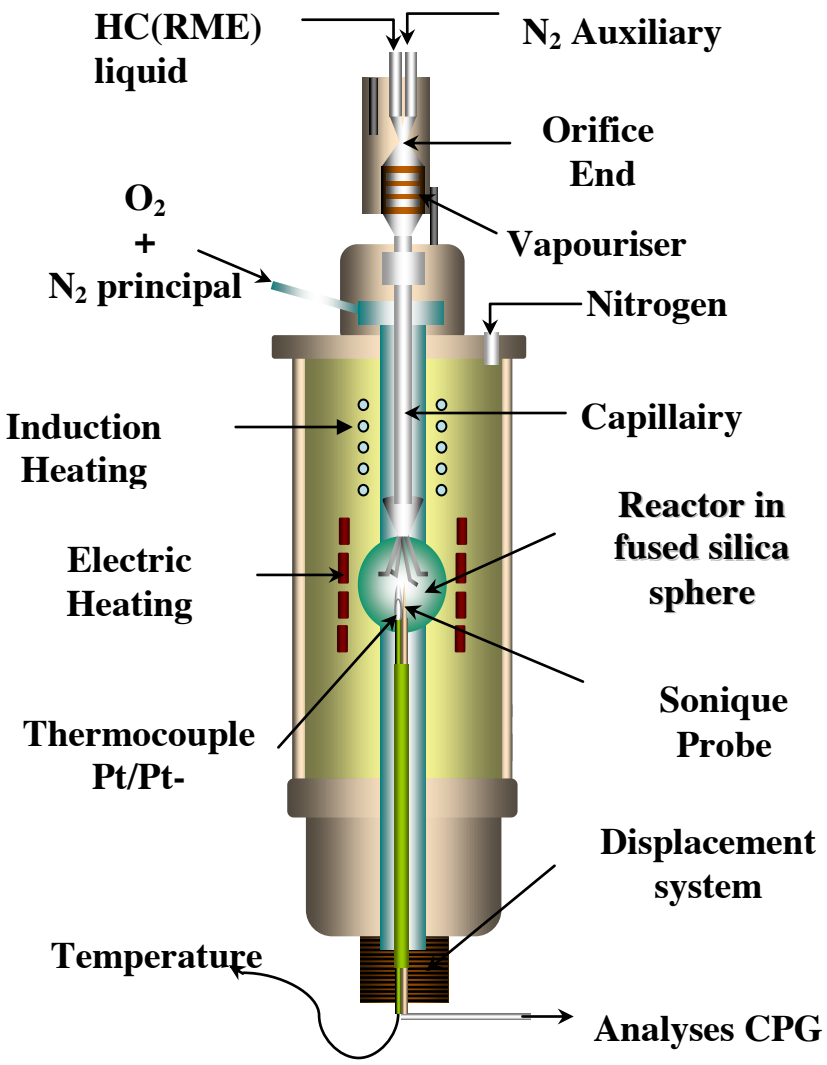

Figure 3.2: Schematic view of Jet Stirred Reactor

The Jet Stirred Reactor set up consists of a small sphere of 40 mm diameter (30.5cm^3) (Fig 3.1) made of fused silica to minimize wall catalytic reactions, equipped with four nozzles of 1 mm internal diameter for the admission of gases. The nozzle's outlets are located in the equatorial place of the spherical reactor allowing perfect stirring and recycling of the gases within the reactor [3.1]. The reactor is surrounded by two independent insulating heating wires, located inside a stainless steel pressure resistant jacket filled with insulating material. Spatial homogeneity inside the reactor prevails when it is operated at steady state. In order to maintain the reactor at desired working temperature, it is used to place inside a regulated oven, typically maintained at 1.5 kW. The temperature of reactor wall and of the gases upstream are measured by insulated thermocouples (Thermocoax) and regulated by electronic controllers. The thermal homogeneity and temperature of the gases inside the reactor is measured by a thermocouple

(0.1mm, Pt-Pt/Rh 10% inside a thin-wall fused silica tube) (measurement gradients <2 K/cm) fixed along the vertical axis of the reactor. The reactor has a low-pressure sonic fused-silica microprobe to collect reaction samples for analysis. The pressure is kept constant in time with a pressure regulator installed on the exit flow line. Working at high pressure (up to 40 bars) is possible by means of electronically controlled pressure balancing inside and outside the reactor [3.2] [3.3].

3.2 Experimental Procedure

As explained in introduction of this chapter, aim of this chapter is to carry out RME oxidation at atmospheric (1bar) & high pressure (10 to 40 bar) in JSR and generate experimental database. JSR set up is explained in previous section. This section describes the detailed experimental procedure to carry out RME oxidation in JSR. Figure 3.3 shows the schematic diagram of complete experimental set up including JSR, offline and online gas analyzers.

The fuel (RME) was diluted with the flow of nitrogen (100l/h), (<50ppm of O_2; <1000ppm of Ar; <5ppm of H_2), and mixed with oxygen-nitrogen flow at the entrance of the reactor. The mixing time was around $1/70^{th}$ of residence time inside the reactor. The residence time of the mixture in injector was 300 times less than the mean residence time in the reactor to prevent pyrolysis or oxidation of the mixture in injectors. The pressure and residence time inside the jet stirred reactor were kept constant. High purity oxygen (99.995% pure) was used in these experiments [3.4]. A high degree of dilution (0.05% of fuel mole) was used to reduce temperature gradients, thus making operation at steady state feasible. The dilution was achieved by using the flow of auxiliary nitrogen (N_2). Due to this dilution flames do not appear in jet stirred reactor.

A pump (Shimatzu LC10 AD-VP) was used to deliver the fuel (RME) to an atomizer-vaporizer assembly maintained at 290°C and located at top of JSR. A fuel (Rapeseed oil Methyl Ester) was sonically degassed before use.The liquid fuel (RME) was vaporised in this atomizer-vaporizer before injecting into the reactor. All the gases were delivered by mass flow controller and pre-heated to reduce the temperature gradient in the JSR. The gases were heated by means of an electrically insulated resistor (Thermocoax) surrounding the Jet stirred reactor.

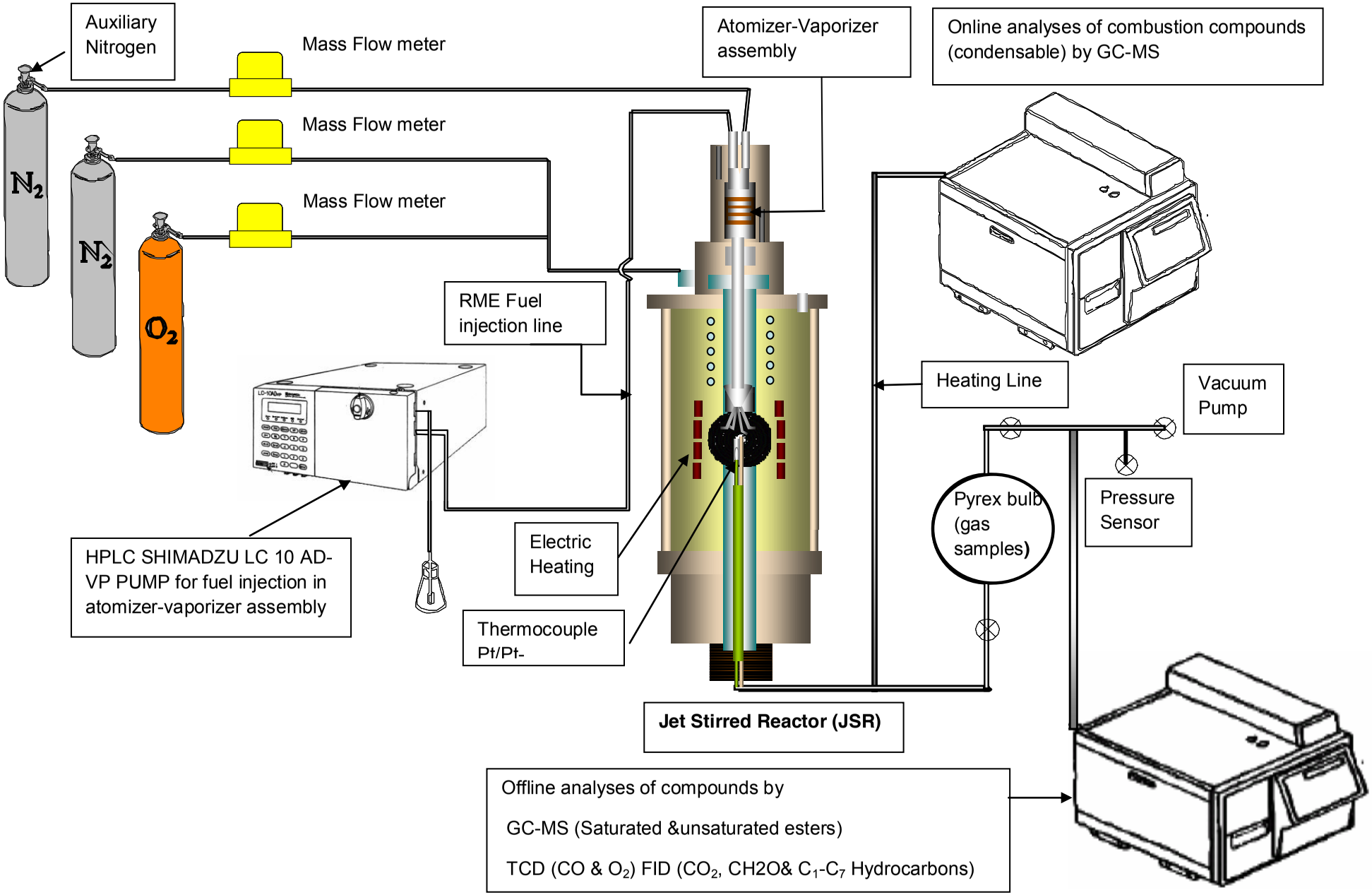

Figure 3.3: Schematic diagram of JSR and experimental set up

The reactants flowed continually into the reactor and the temperature of the gases inside the JSR was varied stepwise. The temperature at the top and bottom of reactor was measured continuously by thermocouple moving axially. The 1st gas sample was collected in 1 lit pyrex bulb for off-line analysis, 1.5hrs after RME was injected in the reactor. The reacting mixtures samples were taken on regular intervals till oxidation of RME was completed. The gas sample was also analyzed on-line by using GC-MS

3.3 The composition of Rapeseed oil methyl ester (RME)

The methyl ester of rapeseed oil is a complex mixture of C_{14}, C_{16}, C_{18}, C_{20}, and C_{22} methyl esters. The carbon chain of RME is highly saturated (60% wt C_{18} with one double bond). The elementary composition of RME has 77.2% carbons, 11.9% hydrogen and 10.9% oxygen. The Rapeseed oil methyl ester (RME) used in this experimental work was provided by COGNIS France. The composition of Rapeseed oil methyl ester (RME) used for oxidation experiments in this project is described in table 3.1.

Fatty Acid Composition (wt %)	C_{14}	C_{16}	C_{18}	C_{20}	C_{22}
Mole %	0.10	5.40	92.00	2.00	0.50

Table 3.1: the composition of RME

3.3.1 Experimental Conditions

The oxidation of RME was done at 1 and 10 bar over various temperature ranges for oxygen rich to fuel rich conditions. Due to experimental set-up limitations experiments were carried out up to 10 bar only. The present experiments have been performed at steady state and constant mean residence times. C.Morin [3.6] combusted Rapeseed oil methyl ester (RME) and Sunflower oil methyl ester (SME) in same JSR set up. So conditions used in current experimental work are based on results and observations from her oxidation work. These conditions are ideal conditions to produce chemical kinetics reaction mechanism. The two different sets of residence times are used for 1 bar and 10 bar experiments, considering the limitations like total flow rate in jet-stirred reactor, flow limits like flow of auxiliary Nitrogen used for dilution and temperature

control inside the reactor. The operating conditions for oxidation experiments are described in table 3.2.

The theoretical reaction of RME oxidation is:

$$C_{18}H_{34}O_2 \ (\text{RME}) + 25.5\ O_2 \longrightarrow 18CO_2 + 17\ H_2O \qquad (3.1)$$

Theoretical value of stoichiometric ratio for oxygen in reaction for combustion of RME is 25.5, where as we have used 25.17 for RME having formula $C_{17.92}H_{33}O_2$

Sr No	Fuel	P (bar)	Φ	%HC mol	$\%O_2$ mol	$\%N_2$ mol	τ (sec)	Working T(^{0}K)
1.1	Oxygen rich	1	0.25	0.05	5.03	94.92	0.07	869 to 1155
1.2	Oxygen rich		0.5	0.05	2.52	97.43	0.07	950 to 1318
2.1	RME rich		1.0	0.05	1.26	98.69	0.1	950 to 1400
2.2	RME rich		1.5	0.05	0.84	99.11	0.1	950 to 1400
Sr No	**Fuel**	**P (bar)**	**Φ**	**%HC mol**	**$\%O_2$ mol**	**$\%N_2$ mol**	**τ (sec)**	**Working T(^{0}K)**
3.1	Oxygen rich	10	0.5	0.05	2.52	97.43	1.0	800 to 1018
3.2	Oxygen rich		0.75	0.05	1.68	98.27	1.0	800 to 1045
4.1	RME rich		1.0	0.05	1.26	98.69	1.0	800 to 1018
4.2	RME Rich		1.5	0.05	0.84	99.11	1.0	800 to 1073

Where, HC = Hydrocarbon/Fuel, Φ = Equivalence ratio, τ = residence time
T **=** Temperature

Table 3.2: the operating conditions for oxidation of RME

Equivalence ratio can be defined as ratio of actual fuel/air or oxidiser ratio to stoichiometric fuel/air or oxidiser ratio.

$\Phi = (n\ C_{18}H_{34}O_2/\ nO_2)_{act} / (n\ C_{18}H_{34}O_2/\ nO_2)_{st}$

Where n = number of moles

The flow of oxygen and nitrogen for each equivalence ratio (Φ) was calculated from following equation:

$$\%\ O_2 = 25.17 * \%\ HC / \Phi$$

% N_2 = 100 - %HC -% O_2

For example at stoichometric (Φ=1) condition

% O_2 = 25.17 * 0.05/1 = 1.258

% N_2 = 100 – 0.05 -1.258 = 98.69

Where, 25.17 is Stoichometric ratio.

3.4 Calculation of gas (reactant) flow rate in the reactor

The calculation of gas flow rate in the reactor was carried out by using expression of residence time, τ, inside the reactor and by assuming ideal gas behavior. To perform experiments with constant residence time and varying temperature, it was necessary to minimize flow rate of reactants when temperature is increasing [3.5]. At higher temperature it was too difficult to control auxiliary Nitrogen flow rate.

$$\tau = \frac{V_r}{D_t} \cdot \frac{T_{amb}}{T} \cdot \frac{P}{P_{amb}}$$

Where,

τ	Average residence time of gas in the reactor (s)
V_r	Volume of reactor (cm^3)
D_t	Total flow rate entering the reactor ($cm^3.s^{-1}$)
T_{amb}	Ambient Temperature (°K)
T	Working Temperature (°K)
P_{amb}	Ambient Pressure (atm)
P	Working Pressure (atm)

From this equation and initial mole fractions Xi entering the reactor, it was possible to calculate flow rates of each reactant [3.5].

$$Di = Xi \cdot D_t = X_i \cdot \frac{V_r}{\tau} \cdot \frac{T_{amb}}{T} \cdot \frac{P}{P_{amb}}$$

For example calculating flow rate of O_2 at stoichometric condition and P = 10 bar

$DO_2 = XO_2 * D_t$

T_{amb} = 295 K, T= 800 K, P= 10 bar, P_{amb} = 1 atm

Vr = 39 cm^3, τ = 1sec

D_t = (39* 0.001)/ (1/3600) * 295/800 * 10/1

D_t = 517.7 l/hr

XO2 = % O_2 / 100 = 1.26 /100 = 0.0126

DO_2 = 517.7 * 0.0126 = 6.52 l/hr

As hydrocarbon (fuel) was injected in its the form, it was necessary to express flow rate of the liquid injected D_{HC} (l) as function of flow rate of desired gas D_{HC} (g)

$$D_{HC}(l) = D_{HC}(g) \cdot \frac{M \cdot P_{amb}}{\rho \cdot R \cdot T_{amb}}$$

Where

M	Molar mass of hydrocarbon
R	Universal gas constant
ρ	Density of hydrocarbon fuel (liquid)

3.5 Analysis

The analytical techniques (Gas Chromatography/Mass Spectroscopy, Flame Ionization Detector, Thermal Conductivity Detector) used were same as that used in previous experimental work (oxidation of hydrocarbons) done at ICARE-CNRS [3.1]. The reacting mixtures were probe sampled using a low-pressure sonic fused-silica microprobe. The samples (ca. 4 kPa) were taken at steady temperature and residence time. The compound analysis is based on two types of compounds namely condensable (low vapor-pressure) and non-condensable (high vapor-pressure). Figure 3.3 shows schematic diagram of experimental set-up and analytical tools used for RME oxidation. The condensable compounds were analyzed on-line using a GC-MS, where as non-condensable species, permanent gases were analyzed off-line after collection and storage in 1 L Pyrex bulbs.

These compounds were analyzed using several types of detectors like Flame Ionization Detector (FID), Thermal Conductivity (TCD), and Mass Spectrometer (MS). In all the analysis the low pressure samples were pressurized using a piston system to 600 -800 torr before injection in order to improve the species detection [3.5] [3.7]. All the products were analysed by chromatographic peak identification. The O_2 and CO were analysed on TCD where as CH_2O and CO_2 were measured by FID after hydrogenation on a Ni/H_2 catalyst connected to the exit of the GC column. The C_1 to C_8 hydrocarbons were analysed on FID (Flame Ionisation Detector). Additional GC/MS analysis was carried out to obtain traces of saturated, unsaturated esters and compounds above C_9.

3.5.1 Flame Ionization Detector (FID)

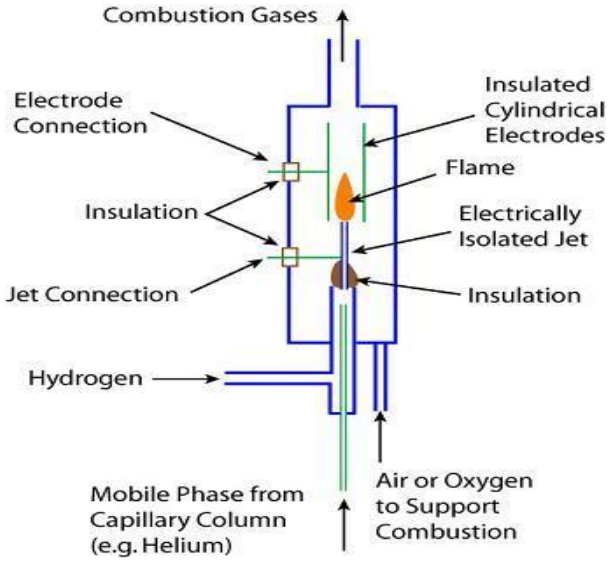

Figure 3.4: Flame Ionization Detector

FID is commonly used gas chromatographic detector for volatile hydrocarbons and many carbon containing compounds. It uses an air-hydrogen flame to produce ions. Molecules that contained carbon and hydrogen respond best in FID but presence of 'heteroatom' in a molecule decreases the detector's response. The disadvantage of FID is that it destroys the sample [3.8].

The detector requires the separate gas supplier with their flow regulators. The gases used are hydrogen for combustion, helium or nitrogen for the carrier gas and oxygen or air as combustion agent. The effluent from GC column passes through the flame, which breaks down organic molecules and produces ions. The

ions are not formed by thermal ionization but by thermal emission from microscopic carbon particles formed during combustion process. The ions are collected on a biased electrode and produce an electrical signal [3.9]. Under optimal conditions; the response of FID does not change markedly with variations in changes in flow rate, pressure or temperature of mobile gas phase thus giving stable detection. In our analysis CO_2 and CH_2O were measured by FID (Hewlett-Packard 5890 series II) along with C_1 to C_7 hydrocarbons (FID Varian 3400) including olefins.

3.5.2 Thermal Conductivity Detector (TCD)

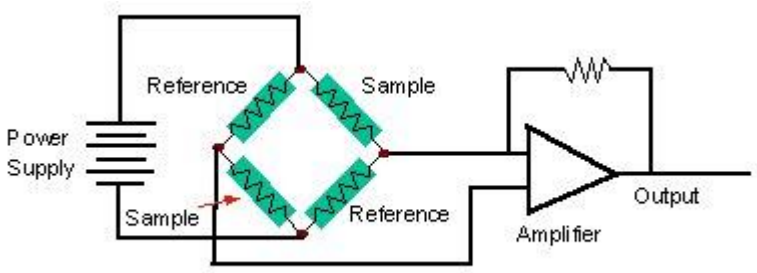

Figure 3.5: Thermal Conductivity Detector

A TCD consists of an electrically heated wire or thermistor. The principle of TCD is to measure electronically the change in thermal conductivity of gas by variation of resistance over thermistor. The temperature of the sensing element depends on the thermal conductivity of the gas flowing around it. The changes in thermal conductivity cause a temperature rise in the element which is sensed as a change in resistance. It is not a very sensitive detector but it is non-specific and non-destructive [3.11].

A TCD comprises of one or more active thermal-sensing elements in two gas streams: the reference stream contains pure carrier gas and the sample stream contains the column effluent [3.10]. Generally two pairs of TCD are used in chromatographs. One pair is placed in the column effluent to detect separated components as they leave the column and another pair is placed before the injector or in separate reference column. The resistances of the two sets of pairs are then arranged in a bridge circuit [3.11]. In our analysis, the oxygenated compounds CO, O_2, CO_2 and CH_2O are analyzed on chromatograph containing 2 columns and 2 detectors. The sample gases are passed through column PoraPLOT U which, traps some CO and O_2. These gases are separated on molecular sieve and then

quantified on TCD (Hewlett Packard 5890 II). The gases left in column (PoraPLOT U) are diverted towards methaniser (Pt/H2) and quantified by FID. The H_2 was measured by TCD (Varian 3300) equipped with column Carboplot P7. The thermal conductivity of Hydrogen is closed to that of Helium, so instead of Helium as gas, N_2 is used in the analysis.

Gases	Thermal Conductivity ($cal.cm^{-1}.s^{-1}.^{0}C$-1 10^{-5})
Helium	34.8
Hydrogen	41.6
Nitrogen	5.8
Argon	4.0
Oxygen	5.9
Carbon Monoxide	5.6
Methane	7.2
Benzene	2.2

Table 3.3: Thermal conductivity of common gases at 0 ^{0}C [3.9]

3.5.3 Gas Chromatography-Mass Spectrometry (GC-MS)

Gas chromatography-Mass spectrometry is a method that combines the features of gas chromatography and mass spectrometry to identify different substances and trace elements in the samples. The gas chromatograph uses the difference in chemical properties between different molecules in a mixture to separate molecules. The retention time taken by molecules allows mass spectrometer downstream to evaluate the molecules separately. It does this by breaking molecule into ionized fragments and detecting these fragments using their mass to charge ratio [3.5] [3.7]. Each molecule has specific fragment spectrum. It is possible to identify a particular molecule accurately by using GC-MS.

In our analyses several gas chromatographs (GC), equipped with capillary columns (Poraplot-U, Molecular Sieve-5A, DB-5ms, Plot Al_2O_3/KCl, Carboplot-P7), were used. We also used two types of mass spectrometer operating in electron impact ionization mode (70 eV).

- Ion trap detector (GC/MS Varian Saturn)

Or

- Quadrupole (GC/MS Varian 1200)

Ion Trap Detector (ITD):

It uses three electrodes to trap ions in a small volume. A mass spectrum is obtained by changing the electrode voltages to eject ions from trap. The advantages of ion-trap mass spectrometer are compact size, ability to trap and accumulate ions.

Quadrupole mass Spectrometer:

It consists of four parallel metal rods. Two opposite rods have an applied potential of voltage. A mass spectrum is obtained by monitoring the ions passing through the quadruple filter as voltages on rods are varied. Hydrocarbons > C6 and oxygenates were measured offline using Varian 3400 MS. The traces of compounds saturated and unsaturated esters along with Benzene, 1-3 Butadiene were measured by Varian 1200(GC/FID).

3.5.4 Analysis of Condensable Compounds

The condensable compounds were analyzed online in gas phase by using GC-MS and FID. This mass spectrometer is connected to sampling probe by transfer line heated at 290 ^{0}C.The gases were collected in 1L Pyrex bulbs. The bulbs were filled up to 80 torr pressure and then gas sample was injected into the GC. The chromatograph is equipped with DB-5ms column and mass spectrometer has ion trap detector to identify compounds. The column in chromatograph and heated transfer line improves the separation of products [3.5]. Thus online analysis of compounds helps to study oxidation of hydrocarbons in the reactor. All condensable compounds were measured by GC/MS and GC/FID technique (Varian 3800).

The following table shows the characteristics of different detectors used.

Chromatograph	Columns	Detectors	Gas Used	Programming and temperature	Products Detected
Hewlett Packard 5890 Series II	CP-PoraPLOT U L = 25 m D_{int} = 0.53 mm Df = 20 µm	Methaniser + FID	He 30 ml/min	T_i = 50 °C t_i = 1.29 min v = 15 °C/min T_f = 180 °C t_f = 8.5 min	CO_2 CH_2O
	CP-Molseive 5Å L = 25 m D_{int} = 0.53 mm Df = 50 µm	TCD			O_2 CO
Varian 3300	CP-CarboPLOT P7 L = 25 m D_{int} = 0.53 mm Df = 25 µm	TCD	N_2 15 ml/min	T = 35 °C t = 5 min Isotherme	H_2
Varian 3400	CP-Al_2O_3/KCl L = 50 m D_{int} = 0.32 mm Df = 5 µm	FID	He 1.5 ml/min	T_i = 70 °C t_i = 0 min v = 10 °C/min T_f = 200 °C t_f = 20 min	HC<C_7
Varian 3400	CPSIL 5CB L=30 m D_{int} = 0.32 mm Df= 1,2 µm DB5MS L= 30 m D_{int} =0.32 mm Df= 1 µm	ITD (GC/MS)	He 1.5ml/min	T_i = 40 °C t_i = 0 min v = 10 °C/min T_f = 200 °C t_f = 20 min	HC>C_6 + Oxygenated

Chromatograph	Columns	Detectors	Gas Used	Programming and temperature	Products Detected
Varian 1200	DB-624 L= 60m D_{int} = 0.32mm Df = 1.8 μm	(GC/FID)	He 20 ml/min	T_i = 40 °C t_i = 2 min v = 15 °C/min T_f = 150 °C t_f = 20 min	Oxygenated (saturated and unsaturated esters)
Varian 3800	DB5MS L = 30 m D_{int}= 0.25 mm Df = 1 μm	ITD (GC/MS)	He 1 ml/min	T_i = 70 °C t_i = 0 min v = 10 °C/min T_l = 250 °C t_l = 0 min v = 20 °C/min T_f = 320 °C t_f=5min	$HC>C_6$ + Oxygenated (online analyses) (Condensable)
		GC/FID		T_i = 60 °C t_i = 3 min v = 12 °C/min T_f = 220 °C t_f = 10 min	

Table 3.4: Detectors used for analysis of compounds

Where

T_i = Initial temperature t_i = Initial time

T_l= Middle temperature t_l= middle time

T_f = Final temperature t_f = final time

v = Change in temperature per min L = Length of column

D_{int} = Diameter of column D_f = Thickness of film inside column

References

3.1 Dagaut.P, Cathonnet.M, Rouan.J-P, Foulatier.R, Quilgars.A, Boettner.J-C, Gaillard.F, James.H, 1986, *A jet-stirred reactor for kinetic studies of homogenous gas-phase reactions at pressures up to ten atmosphere (~1Mpa)*, *J*. Phys E: Instrum 19, 207-209.

3.2 Dagaut.P,2002, *On the kinetics of hydrocarbons oxidation from natural gas to kerosene and diesel fuel*, Physical Chemistry Chemical Physics, 4, 2079-2094

3.3 Dagaut.P, Reuillon.M, Cathonnet.M, 1994, *High Pressure Oxidation of Liquid Fuels From Low to High Temperature.1.n-Heptane and iso-Octane*, Combustion Science and Technology, 95, 233-260

3.4 Philippe Dagaut, Sandro Gaïl, Mayuresh Sahasrabudhe, 2007, *Rapeseed oil methyl ester oxidation over extended ranges of pressure, temperature, and equivalence ratio: Experimental and modeling kinetic study*, Proceedings of Combustion Institute, 31, Issue2 , 2955-2961

3.5 Mati.Karim, 2005, *Cinétique de combustion du gazole à haute pression : étude expérimentale et modélisation*, PhD Thesis, LCSR-CNRS, Orleans, France

3.6 Morin.C, Chauveau.C, Dagaut.P, Gokalp.I and Cathonnet.M, 2004, *Vaporization & Oxidation of liquid fuel droplets at high temperature and high pressure: Application to n-alkanes and vegetable oil methyl esters*, Combustion Science and Technology, 176, 499-529

3.7 Gail.Sandro, 2003, *Étude cinétique de l'oxydation de composés aromatiques en relation avec la combustion du gazole et de l'essence: Approche expérimentale et modélisation cinétique détaillée*, PhD Thesis, LCSR-CNRS, Orleans, France

3.8 www.shsu.edu/~chemistry/primers/FID.html

3.9 www.chromatography-online.org/GC-Detectors/Flame-Ionization/rs36.html

3.10 www.lcgcmag.com/lcgc/article/articleDetail

3.11 www.chemistry.adelaide.edu.au/external/soc-rel/content/tcd.htm

CHAPTER 4

EXPERIMENTAL RESULTS

Chapter 3 described the experimental set-up used for oxidation of RME, details of the Jet-stirred reactor and experimental conditions. It also described the different analytical techniques used for the analysis of experimental results. The RME oxidation experiments were carried out at 1 bar and 10 bar in a Jet Stirred Reactor. This chapter will describe the results obtained from RME oxidation experiments. The results are presented in graphical format in terms of mole fractions against working temperature. This chapter will also cover the effect of pressure and temperature on RME oxidation and esters compounds obtained from GC/FID.

The RME has the following composition in global chemical formula: $C_{18}H_{34}O_2$. The RME oxidation experiments were carried out for fuel lean to fuel rich conditions with residence time of 0.07, 0.1 s and 1 s in a Jet Stirred Reactor. The mass flow rate for RME was the same for 1 bar and 10 bar experiments. As residence time is proportional to pressure (equation 3.4 in section 3.4 of chapter 3), keeping same flow rate results in an increase in residence time by factor of 10 between 1 and 10 bar. So, two different sets of residence times are used for 1 bar and 10 bar experiments. Though Jet stirred reactor is designed for 10-40 bar range, experiments were carried out only at 10 bar, considering the limitations like total flow rate in jet-stirred reactor, flow limits, temperature control and capacity to handle flow of extreme high quantity of gas. Thus experimental conditions used are based on a compromise between conditions required to produce the reaction mechanism (conditions used in previous oxidation work like pressure 1 bar) [4.1] and limitations of the experimental system used. The above conditions are suitable conditions to produce chemical kinetics reaction mechanism. During experimental work following uncertainties were also considered:

Condition	Uncertainties
Reactor Temperature	± 3K
Residence Time	± 0.05 s
Reactor Pressure	± 0.1 atm
Inlet	< 5% for reactants
For measured species	< 10% for concentration higher than 10 ppm

The conditions like temperature, pressure, initial fuel concentration and experimental set-up used in these oxidation experiments are different than typical diesel engine conditions. The commercial diesel engines run at high pressure range (approximately 50-70 bar), whereas, in this research work, the experiments are performed at 1 and 10 bar only. In diesel engine combustion, compression ratio, fuel injection pressure and timing, air/fuel ratio, cylinder pressures are important factors affecting combustion performance and emissions. Diesel engine emission performance and concentration of combustion products vary with engine load and engine speed conditions. The concentration of combustion products and intermediates from diesel engine will be higher than that from Jet-stirred reactor. Though the nature of combustion products/species from RME oxidation experiments is same as that from diesel engines, it is not possible to represent them in terms of real diesel engine combustion.

First the results of 1 bar experiments will be discussed followed by results of the experiments performed at high pressure. The molar concentrations of combustion products (final products and intermediates) were measured by using chemical probe sampling and different gas chromatographs. As described in chapter 3, a carbon balance (difference between total initial carbon concentration in the fuel and total carbon concentration in all combustion products) was calculated for each experiment. A carbon balance was found within +/-10% except for experiments, where the fuel consumption was very low since RME concentration was not measured.

4.1 Results at 1 bar

RME oxidation was studied for fuel-lean to fuel-rich (Φ= 0.25 to 1.5) conditions, at residence time of 0.07 and 0.1 s. As explained before, the operating conditions were based on previous experimental work carried out [4.1] and trial experiments carried out. The temperature range (800 K to 1400 K) for 1 bar experiments is selected after number of trial experiments. The liquid droplets of RME were observed in exit line of JSR, when experiments were carried out below 800 K. The RME liquid droplets were also observed in 1 lit Pyrex bulb in which RME combustion product sample is collected. As RME is highly viscous fuel, the chemical probe (probe used for detecting combustion products) was observed to be blocked for experiments below 800 K. This indicates the incomplete oxidation and RME oxidation takes place at higher temperature range, not at lower temperature i.e below 800 K. The mole fractions of all oxidation products were measured as a function of temperature. These combustion products include all saturated, unsaturated as well as oxygenated compounds. Light saturated and unsaturated hydrocarbons obtained are similar to those obtained by F Billaud [4.2] and Celine Morine [4.1] in their respective works. Figure 4.1 to 4.4 show graphs plotted for mole fractions of different intermediates and combustion products measured from samples obtained from individual experiments carried out with different working temperature range for fuel-lean to fuel-rich (Φ= 0.25 to 1.5) conditions respectively. Figure 4.5 shows carbon balance done for all equivalence ratios (Φ). The effect of equivalence ratio (Φ) and temperature on RME reactivity was observed keeping the total pressure (1 bar) constant.

Following are the products obtained from the oxidation of RME at 1 bar:

- Oxygen, Hydrogen and Carbon dioxide (CO_2),

Hydrocarbon Intermediates obtained from all analytical tools:

- **Saturated Hydrocarbons**: Methane (CH_4), Ethane (C_2H_6), Propane (C_3H_8), iso-Butane (i-C_4H_{10}), n-Heptane (C_7H_{16})
- **Unsaturated Hydrocarbons**: Acetylene (C_2H_2), Ethylene (C_2H_4), Propene (C_3H_6), C_4H_4, 1-Butene (1-C_4H_8), Butyne, 1-Pentene (1-C_5H_{10}), 1-Hexene (1-C_6H_{12}), 1,3CPD, and 1-Heptene (C_7H_{14})
- **Un-regulated Pollutants**: 1,3-Butadiene (1,3-C_4H_6), Formaldehyde (CH_2O), and Benzene (C_6H_6)
- **Regulated Pollutant**: Carbon Monoxide (CO)

The concentration measured for above mentioned products is in PPM quantity; whereas concentration for rest of the intermediate products is in less than 1 ppm quantity. 'NOx' a regular biodiesel combustion product from diesel engines was not observed. NO_x is formed from reaction of free radicals formed from the fuel with N_2. This NO_x formation takes place very early in combustion process and is partly dependent upon the fuel radical concentration. The major sources of N_2 for NO_x formation is N_2 available from air. As only oxidation of fuel was carried out, not combustion using air and the experimental conditions like temperature used in this experimental work was not high enough produce NO_x.

Fuel Lean Conditions (Φ= 0.25, 0.5):

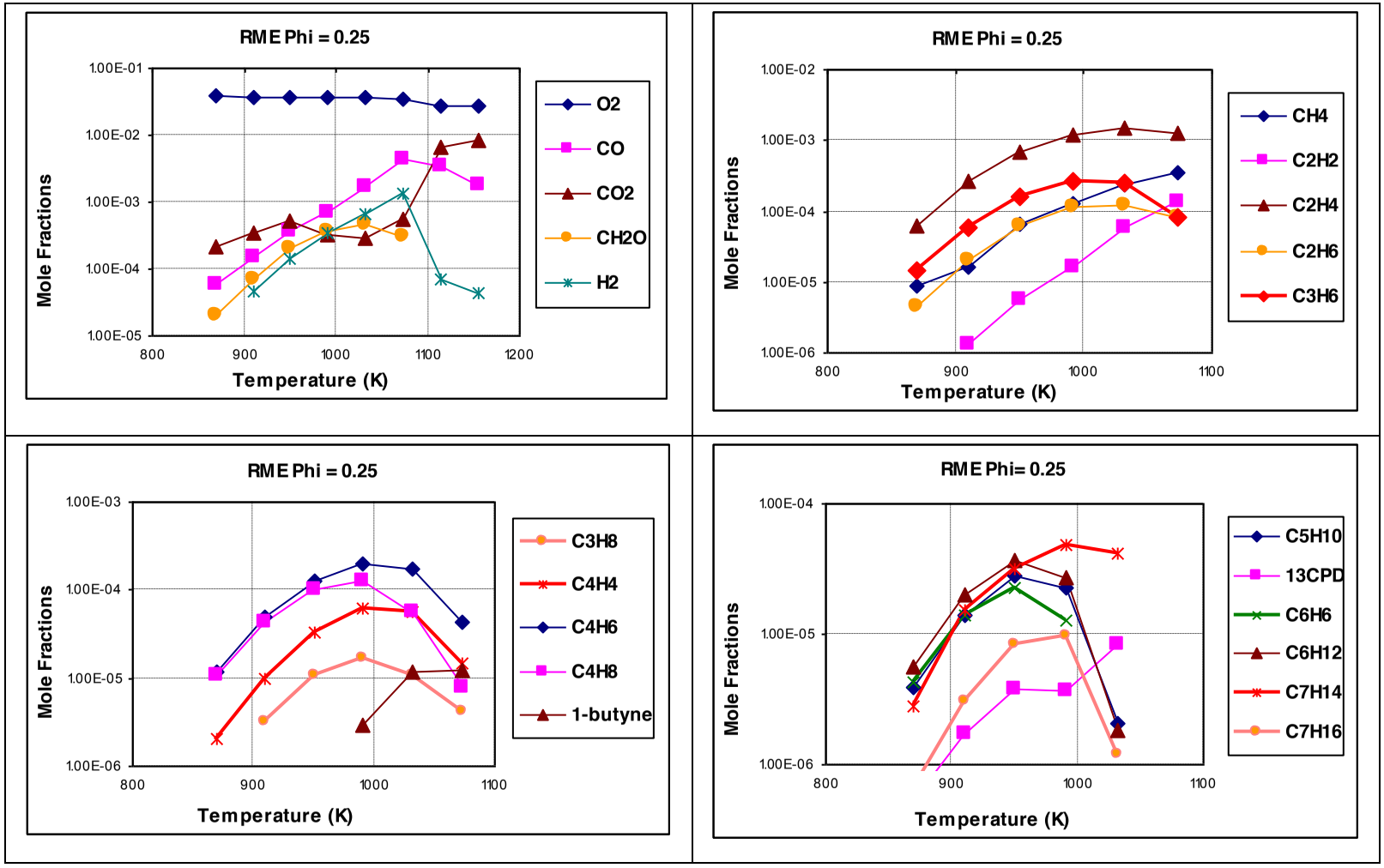

Figure 4.1: Mole fraction profiles of products obtained from oxidation of RME in JSR (τ=0.07s, Φ= 0.25, O_2= 5.03%, N_2=94.92%, RME= 0.05%)

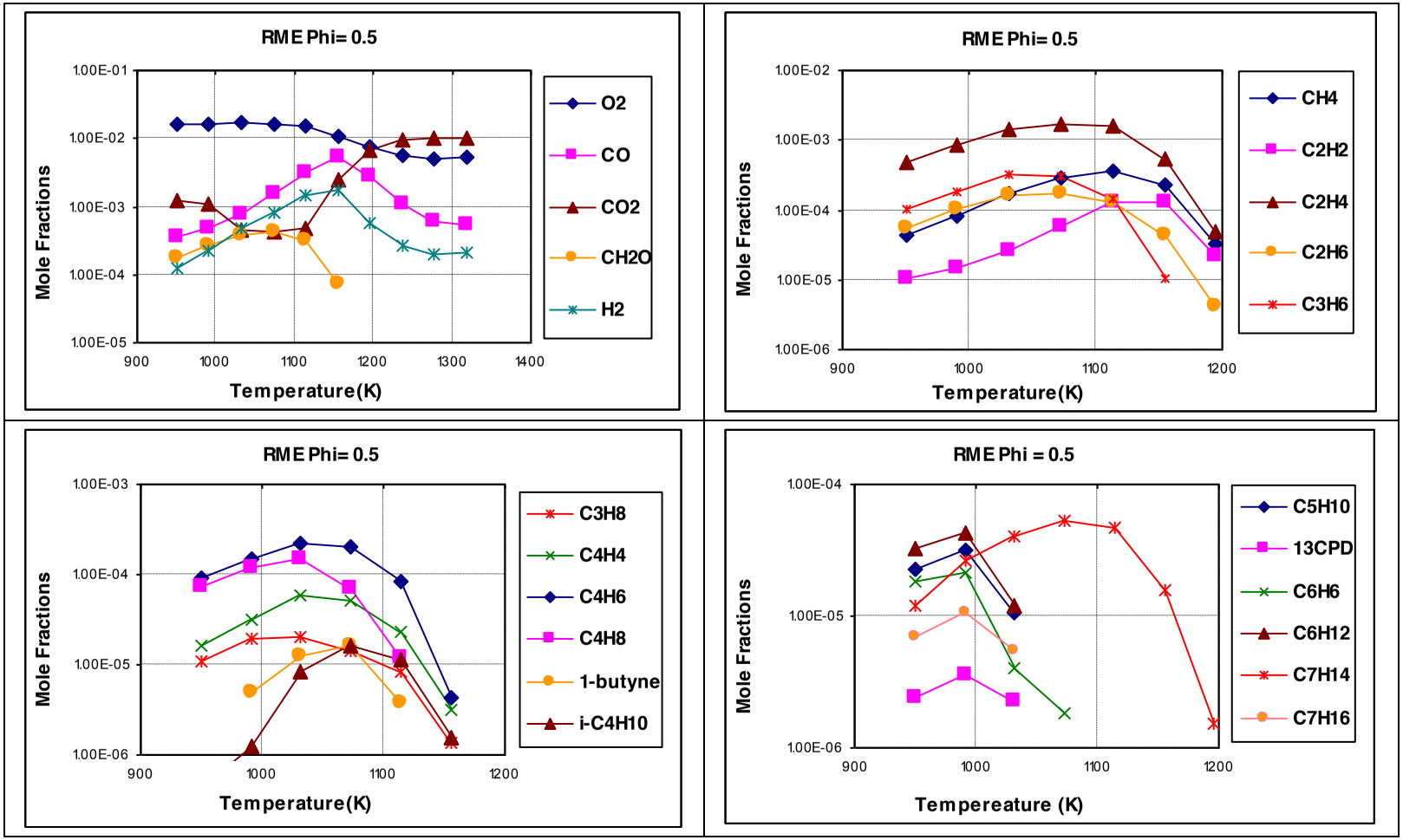

Figure 4.2: Mole fraction profiles of products obtained from oxidation of RME in JSR (τ=0.07s, Φ= 0.5, O_2= 2.52%, N_2= 97.43%, RME= 0.05%)

Figure 4.1 and 4.2 show results for fuel lean conditions. It can be observed from graphs that RME reacted immediately i.e. at initial experimental temperature it yielded saturated, unsaturated hydrocarbon intermediates, and oxygenated intermediates. The early formation of CO_2, the main combustion product in quantity of more than 200 ppm at Φ=0.25 and 1200 ppm at Φ = 0.5, proves that RME is reacting rapidly. It was observed that reactivity increases with increasing temperature. The formation formaldehyde at higher quantity (more than 100 ppm) is in agreement with observation made by J.Pederson [4.6]. J.Pederson observed that formation of aldehydes like formaldehyde is increased due to presence of carbonyl group present in RME [4.6]. The concentration of saturated and unsaturated hydrocarbons reaches a maximum value at higher temperature. The mole fraction level of saturated and unsaturated hydrocarbon compounds was higher between the temperature ranges of 1000-1100K. The formation of intermediates like 1-alkene (1-butene, 1-penten, 1-hexene), dienes and benzene is due to presence of long unsaturated hydrocarbon chain in RME structure.

The major intermediate hydrocarbons observed are Ethylene (C_2H_4) followed by Methane (CH_4), Propene (C_3H_6) and 1,3-Butadiene (1,3 C_4H_6). Carbon Monoxide (CO) and Formaldehyde (CH_2O) are the major oxygenated intermediate compounds.

Stiochiometric (Φ= 1.0):

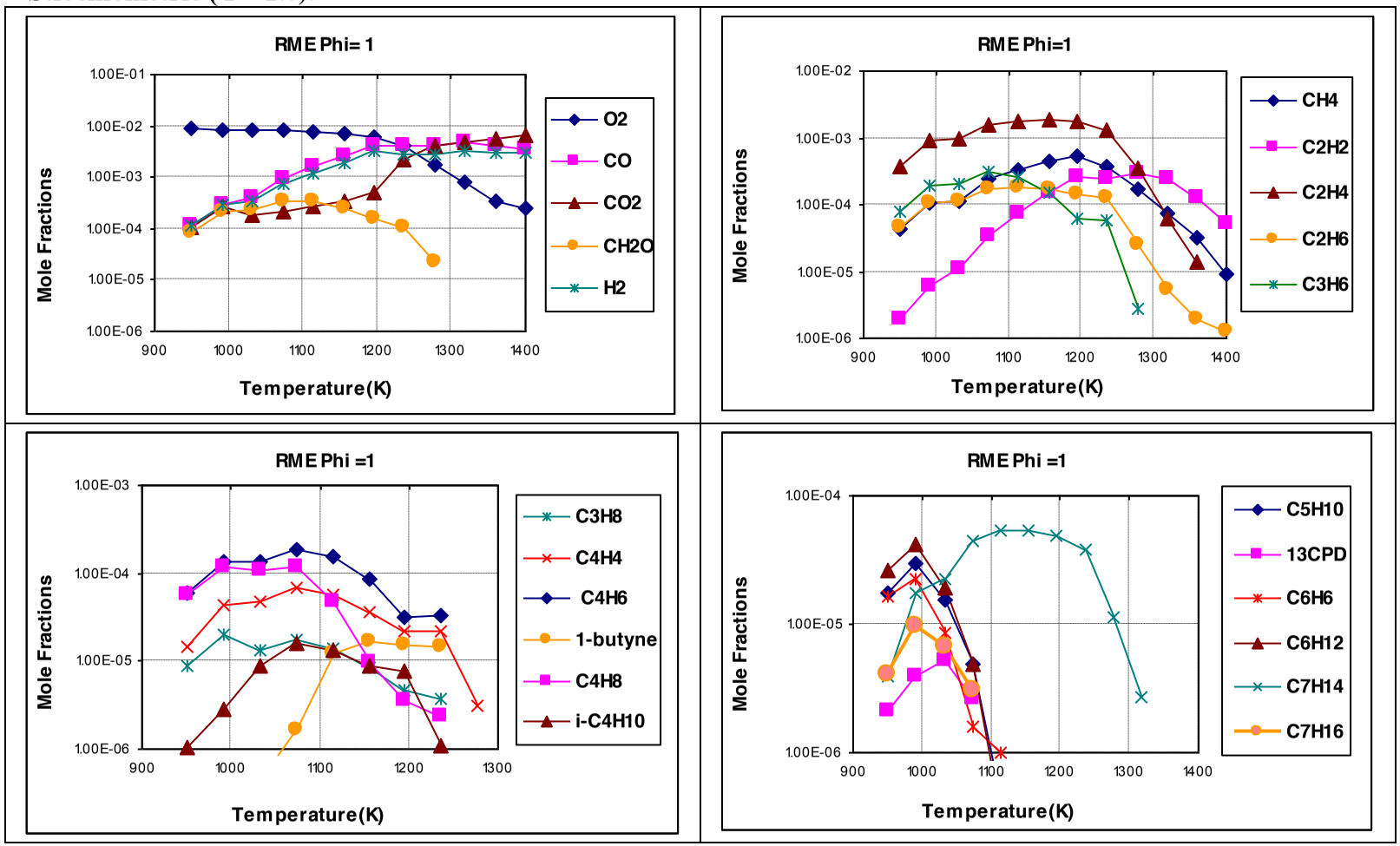

Figure 4.3: Mole fraction profiles of products obtained from oxidation of RME in JSR (τ=0.1s, Φ= 1.00, O_2= 1.26%, N_2= 98.69%, RME= 0.05%)

Fuel-rich condition (Φ= 1.5):

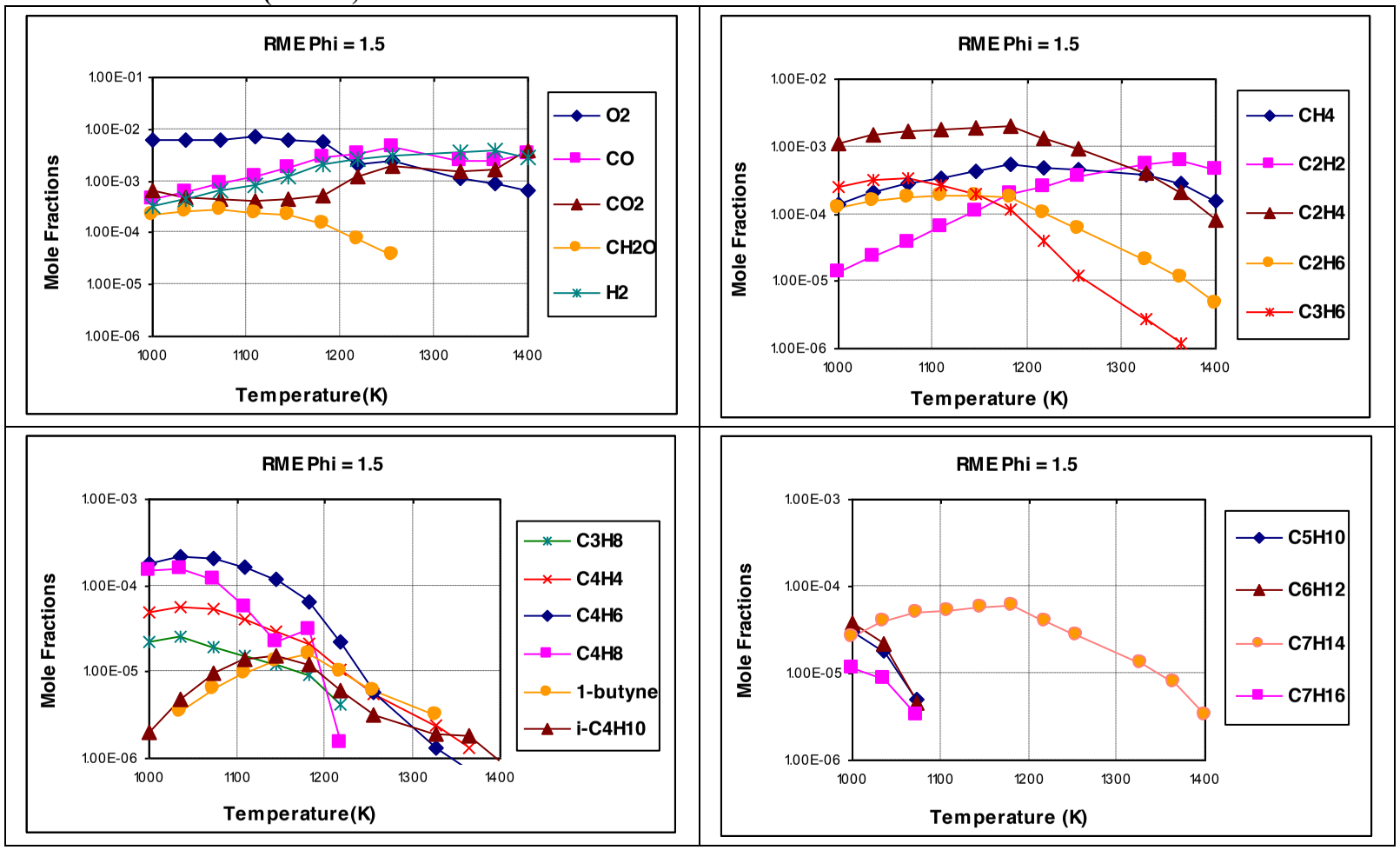

Figure 4.4: Mole fraction profiles of products obtained from oxidation of RME in JSR (τ=0.1s, Φ= 1.50, O_2= 0.84%, N_2= 99.11%, RME= 0.05%)

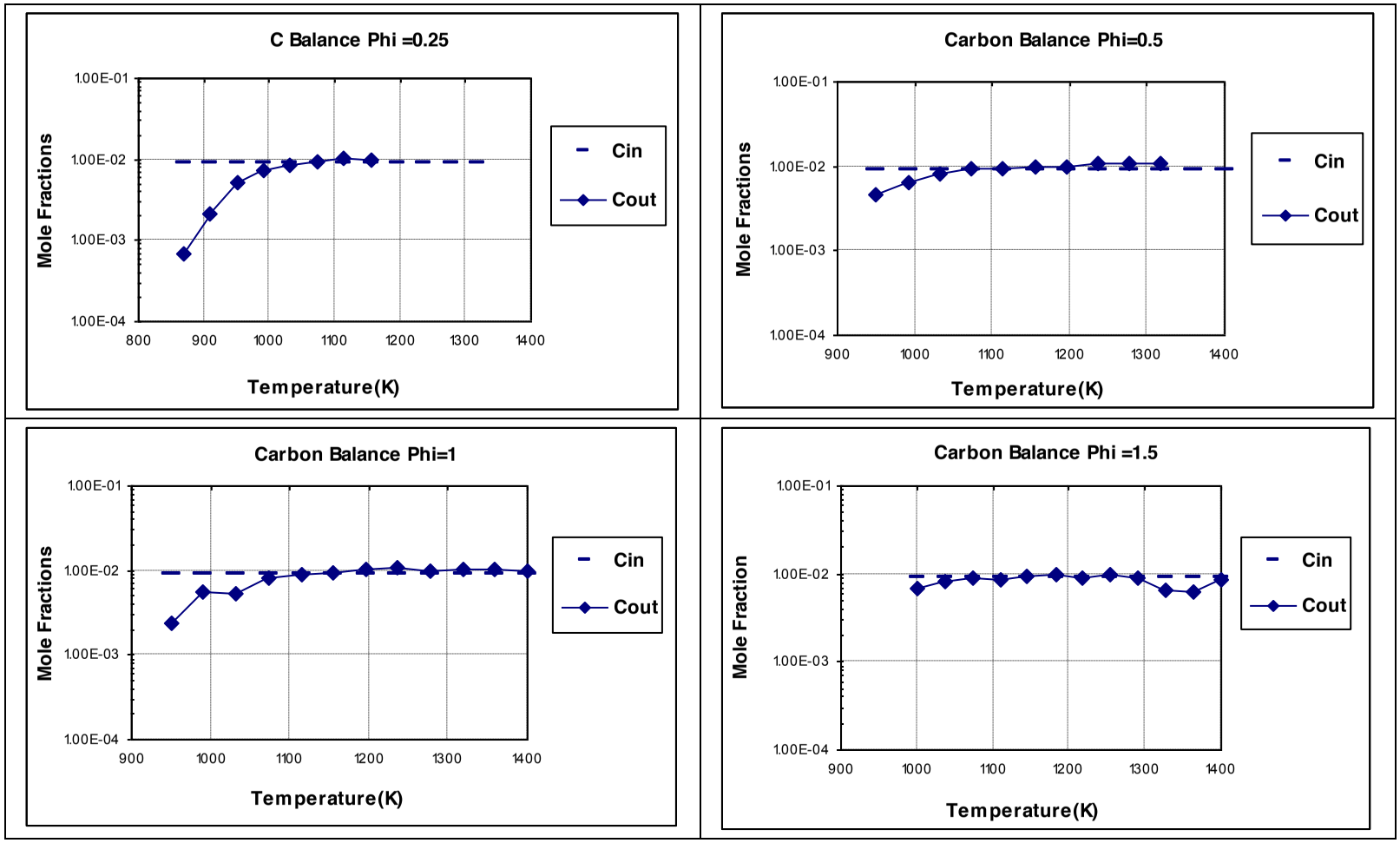

Figure 4.5: Carbon Balance for all equivalence ratios (τ =0.07, 0.1s, Φ= 0.25, 0.5, 1.0 and 1.50)

The figures 4.3 to 4.4 show results for stoichiometric and fuel rich conditions. It was observed, RME reactivity increases with increasing temperature but decreases with increasing equivalence ratio. The working temperature range is changed (it is higher) especially at fuel-rich conditions (1000-1400 K) compared to fuel lean conditions. The rate of oxidation for a given fuel at a given equivalence ratio increases with temperature ; however it decreases with equivalence ratio as less oxygen is available for oxidation. So to enhance the oxidation at fuel- rich mixtures, a higher temperature is needed.

The formation of CO_2 at initial working temperature (950 K for Φ=1.0, 1000K for Φ=1.5) is also observed (100 ppm at Φ=1.0 and 600 ppm at Φ = 1.5), however the concentration is reduced at fuel-rich conditions compared to fuel-lean conditions indicating reactivity is decreased. This early formation CO_2 indicates RME has good combustion properties. The mole fraction level of saturated and unsaturated hydrocarbon compounds was higher between the temperature ranges of 1000-1200 K. The level of saturated and unsaturated hydrocarbon compounds increased in fuel rich conditions.

Maximum Concentration	Φ = 0.25	Φ = 0.5	Φ = 1.0	Φ = 1.5	Trends
Ethylene	1.48×10^{-3}	1.70×10^{-3}	1.92×10^{-3}	2.01×10^{-3}	↑
Methane	3.49×10^{-4}	3.64×10^{-4}	5.20×10^{-4}	5.38×10^{-4}	↑
Propene	2.65×10^{-4}	3.23×10^{-4}	3.13×10^{-4}	3.30×10^{-4}	↑
1,3-Butadiene	1.98×10^{-4}	2.25×10^{-4}	1.88×10^{-4}	2.16×10^{-4}	↑
CO_2	8.24×10^{-3}	1.04×10^{-2}	6.34×10^{-3}	4.01×10^{-3}	↓
CO	4.49×10^{-3}	5.33×10^{-3}	4.93×10^{-3}	4.63×10^{-3}	↓
CH_2O	4.63×10^{-4}	4.21×10^{-4}	3.42×10^{-4}	2.83×10^{-4}	↓

Table 4.1: Maximum mole fractions of the major intermediates at 1 bar

From each plot (Figure 4.1 to 4.4) maximum concentrations of major intermediate gases were extracted and are presented in table 4.1. This result shows that reactivity of RME was higher in fuel lean conditions and it decreased with fuel rich conditions. It was observed from graphs (Figure 4.1 to 4.4) that RME is producing alkenes like Ethylene, propene, aromatics like Benzene and pollutants like 1,3-Butadiene in lesser quantity at fuel-lean conditions. These alkenes along with aldehydes are responsible for ozone formation in atmosphere, so reduction in their emission levels will have positive impact on environmental pollution. The decrease in CO and CH_2O maximum mole fractions can be due to the presence of oxygen in RME. The fuel based oxygen compared to air based oxygen accelerates the combustion process. This fuel based oxygen allows conversion of CO to CO_2 thus reducing CO emission [4.3] [4.4]. However formation formaldehyde (CH_2O) at initial working temperature for fuel rich conditions (230 ppm) is higher than that formed at fuel lean conditions (170 ppm). Figure 4.5 shows the carbon balance done for fuel lean to fuel rich conditions. It was observed that carbon balance was within the range of -/+ 10% especially after 1000K for all fuel conditions. At fuel-lean conditions below 1000 K Carbon-out was less than Carbon-in, because we did not measure un-reacted fuel.

4.2 Results at high pressure (10 bar)

As explained previously, though JSR was designed for pressure up to 40 bar, experiments were done only for 10 bar. During experiments at 10 bar it was difficult to maintain the Nitrogen flow rates (auxiliary and principal) and temperature inside the reactor. Also it was not possible to work at very low fuel lean conditions (Φ = 0.25), so experiment were performed at Φ = 0.75. As pressure increases residence time also increases, so at 40 bar it was be difficult to maintain the total flow rate inside the reactor.

RME oxidation was studied for equivalence ratios of 0.5, 0.75,1 and 1.5 for residence time of 1 s. The residence time used at 10 bar is different than one used at 1 bar (0.07 s and 0.1 s). Figure 4.6 to 4.9 shows graphs plotted for mole fractions of different intermediates and combustion products measured from samples obtained from individual experiments carried out with different working temperature range for fuel-lean to fuel-rich (Φ= 0.5 to 1.5) conditions respectively. The effect of increase in pressure is evaluated by comparing the

results obtained at 1 bar. Also like 1 bar, the effect of equivalence ratio and temperature on RME reactivity was observed keeping pressure constant. As residence used at 1 and 10 bar is different, the comparison between reactivity is more based on mole fraction maxima and profile trends of intermediates.

Following are the products obtained from the oxidation of RME at 10 bar:

- Oxygen, Hydrogen and Carbon dioxide (CO_2)

Hydrocarbon intermediates obtained from different analytical tools:

The intermediates obtained are the same as those detected for experiments at 1 bar

- **Saturated Hydrocarbons**: Methane (CH_4), Ethane (C_2H_6), Propane (C_3H_8)
- **Unsaturated Hydrocarbons**: Acetylene (C_2H_2), Ethylene (C_2H_4), Propene (C_3H_6), C_4H_4, 1-Butene (1-C_4H_8), 1-Pentene (1-C_5H_{10}), 1-Hexene (1-C_6H_{12}), 1,3CPD, and 1-Heptene (C_7H_{14})
- **Un-regulated Pollutants**: 1,3-Butadiene (1,3-C_4H_6), formaldehyde (CH_2O), and Benzene (C_6H_6)
- **Regulated Pollutant**: Carbon Monoxide (CO)

Fuel lean conditions (Φ= 0.5, 0.75):

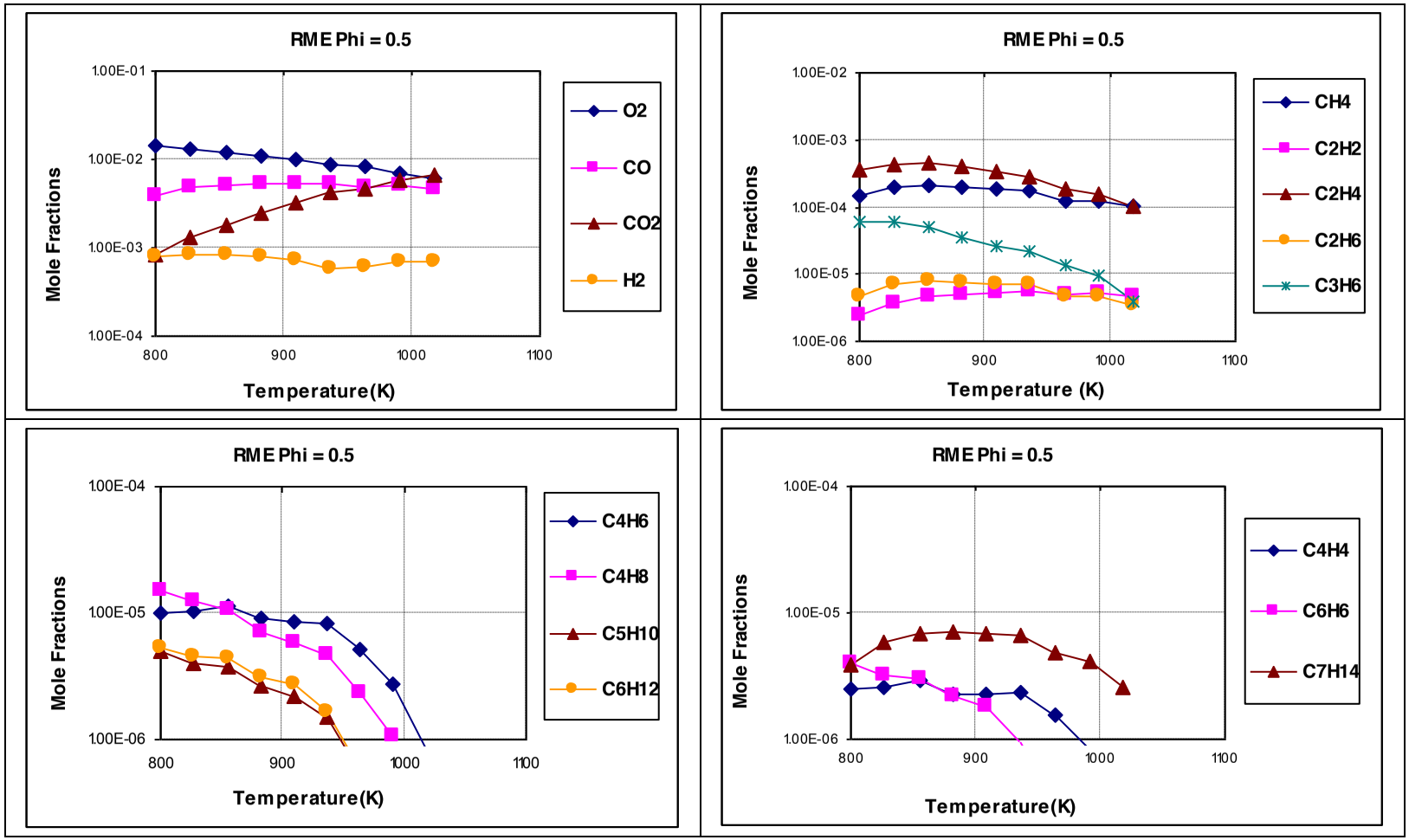

Figure 4.6: Mole fraction profiles of products obtained from oxidation of RME in JSR (τ=1s, Φ= 0.5, O_2=2.52%, N_2=97.43%, RME= 0.05%)

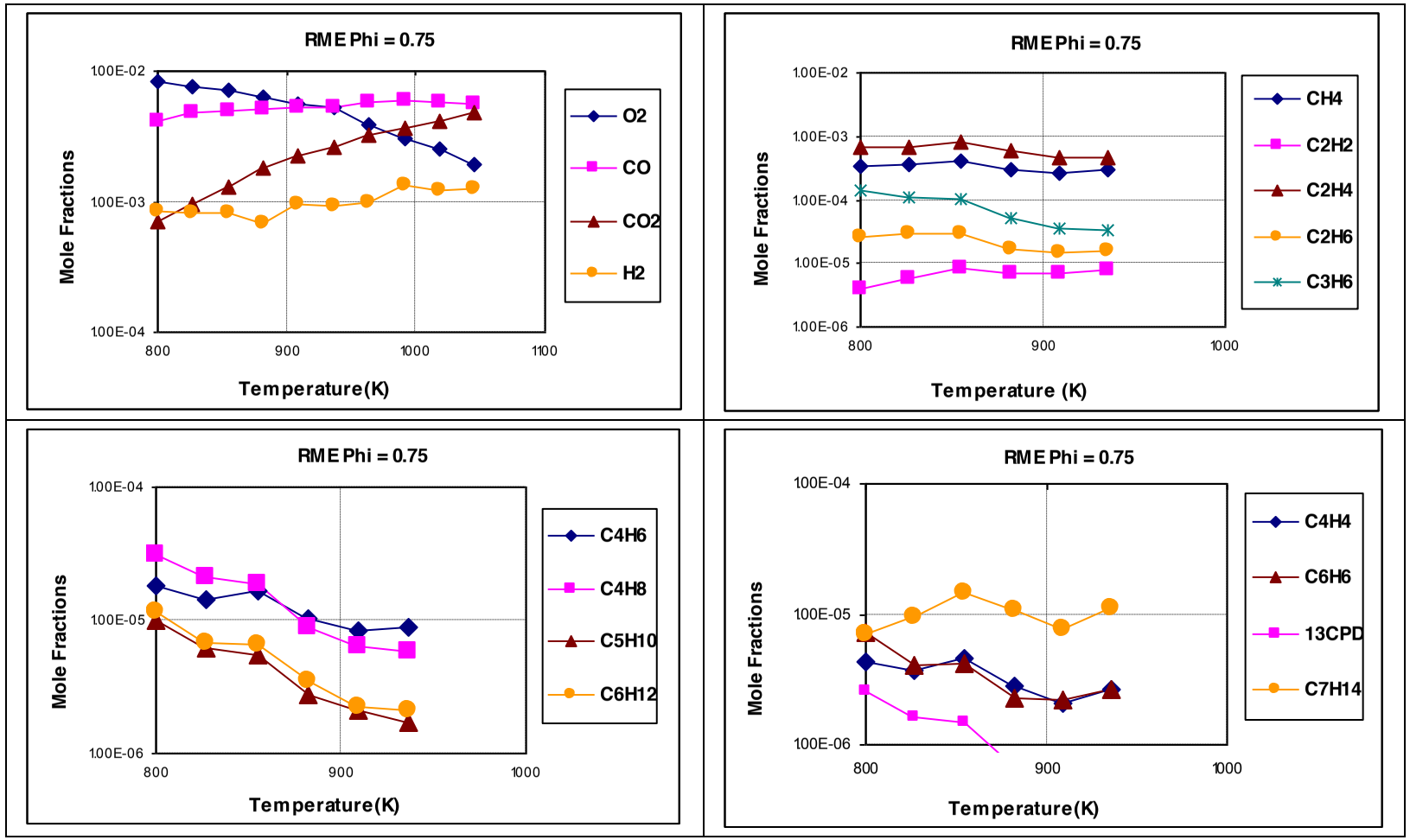

Figure 4.7: Mole fraction profiles of products obtained from oxidation of RME in JSR (τ=1s, Φ= 0.75, O_2= 1.68%, N_2= 98.27%, RME = 0.05%)

Stiochiometric condition (Φ= 1.0):

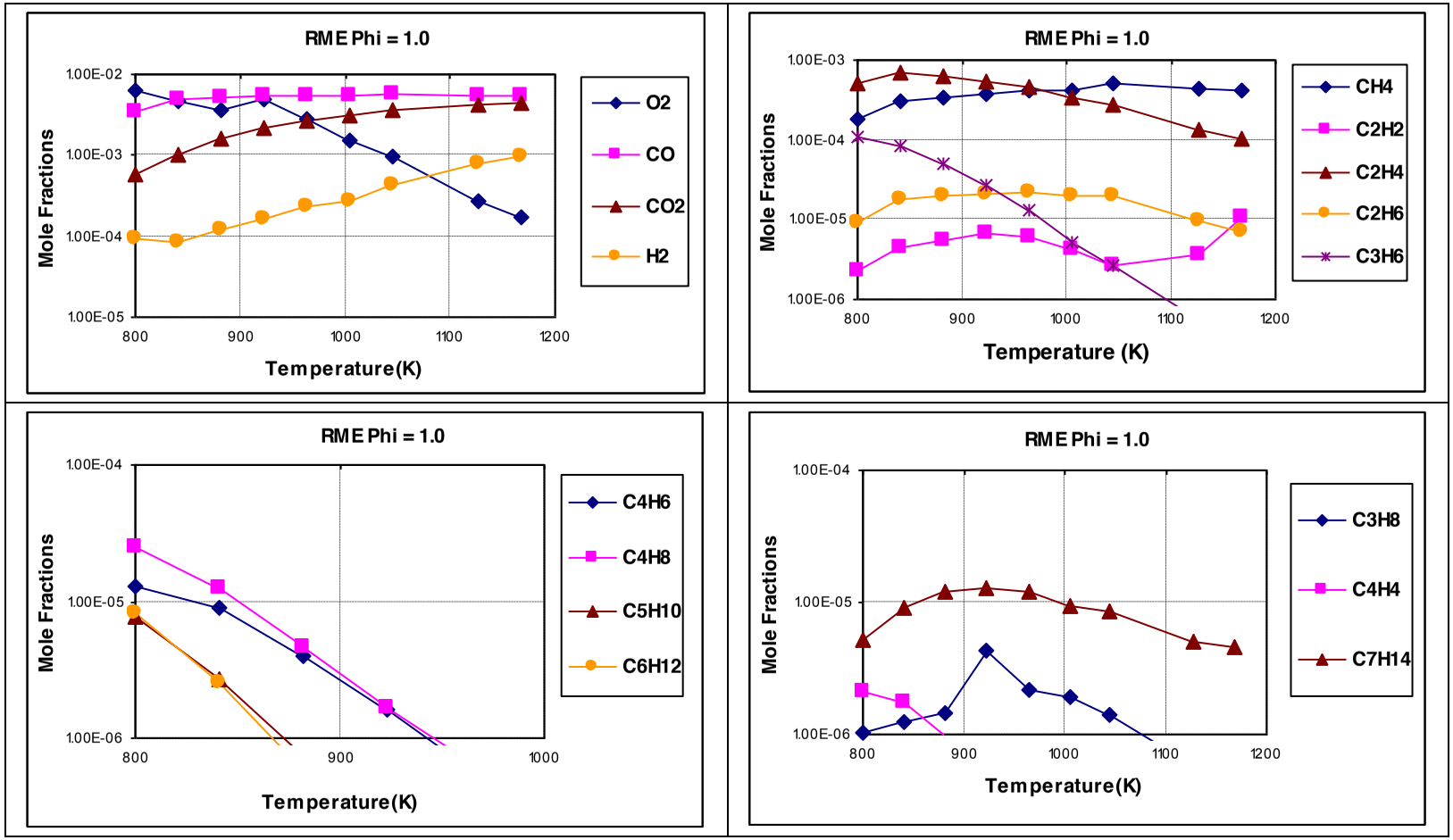

Figure 4.8: Mole fraction profiles of products obtained from oxidation of RME in JSR (τ=1s, Φ= 1.00, O_2= 1.26%, N_2= 98.69%, RME = 0.05%)

Fuel rich condition (Φ= 1.5):

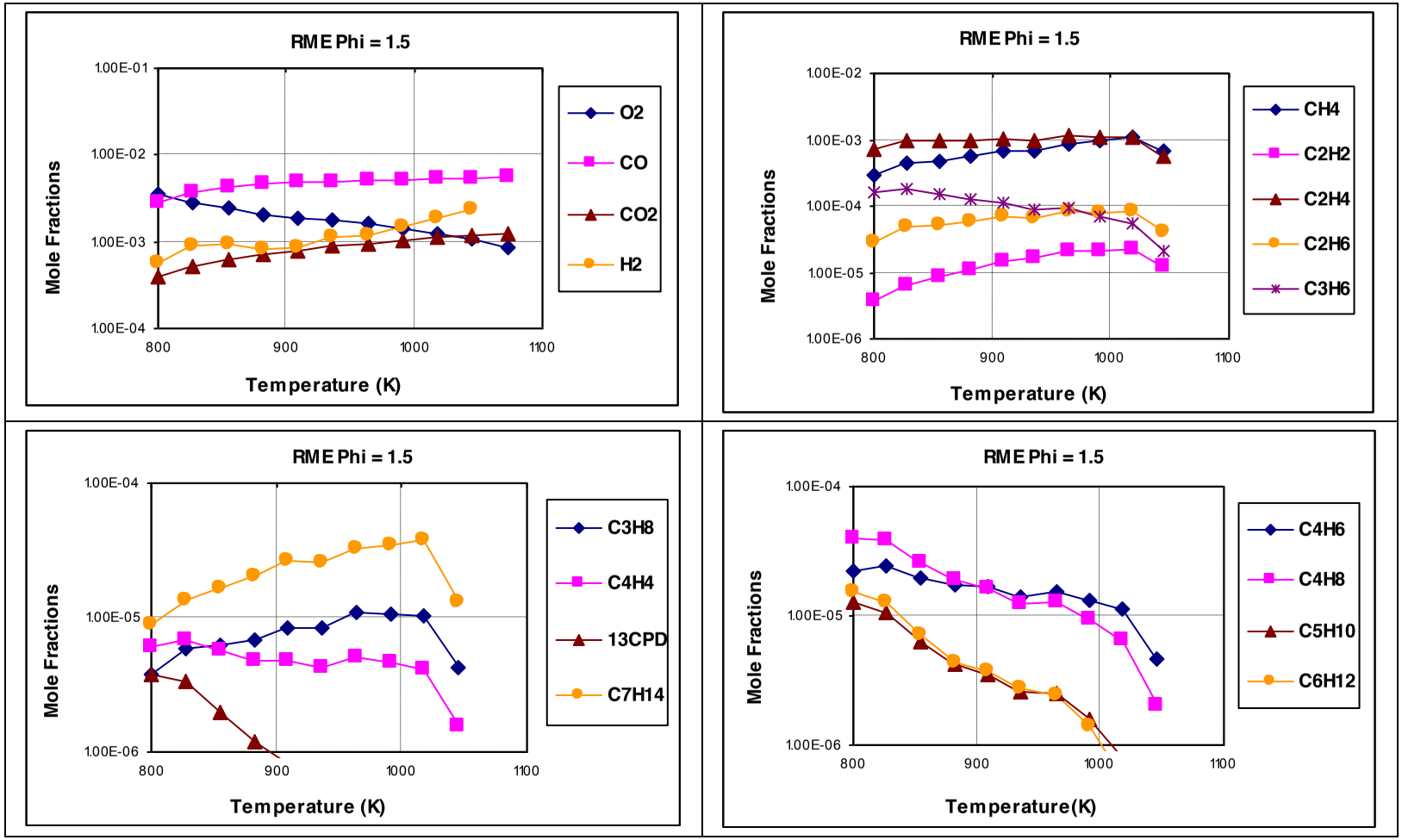

Figure 4.9: Mole fraction profiles of products obtained from oxidation of RME in JSR (τ=1s, Φ= 1.50, O_2= 0.84%, N_2=99.11%, RME = 0.05%)

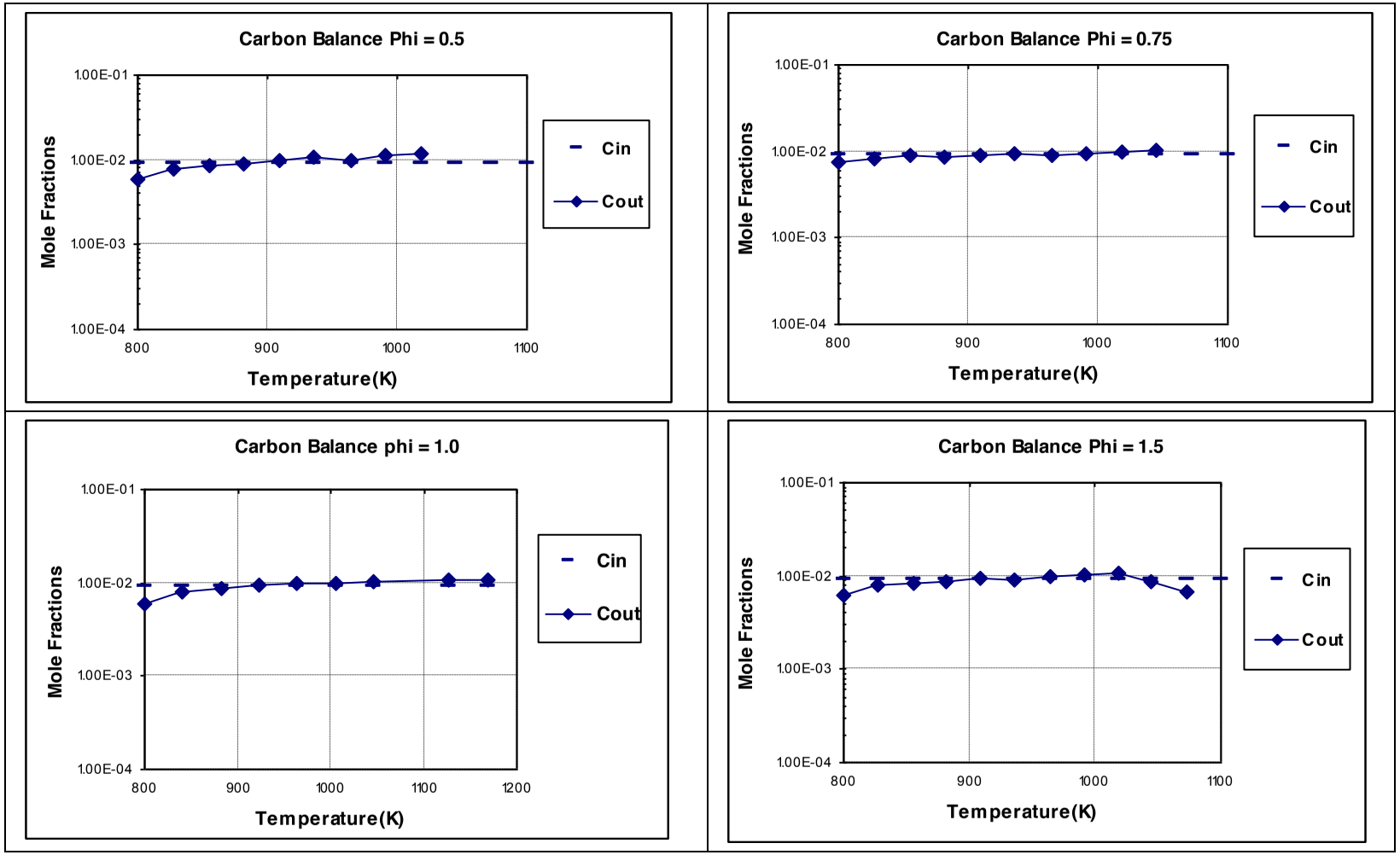

Figure 4.10: Carbon Balance for all equivalence ratios (τ =1s, Φ= 0.5, 0.75, 1.0, and 1.50)

The figures 4.6 to 4.9 show the RME oxidation results for fuel lean conditions (Φ= 0.5, 0.75) to fuel rich conditions (Φ= 1.0, 1.5). At 10 bar also RME reacted rapidly (compared to lighter fuels) yielding CO_2, the main combustion product, similar hydrocarbon and oxygenated intermediates as that from oxidation at 1bar. The change in reactivity and maximum mole fraction level of saturated and unsaturated compounds with respect to increasing equivalence ratio was also observed. It was observed that the reactivity decreases with increasing equivalence ratio and the level of mole fraction maxima of saturated and unsaturated compounds increases in fuel- rich environment. The major intermediate hydrocarbons observed at 10 bar are Ethylene (C_2H_4) followed by Methane (CH_4), Propene (C_3H_6), and Ethane (C_2H_6), where as the major oxygenated intermediate compound observed was Carbon Monoxide (CO). This observation is in agreement with work done by J.Pederson [4.6], Celine Morin [4.1] and F.Billaud [4.2], who worked on oxidation of Rapeseed oil methyl ester (RME) and pyrolysis of Methyl Oleate respectively.

Maximum Concentration	Φ = 0.50	Φ =0.75	Φ = 1.0	Φ = 1.5	Trends
Ethylene	4.50×10^{-4}	8.27×10^{-4}	1.01×10^{-3}	1.13×10^{-3}	↑
Methane	2.06×10^{-4}	4.22×10^{-4}	8.47×10^{-4}	1.12×10^{-3}	↑
Propene	6.16×10^{-5}	1.37×10^{-4}	1.29×10^{-4}	1.87×10^{-4}	↑
Ethane	8.07×10^{-6}	3.01×10^{-5}	6.62×10^{-5}	$8.27x\ 10^{-5}$	↑
CO_2	6.83×10^{-3}	4.87×10^{-3}	1.63×10^{-3}	1.23×10^{-3}	↓
CO	5.33×10^{-3}	5.91×10^{-3}	5.44×10^{-3}	5.60×10^{-3}	↑

Table 4.2: Maximum mole fractions of the major oxidation intermediates at 10 bars

From each plot (Figure 4.6 to 4.9) maximum concentrations of major intermediate gases were extracted and are presented in table 4.2. It was observed from graphs that RME is producing intermediate hydrocarbons like Ethylene,

Methane, Ethane and Propene, aromatics like Benzene (<10 ppm) and pollutant like 1,3-Butadiene (< 50 ppm) and Carbon Monoxide (CO) in lower quantity at fuel-lean conditions. The formation of aromatics in lesser quantity is similar to aromatics formation observed by Krahl and Munack [4.7]. The increase in CO concentration with increasing F/A ratio is similar to observations made by O.M.I Nwafor when he tested diesel engine with RME and its blends. It can be observed from graphs that the highest mole fractions of CO_2 were obtained in fuel-lean conditions. This indicates that combustion efficiency was higher at fuel-lean conditions than fuel-rich conditions. Figure 4.10 shows the carbon balance done for fuel-lean to fuel-rich conditions. It was observed that overall carbon balance was within the range of ± 5% for all fuel conditions especially after 850 K. As carbon calculates total carbon present in inlet fuel and total carbon present in all combustion products, it checks the effectiveness of the combustion.

4.3 The effect of Pressure and Temperature on RME oxidation

It was observed that RME reactivity increases with increasing temperature at 1 bar as well as 10 bar. This means emission of intermediates reduces with increasing temperature. Generally, all intermediates showed same profile trends at 1 bar as well as 10 bar. The main species identified during oxidation of RME at 1 atmosphere and 10 bar are identical but their maximum mole fractions changes with change in pressure and mean residence time (0.07s at 1bar and 1s at 10 bars). Table 4.3 shows maximum mole fractions of major intermediate hydrocarbons at 1 and 10 bar.

Table 4.3 shows that maximum mole fraction value is decreased at high pressure indicating that reactivity of RME is higher at high pressure than at low pressure. Thus RME is emitting alkenes, pollutants like 1,3-Butadiene, Formaldehyde and Benzene in lesser concentration at high pressure especially in fuel lean and stoichiometric conditions. This shows that RME has higher combustion efficiency at high pressure and fuel lean conditions. The CO concentration is decreasing at fuel rich condition for 1 bar, but there is no significance difference for 10 bar. RME has positive effect on CO emission. These findings are in line with those observed by Nwafor [4.5] who reported that CO emission increased with increasing F/A ratio. Similar CO concentration trends were observed at 1 bar and 10 bar experiments in this work. It has been observed

in some diesel engine combustion work higher concentrations of oxygen increases CO emissions [4.4]. This observation is consistent with the results presented in this work. The reduction in emission of hydrocarbon intermediates is important as they are a major contributor to atmospheric pollution and global warming. The aromatic compounds and aldehydes help to form deposits on engines. The reduction in emission concentration of these compounds shows that RME may reduce wear on engines, when combusted in diesel engine.

Compound	1bar (Φ)	10 bar(Φ)
	1.70×10^{-3} (0.5)	4.50×10^{-4} (0.5)
C_2H_4	1.92×10^{-3} (1.0)	1.01×10^{-3} (1.0)
	2.01×10^{-3} (1.5)	1.13×10^{-3} (1.5)
	3.23×10^{-4} (0.5)	6.41×10^{-5} (0.5)
C_3H_6	3.13×10^{-4} (1.0)	1.29×10^{-4} (1.0)
	3.30×10^{-4} (1.5)	1.87×10^{-4} (1.5)
	2.25×10^{-4} (0.5)	1.12×10^{-5} (0.5)
1,3- Butadiene	1.88×10^{-4} (1.0)	1.29×10^{-5} (1.0)
	2.16×10^{-4} (1.5)	2.44×10^{-5} (1.5)
	5.33×10^{-3} (0.5)	5.33×10^{-3} (0.5)
CO	4.93×10^{-3} (1.0)	5.44×10^{-3} (1.0)
	4.63×10^{-3} (1.5)	5.60×10^{-3} (1.5)
	1.04×10^{-2} (0.5)	6.83×10^{-3} (0.5)
CO_2	6.34×10^{-3} (1.0)	1.63×10^{-3} (1.0)
	4.01×10^{-3} (1.5)	1.43×10^{-3} (1.5)

Table 4.3: Maximum mole fractions of major intermediate hydrocarbon at 1bar and 10 bar

Though conditions used in this experimental work are not similar to diesel engine conditions, they produced similar emission trends for intermediates like those obtained from diesel engine work [4.5] [4.7]. The above experimental results show that RME gives better combustion performance at fuel lean conditions and higher temperature, especially at higher pressure. It is known fact that fuel lean mixtures are important in diesel engines [4.1]. Also diesel engines run at higher pressure and temperature. This implies that fuel-lean condition or higher Air/Fuel ratio is more suitable for RME combustion at higher pressure.

4.4 Ester Compounds from GC-MS

All samples obtained from RME oxidation experiments were analyzed on GC-MS for detecting hydrocarbon as well as oxygenated intermediates. The different types of compounds were detected including olefins, cyclic compounds, pollutant like 1,3-Butadiene and traces of Benzene. The prominent saturated and unsaturated esters like Methyl Butanoate were also detected. J.Pederson [4.6] observed similar oxygenated intermediate compounds when he oxidised Rapeseed oil methyl ester and Rapeseed oil with diesel fuel. Figure 4.11 shows different types of compounds obtained from GC-MS analysis.

The major saturated esters obtained from GC-MS analysis of RME oxidation are:

- Methyl Butanoate ($C_5H_{10}O_2$)
- 4-Pentanoic acid, methyl ester ($C_6H_{12}O_2$)
- 5-Hexanoic acid methyl ester ($C_7H_{14}O_2$)
- 6-Heptanoid acid methyl ester ($C_8H_{16}O_2$)

As explained in chapter 1 and 2, combustion kinetics of Biodiesel is investigated experimentally by carrying out the oxidation of Rapeseed oil methyl ester (RME) in a Jet stirred reactor and experimental database is generated. The experimental results showed similitude to diesel combustion. So it will be interesting to compare to these results with diesel oxidation in similar experimental set up. RME oxidation results need to be validated by using simulation approach. As RME structure is a complex mixture of long chain methyl esters (C_{14}-C_{22}), the surrogate fuel model approach can be used as a 1st step to simulate RME oxidation. The surrogate fuel model has been used by Dagaut previously to simulate the combustion kinetics of kerosene and diesel fuel [5.5]. However no surrogate fuel model approach has been used before to model oxidation of commercial biodiesel. Therefore, the oxidation of RME will be simulated using available surrogate fuel chemical kinetics mechanism.

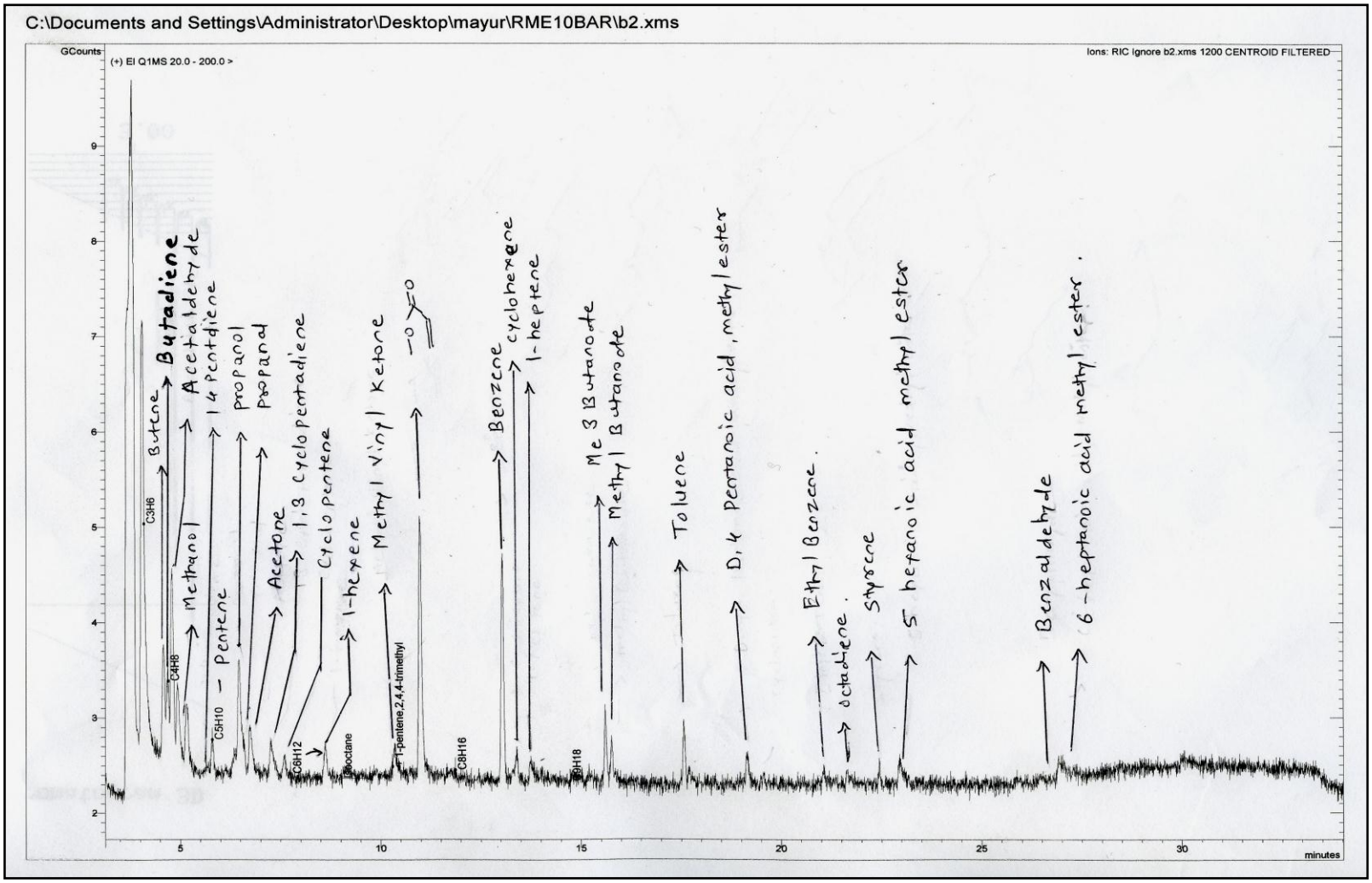

Figure 4.11: Chromatogram from GC-MS

References

4.1 Morin.C, Chauveau.C, Dagaut.P, Gokalp.I and Cathonnet.M, 2004, *Vaporization & Oxidation of liquid fuel droplets at high temperature and high pressure: Application to n-alkanes and vegetable oil methyl esters*, Combustion Science and Technology, 176, 499-529

4.2 Billaud.F and Archambault.D, 1999, *Experimental and modeling study of methyl oleate pyrolysis between 500 and 650 ^{0}C*, J.Chim.Phys, 96, 778-796

4.3 Labeckas.G, Slavinskas.S, 2006, *The effect of rapeseed oil methyl ester on direct injection Diesel engine performance and exhaust emissions*, Energy Conversion and Management, 47, Issue 13-14, 1954-1967

4.4 Makareviciene.V, Sendzikiene.E, Janulis.P, 2006, *Influence of fuel oxygen content on diesel engine exhaust emissions*, Renewable Energy, 31, 2505-2512

4.5 Nwafor.O.M.I, 2004, *Emission characteristics of diesel engine operating on rapeseed methyl ester*, Renewable Energy, 29, 119-129

4.6 Pedersen.R.J, Ingemarsson.A and Olsson.O.J, 1999, *Oxidation of Rapeseed oil, Rapeseed Methyl Ester (RME) and diesel fuel studied with GC/MS*, Chemosphere, 38, 11, 2467-2474

4.7 Krahl.J, Munack.A, Bahadir.M, Schumacher.L and Elser.N, 1996, *Review: Utilization of Rapeseed oil, Rapeseed Oil Methyl Ester or Diesel Fuel: Exhaust Gas Emissions and Estimation of Environmental Effects,* SAE Technical Paper Series Paper no: 962096

CHAPTER 5

COMPARISON WITH COMMERCIAL DIESEL

Chapter 4 described the results obtained from RME oxidation carried out at 1 and 10 bar. It also described the effect of pressure and temperature on RME oxidation and esters compounds obtained from GC/MS. The intermediates and pollutants obtained were similar to hydrocarbons and diesel engine combustion. It was also observed that RME gave better combustion performance at fuel-lean conditions and higher temperature, especially at higher pressure. This shows similarity to commercial diesel fuel combustion. So in this chapter RME oxidation is compared with commercial diesel fuel oxidation on experimental basis. Also the oxidation of RME was simulated using n-hexadecane ($C_{16}H_{34}$) and Methyl Acetate (CH_3COOCH_3) as surrogate model-fuels, which showed similar profile of intermediate and final combustion compounds.

5.1 Experimental Comparison with Commercial diesel fuel

The experimental results obtained from oxidation of RME (biodiesel) at 10 bar for stoichiometric conditions are compared with those obtained from oxidation of commercial diesel fuel. The initial concentration of commercial diesel fuel (the $C_{14.92}$) was scaled to match the initial concentration of carbon in the RME ($C_{17.92}$) experiments. Table 5.1 shows details of experimental conditions for RME and diesel oxidation.

Fuel	Formula	Pressure	Φ	Temperature K	%HC mol
RME	$C_{17.92}H_{33}O_2$	10 bar	1	800 to 1168	0.05%
Diesel	$C_{14.92}H_{29.6}$	10 bar	1	550 to 1175	0.0691%

Table 5.1: Experimental Conditions for RME and Diesel fuel oxidation

Here, the comparison will be done in the form of mole fractions of oxidation products as function of temperature and their profile trends. The graphs are plotted for following species:

- Oxygen, Carbon dioxide (CO_2) (final oxidation product)
- Carbon Monoxide (CO) (main oxygenated intermediate)

- Methane (CH_4), Acetylene (C_2H_2), Ethylene (C_2H_4), Propene (C_3H_6) (the main hydrocarbon intermediates observed in RME oxidation experiments)

The graph in figure 5.1 shows profile trends of intermediates and CO_2 obtained from oxidation of RME (Biodiesel) and commercial diesel. The early formation of CO_2 proves that RME reacted rapidly compared to commercial diesel. It can be seen that RME produces more CO_2 than that of Diesel over the initial temperature range. This early formation of CO_2 is due to presence of ester function ($COOCH_3$) in RME structure. Nwafor [5.3] also observed higher mole fraction of CO_2 from RME compared to diesel when running diesel engine on RME. As CO_2 is a final combustion product, formation of CO_2 in higher quantity indicates that RME gives efficient combustion. Actual proportion in mass between the carbons and hydrogen of RME is 6.5 compared to 6.9 in diesel, which may lead to more complete combustion of biofuels and consequently to higher engine efficiency [5.1] [5.2].

All intermediates obtained in these experiments show same profile trends as those observed from diesel oxidation. It can be seen that RME produced the same mole fractions of regulated pollutant CO and lower quantities of Acetylene (C_2H_2), Propene (C_3H_6) 1,3- Butadiene (C_4H_6) than that from diesel. The above trend is in agreement with results obtained from diesel engine run with RME, except RME produces lower emissions of hydrocarbons and aromatics [5.1] [5.3]. The graph in figure 5.1 shows that RME (Biodiesel) gives combustion performance similar to commercial diesel fuel and it produces same types of intermediate species.

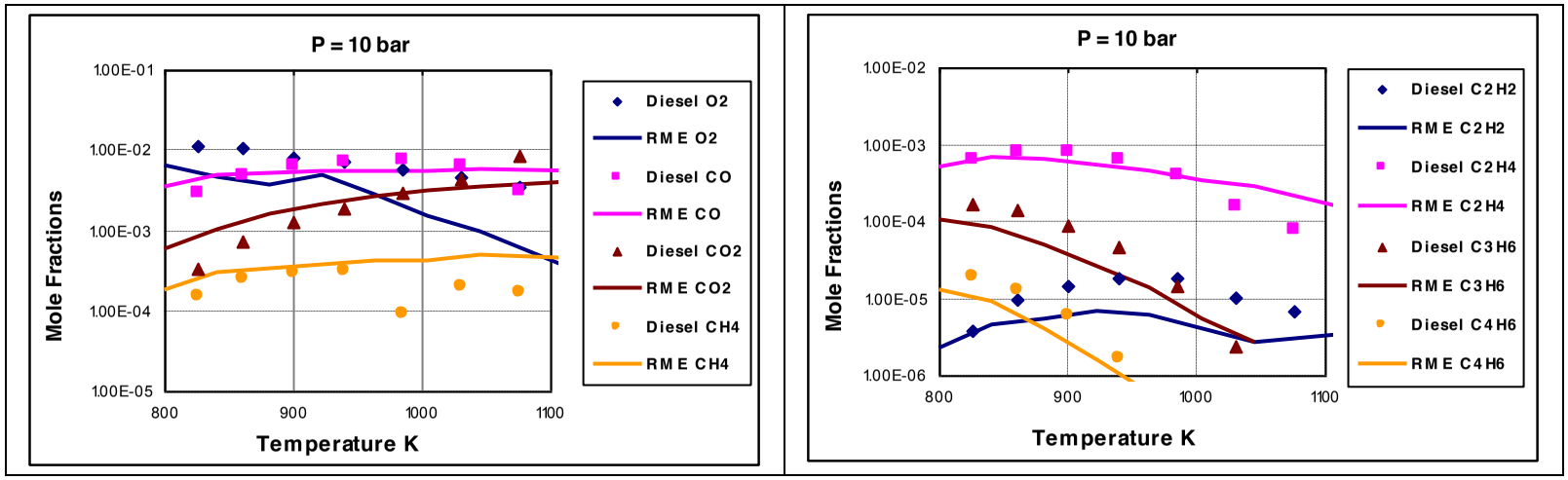

Figure 5.1: Mole fraction profiles of intermediates from oxidation of RME and commercial diesel

5.2 Modeling with surrogate fuels (n-Hexadecane)

The oxidation of RME ($C_{18}H_{34}O_2$) was carried out in a Jet-stirred reactor. The experimental results showed strong similarities to combustion of large n-alkanes and commercial diesel. However these experimental results have to be validated by using simulation approach. As RME structure is a complex mixture of long chain methyl esters (C_{14}-C_{22}), the surrogate model-fuel approach used by Dagaut previously to simulate the combustion kinetics of kerosene and diesel fuel, was followed [5.5]. No surrogate fuel model approach has been used before to model oxidation of such long chain (C_{18}) biodiesel. Therefore, the oxidation of RME was simulated using n-hexadecane ($C_{16}H_{34}$) and methyl acetate (CH_3COOCH_3) as a surrogate model-fuel. The combined n-Hexadecane and Methyl Acetate mechanism will represent long carbon chain and ester function present in structure of RME.

The global chemical formula of n-Hexadecane is $C_{16}H_{34}$. The initial carbon concentration of n-Hexadecane (C_{16}), the surrogate fuel, was scaled to match the initial concentration of carbon in the RME (C_{18}) experiments. The mechanism used here is a detailed chemical kinetic reaction mechanism used for modeling oxidation of n-Hexadecane in a Jet Stirred Reactor [5.4]. It includes high temperature combustion chemistry and pressure-dependencies of unimolecular reactions and of some pressure-dependent bimolecular reactions, where it was appropriate to do so.

The computations were performed using CHEMKIN package and the Perfectly Stirred Reactor (PSR) computer code that estimates species concentrations from the balance between the net rate of production of each species by chemical reaction and the difference between the input and output flow rates of each species. These rates were computed from the kinetic scheme and the rate constants of the elementary reactions calculated at the experimental temperature, using the modified Arrhenius equation:

$$\mathbf{k = A\ T^{b}\ exp(-E/RT)} \qquad (5.1)$$

The schematic diagram for CHEMKIN package with PSR code (Figure 6.1) is presented in chapter 6. The rate constants for reverse reactions

were computed from the corresponding forward rate constants and the appropriate equilibrium constants. The equilibrium constants were calculated by PSR code itself.

$$\mathbf{K_c = k_{forward} / k_{reverse}} \qquad (5.2)$$

The n-Hexadecane reaction mechanism consisted of 225 species & 1841 reversible reactions. The PSR code along with CHEMKIN is described in chapter 6 in detail.

5.2.1 Results at 1 bar

The modeling for RME using n-hexadecane mechanism was done at 1 bar for fuel-lean to fuel-rich conditions (Φ = 0.5 to 1.5), for temperature range of 900 to 1400K. The modeling results were compared with experimental results. The graphs are plotted for oxygenated compounds and olefins (C_2 to C_6). The mole fractions of reactants, intermediates and products were plotted (Figure 5.2 to 5.4) against the temperature. The mole fractions were obtained for oxygen, hydrogen, carbon monoxide (CO),carbon dioxide (CO_2), formaldehyde (CH_2O), methane(CH_4), ethane (C_2H_6), ethene (C_2H_4), acetylene (C_2H_2), propene (C_3H_6),1-butene (1-C_4H_8),1-pentene (1-C_5H_{10}), 1-hexene (1-C_6H_{12}), 1-heptene (C_7H_{14}) and 1,3- butadiene (1,3-C_4H_6). The other compounds detected had low mole fractions (≤ 1 ppm).

Figure 5.2 to 5.4 shows simulation results along with experimental results for fuel-lean to fuel-rich (Φ= 0.5 to 1.5) conditions. The model gives a good description of the experimental results in terms of mole fractions of products and similar profile trends. Overall qualitatively model is predicting experimental results with some discrepancies at lower temperature. The model confirmed the experimental observation that mole fractions of intermediates (saturated, unsaturated as well as oxygenated) reached a maximum value at higher temperature with increasing equivalence ratio.

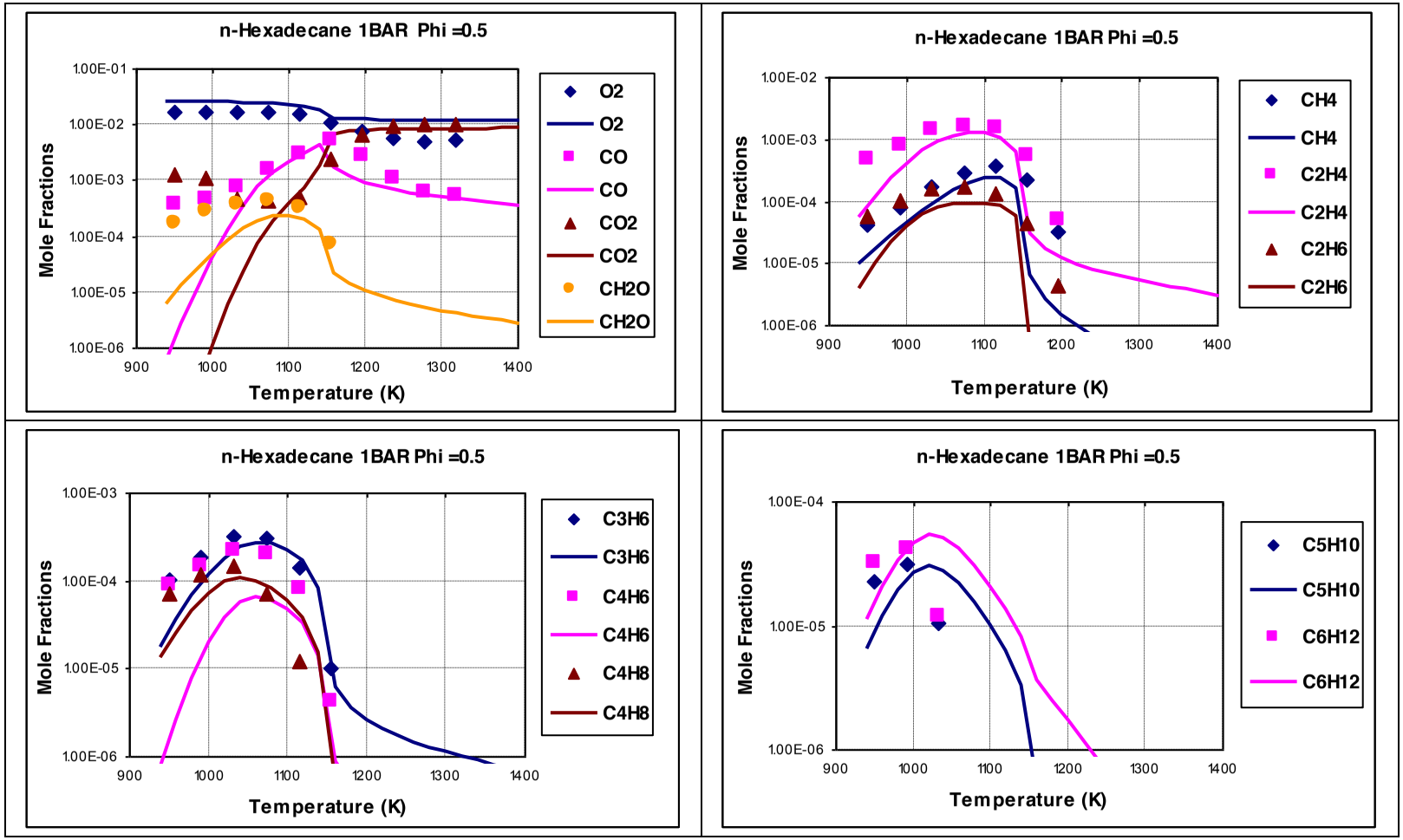

Figure 5.2: The oxidation of RME in a JSR (P = 1bar, Φ = 0.5, τ =0.07 s). The experimental data (large symbols) are compared to the computations (lines surrogate model fuel: n-$C_{16}H_{34}$)

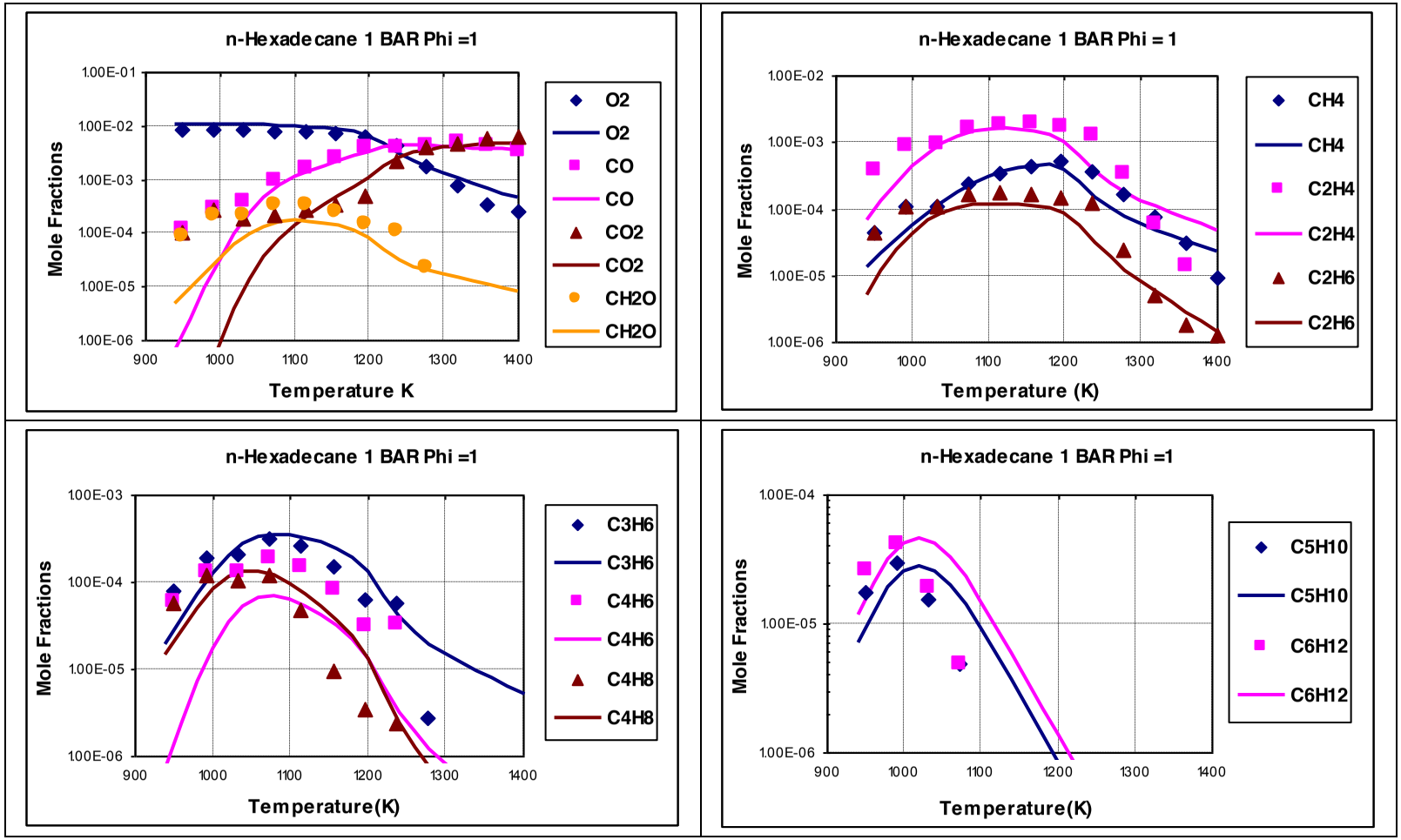

Figure 5.3: The oxidation of RME in a JSR (P = 1bar, Φ = 1, τ = 0.1 s). The experimental data (large symbols) are compared to the computations (lines surrogate model-fuel: n-$C_{16}H_{34}$)

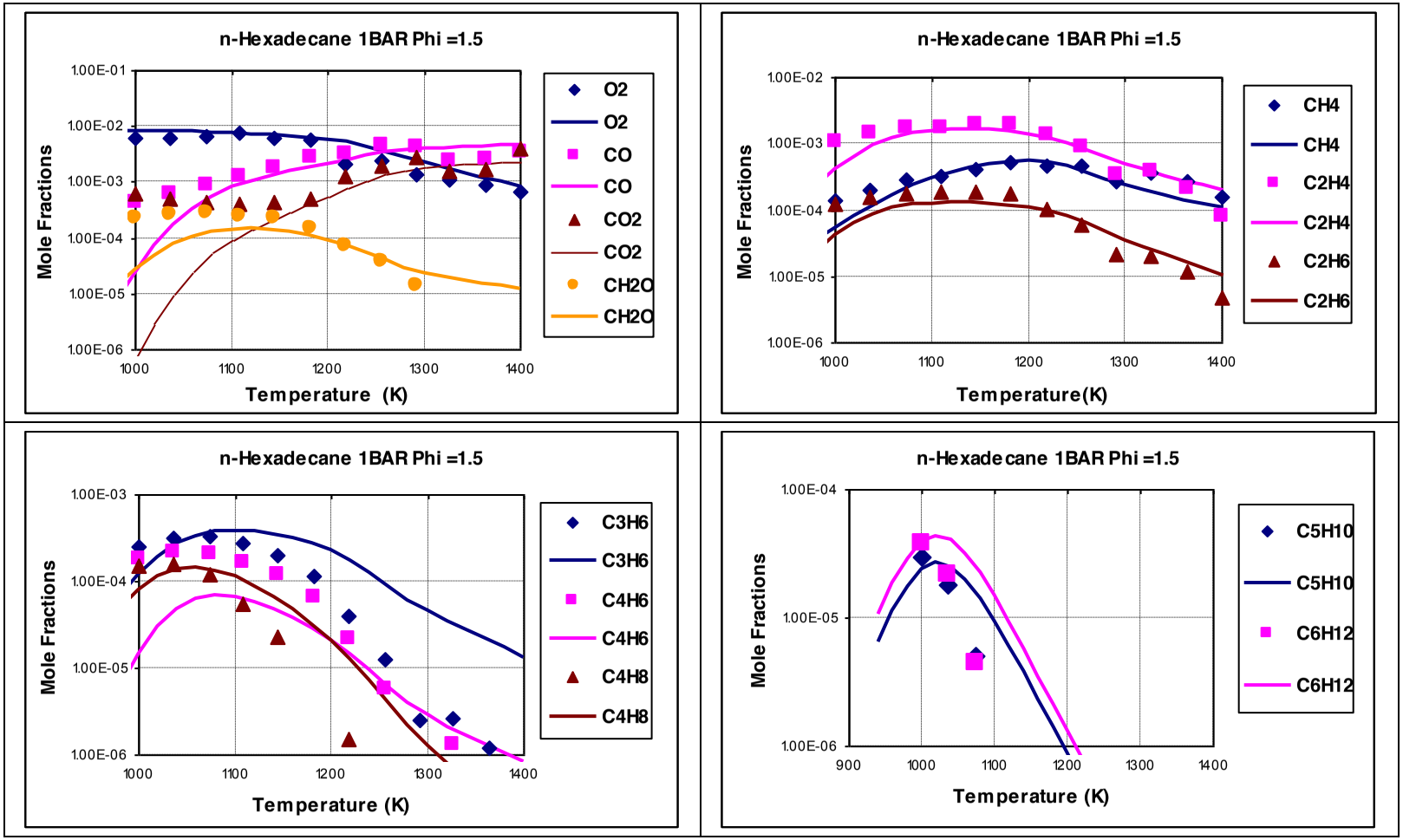

Figure 5.4: The oxidation of RME in a JSR (P = 1 bar, Φ = 1.5, τ = 0.1 s). The experimental data (large symbols) are compared to the computations (lines surrogate model-fuel: n-$C_{16}H_{34}$)

It was observed that intermediates reached maximum mole fractions value particularly in temperature range of 1000 to 1200 K. Regarding the reactivity of RME, again, a good agreement between the data and the model (in terms of profile trends) was obtained. Reactivity can be defined as capacity of atom or molecule to undergo chemical reaction with another atom or molecule. Reactivity refers to rate at which molecule tends to undergo chemical reaction in time. At fuel-lean condition ($\Phi = 0.5$) the maxima in mole fractions of intermediates were lower than measured indicating a higher reactivity. Table 5.2 shows the effectiveness of model in terms of comparison between the maximum mole fractions of major compounds obtained from experiments and simulation. It can be seen from the table the difference in maximum mole fractions is very less.

Compounds	Expt. Max Concn $\Phi = 0.5$	Sim. Max Concn $\Phi = 0.5$	Expt. Max Concn $\Phi = 1.0$	Sim. Max Concn $\Phi = 1.0$	Expt. Max Concn $\Phi = 1.5$	Sim. Max Concn $\Phi = 1.5$
C_2H_4	1.70×10^{-3}	1.27×10^{-3}	1.92×10^{-3}	1.60×10^{-3}	2.01×10^{-3}	1.69×10^{-3}
CH_4	3.64×10^{-4}	2.38×10^{-4}	5.20×10^{-4}	4.53×10^{-4}	5.38×10^{-4}	5.45×10^{-4}
C_3H_6	3.23×10^{-4}	2.72×10^{-4}	3.13×10^{-4}	3.51×10^{-4}	3.30×10^{-4}	3.86×10^{-4}
C_4H_6	2.25×10^{-4}	6.52×10^{-5}	1.88×10^{-4}	6.80×10^{-5}	2.16×10^{-4}	6.85×10^{-5}
CO_2	1.04×10^{-2}	8.31×10^{-3}	6.34×10^{-3}	4.79×10^{-3}	4.01×10^{-3}	2.29×10^{-3}
CO	5.33×10^{-3}	4.15×10^{-3}	4.93×10^{-3}	4.37×10^{-3}	4.63×10^{-3}	4.57×10^{-3}
CH_2O	4.21×10^{-4}	2.27×10^{-4}	3.42×10^{-4}	1.68×10^{-4}	2.83×10^{-4}	1.41×10^{-4}

Table 5.2: Comparison between maximum mole fractions for major compounds from experiments and simulation at 1 bar

As the model reproduced the formation of intermediate hydrocarbons (1-olefins) at an initial temperature, this shows that the fuel reacted very rapidly at these conditions. However the model was not able to reproduce the early formation of oxygenated intermediates such as CO and CH_2O. The model under estimated the formation of CO_2 at the initial temperature for all the fuel conditions (lean to rich). Very good agreement for lighter saturated and unsaturated hydrocarbons (C_1 to C_4) was obtained at all conditions. The model under predicted the formation 1,3 Butadiene (1,3 C_4H_6) for all the fuel conditions. It also over predicted the formation of olefins like 1-pentene (1-C_5H_{10}), 1-hexene (1-C_6H_{12}) at higher temperature i.e. 1100 K. The formation of these olefins above 1100 K indicates that model under predicted reactivity of RME at higher temperature.

5.2.2 Results at 10 bars

The modeling for RME using n-hexadecane mechanism was done at 10 bar for fuel-lean to fuel-rich conditions (Φ = 0.5 to1.5), for temperature range of 800 to 1200K. The results were plotted for oxygenated compounds and olefins (C_2 to C_6). Figure 5.5 to 5.7 shows simulation results with experimental results for fuel-lean to fuel-rich (Φ = 0.5 to1.5) conditions.The model gives a good description of the experimental results in terms of profile trends of reactants, intermediates and products. Though model is able to reproduce profile trends of intermediates, it fails to reproduce the molar concentration of hydrocarbons especially 1-alkenes (Figure 5.6 and 5.7). Regarding the reactivity of RME, again, a good agreement between the data and the model was obtained. The modeling also supported increase in reactivity with increasing pressure. Table 5.3 shows the effectiveness of model in terms of comparison between the maximum mole fractions of major compounds obtained from experiments and simulation. It can be seen from the table 5.3 that the model is not reproducing maximum mole fractions of intermediate hydrocarbons in exact manner especially at fuel lean conditions.

Compounds	Expt. Max Concn Φ = 0.5	Sim. Max Concn Φ = 0.5	Expt. Max Concn Φ = 1.0	Sim. Max Concn Φ = 1.0	Expt. Max Concn Φ = 1.5	Sim. Max Concn Φ = 1.5
C_2H_4	4.50×10^{-4}	7.78×10^{-4}	1.01×10^{-3}	8.84×10^{-4}	1.13×10^{-3}	9.30×10^{-4}
CH_4	2.06×10^{-4}	1.27×10^{-4}	8.47×10^{-4}	3.50×10^{-4}	1.12×10^{-3}	6.54×10^{-4}
C_3H_6	6.16×10^{-5}	3.33×10^{-4}	1.29×10^{-4}	3.22×10^{-4}	1.87×10^{-4}	3.05×10^{-4}
C_2H_6	8.07×10^{-6}	2.09×10^{-5}	6.62×10^{-5}	5.89×10^{-5}	$8.27x\ 10^{-5}$	$8.53x\ 10^{-5}$
CO_2	6.83×10^{-3}	8.60×10^{-3}	1.63×10^{-3}	5.20×10^{-3}	1.23×10^{-3}	2.73×10^{-3}
CO	5.33×10^{-3}	3.60×10^{-3}	5.44×10^{-3}	3.31×10^{-3}	5.60×10^{-3}	3.40×10^{-3}

Table 5.3: Comparison between maximum mole fractions for major compounds from experiments and simulation at 10 bar

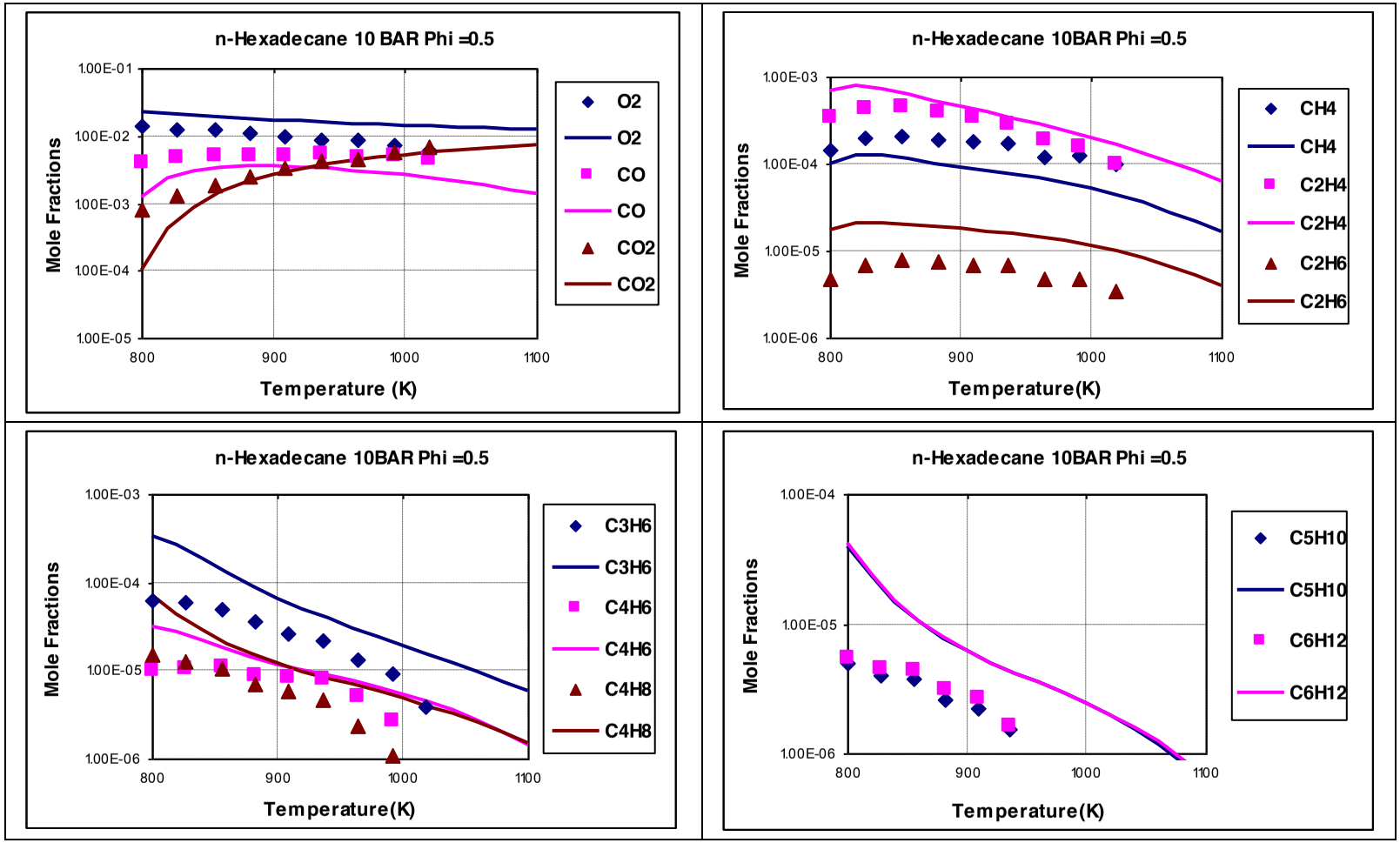

Figure 5.5: The oxidation of RME in a JSR (P = 10bar, Φ = 0.5, τ = 1 s). The experimental data (large symbols) are compared to the computations (lines surrogate model-fuel: n-$C_{16}H_{34}$)

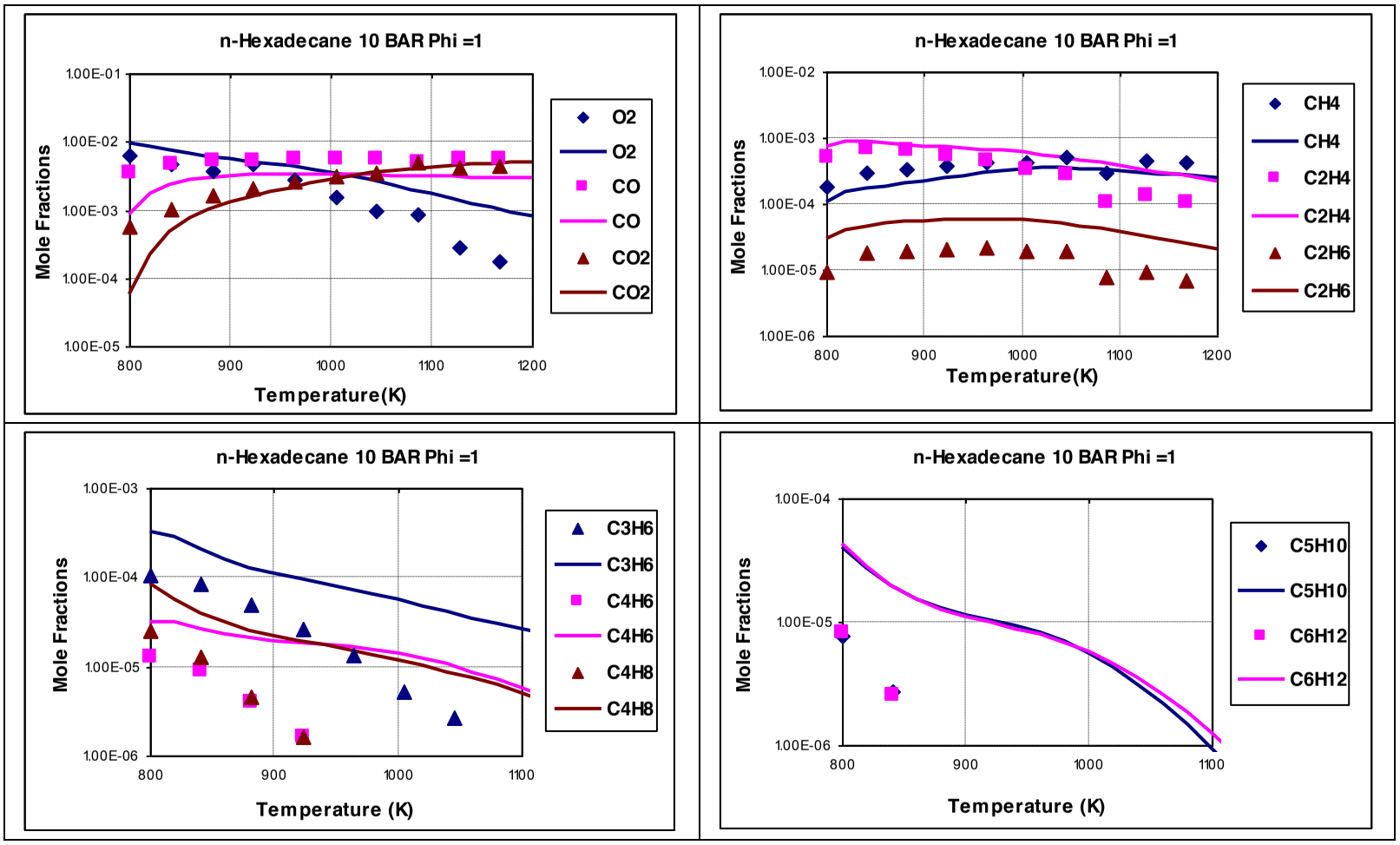

Figure 5.6: The oxidation of RME in a JSR (P = 10bar, Φ = 1, τ = 1 s). The experimental data (large symbols) are compared to the computations (lines surrogate model-fuel: n-$C_{16}H_{34}$)

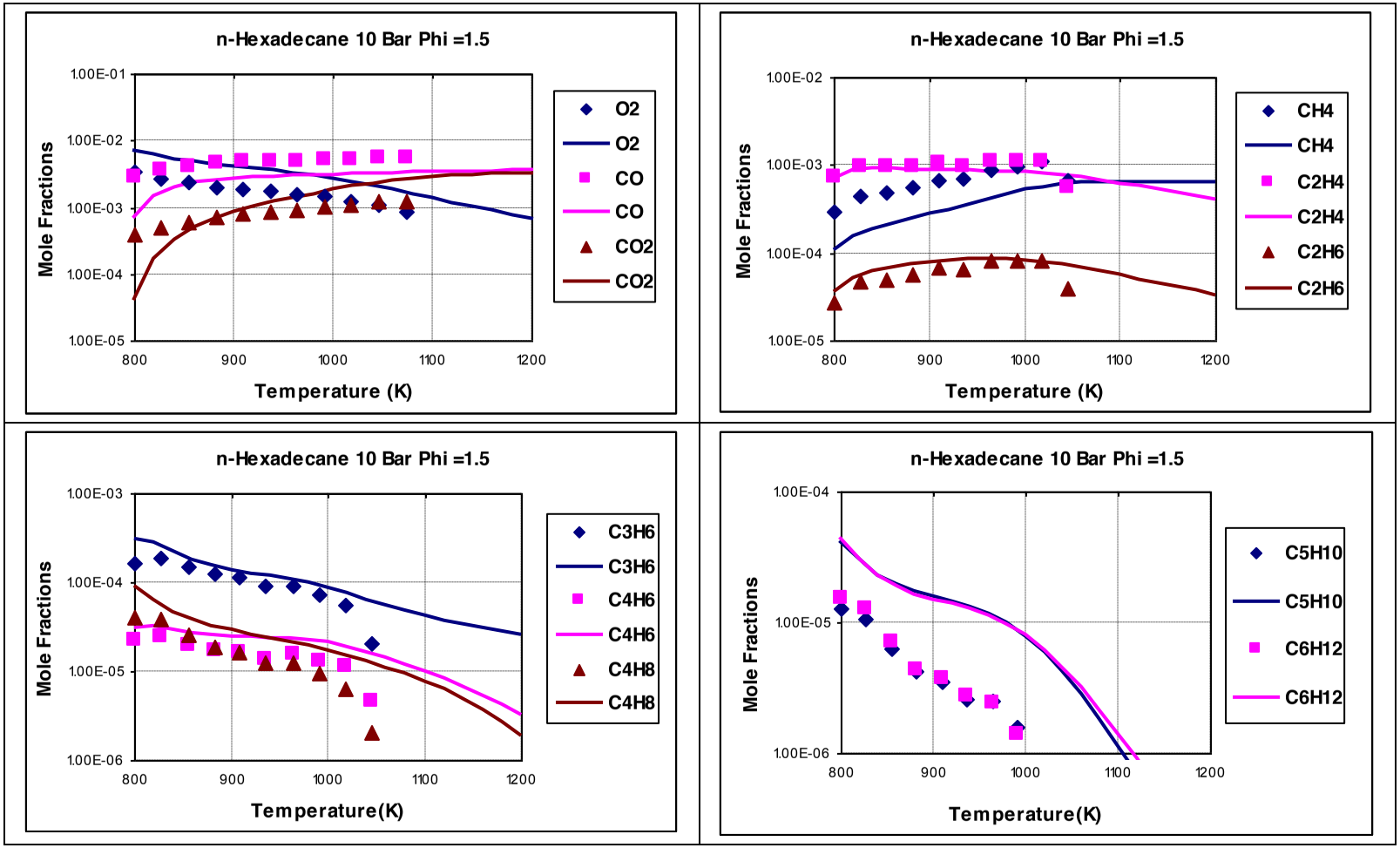

Figure 5.7: The oxidation of RME in a JSR (P = 10 bar, Φ = 1.5, τ = 1 s). The experimental data (large symbols) are compared to the computations (lines surrogate model-fuel: n-$C_{16}H_{34}$)

When results were plotted for fuel-lean to fuel-rich conditions it was observed that intermediates reached maximum mole fractions value particularly in temperature range of 800 to 1000 K indicating lower reactivity. At fuel-lean condition (Φ = 0.5) the maxima in mole fractions of intermediates were lower indicating a higher reactivity (Figure 5.5). At all fuel conditions model is able to reproduce early formation of CO and CO_2, however it over predicted CO_2 at higher temperature for fuel rich conditions.

At fuel lean conditions (Φ = 0.5) the model predicted molar profile trend for C_2H_4, C_4H_6 in agreement with measured, but it under predicted formation of CH_4. It also over-estimated the formation of lighter hydrocarbons; C_2H_6, C_3H_6 and C_4H_8. At stoichiometric conditions (Φ = 1) the model predicts well the formation of CH_4 and C_2H_4 however, it over-estimates the formation of C_3H_6, C_4H_6 and C_4H_8. At fuel rich conditions (Φ = 1.5) model predicts well the formation of C_2H_4, C_2H_6, C_3H_6 and C_4H_6, however over-estimates the mole fractions of CH_4 and C_4H_8. At all fuel conditions model fails to reproduce experimental results for 1-Pentene (1-C_5H_{10}) and 1-Hexene (1-C_6H_{12}). The model over predicted the formation of these compounds for fuel-lean as well as fuel-rich conditions. The main path for formation of 1-Pentene and 1-Hexene is β-scission reaction of n-Hexadecane radicals, where as they are mainly consumed in producing smaller alkyl radicals (C_2-C_3). The graphs (Figure 5.6 & 5.7) for intermediate and fuel-rich conditions showed (Φ = 1 & 1.5) the reactivity of RME was decreasing from fuel-lean to fuel-rich conditions.

Overall n-Hexadecane model reproduced the formation of intermediates and products. The mole fractions of reactants, intermediates and products are in agreement with experimentally measured. The over prediction of 1-Pentene and 1-Hexene by model is may be due to absence of unsaturation in n-Hexadecane structure. Also dienes (1,3 Butadiene) are formed mainly from metathesis reactions of unsaturated hydrocarbons. Metathesis reactions consist of reactions with radicals like OH, H , HO_2. CH_3, C_2H_3 and extracting H from parent molecule. As n-Hexadecane has only saturated alkyl chain in its structure, model with n-Hexadecane is not able to reproduce these olefins in exact manner.

The under prediction of mole fraction for CH_2O and CO is may be due to absence of the carbonyl group and unsaturation in structure of n-Hexadecane. Also, the early formation of carbon dioxide in the experiments is not reproduced by the model, probably due to the pyrolysis of the ester group, as already reported by others studying the combustion of large methyl esters such as Methyl Oleate, Methyl Decanoate [5.8]. The reactions responsible for carbon dioxide early production are of the type:

$$C_nH_mC(=O)OCH_3 \Rightarrow C_nH_mC(=O)O^{\bullet} + CH_3 \quad (5.3)$$

$$C_nH_mC(=O)O^{\bullet} \Rightarrow C_{n-1}H_{m-2}C^{\bullet}H_2 + CO_2 \quad (5.4)$$

The radical formed in reaction 5.3 further decomposes to produce CO_2 and an alkyl radical. This alkyl radical and radical formed in reaction 5.4 further a undergoes number of reactions such as thermal decomposition, reaction with molecular oxygen, chain- propagating reactions consisting of Metathesis reactions, to form smaller alkyl radicals, olefins, alkenyl and diene radicals.

It is observed from diesel engine combustion that concentration of pollutants in exhaust depends on oxygen content of fuel mixtures [5.2]. Also, when diesel engine is fueled with diesel fuel with higher oxygen content, the level of exhaust emission is decreased compared to that from only diesel [5.6]. All RME combustion studies indicate that RME reduces intermediate hydrocarbon emissions. Also the carbonyl group present in ester function of RME promotes formation of Aldehydes [5.7]. So to simulate RME combustion in precise manner, model containing long carbon chain as well as ester group should be used.

5.3 Modeling with n-Hexadecane + Methyl Acetate as model fuel

The modeling with n-hexadecane under predicted the formation of CO and CH_2O. It also failed to reproduce the early formation of CO_2 as detected in the experiments. This early formation of CO_2 is thought to be due to pyrolysis of ester group present in RME structure. Therefore oxidation of RME was simulated using combined oxidation reaction mechanism of n-Hexadecane and Methyl Acetate (CH_3COOCH_3), in an attempt to represent the ester group present in RME structure. The reason for including Methyl Acetate (MA) is that it is a reaction intermediate formed during pyrolysis of methyl esters from rapeseed oil [5.9]. The

chemical kinetic reaction sub-mechanism for oxidation of MA is that used previously by Dagaut et al [5.9]. The thermochemical data for MA and related compounds were computed using THERGAS code. THERGAS is a computer program in CHEMKIN package used for the evaluation of thermochemical data of molecules and free radicals in gas phase. THERGAS code is explained in CHEMKIN section of chapter 6. The combined mechanism consists of 306 species and 1863 reversible reactions.

Here, only reaction sub-mechanism for MA developed by Dagaut et.al is presented. The reaction sub-mechanism was available from Dr. Philippe Dagaut. The reaction sub-mechanism consists of thermal decomposition reactions of MA yielding ketene and methanol (reaction 5.5), acetyl and methyl radicals (reaction 5.6). Acetyl radical (MECOO) then decomposes to give carbon dioxide and methyl radical (reaction 5.7). The sub-mechanism also includes metathesis reactions with O_2, HO_2, OH, H, O, CH_3 and CH_3O (reactions 5.8 to 5.14 and 5.17 to 5.23). The two radicals (CH_3COOCH_2 and CH_2COOCH_3) formed from metathesis reactions, decompose (5.15, 5.24) or react with molecular oxygen (5.16, 5.25-5.26) [5.3] to produce formaldehyde and other radicals.

The reaction sub-mechanism for oxidation of methyl acetate is:

Reactions	**Reaction No**
MECOOME=CH2CO+CH3OH	5.5
MECOOME=MECOO+CH3	5.6
MECOO=>CH3+CO2	5.7
MECOOME+O2=MECOOMY+HO2	5.8
MECOOME+HO2=MECOOMY+H2O2	5.9
MECOOME+OH=MECOOMY+H2O	5.10
MECOOME+H=MECOOMY+H2	5.11
MECOOME+O=MECOOMY+OH	5.12
MECOOME+CH3=MECOOMY+CH4	5.13
MECOOME+CH3O=MECOOMY+CH3OH	5.14
MECOOMY=CH3CO+CH2O	5.15
MECOOMY+O2=>CH2CO+CH2O+HO2	5.16
MECOOME+O2=MYCOOME+HO2	5.17
MECOOME+HO2=MYCOOME+H2O2	5.18
MECOOME+OH=MYCOOME+H2O	5.19
MECOOME+H=MYCOOME+H2	5.20
MECOOME+O=MYCOOME+OH	5.21
MECOOME+CH3=MYCOOME+CH4	5.22
MECOOME+CH3O=MYCOOME+CH3OH	5.23

MYCOOME=CH2CO+CH3O	5.24
MYCOOME+O2=>PROD1+OH	5.25
PROD1=>CH2O+CH2O+CO	5.26
MYCOOME+MYCOOME=C6H10O4	5.27
MECOOMY+MYCOOME=C6H10O4	5.28
MECOOMY+MECOOMY=C6H10O4	5.29

Where,

MECOOME = Methyl Acetate (CH_3COOCH_3)

MECOOMY = $CH_3C(O)CH_2$ MYCOOME = $CH_2C(O)OCH_3$

MECOO = $CH_3C(O)O$ PROD1 = $OCH_2C(O)OCH_2$

5.3.1 Results at 1 bar

The modeling for RME combustion using n-hexadecane and methyl acetate was done at 1 bar for fuel-lean to fuel-rich conditions (Φ = 0.5 to 1.5), for temperature range of 900 to 1400K. The results in the form of mole fractions of all compounds in the product gas as function of temperature of the combustion are plotted in Figure 5.8 to 5.10. The compounds obtained are similar to those from n-hexadecane simulation work. The proportion of n-Hexadecane and Methyl Acetate considered in model fuel was 80 % n-Hexadecane and 20 % Methyl-Acetate on mol basis.

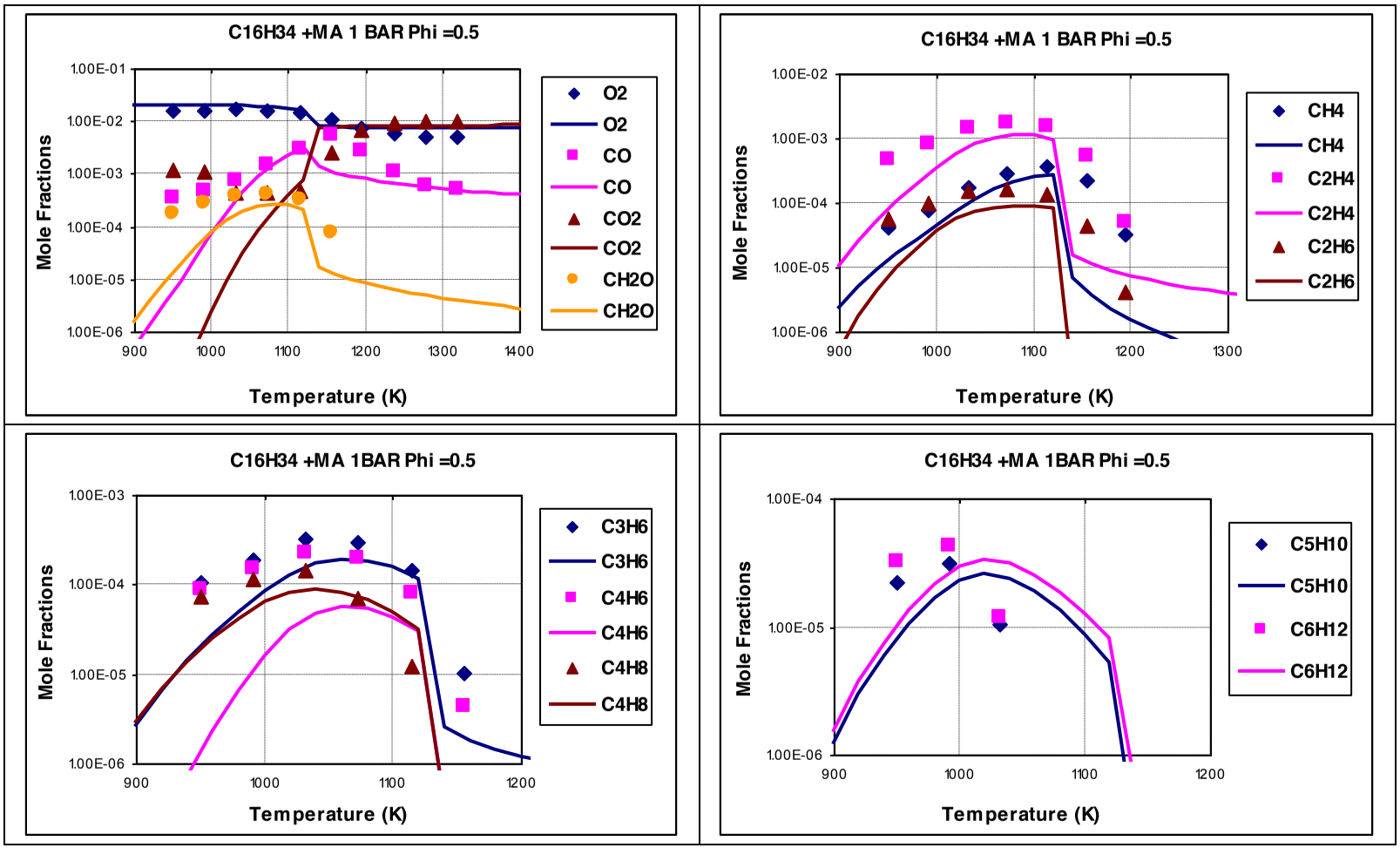

Figure 5.8: The oxidation of RME in a JSR (P = 1bar, Φ = 0.5, τ = 0.07 s). The experimental data (large symbols) are compared to the computations (lines surrogate model-fuel: n-$C_{16}H_{34}$ + MA)

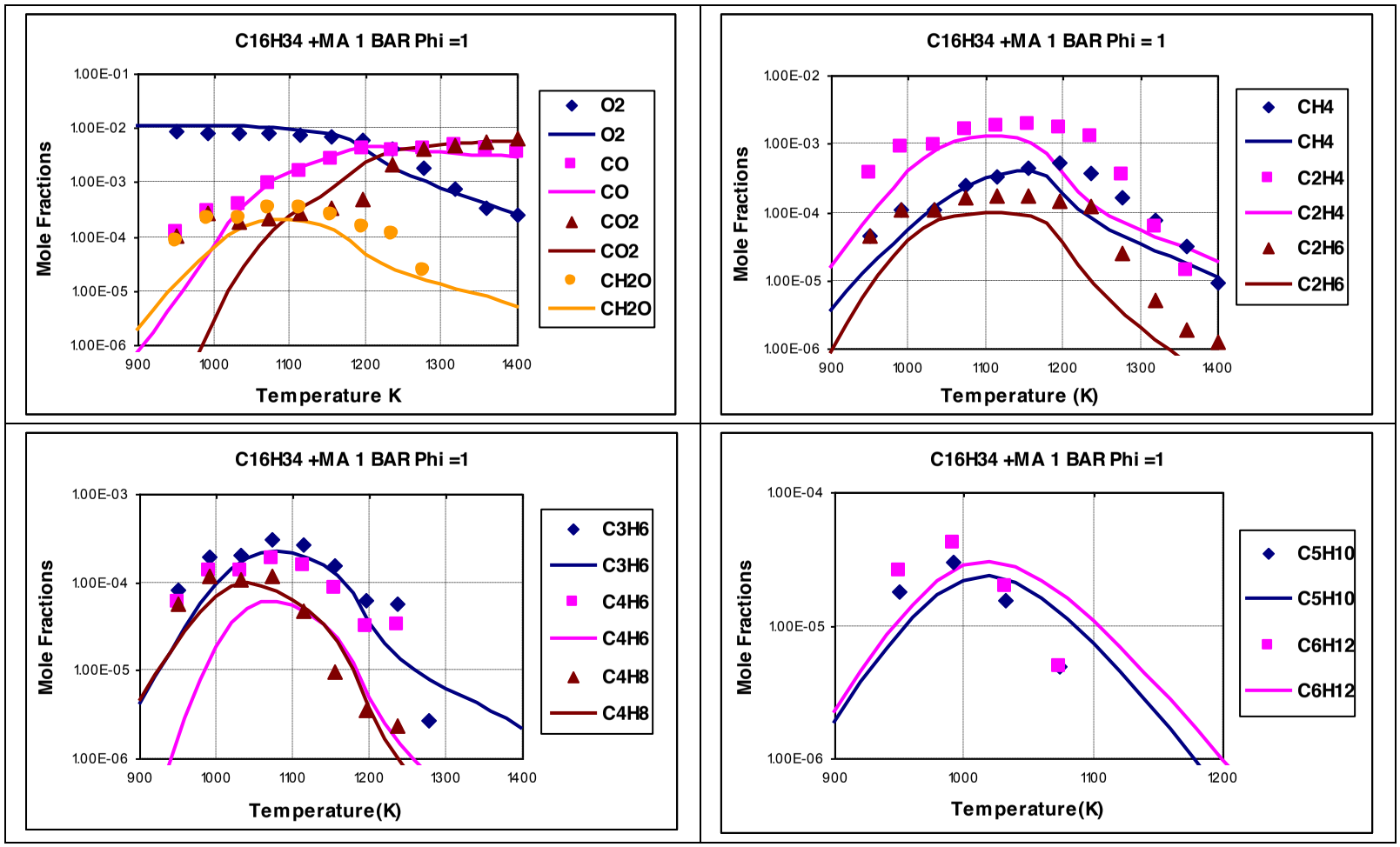

Figure 5.9: The oxidation of RME in a JSR (P = 1bar, Φ = 1, τ = 0.1 s). The experimental data (large symbols) are compared to the computations (lines surrogate model-fuel: n-$C_{16}H_{34}$ + MA)

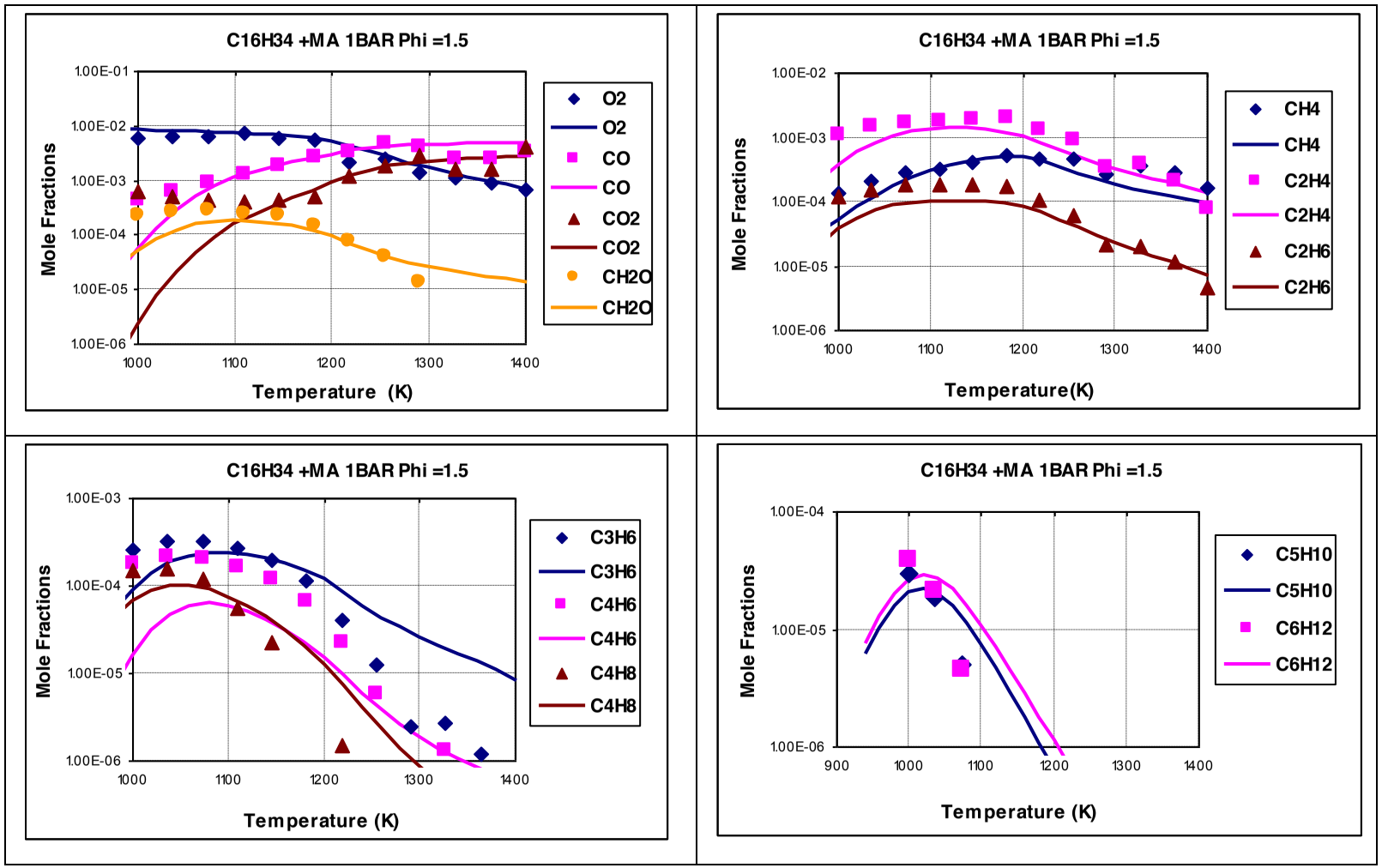

Figure 5.10: The oxidation of RME in a JSR (P = 1bar, Φ = 1.5, τ = 0.1 s). The experimental data (large symbols) are compared to the computations (Lines surrogate model-fuel: n-$C_{16}H_{34}$ + MA)

The modeling results were compared with experimental results. The model gives a description of the experimental results like n-hexadecane in terms of mole fractions of products and similar profile trends. Regarding the reactivity of RME, again, this combined model gives agreement between the data and the model (in terms of profile trends) similar to that from n-hexadecane model.

When graphs were plotted for fuel- lean (Φ = 0.5) to fuel-rich conditions (Φ =1.5) (Figure 5.8 to 5.10), it was observed that the reactivity was again higher at fuel-lean conditions and decreases with an increase in equivalence ratio. Overall this combined model predicted concentration profiles satisfactory for reactants and all hydrocarbon intermediates. Very good modeling of the relative importance of the olefins (C_2 to C_6) was obtained especially at fuel-rich conditions. However, the model under predicted the formation of 1,3-Butadiene (C_4H_6) at all conditions. This is thought to be due to the absence of unsaturated compounds in the fuel mixture. The formation of 1-Pentene (C_5H_{10}) and 1-Hexene (C_6H_{12}) by simulation is improved at all the fuel conditions compared to that obtained from n-Hexadecane.

The model reproduced the formation of formaldehyde (CH_2O) especially at fuel-rich conditions compared to that obtained from n-hexadecane mechanism. However it failed to reproduce early formation of CH_2O at fuel lean conditions. The model also failed to predict early formation of CO_2 for all fuel conditions, whereas profile trend for Carbon monoxide (CO) is improved compared to that obtained from n-hexadecane mechanism. The reason for this improvement in profile trends is MA rapidly produces formaldehyde, CO and lower hydrocarbons (C_1-C_3) during its oxidation.

5.3.2 Results at 10 bar

The modeling for RME combustion using n-hexadecane and methyl acetate as the reaction mechanism was also done at 10 bar for fuel-lean to fuel-rich conditions (Φ = 0.5 to 1.5), over temperature range of 800 to 1200K. Figure 5.11 to 5.13 show the results of n-Hexadecane + MA simulation compared to actual experimental results. The model is describing the experimental results in similar way like n-hexadecane model in terms of profile trends of reactants, intermediates and products. Regarding the reactivity of RME, again, a good

agreement between the data and the model (in terms of profile trends) was obtained similar to that from n-hexadecane.

When graphs were plotted for fuel-lean to fuel- rich conditions (Figure 5.11 to 5.13) it was observed that mole fractions of intermediates (saturated, unsaturated as well as oxygenated) reached their maxima in the temperature range of 800-1000 K. This model also showed that reactivity increased with increasing pressure, decreased with increasing equivalence ratio. The reactivity was higher in fuel-lean condition than fuel-rich condition, similar to that observed from n-hexadecane mechanism. Overall the model predicted similar concentration profiles for reactants, all intermediates and products like that from n-hexadecane. However the model over predicted the mole fractions for 1-C_5H_{10} and 1-C_6H_{12} compared to experimental measurements for all fuel conditions. Also the model over predicted mole fractions for C_3H_6 and C_2H_4 in fuel lean conditions, even though the trend for 1,3-Butadiene (C_4H_6) was improved. The model gives a good description of CO formation, but early formation of CO_2 is still not predicted to a degree that provides 100% confidence.

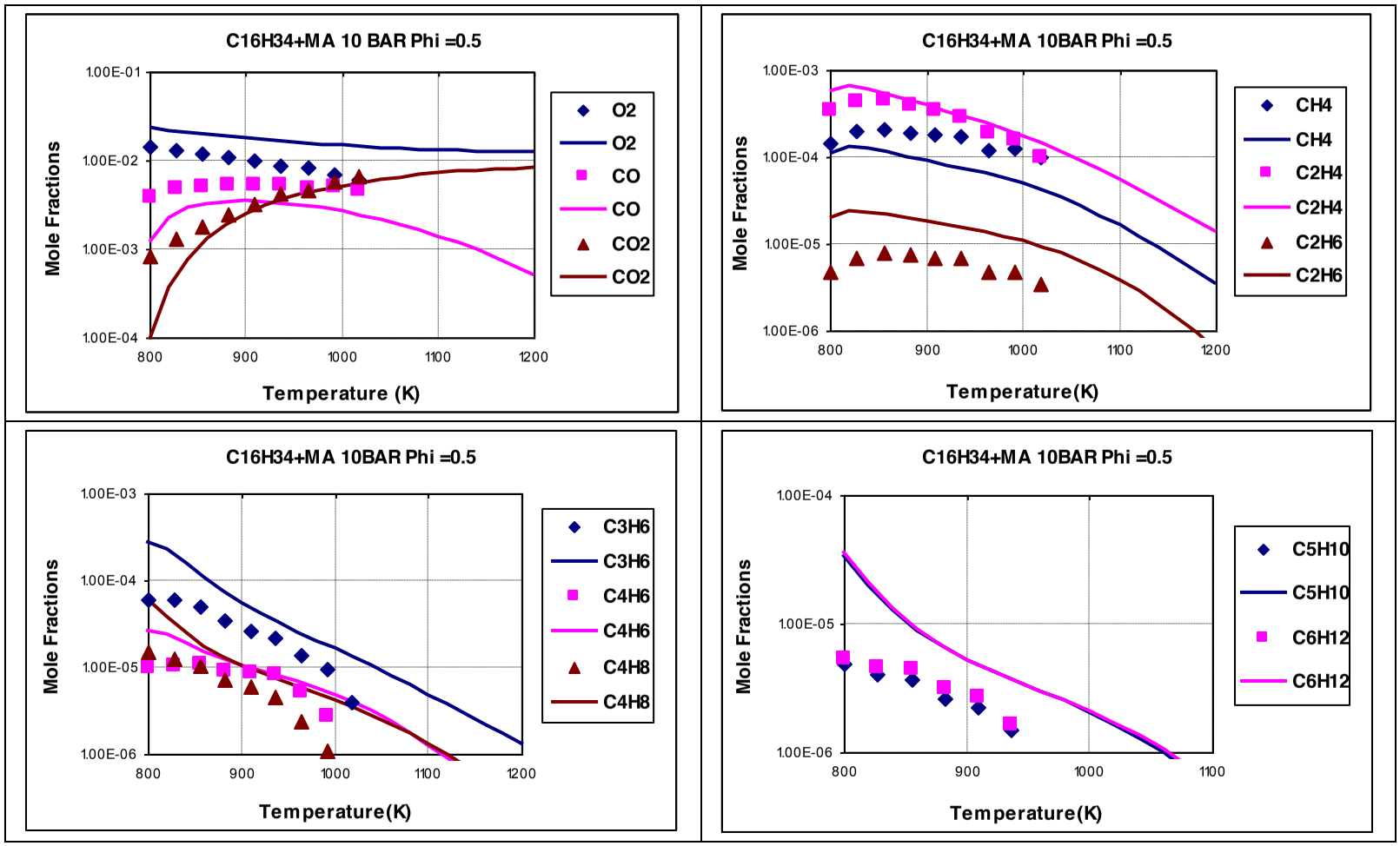

Figure 5.11: The oxidation of RME in a JSR (P = 10bar, Φ = 0.5, τ = 1 s). The experimental data (large symbols) are compared to the computations (lines surrogate model-fuel: n-$C_{16}H_{34}$ + MA)

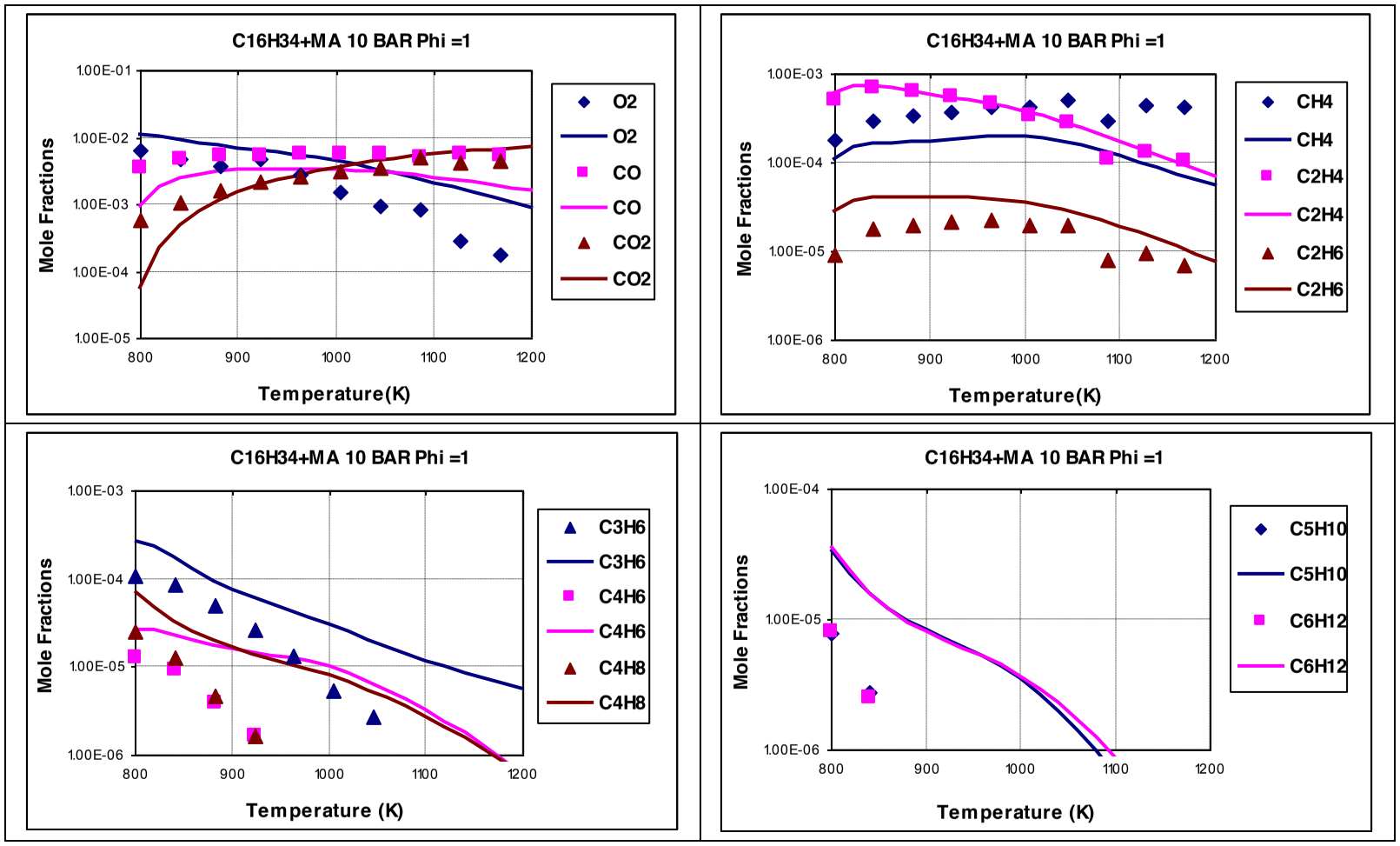

Figure 5.12: The oxidation of RME in a JSR (P = 10bar, Φ = 1.0, τ = 1 s). The experimental data (large symbols) are compared to the computations (lines surrogate model-fuel: n-$C_{16}H_{34}$ + MA)

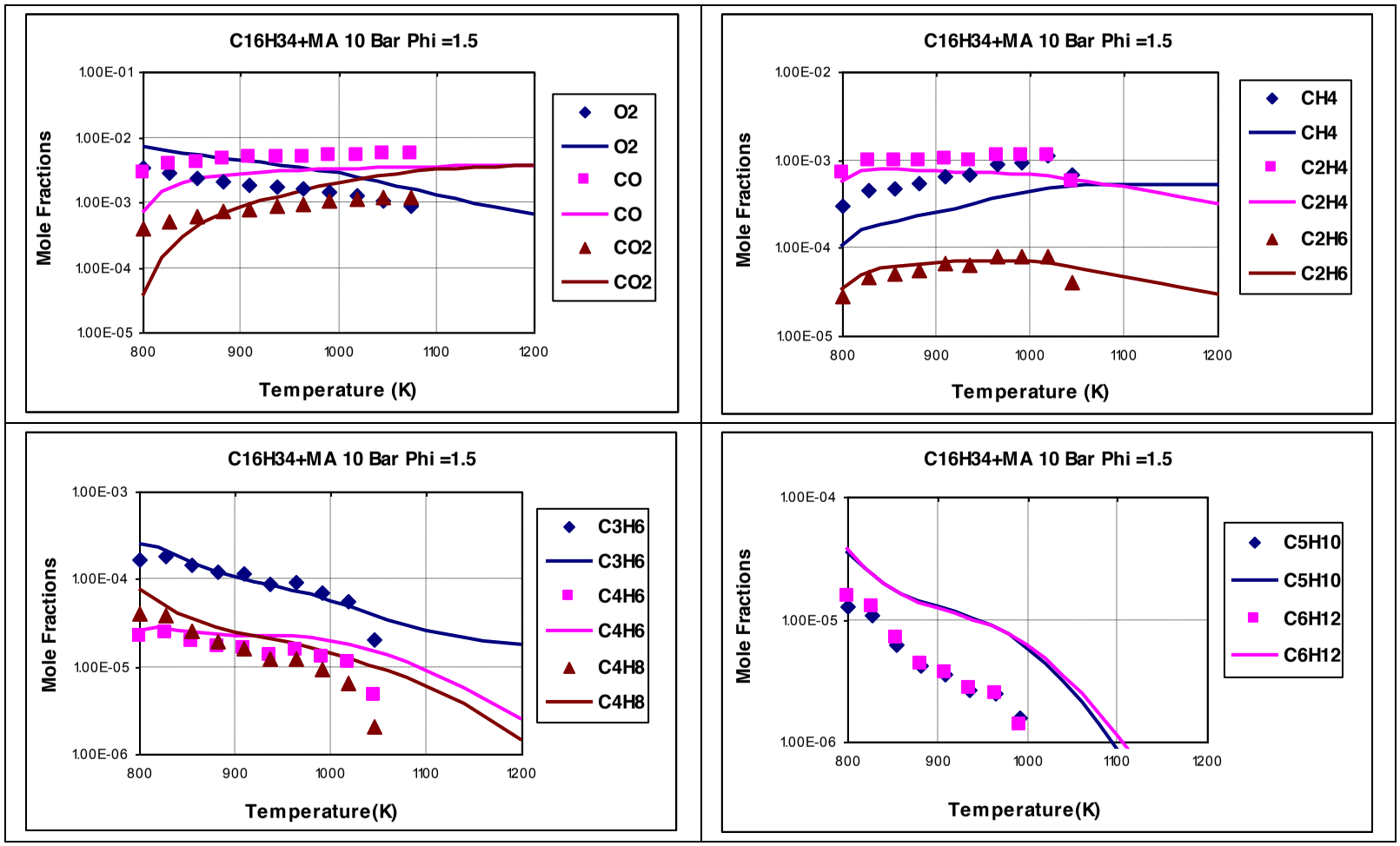

Figure 5.13: The oxidation of RME in a JSR (P = 10bar, Φ = 1.5, τ = 1 s). The experimental data (large symbols) are compared to the computations (lines surrogate model-fuel: n-$C_{16}H_{34}$ + MA)

Overall both models predicted mole fractions of reactants, intermediates and products in satisfactory manner especially for C_1-C_4 hydrocarbons, however formation of pollutants like CO, CH_2O and 1,3-Butadiene is either over predicted or under predicted. This modeling work confirms the efficiency of using surrogate model-fuels for modeling the combustion of commercial fuels, as demonstrated before for oxidation of kerosene [5.5] and a diesel fuel. It also shows that oxidation of long carbon chain Biodiesel like RME can be simulated using surrogate model-fuels, but with some limitations and less accuracy.

The above models lack the presence of unsaturation as well as ester groups associated with a long carbon chain in their structures. It is known fact that formation of aldehydes is favored by presence of unsaturation in RME [5.7]. It can be seen from MA sub mechanism, Methyl Acetate thermally decomposes to give Acetyl radical (CH3COO), which ester radical (reaction 5.6) and this acetyl radical decomposes to give CO_2 and methyl radical (reaction 5.7). The major route for CO_2 formation is through decomposition of acetyl radical only. So the early production of CO_2 in RME combustion may be associated with pyrolysis of ester function as well as with chemistry associated with saturated and un-saturated ester compounds and intermediates formed from parent RME molecule. The above results show that model with long saturated carbon chain and ester function doesn't reproduce RME or Biodiesel oxidation results in exact manner. So the model for RME oxidation has to be developed considering chemistry associated with unsaturation (carbon double bond) and ester chemical function with long carbon chain present in RME structure. These improvements may help in predicting early formation of CO_2 and formation of pollutant like 1,3-Butadiene (C_4H_6).

The chemical kinetic mechanism for RME oxidation will be developed using modeling tools like CHEMKIN simulation package and PSR code. The mechanism will be based on a typical high temperature combustion chemical kinetic mechanism.

References

5.1 Labeckas.G, Slavinskas.S, 2006, *The effect of rapeseed oil methyl ester on direct injection Diesel engine performance and exhaust emissions*, Energy Conversion and Management, 47, Issue 13-14, 1954-1967

5.2 Makareviciene.V, Sendzikiene.E, Janulis.P, 2006, *Influence of fuel oxygen content on diesel engine exhaust emissions*, Renewable Energy, 31, 2505-2512

5.3 Nwafor.O.M.I, 2004, *Emission characteristics of diesel engine operating on rapeseed methyl ester*, Renewable Energy, 29, 119-129

5.4 Dagaut.P, Ristori.A and Cathonnet.M, 2001, *The Oxidation of n-Hexadecane: Experimental and Detailed Kinetic Modeling*, Combustion and Flame, 125, 1128-1137

5.5 Dagaut.P and Cathonnet.M, 2006, *The ignition, oxidation and combustion of kerosene: A review of experimental and kinetic modeling*, Progress in Energy and Combustion Science, 32, Issue1, 48-92

5.6 Janulis.P, 2004, *Reduction of energy consumption in biodiesel fuel life cycle*, Renewable Energy, 29, 861-871

5.7 Pedersen.R.J, Ingemarsson.A and Olsson.O.J, 1999, *Oxidation of Rapeseed oil, Rapeseed Methyl Ester (RME) and diesel fuel studied with GC/MS*, Chemosphere, 38, 11, 2467-2474

5.8 Billaud.F and Archambault.D, 1999, *Experimental and modeling study of methyl oleate pyrolysis between 500 and 650 ^{0}C*, J.Chim.Phys, 96, 778-796

5.9 Dagaut.P, Smoucovit.N and Cathonnet.M, 1997, *Methyl Acetate Oxidation in a JSR: Experimental and Detailed Kinetic Modeling Study*, Combustion Science and Technology, 127, 275-291

CHAPTER 6
MODELING THEORY AND TOOLS

Chapter 5 described the comparison of RME oxidation results with diesel combustion. RME combustion results were simulated using a surrogate fuel model of n-hexadecane ($C_{16}H_{34}$) and of n-hexadecane + methyl acetate ($C_{16}H_{34}$ + CH_3COOCH_3). However, these models were not able to reproduce the experimental results in exact manner. So new kinetic mechanism needs to be developed for RME oxidation. This chapter will define chemical reaction mechanism and it will describe the modeling tools used in this study to identify the correct kinetics; CHEMKIN simulation package and Perfectly Stirred Reactor (PSR) code. It also covers the literature survey on chemical kinetic modeling study of Biodiesel combustion and structure of typical high temperature chemical kinetic mechanism. The last part of chapter explains the development of chemical kinetic mechanism for oxidation of RME.

A chemical reaction mechanism is the step by step sequence of elementary reactions by which overall chemical change occurs. An elementary step is a basic building block of complex reaction. The elementary processes in a reaction mechanism describe the molecular reaction and changes it undergoes during reaction. It also describes the transition state or order that bonds form or break and rate of each elementary step. The reaction mechanism is also accounted for reaction intermediates, which are stable molecules and do not appear in experimentally determined rate low because they are formed in one step and consumed in a subsequent step.

The CHEMKIN package is software designed to facilitate simulations of elementary chemical reactions in flowing systems. CHEMKIN is a highly structured & modular package that requires the manipulation of a number of programs, subroutines & data files. This package developed at the National Sandia Laboratories of Livermore (Kee and al., 1993) allows modelling the whole gas phase. The advantage of CHEMKIN is its general-purpose and problem-independent structure which, allows the analyst to work with same chemical input regardless of the particular problem [6.1].

The Perfectly Stirred Reactor (PSR) code is a FORTRAN computer program that predicts the steady-state temperature and species composition in a perfectly stirred reactor. The model accounts for finite-rate elementary chemical reactions. The governing equations are a system of non-linear algebraic equations that are solved using a hybrid Newton/ time-integration method. The program runs in conjugation with the CHEMKIN package, which handles the chemical reaction mechanism [6.2].

6.1 CHEMKIN

The CHEMKIN package is composed of two blocks of FORTRAN code and two files:

- An Interpreter (code)
- The Gas-Phase Subroutine Library (code)
- The Thermodynamic Database (file)
- The Linking File (file)

As shown in figure 6.1, the typical input files to Chemkin Interpreter are Chem.inp and therm.dat. The Chem.inp file contains detailed reaction mechanism and species, elements appearing in the mechanism. The reaction mechanism section contains the number of chemical reactions, followed by values for a Pre-exponential factor, temperature exponent and activation energy representing a typical Arrhenius type rate expression [6.1]. The thermodynamic database file (therm.dat) contains thermodynamic data of species given as polynomial. The thermodynamic data of species is calculated using THERGAS code. THERGAS is based on group or bond additive approach. This thermodynamic data is a function of temperature as input file to THERGAS code contains a temperature range over which polynomial fits to thermodynamic data are valid.

The interpreter is a program that reads a symbolic description of a reaction mechanism and then extracts the needed thermodynamic data for each species involved from the thermodynamic database. The primary output from the Interpreter is a Linking file or binary file called Chem.bin. The other output is printed output file ‘Chem.out’, which contains list of elements, species and reaction mechanism. This file also shows diagnostic error messages [6.1].

Once the interpreter is executed and the Linking File is created, the user is ready to use Gas-Phase Subroutine Library. The Gas-Phase Subroutine Library has over 100 subroutines that give information on elements, species, reactions, equation of state, thermodynamic properties and chemical production rates. The selection of Chemkin subroutines for any given problem begins by finding the appropriate equations [6.1].

The different types of calculation/application codes like PSR and SENKIN are used. PSR allows modeling of the experiments conducted in Perfectly Stirred Reactor/ Jet Stirred Reactor, whereas SENKIN allows modeling of shock tube experiments [6.1]. The PSR code is described in detail later in this chapter. The input to the PSR is in Keyword format, which defines a particular reactor and parameters needed to solve it. The other input file is 'Restart' file, which contains the solution from a previously calculated computer solution in order to restart a simulation. There are three outputs from the PSR code; save file, Recover file and Print output. The 'Save' file is written after the successful completion of problem. This file contains the first-order sensitivity coefficients and rate of production values. The 'Recover' file is written after every successful completion of converged Newton iterations. It is also used to restart a problem, which has terminated due to CPU time limits. The Print file contains solution in terms of exit mole fraction of all species. All input and output from code are in terms of mole fraction [6.2].

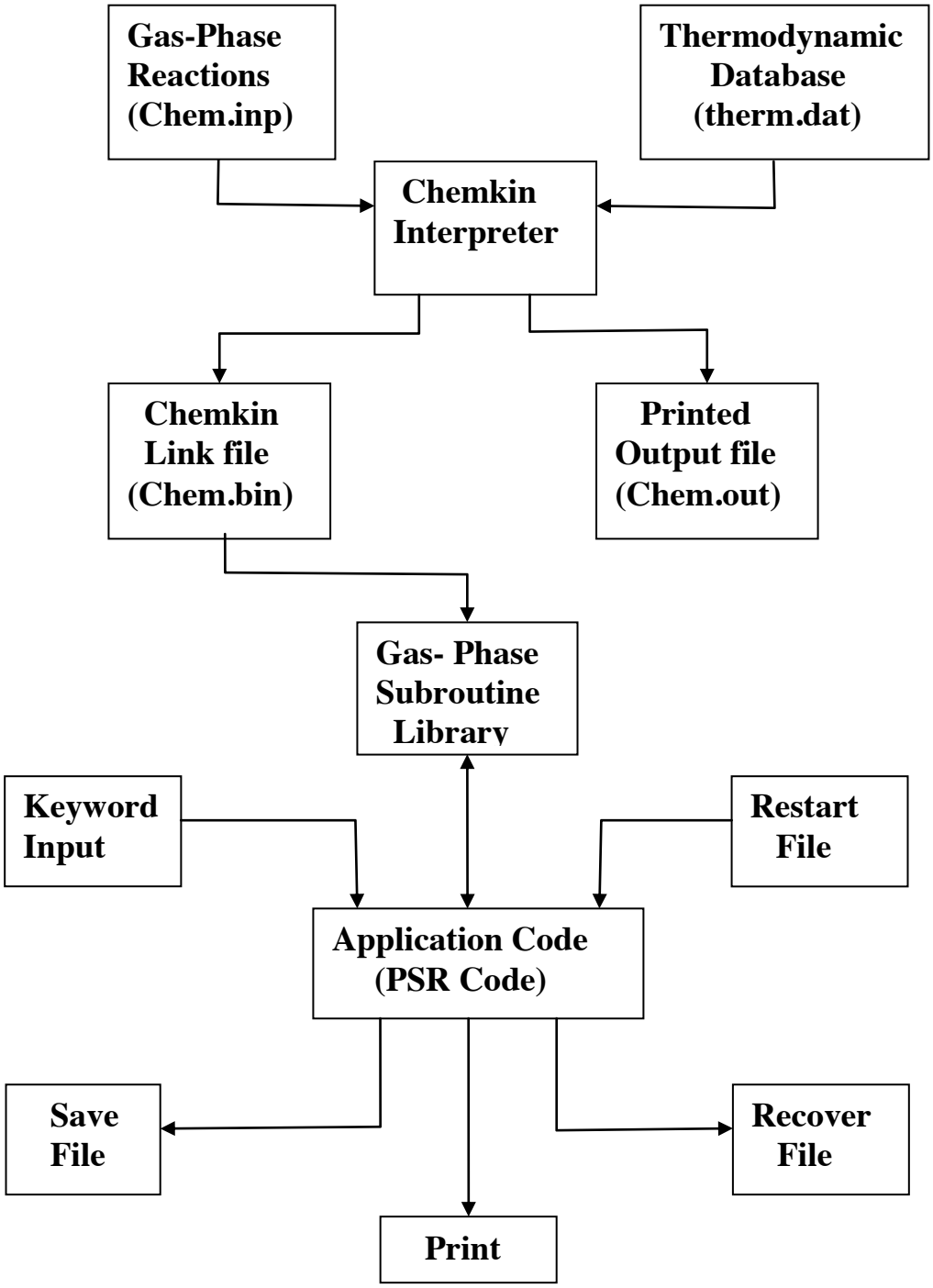

Figure 6.1: Schematic diagram of the CHEMKIN package with PSR code

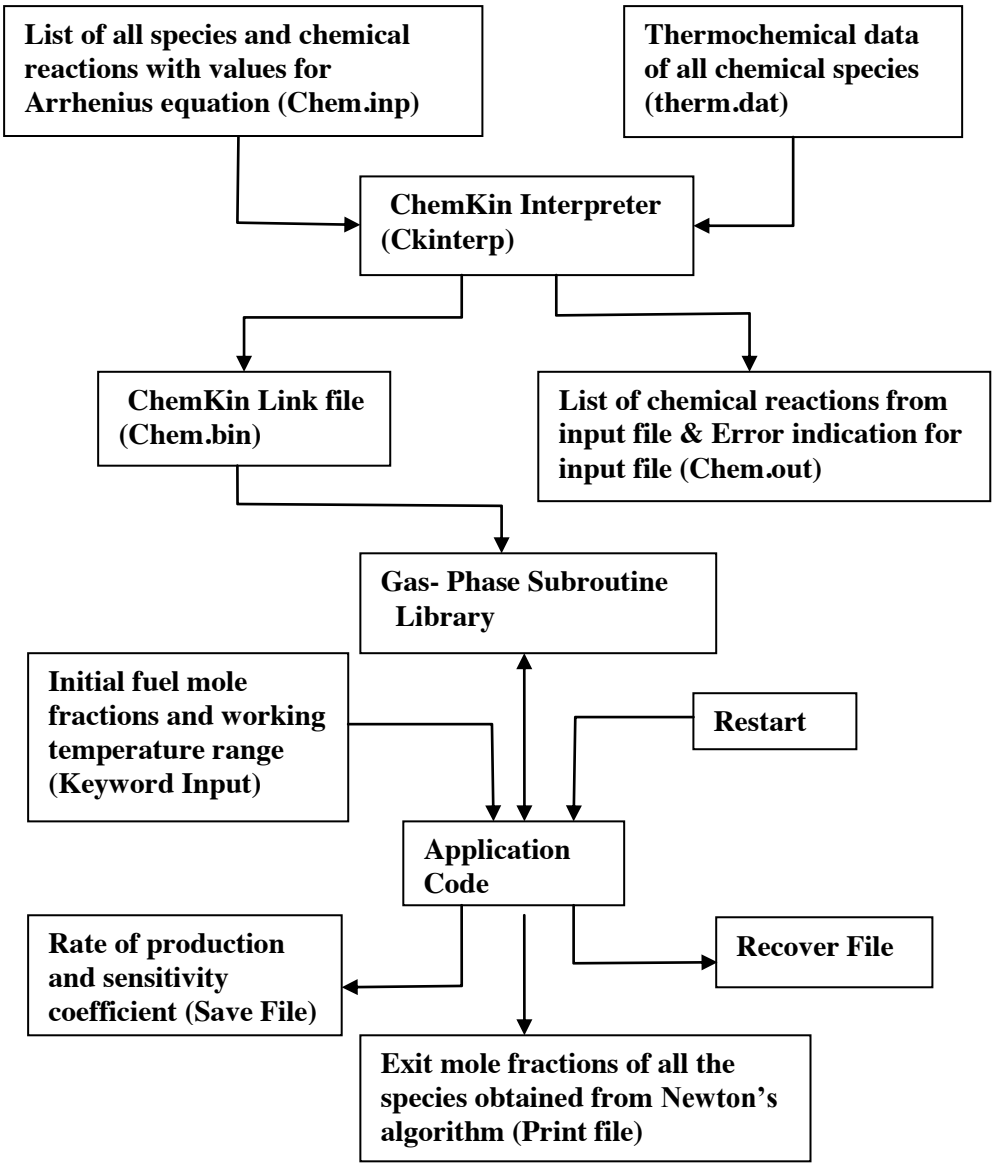

Figure 6.2: Flow chart for simulation process using CHEMKIN package with PSR code

6.2 Standard State Thermodynamic properties

The thermodynamics data used are formatted according to the NASA (National Aeronautics and Space Administration, USA) chemical equilibrium code format. In this case, seven coefficients are needed to describe the key physical properties as a function of working temperature ranges. The five coefficients are for molar heat capacities C_{p_i} and two integration constants for enthalpy and entropy [6.1].

The seven coefficients corresponding to two temperature ranges are [6.4]:

- The coefficients a_{8k} to a_{14k} are used to compute the thermochemistry in the range $300 \leq T \leq 1000$ K
- The coefficients a_{1k} to a_{7k} are used to compute the thermochemistry in the range $<1000 \leq T \leq 5000$ K. The value for these coefficients will different for specific heat capacity, entropy and enthalpy

The equations are [6.1]:

For Specific Heat Capacity

$$\frac{C^0_{Pk}}{R} = a_{1k} + a_{2k} T_k + a_{3k} T_k^2 + a_{4k} T_k^3 + a_{5k} T_k^4 \qquad (6.1)$$

For Standard Enthalpy

$$\frac{H^0_k}{RT_k} = a_{1k} + \frac{a_{2k}}{2} T_k + \frac{a_{3k}}{3} T_k^2 + \frac{a_{4k}}{4} T_k^3 + \frac{a_{5k}}{5} T_k^4 + \frac{a_{6k}}{T_k} \qquad (6.2)$$

For Standard Entropy

$$\frac{S^0_k}{R} = a_{1k} \ln T_k + a_{2k} T_k + \frac{a_{3k}}{2} T_k^2 + \frac{a_{4k}}{3} T_k^3 + \frac{a_{5k}}{4} T_k^4 + a_{7k} \qquad (6.3)$$

Where a_{1k} to a_{7k} correspond to coefficients in region $1000 \leq T_k < 5000$

The equation for standard state Gibbs Free Energy is given as

$$\Delta G^0 = H^0 - TS^0 \qquad (6.4)$$

The equilibrium thermodynamics is $K_{ci} = K_{fi}/K_{ri}$

$$K_{ci} = \frac{K_{fi}}{K_{Pi}\left(\frac{P_T}{RT}\right)\sum_{k=1}^{K} \gamma_{ki}} \qquad (6.5)$$

Where K_{fi} – Forward rate constant of the i^{th} reaction

K_{pi} – Equilibrium constant in pressure units for i^{th} reaction

K_{ci} – Equilibrium constant of the i^{th} reaction

$$\Delta G^0 = \sum X_i G_i^{\theta}{}_{(Products)} - \sum X_i G_i^{\theta}{}_{(reactants)} = -RT \ln (K_{Pi}) \qquad (6.6)$$

6.3 Chemical Reaction Rate Expression

The elementary reversible reaction involving chemical species is represented, for example for component i, as:

$$\sum_{k=1}^{K} \upsilon'_{ki} X_k \Leftrightarrow \sum_{k=1}^{K} \upsilon''_{ki} X_k \quad \text{Where i = 1.... } I \tag{6.7}$$

Where stoichiometric coefficients (υ) are integer numbers and 'X_k' represents the chemical symbol for kth species. The superscript ' indicates forward stoichiometric coefficients while " indicates reverse stoichiometric coefficients. For non-elementary reactions, equation 6.7 shows reaction expression, but stoichiometric coefficients may be non-integers [6.1].

The production rate $\acute{\omega}_k$ of kth species is represented by summation of the rate- of- progress variables (equation 6.8) for all reactions involving K species [6.1]. The reaction progress kinetic analysis involves a system in which the concentrations of multiple reactants are changing over the course of the time.

$$\acute{\omega}_k = \sum_{i=1}^{I} \upsilon_{ki} q_i \qquad (k = 1,.....K) \tag{6.8}$$

Where

$$\upsilon_{ki} = \upsilon''_{ki} - \upsilon'_{ki} \tag{6.9}$$

The rate of progress variable q_i for the ith reaction is given by difference of forward & reverse rates as

$$q_i = k_{fi} \prod_{k=1}^{K} (X_k)^{\upsilon'_{ki}} - k_{ri} \prod_{k=1}^{K} (X_k)^{\upsilon''_{ki}} \tag{6.10}$$

Where (X_k) is the major concentration of the kth species and K_{fi} & K_{ri} are the forward and reverse rate constants of the ith species. The rate of the progress of a reaction is evaluated using the concentration of each reactant or product species raised to the power of its stoichiometric coefficient. The equation 6.10 is always

valid when mass balance oriented kinetics is obeyed and when mechanism is written in terms of elementary reactions [6.1].

The forward rate constants of i reactions are generally expressed as:

$$K_{fi} = A_i T^{\beta i} \exp\left(\frac{-E_i}{R_c T}\right) \tag{6.11}$$

Where

A_i = Pre exponential factor

β_i = the temperature coefficient

E_i = the activation energy

R_c = gas constants

In chemical kinetics, reverse rate constant is related to forward rate constant through the equilibrium constant by

$$K_{r_i} = K_{fi} / K_{ci} \tag{6.12}$$

Although K_{c_i} is given in concentration units, the equilibrium constants are determined from the thermodynamic properties in pressure units and are related by

$$K_{c_i} = K_{p_i}\left(\frac{P_{\text{atm}}}{RT}\right)^{\sum_{k=1}^{K} \upsilon_{ki}} \tag{6.13}$$

The equilibrium constant K_{p_i} is obtained from the relationship

$$\Delta G^0 = -RT \ln (K_{pi}) \tag{6.14}$$

6.3.1 Three-Body Reactions

In some reactions 'Third body' or 3rd reactant species (M) is required for the reaction to proceed; this is often the case in dissociation or recombination reactions, such as

$$H + O_2 + M \rightleftharpoons HO_2 + M \tag{6.15}$$

When third body is needed, the concentration of the effective third body must appear in the expression for the rate of progress variable [6.1].

6.3.2 Pressure Dependent Reactions

Under certain conditions, some reaction rate expressions depend on pressure as well as temperature. These include two types of reactions namely: unimolecular/recombination fall-off reactions and chemically activated bimolecular reactions. Rates for unimolecular/ recombination fall-off reactions increases with increasing pressure, while rates for chemically activated bimolecular reactions decreases with increasing pressure [6.1]. These are important chain reactions of combustion kinetics. The RME oxidation mechanism has incorporated set of pressure dependent unimolecular and bimolecular reaction with their Arrhenius parameters and activation energy values. There are several methods or approaches to represent the rate expressions in the fall-off region. The simplest method amongst these methods is 'Lindemann's Approach or Theory'. The other approach is Troe's fall off form. The Lindemann theory along with Troe's form is explained in next section.

6.4 The Lindemann Theory

This theory forms basis for all modern theories of unimolecular reactions. As fuel is consumed mainly in unimolecular initiation reactions in high temperature combustion chemistry, these reactions are important for developing combustion kinetics. The main concepts of the theory are [6.1] [6.4]:

a) By collisions, a certain fraction of the molecules become energized (A^*) i.e. gain energy in excess of critical quantity E_0. The rate of energization process depends upon the rate of the bimolecular collisions.

The process is written as

$$A + M \xrightarrow{k_1} A^* + M \qquad (6.16)$$

M can represent a product molecule or an added inert gas molecule or second molecule of reactant. The rate constant k_1 is energy-independent and is calculated from collision theory equation.

b) Energized molecules are de-energized by collisions. This is the reverse of the collision process explained in equation 6.16 and is written as

$$A^* + M \xrightarrow{k_2} A + M \qquad (6.17)$$

Here k_2 is taken to be energy-independent and is equated with the collision number Z_2, i.e. it is assumed that every collision of A^* leads to de-energization.

c) There is a time lag between the energization and unimolecular dissociation or isomerization of the energized molecule. The unimolecular dissociation process also occurs with a rate constant independent of the energy content of A^*.

$$A^* \xrightarrow{k_3} B + C \qquad (6.18)$$

In Lindemann's approach, parameters for high-pressure limit (K_∞) and the lower pressure limit (K_0) are calculated as follows [6.1]

$$K_0 = A_0\, T^{\beta 0} \exp - (E_0/R_C\, T) \qquad (6.19)$$

$$K_\infty = A_\infty\, T^{\beta \infty} \exp - (E_\infty/R_C\, T) \qquad (6.20)$$

The rate constant at any pressure is describes as

$$K = K_\infty \left(\frac{P_r}{1+P_r}\right) F \qquad (6.21)$$

Where 'F' is broadening factor and reduced pressure Pr is given by

$$P_r = \frac{K_0(M)}{K_\infty} \qquad (6.22)$$

Where (M) is the concentration of the mixture, and the units for K are cm^3/moles-sec, K_0 are cm^6/$moles^2$-sec and K_∞ is cm^3/moles-sec.

If F is unity in equation 6.21 then it is Lindemann form, where as in the Troe's form equation for F is

$$\text{Log } F = \left(1 + \left(\frac{\log P_r + c}{n - d(\log P_r + c)} \right)^2 \right)^{-1} \log F_{cent} \qquad (6.23)$$

The constant in above equation are

$$C = -0.4 - 0.67 \log F_{cent}$$

$$n = -0.75 - 1.27 \log F_{cent}$$

$$d = 0.14$$

And

$$F_{cent} = (1 - a) \exp\left(\frac{-T}{b}\right) + a \exp\left(\frac{-T}{c}\right) + \exp\left(\frac{-d}{T}\right) \qquad (6.24)$$

Where 'F_{cent}' is falloff parameter

The Troe's form allows considering pressure dependency for a rate constant in a precise way. It allows determining the difference between experimental rate constants and those from Lindemann's theory. The rate constant is corrected by using factor of expansion 'F' ($K_{Troe} = K_{Lindemann}$ F). This factor of expansion is calculated from the centring parameter F_{cent}, which is calculated by using Troe's formula for temperature dependence of F_{cent} and parameters a, b, c, d [6.1].

6.5 The Perfectly Stirred Reactor (PSR) Code

This section describes the components of PSR code, which includes well-stirred reactor equation, numerical solution method like Newton's algorithm and analytical tools like sensitivity analysis.

6.5.1 Well Stirred Reactor Equation

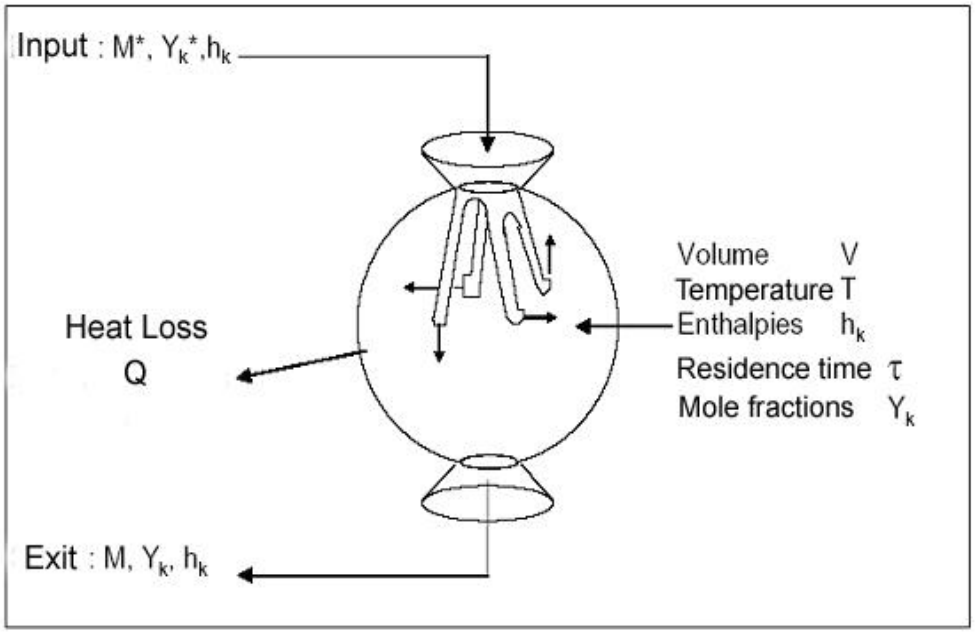

Figure 6.3: Schematic Representation of a Well-Stirred Reactor [6.2]

As the mixing in the reactor chamber is intense, it is assumed that temperature, and composition in the reactor is the same as that of the exit from reactor.

The mass flow rate is given as m^0

The species conservation equation is given by

$$m^0 (Y_k - Y^*_k) - \acute{\omega}.W_k.V = 0 \qquad (6.25)$$

The equation of conservation of energy is given as

$$m^0 \sum_{k=1}^{K} \left(Y_k h_k - Y^*_k h^*_k \right) + Q = 0 \qquad (6.26)$$

Where Y_K is mass fraction of the K^{th} species (there are K species); W_k. the molecular weight of K^{th} species, V the reactor volume, ώ is molar rate of the production by chemical reaction of the K^{th} species per unit volume; h_k, the specific enthalpy of the K^{th} species, Q the reactor heat loss. The superscript (*) indicates the inlet conditions. The energy conservation equation is not required in our

simulation work since the experimentally measured temperature is used as an input [6.2].

The total residence time is given by

$$\tau = \rho \frac{V}{m^0} \tag{6.27}$$

Where mass density ρ is calculated from the ideal gas equation of state

$$\rho = \frac{P\,\overline{W}}{RT} \tag{6.28}$$

Here P is the pressure; T is the temperature, R the universal gas constant and $\overline{W}$ is the mixture's mean molecular weight. The residence time is often used as a characteristic parameter of the reactor rather than the mass flow rate. The analogues time-dependent equation for mass conservation of each species is

$$\rho.V.\frac{dY_k}{dt} = -\,m^0.\left(Y_k - K^*_k\right) + \acute{\omega}.W_k.V \tag{6.29}$$

$$\frac{dY_k}{dt} = -\frac{1}{\tau}\left(Y_k - Y^*_k\right) + \frac{\acute{\omega}.W_k}{\rho} \tag{6.30}$$

Equations 6.25 and 6.26 form a set of K+1 non-linear algebraic equations, the solution of which are the temperature and mass fractions. Even though we seek the solution to the steady-state equations, the computational algorithm often requires a partial solution of the related problem [6.2].

6.5.2 Numerical solution method

A modified Newton algorithm solves the system of algebraic equation. However if during the course of the integration the Newton's algorithm fails to converge, the solution estimate is conditioned by a time integration. The algorithm needs a starting estimate of the solution (temperature and mass fraction) from which to begin its iteration. If no reasonable starting estimate is available, the program can begin its iteration process from a given equilibrium composition at an estimated or specified reactor temperature. The equilibrium state is calculated

by minimization of the Gibbs-free energy function. In different problems, it may be helpful to begin with the equilibrium composition and an artificially long residence time. For an infinite residence time, the equilibrium composition is the solution to the well-stirred reactor problem and thus convergence should be rapid.

The algorithm solves the problem in two parts. First, the species equations are solved at the estimated temperature. This serves to determine a mixture composition that is 'consistent' with residence time and temperature. The output of algorithm or iteration gives exit mole fractions of all the species incorporated in reaction mechanism. After determining this consistent solution, the energy equation is solved simultaneously with the species equations. The initial values of specific enthalpy (h) are generated by code. However when reactor temperature is measured experimentally, it is preferable to use that temperature in the model. Therefore, in the present study, instead of solving the energy equation twice, we used the experimentally measured temperatures in the computation inputs [6.2].

6.5.3 Time stepping

Determining the steady solution by solving the transient equations to a steady state is very reliable but a slow process. As the transient computation is very robust, it is applied in the cases where Newton's method is not converging.

After solving the transient equations for a given number of time steps the algorithm returns to Newton iteration. As a result of time stepping, the trial solution is hopefully closer to the true solution and thus it is more likely to be within Newton's convergence domain. If the program fails to converge on a time step, the user has two choices: one is to choose smaller time steps; another is to try new starting estimates [6.2].

6.5.4 Sensitivity Analysis

The sensitivity analysis is often an invaluable tool in helping to interpret the results of stirred reactor and flame experiments. In sensitivity analyses, we consider the first order sensitivity coefficients of the temperature and mass fractions with respect to the rate coefficients and hence determine what coefficients in the description of chemical reaction mechanism are important [6.2].

The sensitivity coefficients are defined by matrix (dF/dα), were F is a residual vector composed of the residuals of the energy equation and species equation. 'α' is consists of value of 'A' from Arrhenius reaction rate expression. In the computer code, we compute normalized sensitivity coefficients in the form of logarithmic derivatives.

$$S_{k,i} = \frac{\partial \ln Y_k}{\partial \ln K_i} = \frac{K_i}{Y_k}\left(\frac{\partial Y_k}{\partial K_i}\right) \tag{6.31}$$

By using the sensitivity analysis, we can determine the reactions having influence on the calculated concentrations, independent of reaction flows

- The positive coefficients indicate an increase in concentration of species k with increased rate of reaction i.
- The negative coefficients correspond to a decreased concentration of species k with increase in rate of reaction i.

6.5.5 Rate of production analysis

It is interesting to determine how each reaction contributes to the production or destruction of the species. The molar production of species is given by

$$\dot{\omega}_k = \sum_{i=1}^{I} \upsilon_{ki} q_i \tag{6.32}$$

Where υ_{ki} is the stoichiometric coefficient and q_i is the rate of progress variables for the *I* reactions. The contribution to the rate of production of species K for reaction I is therefore simply

$$C_{ki} = \upsilon_{ki}\, q_i \tag{6.33}$$

As this analysis gives set of reactions generating important reaction path way, it is supplementary to the sensitivity analysis .But these reactions are not necessarily sensitive to the modification of their kinetic parameters [6.2]. PSR code gives Absolute rate of production in moles/cc-sec and Normalized rate of production coefficients. The normalized rate of production coefficient for any reaction is calculated by dividing absolute of rate of production for that reaction by total absolute rate of production for all reactions and then multiplied by 100.

6.5.6 Chemical Kinetic modeling study of Biodiesel Combustion:

As covered in chapter 2, a range of experiments on vegetable oil and Biodiesel combustion in different diesel engines had been carried out. However information available about chemical kinetic models developed for combustion of these fuels is not so well developed. The kinetic models available are more suitable for pyrolysis of vegetable oils and their esters or for combustion of small alkyl esters (up to C_4). Chapter 2 explains only literature survey about diesel engine combustion of biodiesel, whereas literature survey about combustion kinetics of Biodiesel is explained in this section.

Daguat et al. [6.3] studied Methyl Acetate oxidation in a Jet Stirred Reactor. Methyl Acetate is a reaction intermediate formed during pyrolysis of alkyl esters. The chemical kinetic mechanism for Methyl Acetate oxidation is based on the mechanism developed for ethane, ethylene, propane and propene oxidation. Formaldehyde was observed as the main intermediate oxidation product. Billaud and Archambault [6.4] developed chemical kinetic mechanism for Methyl Oleate pyrolysis in tubular flow reactor at atmospheric pressure. The model estimated light unsaturated hydrocarbons like propene, butene in well manner. In general, model gave good agreement with experimental results about formation of olefins and smaller esters.

Good and Francisco [6.5] studied the oxidation of Methyl Formate and Dimethyl Ether. They used ab initio techniques and provided information about important reaction pathways in the oxidation. Fisher et al. [6.6] developed a kinetic reaction mechanism for oxidation of Methyl Butanoate, which is a surrogate for Biodiesel and Methyl Formate. The mechanism was tested against limited experimental data obtained under lower-temperature, sub atmospheric conditions in a closed vessel. The model predicted region of negative temperature coefficient and dependence of overall reaction rate on temperature for both the esters. The fisher mechanism was later re-validated by Gail [6.7] and others against Methyl Butanoate oxidation in Jet Stirred Reactor.

Marchese [6.8] studied Methyl Butanoate oxidation in flow reactor at 12.5 atm, over a temperature range of 500-900 K. The experimental results were simulated using the kinetic mechanism developed by Fisher. The model gave good

agreement with experimental results under stoichiometric conditions. It over predicted the reactivity at fuel-rich conditions and under predicted at fuel-lean conditions. Gasnot et al. [6.9] developed a kinetic mechanism for ethyl acetate oxidation with sub-mechanisms for vinyl acetate and acetic acid. The above modeling work reproduces oxidation of methyl ester but it does not represent diesel fuel or practical Biodiesel with carbon chain of C_{16} to $C_{20\text{-}22}$

6.6 High Temperature Chemical Kinetics Mechanism

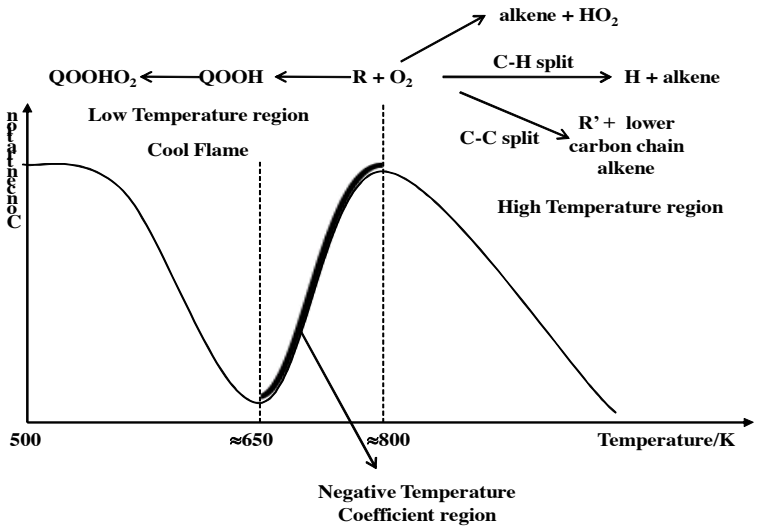

Figure 6.4: Schematic Representation of a temperature zones for oxidation

The kinetic mechanism of hydrocarbon oxidation varies with temperature and pressure [6.11]. Figure 6.4 shows three different temperature zones for oxidation as per temperature range; namely low temperature, negative temperature coefficient and high temperature [6.11]. A chemical kinetic mechanism is developed as per these oxidation temperature zones. A chemical kinetic mechanism developed for oxidation below 650 K is a lower temperature mechanism or chemistry and a chemical kinetic mechanism developed for T ≥ 800K is a high temperature mechanism [6.11]. A lot of work has been done on development of chemical kinetic mechanism for hydrocarbon oxidation and outlines for such mechanism have been developed [6.10]. The typical high

temperature mechanism consists of initiation, chain propagation, addition and termination reactions [6.10].

Initiation:

Initiation reactions deal with the reaction of hydrocarbon with oxygen forming alkyl and hydroperoxy radicals at high temperature, reactions of unimolecular and thermal decomposition. A unimolecular reaction is a reaction, involving one molecular entity. Amongst all these reactions unimolecular and thermal decomposition are more important than oxidation [6.10]. At initial working temperature of oxidation in JSR, fuel is mostly consumed in these initiation reactions only and maximum conversion of fuel takes place by these reactions only.

$$RH + O_2 \rightarrow R^{\cdot} + HO_2^{\cdot} \quad (6.34)$$

$$RH\ (+M) \rightarrow R'^{\cdot} + R''^{\cdot}\ (+M) \quad (6.35)$$

$$RH\ (+M) \rightarrow R^{\cdot} + H^{\cdot}\ (+M) \quad (6.36)$$

Where, $R^{\cdot}$, $R'^{\cdot}$, $R''^{\cdot}$ are alkyl radicals.

Chain propagation reactions:

In these reactions, alkyl radicals formed from initiation reactions decomposes to give different carbon chain olefins and smaller alkyl or alkenyl radicals.

$$R^{\cdot}\ (+M) \rightarrow \text{Olefins} + R'^{\cdot}\ (+M) \quad (6.37)$$

$$R^{\cdot}\ (+M) \rightarrow \text{Olefins} + H^{\cdot}\ (+M) \quad (6.38)$$

Chain propagating reactions also consist of metathesis reactions i.e. H abstraction reactions (reaction 6.39) giving intermediate radicals. For H abstraction, there can be number of sites available depend on alkyl chain.

$$RH + X \rightarrow R^{\cdot} + HX \quad (6.39)$$

Where X = $H^{\cdot}$, $^{\cdot}O^{\cdot}$, $^{\cdot}OH$, $^{\cdot}HO_2$, CH_3, C_2H_3, C_2H_5, C_4H_7, and $R^{\cdot}$ = alkyl radical

Addition Reaction:

Hydrogen present in environment reacts with oxygen giving $^{\cdot}OH$ and $^{\cdot}O^{\cdot}$ radicals.

$$H^{\cdot} + O_2 \rightarrow {}^{\cdot}OH + {}^{\cdot}O^{\cdot} \quad (6.40)$$

In addition reaction, the addition of $H^{\cdot}$ radical with oxygen gives hydroperoxy radical (reaction 6.41). Metathesis of those hydroperoxy radicals with alkyl radicals gives Hydrogen Peroxide, which decomposes to give two OH radicals.

$$H^{\cdot} + O_2 (+M) \rightarrow HO_2^{\cdot} (+M) \quad (6.41)$$

$$HO_2^{\cdot} + RH \rightarrow H_2O_2 \quad (6.42)$$

$$H_2O_2 \rightarrow 2\ {}^{\cdot}OH \quad (6.43)$$

Termination Reactions:

It involves recombination reactions of intermediate radicals to form termination products like stable molecules. In termination reactions, mainly alkyl radicals and methyl radicals recombine to give termination products. In addition, different intermediate radicals also recombine to give products. For example in reaction 6.45 methyl and ethyl radical recombine to form Methane and Ethene molecule.

$$CH_3^{\cdot} + R^{\cdot} \rightarrow \text{ Products of termination} \quad (6.44)$$

$$CH_3 + C_2H_5 \rightarrow C_2H_4 + CH_4 \quad (6.45)$$

6.7 Rapeseed Oil Methyl Ester (RME) Oxidation Mechanism

The mechanism for oxidation of Rapeseed Oil Methyl Ester is based on mechanism developed for oxidation of n-Hexadecane [6.12] and pyrolysis of Methyl Oleate [6.13] [6.14]. This mechanism consists of two parts; first part is mechanism for C_1-C_8 compounds chemistry, which is based on n-Hexadecane oxidation mechanism, developed at CNRS [6.12]. The 2nd part is a mechanism consisting of reactions developed for Rapeseed oil Methyl Ester (RME C_{18}), based on hydrocarbon oxidation chemistry at high temperature. The detailed mechanism and the nomenclature for this mechanism are presented in appendices A and E respectively. RME molecule consists of linear chain of 17 carbon atoms with a C=O and an OCH_3 group at one end (Figure 6.5).

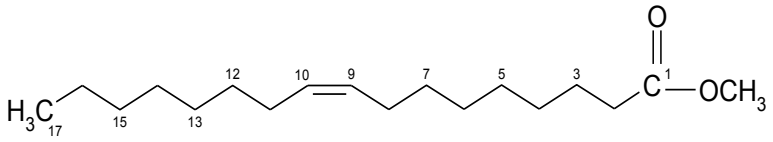

Figure 6.5: Structure of RME (C17:d9) with carbon chain C_1 to C_{17}

Here C17:d9 is a nomenclature used for RME, where C_{17} represents carbon atom number in RME chain and d9 represents position of unsaturation i.e. double bond at carbon no 9.

The mechanism for oxidation of RME consists of:

- Initiation reactions including unimolecular decomposition and bimolecular reactions
- Metathesis Reactions
- Isomerization of radicals
- Decomposition of radicals by β scission
- Termination Reactions

These reactions are labeled from number 1 to 7 as shown in figure 6.6.

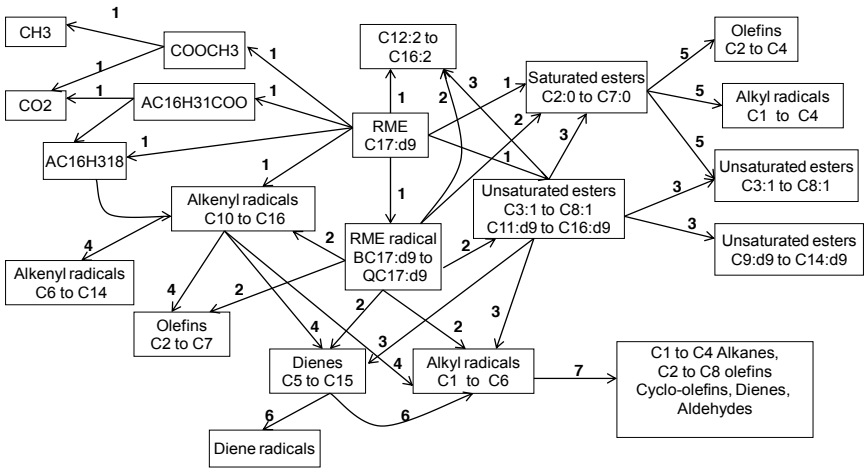

Figure 6.6: Flow diagram for kinetic mechanism for oxidation of RME

1. Unimolecular decomposition of RME gives saturated and unsaturated ester radicals, alkenyl, alkyl and other radicals. Metathesis reaction with O_2, O, OH, H, HO_2, and CH_3 to C_2H_5 gives RME radicals.
2. Isomerization and β scission of RME radicals again gives saturated and unsaturated esters, alkenyl and alkyl radicals, olefins and dienes.
3. Metathesis reaction, Isomerization and β scission of long chain unsaturated esters giving smaller unsaturated esters and saturated esters, alkyl radicals and dienes.
4. Metathesis reaction, Isomerization and β scission of alkenyl radicals gives smaller alkenyl radicals, olefins, smaller alkyl radicals and dienes.
5. Metathesis reaction, Isomerization and β scission of saturated esters gives smaller olefins, smaller alkyl radicals and small carbon chain unsaturated esters.
6. Dienes decompose to give alkyl and diene radicals.
7. Metathesis reaction, Isomerization and β scission reactions with alkyl radicals (C_1 to C_8) give smaller alkanes, olefins, dienes, cyclo-olefins and aldehydes.

These stages are describes in more detailed in the following sections.

Initiation Reactions:

Initiation reactions include unimolecular decomposition and reactions of O_2 with RME. The unimolecular decomposition has reactions for C-C, O-CH3 bond breakage and also reactions for thermal decomposition giving H radical and unsaturated ester radicals. These initiation reactions are most important reaction as they form 1st set of intermediate compounds from RME molecule, which further on decompose to form all intermediate hydrocarbons and pollutants. The structure of RME with different bond breaking sites is given in figure 6.7, where as bond energy values for these bonds are given in table 6.1.

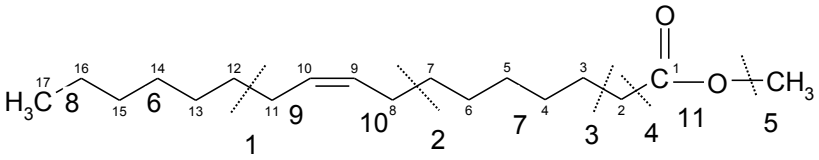

Figure 6.7: Structure of RME with chain breaking sites (1 to 11)

1112. C17:d9=>KC11:d9+AC6H13 (Bond No1)

1113. C17:d9=>AC10H192+GC7:0 (Bond No 2)

The C-C bonds at bond number 1(located at C_{11}-C_{12}) and 2 (located at C_7-C_8) are weakest bonds in the RME structure and are the first part of its chain to break. These reactions give us saturated and unsaturated ester radicals, alkyl radical and alkenyl radical. In Chemkin input file (chemical reaction mechanism file) these reactions are described as reaction no 1112 and 1113. As the O-CH_3 (bond number 5) is, also a weak bond it is possible to break it giving radical and CH_3 (reaction no 1120 in chemical reaction mechanism). The long alkenyl chain at bond 3 and 4 (located at C_1-C_2 and C_3-C_4) gives us saturated ester radical and alkenyl radicals (reaction no 1118 and 1119 in chemical reaction mechanism).

1118. C17:d9=>AC15H297+BC2:0 (Bond No 3)

1119. C17:d9=>AC16H318+COOCH3 (Bond No 4)

1120. C17:d9=>AC16H31COO+CH3 (Bond No 5)

Bond number	Bond Energy Kcal/mol
1	70
2	70
3	82.6
4	83
5	84
6	86
7	86
8	89.8
9	98
10	98
11	98

Table 6.1: Bond energy values for RME [6.15]

Unimolecular decomposition reactions mainly gave us 4 types of compounds, namely:

1. Unsaturated long chain ester radicals
2. Saturated ester radicals
3. Alkenyl radicals
4. Small alkyl radicals

Thermal decomposition of RME gives H and RME (e.g. BC17:d9) radical.

1137. C17:d9=H+BC17:d9

The RME is oxidized giving RME radicals and hydroperoxy radicals.

1123. C17:d9+O2=HO2+BC17:d9

All the radicals formed from the initiation are thermally decomposed and oxidized, giving other radicals and dienes.

Metathesis Reactions:

Metathesis reactions consist of extracting H from long alkenyl chain forming ester (RME) radicals and other radicals or olefins.

The metathesis reaction is represented as:

$$C17{:}d9 + X \longrightarrow C17{:}d9^{*} + XH \qquad (6.46)$$

Where

X = O, OH , H , HO_2. CH_3, C_2H_3, C_2H_5

Total of 16 sites are available for abstracting H by metathesis reaction in RME molecule, so we have written metathesis reactions for RME considering each radical site available in RME structure.

Decomposition of RME radicals:

The RME radicals formed from initiation and metathesis reactions decompose by a β scission reaction giving unsaturated and saturated ester radicals, alkenyl and diene radicals and olefins.

$$C17{:}d9^{*} \xrightarrow{\beta} R^1 + R^2 \qquad (6.47)$$

1299. DC17:d9=AC12H234+C5:1

$$C17{:}d9^{*} \xrightarrow{\beta} R^3 + R^4 \qquad (6.48)$$

1300. DC17:d9=C15H2817+BC2:0

$$C17{:}d9^{*} \xrightarrow{\beta} R^5 + R^6 \qquad (6.49)$$

1312. MC17:d9=KC11:d9+AC6H12

Where

R^1 = Alkenyl radical R^2 = Smaller Unsaturated ester radical

R^3 = Diene R^4 = Saturated ester radical

R^5 = Unsaturated ester radical R^6 = Olefins

Isomerization of radicals:

The isomerization reaction changes the position of the radical site on molecule. In this mechanism, we have used 1-4, 1-5 and 1-6 isomerizations. It includes isomerization of primary to secondary, secondary-to-secondary and secondary to primary isomerization.

1248. BC17:d9 => EC17:d9 (1-4 isomerization)

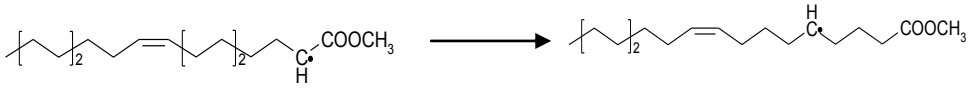

1249. BC17:d9 => FC17:d9 (1-5 isomerization)

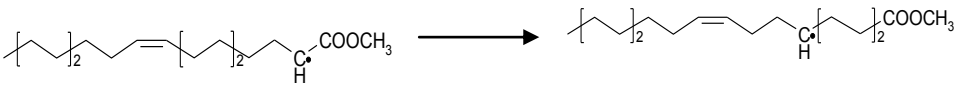

1250. BC17:d9 => GC17:d9 (1-6 isomerization)

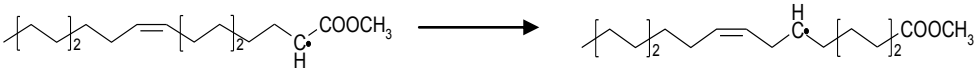

Decomposition by β scission:

The decomposition by β scission reaction is applicable to all the radicals formed, but radicals or products formed by β scission reactions depend on the position of the radical site. These reactions are important as β scission of long carbon chain radicals form intermediate hydrocarbons like olefins, 1-3 Butadiene and smaller hydrocarbon radicals. These small hydrocarbon radicals decompose further on to give smaller radicals and olefins.

In this mechanism, long carbon-chain ester radicals, alkenyl and diene radicals are decomposed by β scission. These radicals give small carbon chain saturated and unsaturated ester radicals, small carbon chain alkenyl, alkyl, diene radicals and olefins. For example in reaction no 1372, an unsaturated ester radical with 16 carbon chain decomposes to give unsaturated ester compound with 6 carbon chain and 3-Decene radical.

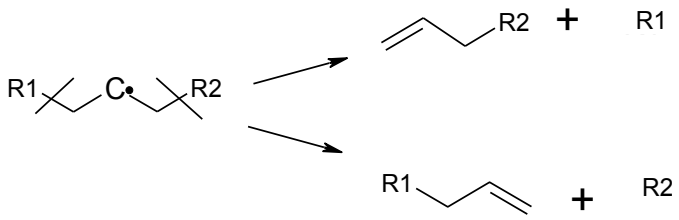

1372. EC16:d9=AC10H193 + C6:1

1373. EC16:d9=C13H2416 + CC3:0

Termination Reactions:

The termination reactions are the recombination of smaller alkyl as well as ester radicals to give products like olefins, saturated and unsaturated esters.

This chapter described the modeling tools like CHEMKIN simulation package and Perfectly Stirred Reactor (PSR) used in simulating the combustion of hydrocarbons and biofuels. The literature survey on chemical kinetic modeling study of biodiesel combustion was also explained in detail. A typical high temperature chemical kinetic mechanism is explained in section 6.6 of this chapter. Finally, section 6.7 covers the development of Rapeseed Oil Methyl Ester (RME) oxidation mechanism. RME oxidation is simulated using the chemical kinetic mechanism explained in section 6.7. The results of this simulation work are explained in chapter 7 along with rate of production and sensitivity analysis.

References

6.1 Kee.R.J, Rupley.F.M, Meeks.E, and Miller.J.A, 1996, *Chemkin III: A FORTRAN chemical kinetics package for the analysis of gas-phase chemical and plasma kinetics*, Report No.SAND96-8216, Sandia National Laboratories, Livermore, CA

6.2 Glarborg.P, Kee.R.J, Grcar.J.F, and Miller.J.A, 1986, *PSR: A FORTRAN program for modeling well-stirred reactors*, Report No.SAND86-8209, Sandia National Laboratories, Livermore, CA

6.3 Dagaut.P, Smoucovit.N and Cathonnet.M, 1997, *Methyl Acetate Oxidation in a JSR: Experimental and Detailed Kinetic Modeling Study*, Combustion Science and Technology, 127, 275-291

6.4 Billaud.F and Archambault.D, 1999, *Experimental and modeling study of methyl oleate pyrolysis between 500 and 650 ^{0}C*, J.Chim.Phys, 96, 778-796

6.5 Good.D.A, Francisco.J.S, 2000, *Tropospheric Oxidation Mechanism of Dimethyl Ether and Methyl Formate*, J.Phys.Chem, A 104, Issue 6, 1171-1185

6.6 Fisher.E.M, Pitz.W.J, Curran.H.J, Westbrook.C.K, 2000, *Detailed Chemical Kinetic Mechanisms for Combustion of Oxygenated Fuels*, Proceedings of Combustion Institute, 28, 1579-1586

6.7 Gail.S, Thomson.M.J, Sarathy.S.M, Syed.S.A, Dagaut.P, Dievart.P, Marchese.A.J, 2007, *A wide-ranging kinetic modeling study of methyl butanoate combustion*, Proceedings of Combustion Institute, Volume 31, Issue 1, 305-311

6.8 Marchese.A.J, Angioletti.M, Dryer.F.L, 2004, Internation Symposium on Combustion, Work-in-progress poster, 1F1-03

6.9 Gasnot.L, Decottignies.V, Pauwels.J.F, 2005, *Kinetics modeling of ethyl acetate oxidation in flame conditions, Fuel*, Volume 84, Issue 5, 505-518

6.10 Warnatz.J, 1993, *Hydrocarbon Oxidation at High Temperatures*, Ber.Bunsenges.Phys.Chem, 87, 1008-1022

6.11 Mati.K, 2005, *Cinétique de combustion du gazole à haute pression : étude expérimentale et modélisation*, Doctoral Thesis, University of Orleans, France

6.12 Dagaut.P, Ristori.A and Cathonnet.M, 2001, The *Oxidation of n-Hexadecane: Experimental and Detailed Kinetic Modeling*, Combustion and Flame, 125, 1128-1137

6.13 Billaud.F and Archambault.D, 1999, *Experimental and modeling study of methyl oleate pyrolysis between 500 and 650* ^{0}C, J.Chim.Phys, 96, 778-796

6.14 Archambault.Damien, 1997, *Valorisation non alimentaire de l'huile de colza: Pyrolyse de l'oleate de methyle*, Doctoral Thesis, I.N.P.L, Nancy, France

6.15 Osmont.A, 2007, *Elaboration d'une méthode théorique de calcul des enthalpies de formation en phase gazeous et condensée des molécules et radicaux de masse molaire élevée : Application à l'énergétique*, Doctoral Thesis, University of Orléans France

CHAPTER 7

MODELING RESULTS

Chapter 5 described the comparison of RME oxidation experimental results with diesel combustion on experimental and simulation basis. RME combustion results were simulated using surrogate fuel models using n-hexadecane ($C_{16}H_{34}$) and methyl acetate (CH_3COOCH_3) to represent the RME molecule. However, mechanisms used in these surrogate fuel models are not able to reproduce the experimental results in an exact manner. So considering the structure of RME, a new mechanism was developed for RME oxidation. Chapter 6 described the development of this new mechanism along with the modeling tools used (ChemKin simulation package and Perfectly Stirred Reactor (PSR) code). This chapter describes the simulation results for RME oxidation at 1 bar and 10 bar. It also includes analysis of results using tools like Rate of Production and Sensitivity Analysis.

7.1 Modeling with Rapeseed oil Methyl Ester (RME) as model fuel

As early formation of CO_2 was not detected by surrogate model fuels explained in chapter 5, a new chemical kinetic mechanism was developed for RME oxidation considering the degree of unsaturation and the presence of an ester function present in the RME structure. This mechanism also includes the chemistry associated with unsaturated, saturated intermediate esters and intermediate hydrocarbons formed during oxidation of RME. In the new mechanism, chemistry for C_1-C_8 compounds is based on the n-Hexadecane oxidation mechanism developed by Ristori et al [7.1]. The remaining chemistry is based on a high temperature hydrocarbon oxidation mechanism including chemistry for all C_9-C_{18} compounds (saturated & unsaturated esters, dienes and alkyl compounds). The detailed development of mechanism was already explained in Chapter 6. The thermochemical data for RME and related compounds was computed using the THERGAS code. The computations were performed using the Perfectly Stirred Reactor (PSR) code. The mechanism consists of 2652 reversible reactions and 496 species. All reactions except initiation reactions are reversible in this mechanism. The detailed reaction mechanism is given in appendix A. The rate expressions for initiation reactions, H atom abstraction, Isomerization reactions are given in table 7.1 to 7.4. The rate expressions given in table 7.1 and 7.2 are for

initiation and H atom abstraction reactions associated with RME. Table 7.3 gives rate expressions for Isomerization reactions and table 7.4 gives rate expression for H atom abstraction reactions applicable to RME, RME radicals, intermediate unsaturated (C_{16} to C_{10}) and saturated ester radicals, alkyl radicals. As initiation and thermal decomposition are important irreversible reactions, model fitting is done mainly for these reactions only. The model fitting done for initiation reactions is well within accepted range. The model fitting values are modified pre-exponential factor and activation energy values to fit the model as per experimental results. It was observed that initiation reactions were most influential reactions and values of pre-exponential factor (A) and activation energy (E) for these reaction have impact on chemical kinetics and simulation results. The reactions with '**=>**' symbol represents irreversible reactions and reactions with '**=**' symbol are reversible reactions.

Reactions	A	b	E_a	Fitting Values	References
C17:d9=>PC16:d9+CH3	2.51 X 10^{+17}	0.0	83000	A*10 E_a - 2400	7.4
C17:d9=>OC15:d9+C2H5	2.51 X 10^{+17}	0.0	79000	A*10 E_a - 2900	7.4
C17:d9=>NC14:d9+NC3H7	2.51 X 10^{+17}	0.0	79000	A*10 E_a - 2900	7.4
C17:d9=>MC13:d9+PC4H9	2.51X 10^{+17}	0.0	79000	A*10 E_a - 2900	7.4
C17:d9=>LC12:d9+AC5H11	2.51X 10^{+17}	0.0	79000	A*10 E_a - 2900	7.4
C17:d9=>KC11:d9+AC6H13	2.51X 10^{+17}	0.0	70800	A*10	7.4
C17:d9=>AC10H192+GC7:0	2.51X 10^{+17}	0.0	70800	A*10	7.4
C17:d9=>AC11H213+FC6:0	2.51X 10^{+17}	0.0	79000	A*10 E_a - 2900	7.4
C17:d9=>AC12H234+EC5:0	2.51X 10^{+17}	0.0	79000	A*10 E_a - 2900	7.4
C17:d9=>AC13H255+DC4:0	2.51X 10^{+17}	0.0	79000	A*10 E_a - 2900	7.4
C17:d9=>AC14H276+CC3:0	2.51X 10^{+17}	0.0	79000	A*10 E_a - 2900	7.4
C17:d9=>AC15H297+BC2:0	2.51X 10^{+17}	0.0	77000	A*10 E_a - 2000	7.4
C17:d9=>AC16H318+COOCH3	2.51X 10^{+17}	0.0	78000	A*10 E_a - 7400	7.4
C17:d9=>AC16H31COO+CH3	2.51X 10^{+18}	0.0	73000	A*10 E_a - 3000	7.4
AC16H31COO=>AC16H318+CO2	2.51X 10^{+20}	0.0	82000	E_a - 3000	7.4
COOCH3=>CO2+CH3	1.50X 10^{+11}	0.0	32700		7.4

Table 7.1: Rate expressions for initiation reactions with RME
(k= A T^b exp [-E/RT], (Units: s, K, cal/mole, cm^3)

Reactions	A	b	E_a	References
C17:d9 + O2 = HO2 + QC17:d9	2.50X 10^{+13}	0.0	49000	7.1
C17:d9 + O2 = HO2 + BC17:d9 TO PC17:d9	4.00X 10^{+13}	0.0	47600	7.1
C17:d9 = H + BC17:d9 TO QC17:d9	1.00X 10^{+15}	0.0	100000	7.1
C17:d9 + H = H2 + BC17:d9 TO QC17:d9	1.20X 10^{+07}	2.0	5000	7.1
C17:d9 + O = OH + BC17:d9 TO QC17:d9	1.13X 10^{+03}	3.3	1653	7.1
C17:d9 + OH = H2O + QC17:d9	1.41X 10^{+07}	1.8	974	7.1
C17:d9 + OH = H2O + BC17:d9 TO PC17:d9	1.13X 10^{+06}	2.0	-1391	7.1
C17:d9 + HO2 = H2O2 + BC17:d9 TO QC17:d9	4.88X 10^{+12}	0.0	18500	7.1
C17:d9 + CH3 = CH4 + QC17:d9	1.30X 10^{+12}	0.0	11600	7.1
C17:d9 + CH3 = CH4 + BC17:d9 TO PC17:d9	8.00X 10^{+11}	0.0	9500	7.1
C17:d9 + C2H3 = C2H4 + QC17:d9	1.00X 10^{+12}	0.0	18000	7.1
C17:d9 + C2H3 = C2H4 + BC17:d9 TO PC17:d9	8.00X 10^{+12}	0.0	16800	7.1
C17:d9 + C2H5 = C2H6 + QC17:d9	1.00X 10^{+15}	6.0	13400	7.1
C17:d9+ C2H5 = C2H6 + BC17:d9 TO PC17:d9	1.00X 10^{+15}	0.0	8400	7.1

Table 7.2: Rate expressions for H atom abstraction reactions with RME ($k= A T^b \exp[-E/RT]$, (Units: s, K, cal/mole, cm^3)

Reactions	A	b	E_a	References
$R_{(primary)}$ => $R_{(secondary)}$ (1-4)	5.01X 10^{+11}	0.0	17300	7.4
$R_{(primary)}$ => $R_{(secondary)}$ (1-5)	8.61X 10^{+10}	0.0	12000	7.4
$R_{(primary)}$ => $R_{(secondary)}$ (1-6)	1.48X 10^{+10}	0.0	17400	7.4
$R_{(secondary)}$ => $R_{(secondary)}$ (1-4)	5.01X 10^{+11}	0.0	17300	7.4
$R_{(secondary)}$ => $R_{(secondary)}$ (1-5)	8.61X 10^{+10}	0.0	12000	7.4
$R_{(secondary)}$ => $R_{(secondary)}$ (1-6)	1.48X 10^{+10}	0.0	17400	7.4
$R_{(secondary)}$ => $R_{(primary)}$ (1-4)	7.52X 10^{+11}	0.0	19800	7.4
$R_{(secondary)}$ => $R_{(primary)}$ (1-5)	1.29X 10^{+11}	0.0	14500	7.4
$R_{(secondary)}$ => $R_{(primary)}$ (1-6)	2.11X 10^{+10}	0.0	19900	7.4

Table 7.3: Rate expressions for Isomerization reactions ($k= A T^b \exp[-E/RT]$, (Units: s, K, mole/cal, cm^3)

Reactions	A	b	E_a	References
R + O2 = HO2 + R1	1.40X 10^{+13}	0.0	39000	7.1
R + O = OH + R1	1.00X 10^{+13}	0.0	4000	7.1
R + OH = H2O + R1	1.00X 10^{+13}	0.0	1230	7.1
R + HO2 = H2O2 + R1	1.00X 10^{+11}	0.0	17000	7.1
R + H = H2 + R1	1.00X 10^{+13}	0.0	3900	7.1
R + CH3 = CH4 + R1	2.00X 10^{+11}	0.0	7300	7.1
R + C2H3 = C2H4 + R1	2.00X 10^{+11}	0.0	7300	7.1
R + C2H5 = C2H6 + R1	1.26X 10^{+15}	0.0	10400	7.1
+R = H + R1	1.15X 10^{+15}	0.0	100000	7.1

Table 7.4: Rate expressions for H atom abstraction reactions ($k= A T^b \exp[-E/RT]$, (Units: s, K, mole/cal, cm^3)

*Where, R & R1 = Saturated, unsaturated esters radical and alkyl radicals

* Where R is RME radical and R1 is a fatty acid ester radical

RME oxidation experimental results are presented in chapter 4. RME oxidation was simulated using new chemical kinetic mechanism explained in chapter 6. Here simulation results are presented for 1 & 10 bar for fuel-lean to fuel-rich conditions. RME chemical kinetic model calculates and gives exit mole fractions for all reactants, intermediate species and combustion products at user defined temperature range and equivalence ratio. These exit mole fractions are compared with mole fractions obtained from experiments and are presented in the form of graphical representation. The experimentation observations are also explained by using simulation work.

RME simulation results for 1 bar are presented in section 7.2 along with sensitivity analysis and rate of production analysis. The rate of production analysis gives set of reactions, which are mainly responsible for consuming fuel molecule during its oxidation. 'R' is rate of production or consumption in rate of production analysis. 'R' with positive value, is normalized rate of production and with negative value, it is normalized rate of consumption. The absolute rate of production is expressed in moles/cc-sec. The rate of production analysis was done for RME and pollutants like CH_2O and 1,3-Butadiene at 1 bar. A sensitivity analysis gives a set of reactions, which are sensitive to modification of kinetic parameters and changes to their kinetic parameters can affect the reactivity of fuel or hydrocarbon.

7.2 Results at 1 bar

The modeling for RME using RME as model fuel was done at 1 bar for fuel-lean to fuel-rich conditions (Φ = 0.25 to 1.5), for temperature range of 900 to 1400K. The mole fractions of important oxygenated compounds, intermediate olefins (C_2 to C_6) and products are plotted against the temperature. Figure 7.1 to 7.4 shows simulation results with experimental results plotted for all fuel conditions. The mole fractions were obtained for oxygen, hydrogen, carbon monoxide (CO),carbon dioxide (CO_2), formaldehyde (CH_2O), methane(CH_4), ethane (C_2H_6), ethene (C_2H_4), acetylene (C_2H_2), propene (C_3H_6),1-butene (1-C_4H_8),1-pentene (1-C_5H_{10}), 1-hexene (1-C_6H_{12}), 1-heptene (C_7H_{14}) and 1,3-butadiene (1,3-C_4H_6).

Figure 7.1 and 7.2 shows the predicted and experimentally measured concentrations, expressed as mole fractions, for key RME oxidation products for fuel-lean conditions (Φ = 0.25 and 0.5),. The results in figure 7.1 and 7.2 shows that the model predicts the similar profile trends as found in the experiment; in that as the temperature of the reaction is increased from 900 K, the concentration of decomposition products CO, CO_2 and CH_2O increases while the concentration of unused oxygen reduces (figure 7.1 and 7.2 a). However after 1100 K, the model deviates slightly from the experimental results.

Figure 7.1 (b, c, and d) and 7.2 (b, c and d) for long chain intermediate hydrocarbons shows that their concentration increases up to 1000 to 1100 K, and then starts decreasing. The temperature of 1100 K therefore seems to be a limit where smaller hydrocarbon molecules are themselves reacted with oxygen to form CO, CO_2, and CH_2O. This would explain the decrease in oxygen concentration observed during the experiment. The model agrees with their experimental observations although the predicted concentrations are an order of magnitude different from what was experimentally measured.

Figure 7.1.a and 7.2.a highlights the importance of the CO_2 formed during the combustion. The experimental measurements show that CO_2 concentrations rise gradually, they are constant over the temperature range of 980 to 1050 K for Φ = 0.25 and 1000 to 1100 K for Φ = 0.5. After 1050 K (figure 7.1.a) and 1100 K (figure 7.2.a) concentrations of CO_2 rise sharply. The each fraction of CO_2 in the model is as result of the chemistry associated with the ester function present in the RME structure. The early formation of CO_2, CO for temperature range 850-950 K (Φ = 0.25) and 900-1000K (Φ = 0.5) in the experiment shows that there must be breakdown of longer chain molecules early in the oxidation process. This can be attributed to the breakdown of functional groups such as the ester function present in the RME structure. Although the new model for RME oxidation developed in this work has these reactions present, it is still unable to predict accurately the early formation of CO_2, CO and CH_2O at fuel lean conditions (Φ = 0.25. 0.5).

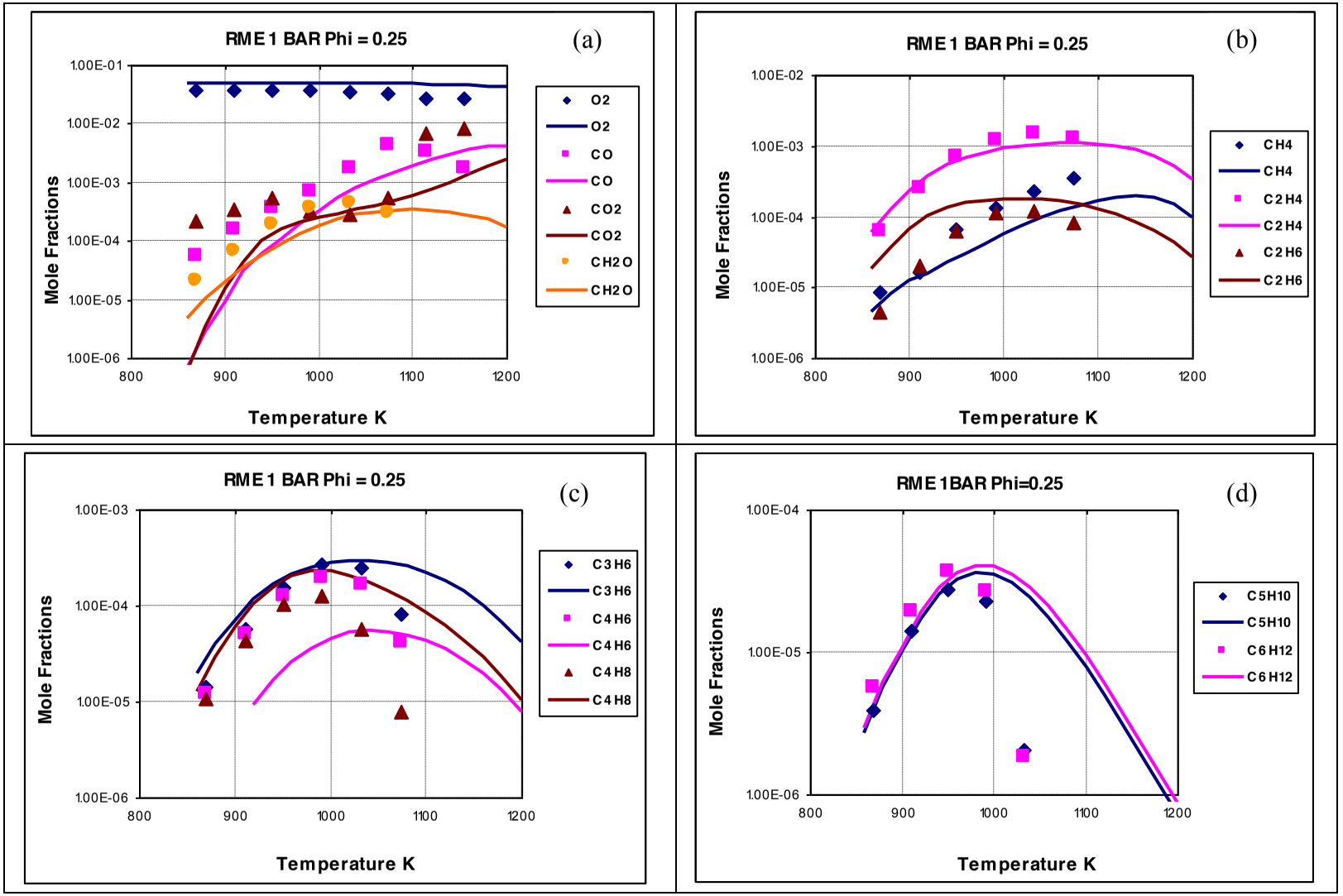

Figure 7.1: The oxidation of RME in a JSR (P = 1bar, Φ = 0.25, τ =0.07 s). The experimental data (large symbols) are compared to the computations (lines model fuel: RME)

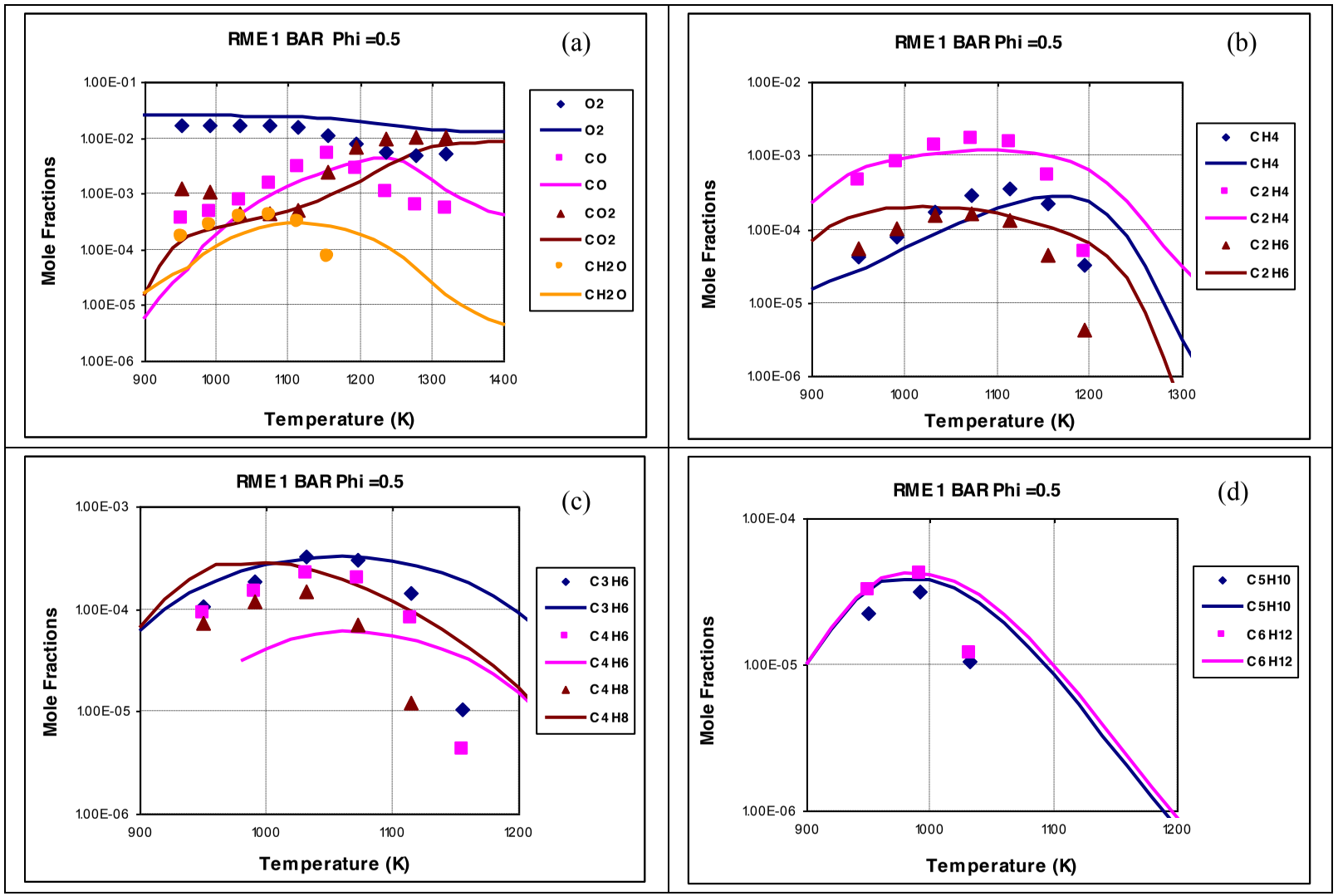

Figure 7.2: The oxidation of RME in a JSR (P = 1bar, Φ = 0.5, τ =0.07 s). The experimental data (large symbols) are compared to the computations (lines model fuel: RME)

Results at fuel- lean (Φ = 0.25, 0.5):

At fuel- lean (Φ = 0.25, 0.5) conditions (figure 7.1 and 7.2), the model reproduced the formation of intermediate hydrocarbons like 1-olefins at initial temperature (at 940 K CH_4 = 24 ppm C_2H_4 = 534 ppm, C_3H_6 = 146 ppm, C_4H_8 = 196 ppm, C_5H_{10}= 27 ppm and C_6H_{12}= 28 ppm), it indicates that the fuel reacted very rapidly at initial working temperature. The model predicts the concentration for C_1-C_3 intermediate hydrocarbons, CH_2O better than CO and CO_2. The table 7.5 shows the reactions along with Rate of Production, responsible for RME consumption and re-production at 940 K. As mentioned in chapter 6 RME is mainly consumed in initiation reactions (at 940 K, reaction no 1112, 113 and 1120) producing alkyl, alkenyl radicals and saturated esters. It can be seen from table 7.5 RME consumption is primarily through reaction no 1120 (42.9%). However RME is also reproduced by oxidation reactions (reaction 1124 and 1128), which are reversible reactions.

Reaction No	Reactions	Normalized Rate Of Production (ROP) Coefficients	Absolute Rate Of Production (ROP) moles/cc-sec
RME			
1112	C17:d9=>KC11:d9+AC6H13	-0.139	-1.05E-08
1113	C17:d9=>AC10H192+GC7:0	-0.139	-1.05E-08
1120	C17:d9=>AC16H31COO+CH3	-0.429	-3.23E-08
1124	C17:d9+O2<=>HO2+CC17:d9	0.102	6.60E-13
1128	C17:d9+O2<=>HO2+GC17:d9	0.107	6.89E-13

Table 7.5: Rate of production and consumption for RME at 940 K

Figure 7.1 and 7.2 shows that at both fuel-lean conditions (Φ = 0.25, 0.5) model failed to re-produce early formation of CO_2. At Φ = 0.5 condition in simulation work, CO_2 is produced in quantity of 108 ppm (940 K) and 168 ppm (960K) only, compared to 1200 ppm (950K) obtained experimentally. As mentioned in chapter 4 and 5 this early formation of CO_2 is mainly from reaction no 1121 (99.3%) which is associated with the ester function (CH_3COOCH_3) present in the RME structure. However table 7.6 show CO_2 is mainly consumed in a recombination reaction (99.9%, reaction no 1122) to form an ester, although the rate of consumption is several order of magnitude lower than CO_2 production.

Reaction No	Reactions	Normalized Rate Of Production (ROP) Coefficients	Absolute Rate Of Production (ROP) moles/cc-sec
CO_2			
1121	AC16H31COO=>AC16H318+CO2	0.993	1.95E-08
1122	COOCH3<=>CO2+CH3	-0.999	-1.96E-11
CH_2O			
48	CH3+O2<=>CH2O+OH	0.141	1.01E-09
98	CH3O+M<=>CH2O+H+M	0.478	3.42E-09
467	C4H8+OH<=>CH2O+NC3H7	0.204	1.46E-09
2646	C2H3+O2<=>CH2O+HCO	0.126	8.97E-10
111	CH2O+HO2<=>HCO+H2O2	-0.173	-1.31E-10
112	CH2O+OH<=>HCO+H2O	-0.421	-3.18E-10
116	CH2O+CH3<=>HCO+CH4	-0.384	-2.90E-10
CO			
30	HCO+O2<=>CO+HO2	0.351	1.70E-09
428	C2H3CO+M=>C2H3+CO+M	0.546	2.65E-09
589	OC4H6=>C3H6+CO	-0.237	-1.77E-11
608	C4H5O=>CO+AC3H5	-0.508	-3.79E-11

Table 7.6: Rate of production and consumption for oxygenated compounds at 940 K

The model is under predicted the profile trends and concentrations of formaldehyde (CH_2O) and CO at initial working temperature range (940 K to 960 K) compared to experimentally observed quantities (more than 100 ppm). At these conditions formaldehyde (CH_2O) is mainly consumed in metathesis reactions (42% and 38%, reaction no 112, 116) mentioned in table 7.6 and CO is consumed in recombination reactions (reaction no 589 and 608). However model is able to reproduce formation of CO, CO_2 and CH_2O at higher temperatures. As mentioned in chapter 4, at higher temperatures, the fuel based oxygen i.e. oxygen present in fuel structure compared to air based oxygen, accelerates the combustion process. P.Janulis [7.6] observed that this fuel based oxygen allows conversion of CO to CO_2 thus reducing CO emission. It can be seen from reactions 21, 22 and 229 in table 7.7 at higher temperatures CO_2 (1240 ppm at 1180 K) is mainly produced from CO and HCCO radicals, not only by initiation reaction. Thus the reproduction of the oxygenated contents present in RME structure helps to increase the combustion efficiency.

Reaction No	Reactions	Normalized Rate Of Production (ROP) Coefficients	Absolute Rate Of Production (ROP) moles/cc-sec
CO			
21	CO+HO2<=>CO2+OH	-0.372	-2.13E-08
22	CO+OH<=>CO2+H	-0.625	-3.57E-08
25	HCO+M<=>H+CO+M	0.280	1.51E-07
30	HCO+O2<=>CO+HO2	0.375	2.02E-07
CO_2			
21	CO+HO2<=>CO2+OH	0.117	2.13E-08
22	CO+OH<=>CO2+H	0.196	3.57E-08
63	CH2+CO2<=>CH2O+CO	-0.734	-1.22E-11
89	SCH2+CO2<=>CH2O+CO	-0.265	-4.42E-12
229	HCCO+O2<=>CO2+CO+H	0.234	4.27E-08
1121	AC16H31COO=>AC16H318+CO2	0.249	4.55E-08

Table 7.7: Rate of production and consumption for CO, CO_2 at 1180 K

The experimental results showed that intermediates reached maximum mole fractions value particularly in temperature range of 950 to 1100 K. Figure 7.1 and 7.2 shows that at both fuel-lean conditions (Φ = 0.25, 0.5) the model over predicts the reactivity for 1,3-Butadiene (C_4H_6) and under predicts the reactivity for C_4H_8 at Φ = 0.5 conditions. It can be seen from figure 7.2 that the model under predicts the mole fraction of C_4H_6 at 1020K, whereas it over predicts the mole fractions at higher temperatures (1160K). At 1020K 1-3 Butadiene was mainly produced from Methyl Allyl (MEALL) in reaction no 524 and consumed in metathesis reaction of C_4H_6 with O radical in reaction 588. Table 7.9 shows the reaction associated with C_4H_6 production and reduction at 1020 K. However at higher temperature (1160K) apart from Methyl Allyl, C_4H_6 is also produced from decomposition of Methyl Heptenoate radical (EC7:1) (reaction no 1671 in table 7.8). At all temperatures C_4H_8 is produced from recombination of smaller radicals & decomposition of alkenyl radical and it is mainly consumed in metathesis reactions. Table 7.8 shows the reactions and rate of production for C_4H_6 and C_4H_8 at 1160 K.

Reaction No	Reactions	Normalized Rate Of Production (ROP) Coefficients	Absolute Rate Of Production (ROP) moles/cc-sec
C_4H_6			
524	MEALL<=>C4H6+H	0.598	1.81E-08
586	C4H6+OH<=>HOC4H6	-0.210	-5.34E-09
588	C4H6+O=>OC4H6	-0.359	-9.13E-09
1671	EC7:1<=>C4H6+CC3:0	0.160	4.84E-09
C_4H_8			
461	C4H8<=>AC3H5+CH3	0.564	3.04E-08
466	C4H8+OH<=>MEALL+H2O	-0.184	-9.15E-09
467	C4H8+OH<=>CH2O+NC3H7	-0.128	-6.36E-09
469	C4H8+O<=>C3H6+CH2O	-0.157	-7.83E-09
473	C4H8+H<=>SC4H9	-0.113	-5.62E-09
933	CC7H15<=>C4H8+NC3H7	0.403	2.17E-08

Table 7.8: Rate of production and consumption for C_4H_6, C_4H_8 at 1160K

Reaction No	Reactions	Normalized Rate Of Production (ROP) Coefficients	Absolute Rate Of Production (ROP) moles/cc-sec
C_4H_6			
524	MEALL<=>C4H6+H	0.435	5.05E-09
525	MEALL+O2<=>C4H6+HO2	0.100	1.16E-09
538	MEALL+AC3H5<=>C4H6+C3H6	0.267	3.10E-09
586	C4H6+OH<=>HOC4H6	-0.376	-1.16E-09
588	C4H6+O=>OC4H6	-0.259	-7.96E-10
C_5H_{10}			
765	AC5H10<=>C2H5+AC3H5	-0.584	-2.42E-09
768	AC5H10+OH<=>C5H913+H2O	-0.248	-1.03E-09
932	DC7H15<=>AC5H10+C2H5	0.352	3.47E-09
1845	DC16H318<=>AC5H10+AC11H213	0.446	4.41E-09
C_6H_{12}			
894	AC6H12<=>NC3H7+AC3H5	-0.490	-2.36E-09
896	AC6H12<=>2C3H6	-0.158	-7.63E-10
899	AC6H12+OH<=>C6H1113+H2O	-0.172	-8.32E-10
931	CC7H15<=>AC6H12+CH3	0.769	8.57E-09
1847	EC16H318<=>AC6H12+AC10H192	0.165	1.83E-09

Table 7.9: Rate of production and consumption for intermediate hydrocarbons at 1020K

Figure 7.1 and 7.2 shows that the model is able to reproduce the formation of important alkenes like 1-C_5H_{10} and 1-C_6H_{12} in a precise manner up to temperature range of 1000 K. The model over predicts the formation of these alkenes at higher temperatures (above 1000 K). Table 7.9 shows reactions associated with production and consumption of 1-C_5H_{10} and 1-C_6H_{12}. As mentioned in chapter 4 these olefins are mainly produced from decomposition of the Hexadecene radical ($C_{16}H_{31}$:8), which is formed from the decomposition of RME (reactions 1845, 1847 in table 7.9). Apart from Hexadecene radical ($C_{16}H_{31}$:8), decomposition of Heptane radical produces 1-C_5H_{10} and 1-C_6H_{12} in reaction no 932 and 931 respectively. As observed in other RME combustion work, long unsaturated chain present in RME structure is responsible for producing these olefins [7.7] [7.8]. 1-C_5H_{10} is mainly consumed in decomposition in (reaction 765) and metathesis reaction (reaction no 768) where as 1-C_6H_{12} is mainly consumed in decomposition reaction only (reaction no 894 and 896 in table 7.9).

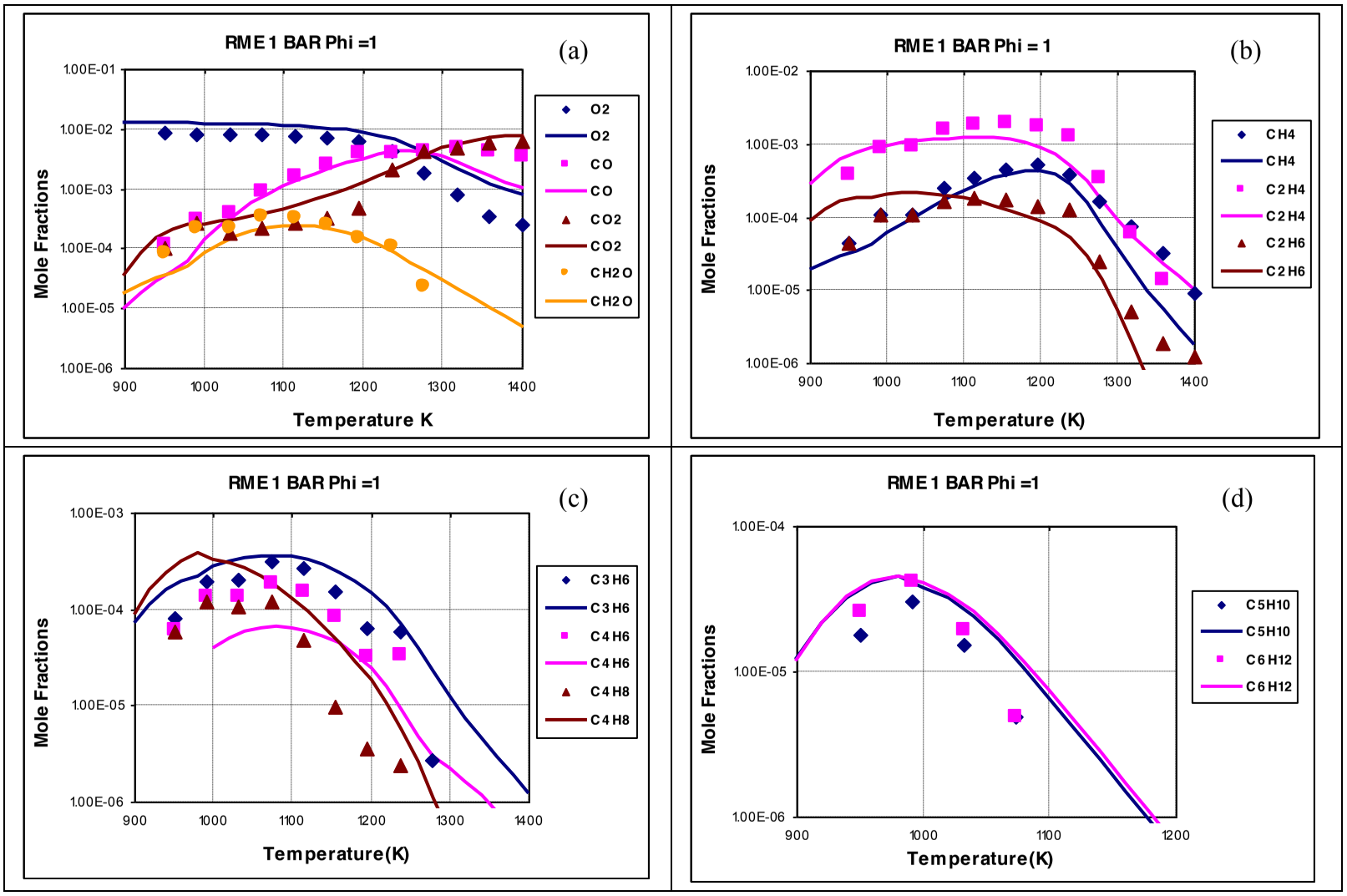

Figure 7.3: The oxidation of RME in a JSR (P = 1bar, Φ = 1, τ = 0.1 s). The experimental data (large symbols) are compared to the computations (lines model-fuel: RME)

Result at stoichiometric condition (Φ = 1.0):

Figure 7.3 shows the results at stoichiometric condition (Φ = 1.0) for key RME oxidation products. The results in figure 7.3 shows that the model reproduces the similar profile trends as found in the experiment. The profile trends show that as the temperature of the reaction is increased from 900 K to 1200 K, the concentration of decomposition products CO, CO_2 and CH_2O is increased (figure 7.3 a). However after 1200 K, the model deviates slightly from the experimental results. The model is able to reproduce early formation of CO and CO_2 better than that predicted from fuel lean conditions.

Figure 7.3 b, c, and d for long chain intermediate hydrocarbons shows that their concentration increases up to about to 1200 K, and then starts decreasing. The temperature of 1200 K therefore seems to be a limit where smaller hydrocarbon molecules start reacting with molecular oxygen. The model gives good agreement with experimental observations in terms of profile trends of CH_4, C_3H_6, C_5H_{10} and C_6H_{12} except model under predicts CO formation at high temperature.

Reaction No	Reactions	Normalized Rate Of Production (ROP) Coefficients	Absolute Rate Of Production (ROP) moles/cc-sec
CO_2			
63	CH2+CO2<=>CH2O+CO	-0.868	-5.11E-14
89	SCH2+CO2<=>CH2O+CO	-0.132	-7.75E-15
1121	AC16H31COO=>AC16H318+CO2	0.989	1.56E-08
CH_2O			
98	CH3O+M<=>CH2O+H+M	0.468	2.39E-09
111	CH2O+HO2<=>HCO+H2O2	-0.139	-1.03E-10
112	CH2O+OH<=>HCO+H2O	-0.354	-2.63E-10
114	CH2O+H<=>HCO+H2	-0.160	-1.18E-10
116	CH2O+CH3<=>HCO+CH4	-0.333	-2.47E-10
467	C4H8+OH<=>CH2O+NC3H7	0.260	1.33E-09
2646	C2H3+O2<=>CH2O+HCO	0.115	5.89E-10
CO			
21	CO+HO2<=>CO2+OH	-0.464	-6.90E-12
22	CO+OH<=>CO2+H	-0.514	-7.65E-12
30	HCO+O2<=>CO+HO2	0.281	1.34E-09
28	C2H3CO+M=>C2H3+CO+M	0.539	2.57E-09

Table 7.10: Rate of production and consumption for oxygenated compounds at 940 K

The rate of production analysis (ROP) in table 7.10 shows the path responsible for the early formation of CO_2. It can be seen from table 7.10, at the initial working temperature (940K), CO_2 is mainly produced from initiation reaction (reaction no 1121) associated with the ester group present in the RME structure. However it is mainly consumed in reaction no 63 mentioned in table 7.10 for formation of CO and formaldehyde (CH_2O). This CO_2 consumption path i.e. reaction no 63, is different than one observed at fuel-lean conditions. At fuel lean conditions CO_2 is consumed in a recombination reaction (reaction no 1122 in table 7.6) to form an ester group. So this CO_2 contribution to produce CO at stoichiometric conditions (reactions 63 and 89 in table 7.10) can explain the observations made by O.I Nwafor, that as Fuel/Air ratio increases, CO emissions increases for RME [7.7].

The model shows that at this temperature (940K) CO is mainly consumed to produce CO_2 (reaction no 21 and 22 in table 7.10). As CO_2 is produced from reaction path associated with ester function (reaction no 1121) and reaction associated with CO (reaction no 21 and 22), it justify the observations of Nwafor [7.7] and comparison with diesel in chapter 5, that RME produces more CO_2 than commercial diesel. The formaldehyde is mainly produced from third body reaction with Methoxy radical (CH_3O) (reaction no 98 in table 7.10) and metathesis reaction with 1-butene (reaction no 467). At 940 K, RME is mainly consumed by initiation reactions outlined in table 7.11, producing alkyl, alkenyl radicals and saturated esters (reaction no 1112, 1113 and 1120). As reactions of RME with molecular Oxygen are reversible reactions, RME is also reproduced by these oxidation reactions (reaction no 1124, 1127, and 1128 in table 7.11).

Reaction No	Reactions	Normalized Rate Of Production (ROP) Coefficients	Absolute Rate Of Production (ROP) moles/cc-sec
RME			
1112	C17:d9=>KC11:d9+AC6H13	-0.132	-7.42E-09
1113	C17:d9=>AC10H192+GC7:0	-0.132	-7.42E-09
1120	C17:d9=>AC16H31COO+CH3	-0.407	-2.28E-08
1124	C17:d9+O2<=>HO2+CC17:d9	0.115	5.00E-13
1127	C17:d9+O2<=>HO2+FC17:d9	0.102	4.46E-13
1128	C17:d9+O2<=>HO2+GC17:d9	0.120	5.20E-13

Table 7.11: Rate of production and consumption for RME at 940 K

At higher temperatures (1320K) CO is mainly consumed by producing CO_2 (reaction no 22 in table 7.12). As normalized rate of production for CO at 1320K is lower than the its rate of consumption (reaction no 22 and 25 in table 25), the mole fractions of CO are underestimated in figure 7.3, compared to experimental results after 1320K. At 1320K, CO_2 is mainly produced from reactions like metathesis and oxidation reactions with intermediate species like CO, HCCO (reaction no 22 & 229 in table 7.12). The conversion of these intermediate species (CO, HCCO) to final combustion product CO_2 in reaction 22 and 229, explains the experimental observation that RME reactivity increases with increasing temperature.

Reaction No	Reactions	Normalized Rate Of Production (ROP) Coefficients	Absolute Rate Of Production (ROP) moles/cc-sec
CO			
22	CO+OH<=>CO2+H	-0.988	-3.91E-07
25	HCO+M<=>H+CO+M	0.560	3.61E-07
CO_2			
22	CO+OH<=>CO2+H	0.735	3.91E-07
63	CH2+CO2<=>CH2O+CO	-0.625	-2.61E-09
89	SCH2+CO2<=>CH2O+CO	-0.338	-1.41E-09
229	HCCO+O2<=>CO2+CO+H	0.116	6.18E-08
RME			
1112	C17:d9=>KC11:d9+AC6H13	-0.146	-6.68E-09
1113	C17:d9=>AC10H192+GC7:0	-0.146	-6.68E-09
1120	C17:d9=>AC16H31COO+CH3	-0.630	-2.89E-08
1138	C17:d9<=>H+CC17:d9	0.114	6.88E-16
1142	C17:d9<=>H+GC17:d9	0.130	7.81E-16
1150	C17:d9<=>H+QC17:d9	0.132	7.98E-16

Table 7.12: Rate of production and consumption for CO, CO_2 and RME at 1320 K

For C_1-C_4 compounds, the model under predicts the reactivity at lower temperatures, whereas the profile trend for 1,3 Butadiene is improved compared to fuel-lean conditions. The early formation of the intermediate hydrocarbons like 1-olefins at initial temperature (at 940 K CH_4 = 28.5 ppm C_2H_4 = 607 ppm, C_2H_6 = 162 ppm, C_3H_6 = 158 ppm, C_4H_8 = 242 ppm, C_5H_{10}= 32 ppm and C_6H_{12}= 32 ppm), indicates that the fuel has reacted very rapidly. Figure 7.3 shows that the model over predicts the formation of C_2H_6, C_3H_6, C_4H_8 and it is unable to produce

1,3 Butadiene at the initial working temperature i.e. 940 K. However the model is able to reproduce Propene (C_3H_6) and 1-Butene (C_4H_8) at 1120K in precise manner.

The reactivity of RME at stoichiometric condition (Φ = 1.0) is lower compared to fuel lean conditions (Φ = 0.25, 0.5). It was observed that mole fractions of intermediates (saturated, unsaturated as well as oxygenated) reached their maximum value at higher temperatures particularly in temperature range of 1000 to 1200 K. At 1140 K the rate of consumption for RME is higher than rate of production. Table 7.13 shows the rate of production (ROP) for important intermediate species at 1140K.

Reaction No	Reactions	Normalized Rate Of Production (ROP) Coefficients	Absolute Rate Of Production (ROP) moles/cc-sec
C_2H_6			
118	C2H6+OH<=>C2H5+H2O	-0.427	-7.40E-09
120	C2H6+H<=>C2H5+H2	-0.408	-7.06E-09
2618	2CH3(+M)<=>C2H6(+M)	0.530	1.73E-08
C_2H_4			
136	C2H4+OH<=>C2H3+H2O	-0.306	-1.63E-08
137	C2H4+O<=>CH3+HCO	-0.146	-7.76E-09
138	C2H4+O<=>CH2HCO+H	-0.243	-1.29E-08
142	C2H4+CH3<=>C2H3+CH4	-0.216	-1.15E-08
729	AC5H11<=>C2H4+NC3H7	0.145	2.61E-08
2620	C2H4+H(+M)<=>C2H5(+M)	0.215	3.86E-08
2629	NC3H7(+M)<=>C2H4+CH3(+M)	0.325	5.86E-08
C_3H_6			
300	C3H6+OH<=>AC3H5+H2O	-0.180	-9.14E-09
310	C3H6+H<=>AC3H5+H2	-0.371	-1.89E-08
426	ACROL+AC3H5=>C2H3CO+C3H6	0.100	8.14E-09
2651	C3H6<=>AC3H5+H	0.390	3.18E-08
C_4H_6			
159	C2H3+C2H4<=>C4H6+H	-0.152	-2.14E-09
524	MEALL<=>C4H6+H	0.517	1.02E-08
586	C4H6+OH<=>HOC4H6	-0.188	-2.64E-09
588	C4H6+O=>OC4H6	-0.294	-4.14E-09
1671	EC7:1<=>C4H6+CC3:0	0.171	3.36E-09

Table 7.13: Rate of production and consumption for intermediate hydrocarbons at 1140 K

It can be seen from table 7.13 at 1140 K, Ethane (C_2H_6), Ethylene (C_2H_4), Propene (C_3H_6) and 1,3 Butadiene (C_3H_6), are pre-dominantly consumed in metathesis reactions (reaction no 120, 136 to 138, 300, 310, 586 and 588). Ethane is mainly formed by recombination of methyl radicals (reaction no 2618) and Ethylene is formed by third body reaction (reaction no 2629). 1, 3 Butadiene is formed from decomposition of methyl allyl (reaction no 524). These three reactions have highest normalized rate of production coefficients compared to other reactions. At higher temperatures (1320 K), the model is predicting Ethane (C_2H_6) and Ethylene (C_2H_4) in precise manner. Table 7.14 shows rate of production and consumption for C_2H_6, C_2H_4 at 1320 K. At 1320 K also recombination of methyl radicals (reaction no 2618) is responsible for producing Ethane. However ROP for this reaction (reaction 2618) is much higher at 1320 K compared to that obtained at 1120K.

Reaction No	Reactions	Normalized Rate Of Production (ROP) Coefficients	Absolute Rate Of Production (ROP) moles/cc-sec
C_2H_6			
118	C2H6+OH<=>C2H5+H2O	-0.442	-8.61E-09
119	C2H6+O<=>C2H5+OH	-0.128	-2.49E-09
120	C2H6+H<=>C2H5+H2	-0.424	-8.26E-09
2618	2CH3(+M)<=>C2H6(+M)	0.971	1.91E-08
C_2H_4			
136	C2H4+OH<=>C2H3+H2O	-0.330	-6.77E-08
137	C2H4+O<=>CH3+HCO	-0.211	-4.32E-08
138	C2H4+O<=>CH2HCO+H	-0.351	-7.19E-08
729	AC5H11<=>C2H4+NC3H7	0.113	2.37E-08
2620	C2H4+H(+M)<=>C2H5(+M)	0.257	5.41E-08
2629	NC3H7(+M)<=>C2H4+CH3(+M)	0.217	4.55E-08

Table 7.14: Rate of production and consumption for C_2H_6, C_2H_4 at 1320 K

Reaction No	Reactions	Normalized Rate Of Production (ROP) Coefficients	Absolute Rate Of Production (ROP) moles/cc-sec
AC_5H_{10}			
736	BC5H11<=>AC5H10+H	-0.100	-4.38E-11
765	AC5H10<=>C2H5+AC3H5	-0.170	-7.45E-11
768	AC5H10+OH<=>C5H913+H2O	-0.518	-2.27E-10
771	AC5H10+H<=>C5H913+H2	-0.167	-7.32E-11
932	DC7H15<=>AC5H10+C2H5	0.413	1.78E-09

1845	DC16H318<=>AC5H10+AC11H213	0.315	1.35E-09
2428	GC10H192<=>AC5H10+C5H925	0.136	5.87E-10
AC_6H_{12}			
884	BC6H13<=>AC6H12+H	-0.162	-7.94E-11
894	AC6H12<=>NC3H7+AC3H5	-0.171	-8.40E-11
896	AC6H12<=>2C3H6	-0.129	-6.31E-11
899	AC6H12+OH<=>C6H1113+H2O	-0.357	-1.75E-10
931	CC7H15<=>AC6H12+CH3	0.814	3.76E-09
1847	EC16H318<=>AC6H12+AC10H192	0.110	5.06E-10

Table 7.15: Rate of production and consumption for 1-Pentene and 1-Hexene at 940 K

Reaction No	Reactions	Normalized Rate Of Production (ROP) Coefficients	Absolute Rate Of Production (ROP) moles/cc-sec
AC_5H_{10}			
765	AC5H10<=>C2H5+AC3H5	-0.633	-1.36E-09
768	AC5H10+OH<=>C5H913+H2O	-0.179	-3.85E-10
771	AC5H10+H<=>C5H913+H2	-0.099	-2.13E-10
932	DC7H15<=>AC5H10+C2H5	0.365	2.48E-09
1845	DC16H318<=>AC5H10+AC11H213	0.432	2.93E-09
AC_6H_{12}			
894	AC6H12<=>NC3H7+AC3H5	-0.505	-1.29E-09
896	AC6H12<=>2C3H6	-0.187	-4.80E-10
899	AC6H12+OH<=>C6H1113+H2O	-0.117	-3.00E-10
931	CC7H15<=>AC6H12+CH3	0.787	5.88E-09
1847	EC16H318<=>AC6H12+AC10H192	0.159	1.19E-09

Table 7.16: Rate of production and consumption for 1-Pentene and 1-Hexene at 1000 K

Figure 7.3 shows that the model is able to reproduce formation of important alkenes like 1-Pentene (1-C_5H_{10}) and 1-Hexene (1-C_6H_{12}) in reasonable manner up to temperature range of 1040 K. The model over predicts formation of these alkenes at higher temperatures (above 1050 K). The model reproduces experimental observation that 1-Pentene and 1-Hexene reach their concentration maxima at 990-1000 K. It can be seen from table 7.15, at 940 K 1-Pentene is mainly consumed in metathesis reaction (reaction no 768) and produced by decomposition of alkyl radical (reaction no 932), whereas at 1000K it is mainly consumed in decomposition reaction to form smaller radicals like Ethyl radical (C_2H_5) and Allyl radical (AC_3H_5) (reaction no 765 in table 7.16) and produced

from decomposition of Hexadecene radical ($C_{16}H_{31}$:8) formed from RME (reaction no 1845). Table 7.15 and 7.16 shows the rate production and consumption for 1-Pentene and 1-Hexene at 940 K and 1000 K respectively. 1-Hexene is mainly consumed in metathesis reaction (reaction no 899) and produced from decomposition of Heptyl radical (C_7H_{15}) in reaction no 931 at 940 K, whereas at 1000K, it is mainly consumed in decomposition reaction (reaction no 894) and produced by decomposition of Heptyl radical (C_7H_{15}) only (reaction no 931).

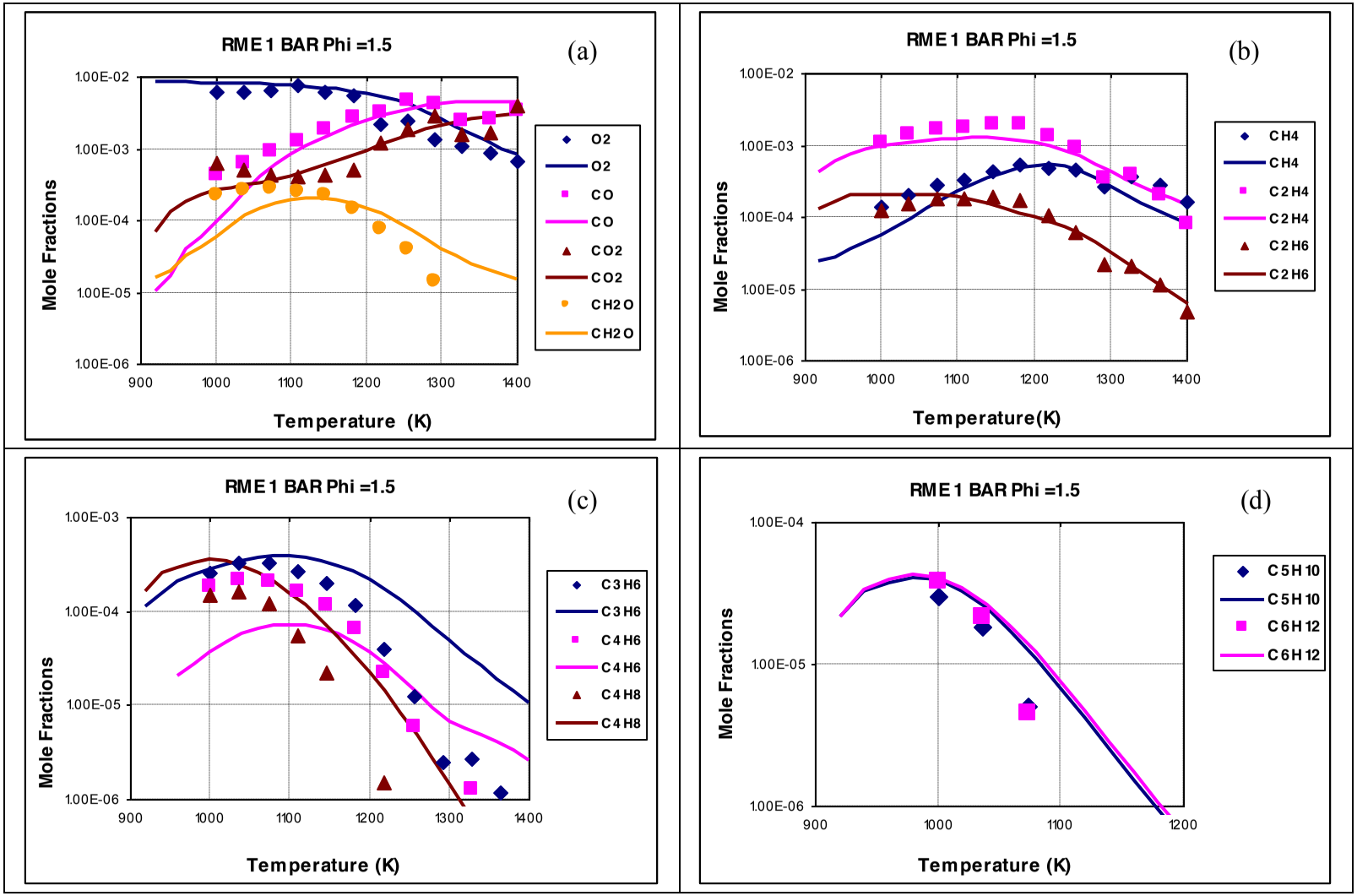

Figure 7.4: The oxidation of RME in a JSR (P = 1 bar, Φ = 1.5, τ = 0.1 s). The experimental data (large symbols) are compared to the computations (lines model-fuel: RME)

Results at fuel- rich conditions (Φ = 1.5):

Though fuel-lean conditions are important in diesel engine combustion, the combustion performance of the fuel is important at fuel-rich conditions (Φ = 1.5). Chapter 4 showed that RME reactivity decreases with increasing equivalence ratio and it was lowest at fuel-rich condition. Figure 7.4 shows the results at fuel-rich condition (Φ = 1.5) for key RME oxidation products. The results in figure 7.4.a shows that the model reproduces early formation of CO_2 reasonably well compared to fuel lean conditions. The increase in CO_2 mole fractions at initial working temperature i.e. 1000 K, with increase in Fuel/O_2 ratio indicates the combustion efficiency of RME. The CO_2 concentration obtained from all experiments is highest (260 ppm) at fuel-rich conditions, which is similar to the observations made during RME combustion in diesel engines [7.5] [7.7]. The CO profile trend at higher temperatures (above 1300 K) is also improved compared to the one predicted at stoichiometric condition. Figure 7.4 b, c, and d for long chain intermediate hydrocarbons shows that their concentration maxima is between 1100 K and 1200 K. The model gives good predictions for CH_4, C_2H_4, C_2H_6, C_5H_{10} and C_6H_{12} except model under predicts formation of C_4H_6 below 1200 K.

Reaction No	Reactions	Normalized Rate Of Production (ROP) Coefficients	Absolute Rate Of Production (ROP) moles/cc-sec
CO_2			
63	CH2+CO2<=>CH2O+CO	-0.836	-5.78E-13
89	SCH2+CO2<=>CH2O+CO	-0.164	-1.14E-13
1121	AC16H31COO=>AC16H318+CO2	0.975	3.08E-08
CH_2O			
98	CH3O+M<=>CH2O+H+M	0.195	1.73E-09
112	CH2O+OH<=>HCO+H2O	-0.221	-3.83E-10
114	CH2O+H<=>HCO+H2	-0.264	-4.59E-10
116	CH2O+CH3<=>HCO+CH4	-0.410	-7.13E-10
467	C4H8+OH<=>CH2O+NC3H7	0.191	1.69E-09
2646	C2H3+O2<=>CH2O+HCO	0.426	3.76E-09
CO			
21	CO+HO2<=>CO2+OH	-0.516	-1.91E-11
22	CO+OH<=>CO2+H	-0.454	-1.68E-11
25	HCO+M<=>H+CO+M	0.219	2.56E-09
30	HCO+O2<=>CO+HO2	0.333	3.88E-09
28	C2H3CO+M=>C2H3+CO+M	0.284	3.31E-09

Table 7.17: Rate of production and consumption for oxygenated compounds at 1000 K

Table 7.17 shows that at 1000 K, the reaction path for CO_2 production (reaction associated with ester function, reaction no 1121) is similar to the one observed at fuel-lean and stoichiometric conditions. At 1000 K CO_2 is mainly consumed by reaction no 63 and 89, thus producing CO and CH_2O; however at this temperature model is not able to reproduce formation of these compounds (CO and CH_2O). At 1000K CO is mainly produced from third body reaction & oxidation of HCO (reaction no 25 and 30 in table 7.17) and consumed mainly in metathesis reaction to produce CO_2 (reaction no 21 & 22). CH_2O is mainly produced from oxidation of the vinyl radical (reaction no 2646) and consumed in metathesis reactions (reaction no 112, 114 &116).

At higher temperatures (1320K) most of the CO is consumed in producing CO_2 (reaction no 22) like at stoichiometric conditions and produced by third body reaction with HCO radical (reaction no 25). It can be seen from figure 7.4 that the model predicts the formation of CO reasonably well even at higher temperatures (above 1300K). Table 7.18 gives rate of production and consumption for CO, CO_2 at 1320 K. At 1320K, CO_2 is mainly produced from reactions such as metathesis, oxidation reactions with intermediate species like CO, HCCO (reaction no 22 & 229). The conversion of these intermediate species to final combustion product CO_2 explains why CO_2 emission is higher from RME combustion in diesel engines [7.7] [7.9].

Reaction No	Reactions	Normalized Rate Of Production (ROP) Coefficients	Absolute Rate Of Production (ROP) moles/cc-sec
CO			
22	CO+OH<=>CO2+H	-0.941	-7.19E-08
25	HCO+M<=>H+CO+M	0.471	2.25E-07
218	CH2CO+H<=>CH3+CO	0.140	6.70E-08
229	HCCO+O2<=>CO2+CO+H	0.172	8.20E-08
CO_2			
22	CO+OH<=>CO2+H	0.328	7.19E-08
63	CH2+CO2<=>CH2O+CO	-0.642	-8.17E-10
89	SCH2+CO2<=>CH2O+CO	-0.344	-4.38E-10
229	HCCO+O2<=>CO2+CO+H	0.374	8.20E-08
1121	AC16H31COO=>AC16H318+CO2	0.132	2.89E-08

Table 7.18: Rate of production and consumption for CO, CO_2 at 1320 K

Very good modeling results are obtained for olefins (C_2 to C_6). The model predicts the profile trends for Methane & Olefins, well throughout the working temperature range (1000 to 1400 K). These are important hydrocarbon intermediates formed during RME combustion. However the model overestimated the formation of C_3H_6 above 1145K and underestimated the formation C_4H_6 up to 1145K, when compared to experimental results. The model confirmed that reactivity of RME decreased with increasing equivalence ratio. It was observed that mole fractions of all intermediates reached their maximum value in temperature range of 1000 to 1200 K. At fuel-rich condition intermediates reached their maximum concentration peak value.

At 1000K and 1080K 1-3 Butadiene (C_4H_6) is mainly produced from thermal decomposition of Methyl Allyl (MEALL) radical (reaction no 524) and metathesis reaction with it (reaction no 528), whereas C_4H_6 is mainly consumed in metathesis reactions (reaction no 586 and 588). Table 7.19 shows the rate of production and consumption for C_4H_6 at different temperatures. Methyl allyl radical is formed mainly from 1-Butene (1-C_4H_8), Tertiary-Butene and β scission of unsaturated ester radicals and alkenyl radicals. It can be seen from figure 7.4, at both these working temperatures (1000 K and 1080 K) model underestimates the formation of C_4H_6. However at higher working temperatures (1220 K and 1320K) the model over predicts the formation of C_4H_6. At these working temperatures C_4H_6 is mainly formed from a decomposition of small carbon chain (C_5-C_7) unsaturated esters (reaction no 1671 and 1721) and hydrogenation of diene radical (C_4H_5) (reaction no 2612). The model is reproducing the experimental observation that 1-3 Butadiene formation increases with increasing Fuel/O_2 ratio.

Reaction No	Reactions	Normalized Rate Of Production (ROP) Coefficients	Absolute Rate Of Production (ROP) moles/cc-sec
At 1000K			
159	C2H3+C2H4<=>C4H6+H	-0.175	-9.62E-11
524	MEALL<=>C4H6+H	0.364	1.80E-09
538	MEALL+AC3H5<=>C4H6+C3H6	0.372	1.83E-09
586	C4H6+OH<=>HOC4H6	-0.332	-1.83E-10
588	C4H6+O=>OC4H6	-0.194	-1.07E-10
At 1080K			
159	C2H3+C2H4<=>C4H6+H	-0.187	-8.64E-10
524	MEALL<=>C4H6+H	0.526	6.62E-09

538	MEALL+AC3H5<=>C4H6+C3H6	0.210	2.64E-09
586	C4H6+OH<=>HOC4H6	-0.216	-1.00E-09
588	C4H6+O=>OC4H6	-0.271	-1.25E-09
At 1220K			
159	C2H3+C2H4<=>C4H6+H	-0.194	-4.17E-09
498	C4H73<=>C4H6+H	-0.115	-2.48E-09
524	MEALL<=>C4H6+H	0.284	6.89E-09
586	C4H6+OH<=>HOC4H6	-0.105	-2.26E-09
588	C4H6+O=>OC4H6	-0.248	-5.34E-09
1671	EC7:1<=>C4H6+CC3:0	0.264	6.41E-09
1721	CC5:1<=>C4H6+COOCH3	0.127	3.08E-09
At 1320K			
159	C2H3+C2H4<=>C4H6+H	-0.218	-6.61E-09
498	C4H73<=>C4H6+H	-0.165	-5.02E-09
588	C4H6+O=>OC4H6	-0.183	-5.54E-09
1671	EC7:1<=>C4H6+CC3:0	0.202	6.24E-09
1721	CC5:1<=>C4H6+COOCH3	0.113	3.48E-09
2612	DC4H513+H<=>C4H6	0.317	9.77E-09

Table 7.19: Rate of production and consumption for C_4H_6 at different temperatures

It can be seen from figure 7.4; the model is predicting Propene (C_3H_6) in precise manner at initial working temperature i.e. at 1000K and 1080K. At 1000 K C_3H_6 is mainly formed from decomposition of alkyl radicals of C_5-C_7 carbon chain (reaction no 735, 892, 934) and third body reaction (reaction no 2628), however it is mainly consumed in metathesis reactions to produce Allyl radical (AC_3H_5, reaction no 310). Table 7.20 shows the rate of production and consumption for C_3H_6 at different temperatures. At 1080 K Propene (C_3H_6) is mainly formed from recombination reaction (reversible reaction of thermal decomposition, reaction no 2651), metathesis reaction with Acrolein (reaction no 426) and decomposition of alkyl radical (reaction 892). At higher temperature (1220 K & 1320 K) C_3H_6 is mainly formed from reversible reaction of thermal decomposition (at 1220 K, reaction no 2651) and recombination of radicals (at 1320 K reaction no 291) indicating that the rate for the reversible reaction is higher compared to rate of reaction for forward reaction.

Reaction No	Reactions	Normalized Rate Of Production (ROP) Coefficients	Absolute Rate Of Production (ROP) moles/cc-sec
At 1000K			
300	C3H6+OH<=>AC3H5+H2O	-0.194	-6.02E-10
310	C3H6+H<=>AC3H5+H2	-0.351	-1.09E-09
735	BC5H11<=>C3H6+C2H5	0.139	5.11E-09
892	BC6H13<=>C3H6+NC3H7	0.239	8.79E-09
934	BC7H15<=>C3H6+PC4H9	0.108	3.99E-09
2628	C3H6+H(+M)<=>NC3H7(+M)	0.111	4.09E-09
At 1080K			
300	C3H6+OH<=>AC3H5+H2O	-0.162	-2.90E-09
310	C3H6+H<=>AC3H5+H2	-0.409	-7.36E-09
426	ACROL+AC3H5=>C2H3CO+C3H6	0.110	6.72E-09
892	BC6H13<=>C3H6+NC3H7	0.142	8.65E-09
2631	SC4H9(+M)<=>C3H6+CH3(+M)	0.101	6.12E-09
2651	C3H6<=>AC3H5+H	0.211	1.28E-08
At 1220K			
300	C3H6+OH<=>AC3H5+H2O	-0.109	-1.07E-08
310	C3H6+H<=>AC3H5+H2	-0.472	-4.64E-08
2651	C3H6<=>AC3H5+H	0.650	7.50E-08
At 1320K			
291	C3H6<=>C2H3+CH3	0.170	2.59E-08
310	C3H6+H<=>AC3H5+H2	-0.541	-8.06E-08
2651	C3H6<=>AC3H5+H	0.702	1.07E-07

Table 7.20: Rate of production and consumption for C_3H_6 at different temperatures

The model is able to reproduce formation important 1-alkenes like 1-Pentene (1-C_5H_{10}) and 1-Hexene (1-C_6H_{12}) in precise manner up to temperature range of 1040 K (Figure 7.4). The model is over predicting formation of these alkenes at higher temperature (above 1050 K). The model is reproducing experimental observation that 1-Pentene and 1-Hexene reach their concentration maxima at 1000-1050 K. At 1000 K 1-Petene is mainly consumed in decomposition reaction (reaction no 765) and produced mainly by decomposition of long carbon chain alkyl radical ($C_{16}H_{31}$, reaction no 1845) formed from Decarboxylation of RME and decomposition of alkyl radical (reaction no 932). Table 7.21 and 7.22 shows the rate of production and consumption for 1-Pentene and 1-Hexene at 1000 K and 1080 K respectively. At 1080K also, 1-Petene is mainly consumed in decomposition reaction to form smaller radicals like Ethyl

(C_2H_5) and Ally radical (AC_3H_5) (reaction no 765) and produced from decomposition of long carbon chain alkyl radical formed from RME (reaction no 1845). At 1000K 1-Hexene is mainly consumed in decomposition reaction to form smaller radicals (reaction no 894) and produced from decomposition of long carbon chain alkyl radical formed from RME ($C_{16}H_{31}$) (reaction no 1847) and decomposition of alkyl radical (reaction no 931). At 1080 K it is mainly consumed in decomposition reaction to produce smaller radicals and 2 Propene (C_3H_6) radicals (reaction no 894). At this temperature it follows the same production path like at 1000 K (reaction no 931 & reaction no 1847). As mentioned in chapter 4 formation of 1-alkenes is due to decomposition of long carbon chain unsaturated compounds i.e. due to presence of unsaturation in RME structure.

Reaction No	Reactions	Normalized Rate Of Production (ROP) Coefficients	Absolute Rate Of Production (ROP) moles/cc-sec
AC_5H_{10}			
765	AC5H10<=>C2H5+AC3H5	-0.980	-8.35E-09
932	DC7H15<=>AC5H10+C2H5	0.173	1.47E-09
1845	DC16H318<=>AC5H10+AC11H213	0.451	3.85E-09
AC_6H_{12}			
894	AC6H12<=>NC3H7+AC3H5	-0.916	-6.47E-09
931	CC7H15<=>AC6H12+CH3	0.618	4.36E-09
1847	EC16H318<=>AC6H12+AC10H192	0.307	2.17E-09

Table 7.21: Rate of production and consumption for 1-Pentene and 1-Hexene at 1000 K

Reaction No	Reactions	Normalized Rate Of Production (ROP) Coefficients	Absolute Rate Of Production (ROP) moles/cc-sec
AC_5H_{10}			
765	AC5H10<=>C2H5+AC3H5	-0.890	-5.53E-09
932	DC7H15<=>AC5H10+C2H5	0.314	2.34E-09
1845	DC16H318<=>AC5H10+AC11H213	0.482	3.59E-09
AC_6H_{12}			
894	AC6H12<=>NC3H7+AC3H5	-0.729	-5.13E-09
896	AC6H12<=>2C3H6	-0.162	-1.14E-09
931	CC7H15<=>AC6H12+CH3	0.753	6.32E-09
1847	EC16H318<=>AC6H12+AC10H192	0.191	1.60E-09

Table 7.22: Rate of production and consumption for 1-Pentene and 1-Hexene at 1080 K

7.2.1 Sensitivity Analysis at 1 bar

A sensitivity analysis helps to identify the rate-limiting reaction steps. The rate-limiting reactions steps are elementary reactions for which change in rate coefficients has large effect on time-dependent solution and accurate rate coefficients are required for these reactions. The objective of this section is to analyze RME oxidation and identify these rate-limiting steps, which can affect the reactivity of RME. A sensitivity analysis was done for all equivalence ratios (Φ = 0.25, 0.5, 1, 1.5) at 980K. At this temperature conversion of RME was more than 50% for fuel-lean as well fuel-rich conditions. Figure 7.5 shows the sensitivity analysis done for oxidation of RME at 1 bar, where values of sensitive coefficients are plotted on X axis for important reactions. The positive coefficients indicate an increase in concentration with constant rate of reaction and the negative coefficients correspond to decrease in the concentration with increase in reaction rate of that corresponding reaction i.e. consumption reactions. For example reaction no 1112 is RME consumption reaction which has negative sensitivity coefficient.

In general, oxidation of RME at all fuel conditions (Φ = 0.25, 0.5, 1, 1.5) is sensitive to the initiation reactions like reaction of C-C bond breaking at the β position in RME structure (reaction no 1112, 1113) and O-CH_3 bond breaking reaction (reaction no 1120). The reaction of O-CH_3 bond breaking (reaction no 1120) has highest negative sensitivity coefficient followed by reaction no 1112 and 1113. It can be seen from figure 7.5 all these three reaction have negative sensitivity coefficients for all fuel conditions

1112	C17:d9 =>KC11:d9 + AC6H13
1113	C17:d9 =>AC10H192 + GC7:0
1120	C17:d9 =>AC16H31COO + CH3

At fuel-lean (Φ = 0.25, 0.5) conditions the oxidation of RME is sensitive to mainly thermal cracking reactions of C_8 unsaturated esters, producing C_8 ester radicals. Following are the reactions for thermal cracking of Methyl Octenoate (C_8:1) & Methyl Pentenoate (C_5:1) esters. These ester radicals are formed from decomposition of C_{11}-C_{16} carbon chain ester radicals, which are obtained from decomposition of RME.

1598	C8:1 = H + FC8:1
1606	C8:1 = H + EC8:1
1614	C8:1 = H + DC8:1
1622	C8:1 = H + CC8:1
1630	C8:1 = H + BC8:1
1712	C5:1 = H + CC5:1

At stoichiometric (Φ = 1) and fuel- rich (Φ = 1.5) conditions the consumption of RME is sensitive to thermal cracking of small carbon chain unsaturated esters (C_5-C_7), producing unsaturated ester radicals with different carbon chain. Following are the reactions of thermal cracking of small carbon chain unsaturated esters.

1654	C7:1 = H + DC7:1
1662	C7:1 = H + CC7:1
1670	C7:1 = H + BC7:1
1692	C6:1 = H + CC6:1
1700	C6:1 = H + BC6:1
1712	C5:1 = H + CC5:1
1720	C5:1 = H + BC5:1

The sensitivity analysis shows that all fuel conditions RME oxidation is sensitive to unimolecular decomposition of RME (Initiation) and thermal cracking of intermediate esters (C8:1 to C5:1). The most influential reactions are RME decomposition reactions (reaction no 1120, 1112 and 1113) with highest sensitivity coefficients, so these are rate-limiting steps for RME oxidation. Any change in rate coefficients or kinetics for these reactions can affect RME oxidation kinetics.

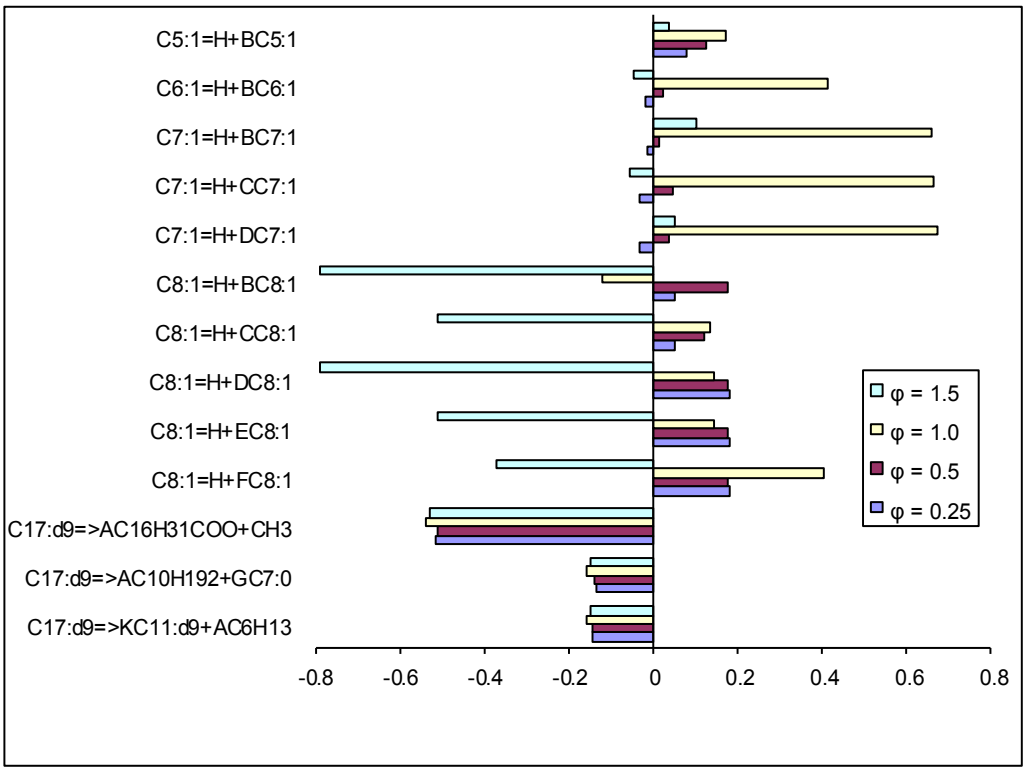

Figure 7.5: Sensitivity Analysis of oxidation of RME at 1 bar

7.2.2 Rate of production (ROP) analysis at 1 bar

The rate of production analysis gives a set of reactions, which are mainly responsible for consuming RME during its oxidation. This analysis also helps to generate important reaction pathways for production/consumption of particular species especially pollutants. The rate of production analysis for oxidation of RME at 1 bar was done at 980K for fuel-lean to fuel-rich conditions. At this temperature, conversion of RME was approximately more than 50%.

At stoichiometric condition ($\Phi = 1$, $\tau = 0.1$ s) RME is mainly consumed by O-CH_3 bond breaking reaction (reaction no 1120) and initiation reactions i.e. C-C bond breakage at β position, (reaction no 1112, 1113), whereas it is reproduce mainly by the metathesis reaction with Hydrogen radical (reaction no 1151, 1159) producing RME radical. The intermediate unsaturated and saturated ester radicals, alkyl radicals and the primary alkyl radical along with carbonyl function are formed from these reactions. These compounds decompose further to give small carbon chain compounds. The following are the important reactions responsible for RME consumption, where 'R' is rate of production or consumption. 'R' with

positive value, is normalized rate of production and with negative value, it is normalized rate of consumption.

Reaction No	Reactions	Normalized Rate Of Production (ROP) Coefficients 'R'	Absolute Rate Of Production (ROP) moles/cc-sec
1112	C17:d9=>KC11:d9+AC6H13	-0.163	-7.42E-09
1113	C17:d9=>AC10H192+GC7:0	-0.163	-7.42E-09
1120	C17:d9=>AC16H31COO+CH3	-0.528	-2.28E-08
1151	C17:d9+H<=>H2+BC17:d9	0.070	1.49E-13
1159	C17:d9+H<=>H2+LC17:d9	0.070	1.97E-13

It can be seen from above table the reaction no 1120 gives the trans-8-Hexadecene radical ($C_{16}H_{31}8$) with a carbonyl group (COO^*) attached to it and methyl radical. Reaction 1112 gives the Methyl 9-decenoate radical (KC11:d9) along with alkyl radical. The reaction 1113 gives the 1-Decene radical ($AC_{10}H_{19}2$) and Methyl Heptanoate radical (GC7:0, saturated ester radical), which is obtained from RME oxidation in JSR (GC-MS analysis) also. Thus the model predicts the reaction path for the formation of intermediate compounds observed from experimental work. The decomposition of these radicals will be discussed further.

At fuel-lean (Φ = 0.25, 0.5) and fuel-rich conditions (Φ = 1.5), RME is mainly consumed by above mentioned reactions (reaction no 1112, 1113 & 1120) and metathesis reaction with C_2H_5 producing C_2H_6 and RME radicals. Following is the set of reaction with normalized rate of consumption and production values at fuel- lean (Φ = 0.5, τ = 0.07 s) condition.

Reaction No	Reactions	Normalized Rate Of Production (ROP) Coefficients	Absolute Rate Of Production (ROP)
1220	C17:d9+C2H5 = C2H6+BC17:d9	-0.013	moles/cc-sec
1221	C17:d9+C2H5 = C2H6+CC17:d9	-0.012	-1.67E-09
1230	C17:d9+C2H5 = C2H6+NC17:d9	-0.012	-1.47E-09
1124	C17:d9+O2<=>HO2+CC17:d9	0.120	-1.51E-09
1127	C17:d9+O2<=>HO2+FC17:d9	0.105	9.46E-13
1128	C17:d9+O2<=>HO2+GC17:d9	0.126	8.49E-13

The RME radicals (BC17:d9 to NC17:d9) formed from above reactions isomerise and decompose to give intermediate unsaturated esters (C_{10} to C_{15}, C_3 to C_8),

small carbon chain saturated esters (C_2 to C_6), alkyl radicals (C_1 to C_{14}), 1-alkenes (C_4-C_7) and Dienes (C_{10} to C16).

As mentioned earlier the radicals formed from initiation reactions decompose to produce small carbon chain intermediate radicals. The decomposition of these radicals is discussed below.

Methyl 9-decenoate radical (KC11:d9):

Reaction No	Reactions	Normalized Rate Of Production (ROP) Coefficients	Absolute Rate Of Production (ROP) moles/cc-sec
1539	KC11:d9=>GC11:d9	-0.989	-7.40E-06
1540	KC11:d9=>FC11:d9	-0.011	-7.50E-08
1546	GC11:d9=>KC11:d9	0.988	7.39E-06
1547	FC11:d9=>KC11:d9	0.010	7.49E-08

Methyl 9-decenoate radical (KC11:d9) is an important intermediate radical formed from initiation reaction by C-C bond breakage at the β position in the RME structure. The ROP for Methyl 9-decenoate radical shows that it is mainly consumed in 1-5 and 1-6 Isomerization reaction (reaction no 1539, 1540), whereas it is reproduced by Isomerization of these radicals only. However all Methyl 9-decenoate radicals decompose to form alkyl radicals, dienes from C_6 to C_{10}, intermediate unsaturated esters like Methyl Octenoate (C8:1) to Methyl Propenoate (C3:1), and saturated intermediate esters like Methyl Pentanoate (C5:0) to Methyl Acetate (C2:0). These radicals further decompose to produce 1-alkenes, dienes and pollutants.

Reaction No	Reaction
1553	GC11:d9=AC3H5+C8:1
1554	GC11:d9=C6H1014+EC5:0
1555	FC11:d9=C4H721+C7:1
1556	FC11:d9=C7H1215+DC4:0
1557	DC11:d9=C6H1131+C5:1
1558	DC11:d9=C9H1616+BC2:0
1559	CC11:d9=C7H1331+C4:1
1560	CC11:d9=C10H1817+COOCH3
1561	BC11:d9=C8H1538+C3:1

Trans-8-Hexadecene radical ($C_{16}H_{31}8$):

Trans-8-Hexadecene radical ($C_{16}H_{31}8$) is formed from Decarboxylation reaction (reaction no 1121). It is longest carbon chain (C_{16}) intermediate hydrocarbon radical formed from RME. This radical is also mainly consumed in 1-4, 1-5 Isomerization to form other Hexadecene radicals (reaction no 1835, 1836). It is reproduced by Isomerization reaction only (reaction no 1839, 1840).

Reaction No	Reactions	Normalized Rate Of Production (ROP) Coefficients	Absolute Rate Of Production (ROP) moles/cc-sec
1121	AC16H31COO=>AC16H318+CO2	0.033	1.76E-08
1835	AC16H318=>DC16H318	-0.871	-5.19E-07
1836	AC16H318=>EC16H318	-0.104	-6.18E-08
1839	DC16H318=>AC16H318	0.840	5.03E-07
1840	EC16H318=>AC16H318	0.103	6.12E-08

All trans-8-Hexadecene radicals ($C_{16}H_{31}8$) decompose to give intermediate alkyl & alkenyl radicals, Dienes (C_{10} to C_{14}), important 1-alkenes like 1-Pentene and 1-Hexene. All decomposition reactions are shown in table below.

Reaction No	Reaction
1843	AC16H318=C2H4+AC14H276
1844	DC16H318=C2H5+C14H2616
1845	DC16H318=AC5H10+AC11H213
1846	EC16H318=NC3H7+C13H2415
1847	EC16H318=AC6H12+AC10H192
1848	FC16H318=PC4H9+C12H2214
1849	FC16H318=AC9H171+AC7H14
1850	GC16H318=AC5H11+C11H2013

1-Decene radical ($AC_{10}H_{19}2$):

Reaction No	Reactions	Normalized Rate Of Production (ROP) Coefficients	Absolute Rate Of Production (ROP) moles/cc-sec
2400	AC10H192=>DC10H192	-0.275	-2.10E-06
2401	AC10H192=>EC10H192	-0.718	-5.80E-06
2411	DC10H192=>AC10H192	0.273	2.08E-06
2412	EC10H192=>AC10H192	0.722	5.83E-06

1-Decene ($C_{10}H_{19}$) radical is also formed from initiation reaction. It is also mainly consumed in 1-4 and 1-5 Isomerization reaction to produce other 1-Decene radicals. The above table shows ROP for 1-Decene radical. All 1-Decene radicals like Hexadecene radicals decompose to give small carbon chain alkyl radicals (C_1 to C_6), Dienes (C_5 to C_9), 1-alkenes (C_4 to C_7).

Methyl Heptanoate (GC7:0):

Reaction No	Reactions	Normalized Rate Of Production (ROP) Coefficients	Absolute Rate Of Production (ROP) moles/cc-sec
1760	GC7:0=>DC7:0	-0.867	-3.20E-06
1761	GC7:0=>CC7:0	-0.104	-3.81E-07
1763	DC7:0=>GC7:0	0.867	3.20E-06
1764	CC7:0=>GC7:0	0.104	3.81E-07

Methyl Heptanoate radical (GC7:0) is longest carbon chain saturated ester radical formed from RME decomposition. This saturated ester was also observed from GC-MS analysis of RME oxidation in JSR. This ester radical is also mainly consumed in 1-4 and 1-5 Isomerization reaction to form other Methyl Heptanoate radicals. These radicals further on decompose to form unsaturated esters like Methyl Pentenoate (C5:1) to Methyl Propenoate (C3:1), Methyl Pentanoate radical (EC5:0), Methyl Acetate radical (BC2:0), alkyl radical, ester group ($COOCH_3$), 1-Pentene and 1-Hexene.

Reaction No	Reaction
1766	GC7:0=C2H4+EC5:0
1767	DC7:0=C2H5+C5:1
1768	DC7:0=AC5H10+BC2:0
1769	CC7:0=NC3H7+C4:1
1770	CC7:0=AC6H12+COOCH3
1771	BC7:0=PC4H9+C3:1

7.2.3 Rate of production analysis for Formaldehyde (CH_2O)

The formaldehyde (CH_2O) is important oxygenated intermediate and pollutant formed during RME oxidation. To understand formation path of CH_2O formation, the rate of production analysis was done for CH_2O at 980K for fuel-

lean to fuel-rich conditions. At this temperature conversion of RME was approximately more than 50%.

At all fuel conditions (Φ = 0.25, 0.5, 1, 1.5), CH_2O is mainly produced from Methoxy radical (CH_3O) (reaction no 98), reaction of 1-Butene (C_4H_8) with OH radial (reaction no 467) and reaction of Vinyl radical (C_2H_3) with molecular oxygen (reaction no 2646). However at all fuel conditions, CH_2O is mostly consumed in metathesis reactions like reaction with methyl radical (reaction no 116) producing Methane and Formyl radical, reaction with OH radical (reaction no 112) producing Formyl radical (HCO) & H_2O.

Reaction No	Reactions	Normalized Rate Of Production (ROP) Coefficients	Absolute Rate Of Production (ROP) moles/cc-sec
98	CH3O+M = CH2O+H+M	0.299	4.54E-09
467	C4H8+OH = CH2O+NC3H7	0.212	3.16E-09
2646	C2H3+O2 = CH2O+HCO	0.290	1.87E-09

Reaction No	Reactions	Normalized Rate Of Production (ROP) Coefficients	Absolute Rate Of Production (ROP) moles/cc-sec
111	CH2O+HO2<=>HCO+H2O2	-0.139	-3.89E-10
112	CH2O+OH<=>HCO+H2O	-0.354	-1.33E-09
114	CH2O+H<=>HCO+H2	-0.160	-7.30E-10
116	CH2O+CH3<=>HCO+CH4	-0.333	-5.43E-10

It can be seen from above table Methoxy radical (CH_3O), 1-Butene (C_4H_8) and Vinyl radical (C_2H_3) are mainly responsible for producing formaldehyde. The following are the reaction paths responsible for producing these radicals.

Methoxy radical (CH_3O):

The Methoxy radical is mainly formed from the reaction of a methyl radical (CH_3) with the hydroperoxy radical (HO_2) (reaction no 44). Methyl radicals are formed from RME decomposition by initiation reactions, β scission of alkyl radicals and small carbon chain esters (C_5-C_8).

Reaction No	Reactions	Normalized Rate Of Production (ROP) Coefficients	Absolute Rate Of Production (ROP) moles/cc-sec
44	CH3+HO2<=>CH3O+OH	0.971	4.54E-09
98	CH3O+M<=>CH2O+H+M	-0.997	-4.74E-09

1-Butene (C_4H_8):

1-Butene, responsible for producing formaldehyde is an important 1-alkene intermediate formed during RME oxidation. 1-Butene is mainly formed from recombination of Methyl and Allyl radical (reaction no 461). It is also formed from decomposition Heptyl radical (C_7H_{15}, reaction no 933). As mentioned earlier methyl radical is formed from RME, alkyl radicals and small carbon chain esters. Allyl radical (C_3H_5) is mainly formed from decomposition of dienes and intermediate ester radicals. Apart from producing formaldehyde, 1-Butadiene is also producing Propane and Methyl Allyl (MEALL), which is responsible for 1-3 Butadiene production.

Reaction No	Reactions	Normalized Rate Of Production (ROP) Coefficients	Absolute Rate Of Production (ROP) moles/cc-sec
461	C4H8<=>AC3H5+CH3	0.627	2.02E-08
466	C4H8+OH<=>MEALL+H2O	-0.214	-2.90E-09
467	C4H8+OH<=>CH2O+NC3H7	-0.223	-3.16E-09
469	C4H8+O<=>C3H6+CH2O	-0.104	-3.04E-10
933	CC7H15<=>C4H8+NC3H7	0.349	1.60E-08

Vinyl radical:

Vinyl radical is mainly formed from decomposition of 1,3-Hexadiene (C_6H_{10}, reaction 2594) and Butene radical (C_4H_7, reaction no 2568). 1-3 Hexadiene is formed from decomposition of C_9 to C_{11} alkene radicals, where as Butene radical is mainly formed from decomposition of dienes (C_9-C_{12}). Vinyl radical is consumed in forming dienes (reaction no 1973, 2174, and 2598) and Methyl Propenoate (C3:1, reaction no 1724).

Reaction No	Reactions	Normalized Rate Of Production (ROP) Coefficients	Absolute Rate Of Production (ROP) moles/cc-sec
1724	C3:1<=>C2H3+COOCH3	-0.142	-4.68E-09
1973	C13H2415<=>C2H3+AC11H21	-0.113	-8.24E-09
2174	C11H2013<=>C2H3+AC9H171	-0.121	-7.31E-09
2568	C4H714<=>C2H4+C2H3	0.135	9.29E-09
2594	C6H1013<=>C2H3+C4H711	0.701	2.09E-08
2598	C5H814<=>C2H3+AC3H5	-0.358	-1.75E-08

7.2.4 Rate of production analysis for 1,3-Butadiene (C_4H_6)

The 1,3-Butadiene (C_4H_6) is an important hydrocarbon intermediate formed during RME oxidation. As surrogate fuel models (n-Hexadecane +Methyl Acetate) as well as RME model failed to reproduce formation of 1,3-Butadiene in precise manner in terms of mole fractions and hence it is important to understand formation path of pollutant like 1,3-Butadiene. The rate of production analysis was done for 1,3-Butadiene at 980K for fuel-lean to fuel-rich conditions. At this temperature, conversion of RME was approximately more than 50%.

At fuel-lean conditions (Φ = 0.25, 0.5), 1,3-Butadiene is mainly produced from thermal decomposition of the Methyl allyl radical (MEALL) (reaction no 524) and its reaction with molecular oxygen and Allyl radical (AC_3H_5) (reaction no 525, 538). Methyl allyl radical is formed mainly from 1-Butene, Tertiary-Butene and β scission of unsaturated ester radicals and alkenyl radicals. The below table shows all main reactions responsible for 1,3 Butadiene (C_4H_6) formation.

Reaction No	Reactions	Normalized Rate Of Production (ROP) Coefficients	Absolute Rate Of Production (ROP) moles/cc-sec
524	MEALL = C4H6+H	0.263	1.24E-09
525	MEALL+O2 = C4H6+HO2	0.164	1.53E-09
538	MEALL+AC3H5 = C4H6+C3H6	0.336	4.46E-09
976	C7H1313 = C4H6+NC3H7	0.105	1.07E-09

At stoichiometric (Φ = 1) and fuel-rich conditions (Φ = 1.5), C_4H_6 is formed by decomposition of the Methyl Allyl (reaction 524) as well as the Methyl Pentenoate (CC5:1) radical (reaction 1721) and Methyl Heptenoate (EC7:1)

(reaction 1671). The reactions 1721 and 1671 proves that at fuel rich conditions unsaturated chain with ester function present in RME structure is contributing in producing 1,3-Butadiene. All these reactions are presented in table below.

Reaction No	Reactions	Normalized Rate Of Production (ROP) Coefficients	Absolute Rate Of Production (ROP) moles/cc-sec
524	MEALL<=>C4H6+H	0.517	1.24E-10
538	MEALL+AC3H5<=>C4H6+C3H6	0.073	4.46E-09
1671	EC7:1<=>C4H6+CC3:0	0.171	1.34E-09
1721	CC5:1<=>C4H6+COOCH3	0.057	1.06E-09

Methyl Heptenoate radical (EC7:1) is important small carbon chain intermediate ester formed during RME combustion. This radical is mainly formed from recombination of 1, 3 Butadiene (C_4H_6) and Methyl Propionate radical (CC3:0) (reaction 1671). It is also formed by reaction of ethyl radical with Methyl Heptenoate (C7:1, reaction 1645), whereas it is consumed in reforming Methyl Heptenoate. Methyl Heptenoate (C7:1) is formed from decomposition of parent RME molecule and intermediate unsaturated ester radicals (C_{10}-C_{16}).

Reaction No	Reactions	Normalized Rate Of Production (ROP) Coefficients	Absolute Rate Of Production (ROP) moles/cc-sec
1645	C7:1+C2H5<=>C2H6+EC7:1	0.203	2.83E-09
1646	C7:1<=>H+EC7:1	-1.00	-5.28E-09
1671	EC7:1<=>C4H6+CC3:0	0.737	2.02E-08

At all fuel conditions (Φ = 0.25, 0.5, 1, 1.5), C_4H_6 is consumed in mainly reactions mentioned in table below. It can be seen from table below 1-3 Butadiene is mainly consumed in forming radicals of intermediate esters like Methyl Pentenoate (C5:1), Methyl Hexenoate (C6:1) and Methyl Heptenoate (C7:1) (reaction1671, 1701, 1721). It is also consumed in forming 2-Butenal (reaction 588) and important hydrocarbon intermediate like Ethylene & Vinyl radical (C_2H_3, reaction 159).

Reaction No	Reactions	Normalized Rate Of Production (ROP) Coefficients	Absolute Rate Of Production (ROP) moles/cc-sec
159	C2H3+C2H4 = C4H6+H	-0.166	-2.43E-10
586	C4H6+OH = HOC4H6	-0.387	-9.68E-10
588	C4H6+O = OC4H6	-0.151	-2.13E-10
1671	EC7:1 = C4H6+CC3:0	-0.688	-3.34E-09
1701	DC6:1 = C4H6+BC2:0	-0.123	-6.23E-09
1721	CC5:1 = C4H6+COOCH3	-0.104	-3.06E-09

Overall at 1 bar conditions, this model reproduced concentration profiles for reactants, all intermediates and products except C_4H_8. The model over predicted the formation of C_4H_8 at fuel-lean & stoichiometric conditions. The model reproduced early formation of CO_2 in good manner especially for stoichiometric and fuel-rich condition. The Rate of Production Analysis (ROP) showed the production and consumption path for CO_2, which explains higher CO_2 emission from RME combustion and higher RME combustion efficiency. It also supported the effect of ester group ($COOCH_3$, i.e. fuel based oxygen) present in RME structure on CO_2 formation. The formation path for important intermediates like 1-Pentene and 1-Hexene was also studied, which confirms the effect of long carbon unsaturated chain present in RME structure on formation of 1-alkenes. The model also confirmed the diesel engine combustion observation that RME has positive effect on intermediate hydrocarbon emission.

The sensitivity analysis showed that RME combustion is sensitive to initiation reactions and unimolecular decomposition of unsaturated esters with small carbon chain of C_5-C_8. The rate of production analysis gave the reaction path for RME consumption during its combustion. RME is mainly consumed in initiation reactions i.e. decomposition and oxidation reactions, producing intermediate radicals and metathesis reactions producing RME radicals, which decompose further to produce intermediate hydrocarbon and ester radicals. The reaction path for important pollutants like formaldehyde (CH_2O) and 1, 3-Butadiene (C_4H_6) was also studied. This analysis confirmed the effect of unsaturation and ester function present in RME structure on formation of these pollutants.

Regarding the reactivity of RME, again, a good agreement between the data and the model (in terms of profile trends) was obtained especially for fuel-rich conditions. The model also proves the experimental observation that RME reactivity decreases with increasing F/O2 ratio and increases with increasing temperature. The reactivity observed was highest at fuel lean conditions. As reactivity was higher at higher temperature and fuel-rich conditions, these conditions look favorable for RME combustion in diesel engine. The recommended fuel conditions for RME combustion in commercial engines are fuel-lean conditions or RME in blends with diesel up to 50%.

7.3 Results at 10 bar

The modeling for RME using RME as model fuel was done at 10 bars for fuel-lean to fuel-rich conditions (phi = 0.5 to 1.5), for temperature range of 800 to 1200K. Figure 7.6 to 7.8 shows the predicted and experimentally measured concentrations, expressed as mole fractions for oxygenated compounds and key RME combustion products (olefins, C_2 to C_6) at 10 bar. Figure 7.6 b and c shows that model predicts similar profile trend as found in experiments for C_1 to C_3, i.e. as reaction temperature is increased from 800 K to 900 K, the concentration of these compounds is increased and after 900 K it starts decreasing. Figure 7.6 d shows that model is also reproducing concentration decreasing profile trend for C_4-C_6 after 850 K. However the deviation between predicted concentration and experimentally measured concentration for these intermediate compounds (C_1-C_6) is very large.

Figure 7.6 to 7.8 (a, b, c and d) shows that RME model under predicted reactivity of RME at all conditions. Figure 7.7.a and 7.8.a. shows that model reproduced early formation of CO_2 at stoichiometric and fuel-rich conditions but it failed to reproduce formation of CO. The model gave good description of experimental results for C_2H_4 and 1, 3-Butadiene (C_4H_6), especially in fuel-rich conditions. Overall the model failed to predict reactivity and formation of major intermediate species like olefins and CO.

It can be seen from figure 7.6 to 7.8 that there are intermediate species formed in a model that are not consumed fast enough to allow fast oxidation of fuel. This disagreement with experimental results can be associated with

inaccurate rate coefficients and pressure dependency considered or some missing reactions in the chemical kinetic model. The unimolecular decomposition reactions are known as pressure dependent reactions and sensitivity analysis at1 bar also showed that RME oxidation is sensitive to initiation reactions which are unimolecular decomposition reactions. The inaccurate rate coefficients for these reactions can contribute to under predict RME reactivity. Also at high pressure, reactions with molecular oxygen are very important. So, the inaccurate rate coefficients or missing reactions for oxidation of intermediate species can also under predict or over predict the reactivity. As figure 7.6 shows that experiments performed at 10 bar started from 800 K instead of 900 K. At this temperature range (800 K), some low temperature combustion chemistry may take place especially in case of reaction with molecular oxygen. We have only considered chemistry associated with high temperature combustion of RME in RME model. The reactions associated with specific chemistry of low temperature combustion need to be developed and incorporated in RME model and effect of low temperature combustion chemistry on RME reactivity needs to be verified.

As there is no enough data available from literature regarding kinetic mechanism for oxidation of long chain esters, it is difficult to develop kinetic mechanism for such long carbon unsaturated ester. The model needs improvement, considering pressure dependency, suitable values of rate coefficients and incorporating effect of low temperature combustion chemistry.

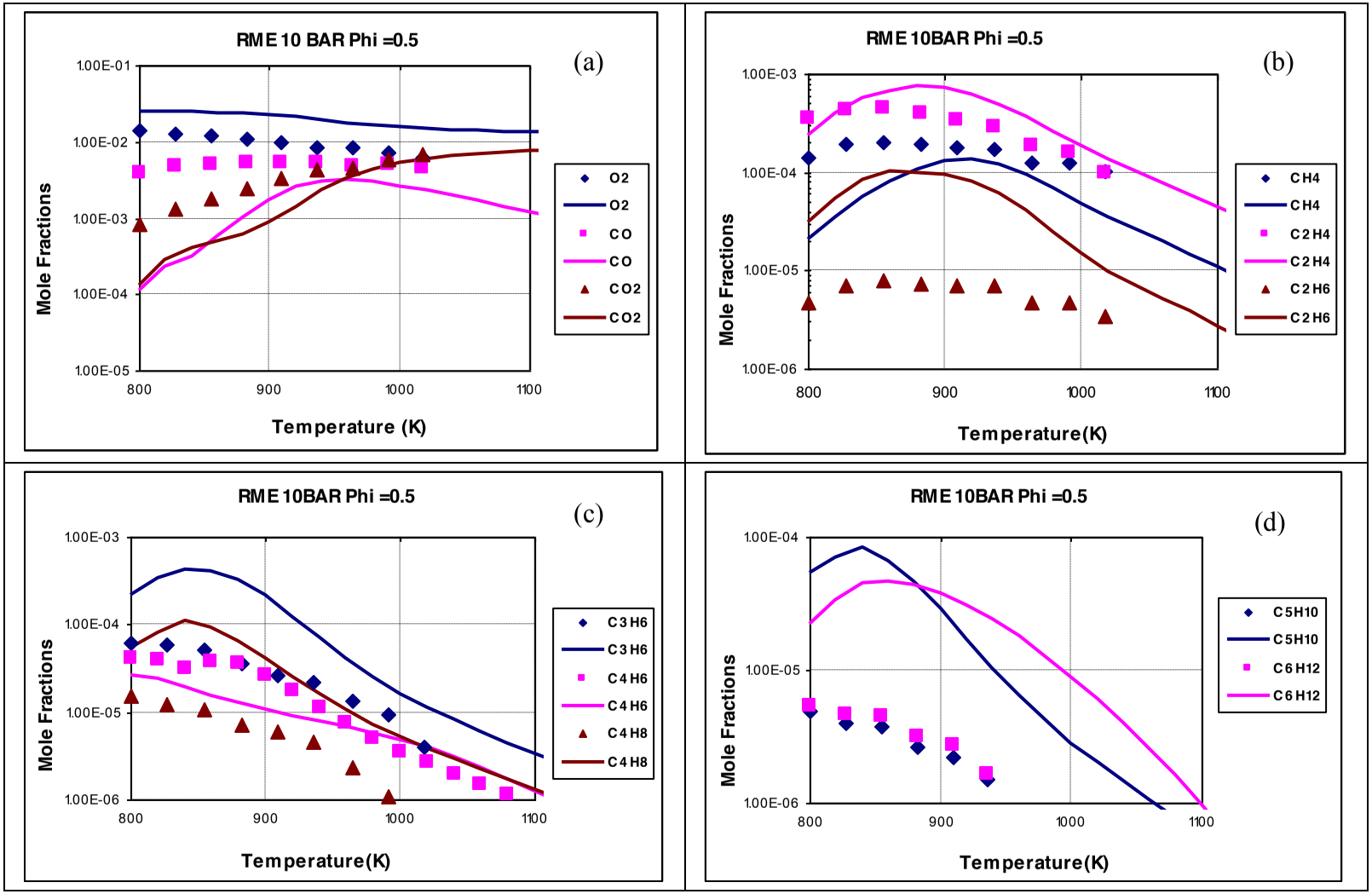

Figure 7.6: The oxidation of RME in a JSR (P = 10bar, φ = 0.5, τ = 1 s). The experimental data (large symbols) are compared to the computations (lines model-fuel: RME)

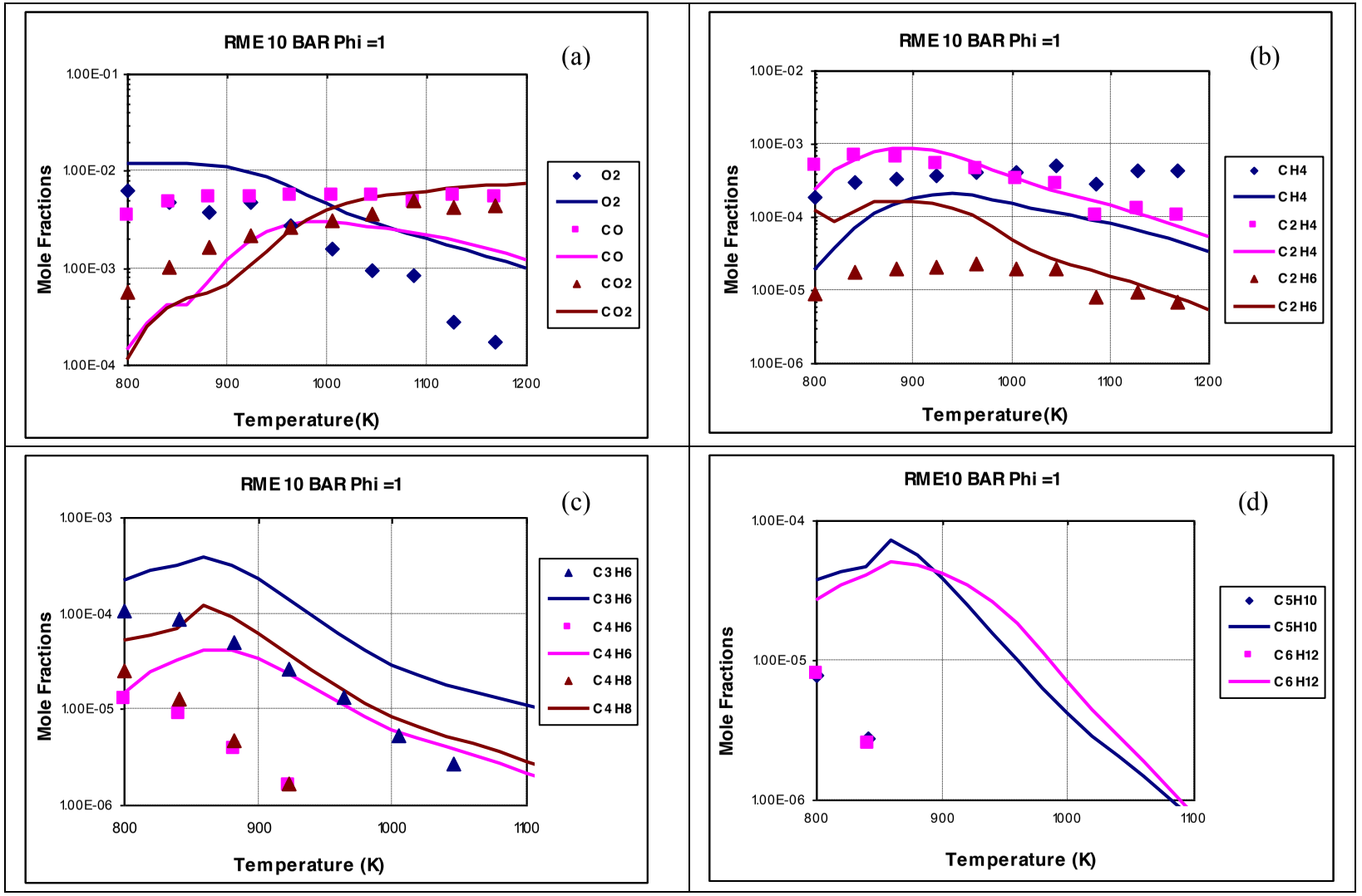

Figure 7.7: The oxidation of RME in a JSR (P = 10bar, φ = 1.0, τ = 1 s). The experimental data (large symbols) are compared to the computations (lines e model-fuel: RME)

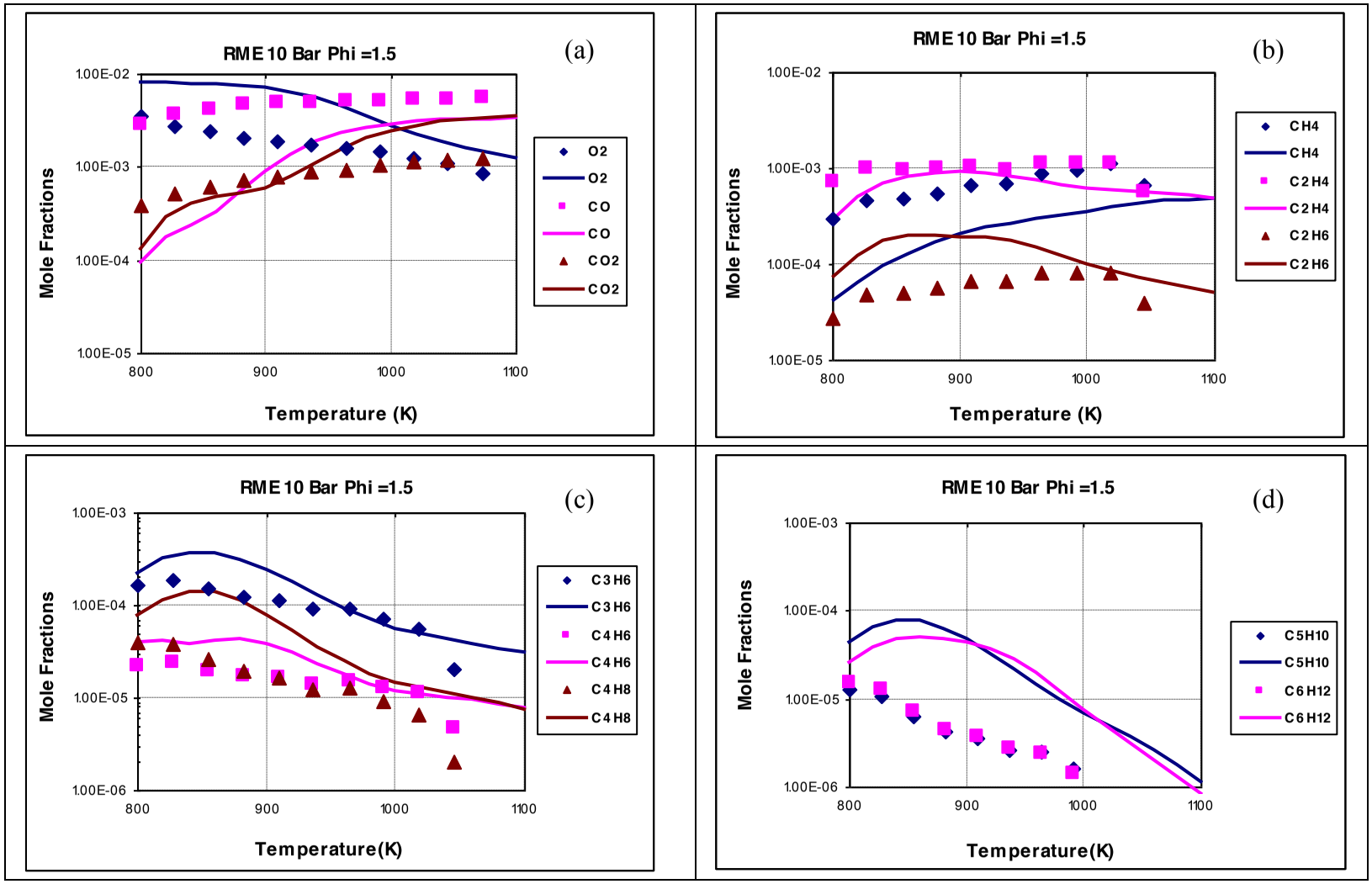

Figure 7.8: The oxidation of RME in a JSR (P = 10bar, φ = 1.5, τ = 1 s). The experimental data (large symbols) are compared to the computations (lines model-fuel: RME)

References

7.1 Dagaut.P, Ristori.A and Cathonnet.M, 2001, *The Oxidation of n-Hexadecane: Experimental and Detailed Kinetic Modeling*, Combustion and Flame, 125, 1128-1137

7.2 Dagaut.P and Cathonnet.M, 2006, *The ignition, oxidation and combustion of kerosene: A review of experimental and kinetic modeling*, Progress in Energy and Combustion Science, 32, Issue1, 48-92

7.3 Dagaut.P, Smoucovit.N and Cathonnet.M, 1997, *Methyl Acetate Oxidation in a JSR: Experimental and Detailed Kinetic Modeling Study*, Combustion Science and Technology, 127, 275-291

7.4 Billaud.F and Archambault.D, 1999, *Experimental and modeling study of methyl oleate pyrolysis between 500 and 650* ^{0}C, J.Chim.Phys, 96, 778-796

7.5 Labeckas.G, Slavinskas.S, 2006, *The effect of rapeseed oil methyl ester on direct injection Diesel engine performance and exhaust emissions*, Energy Conversion and Management, 47, Issue 13-14, 1954-1967

7.6 Makareviciene.V, Sendzikiene.E, Janulis.P, 2006, *Influence of fuel oxygen content on diesel engine exhaust emissions*, Renewable Energy, 31, 2505-2512

7.7 Nwafor.O.M.I, 2004, *Emission characteristics of diesel engine operating on rapeseed methyl ester*, Renewable Energy, 29, 119-129

7.8 Pedersen.R.J, Ingemarsson.A and Olsson.O.J, 1999, *Oxidation of Rapeseed oil, Rapeseed Methyl Ester (RME) and diesel fuel studied with GC/MS*, Chemosphere, 38, 11, 2467-2474

7.9 Krahl.J, Munack.A, Bahadir.M, Schumacher.L and Elser.N, 1996, *Review: Utilization of Rapeseed oil, Rapeseed Oil Methyl Ester or Diesel Fuel: Exhaust Gas Emissions and Estimation of Environmental Effects,* SAE Technical Paper Series Paper no: 962096

CHAPTER 8
RAPESEED OIL COMBUSTION

Chapter 7 described the results obtained from modeling of RME oxidation, carried out at 1 and 10 bar using the new chemical kinetic mechanism developed for RME. It also described the analysis of the modeling results using tools, sensitivity analyses and rate of production. The rate of production analysis was done for important pollutants like Formaldehyde (CH_2O) and 1,3 Butadiene (C_4H_6). This chapter deals with proposed reaction mechanism for the oxidation of Rapeseed oil (RSO) and presents modeling results. The chemical probe of JSR was observed to be blocked during RME oxidation experiments. This problem was observed due to highly viscosity of RME. As viscosity of Rapeseed oil is almost eight times higher than that of RME, potential problems may cause by this higher viscosity during oxidation experiments in JSR. So RSO oxidation experiments were not carried out in JSR. RME represents largest alkyl chain (C_{17}) with unsaturation similar to RSO and as there is no other experimental data available for Rapeseed oil oxidation in Jet Stirred Reactor (JSR), Rapeseed oil methyl ester (RME) oxidation experimental data explained in chapter 4 was used for the modeling work. RME & RSO have similar long carbon alkyl chain (C_{18}) in their structure, so a RSO based mechanism was used to simulate RME oxidation data.

8.1 Rapeseed oil oxidation mechanism

As explained in section 2.4 of chapter 2, the most important constituent of any vegetable oil is triglyceride. The vegetable oils comprise 90 to 98% triglycerides with small amounts of mono and diglycerides. Triglycerides are esters of three fatty acids (R-COOH) and one glycerol (figure 2.6 in chapter 2). Fatty acids vary in their carbon chain length and in the number of double bonds. Decomposition or combustion of vegetable oils i.e. triglycerides gives three fatty acids, Acrolein and Ketene. Typical Rapeseed oil molecule consists of esters of Oleic acid (C18:1), Linoleic acid (C18:2) and Linolenic acid (C18:3), where oleic acid (C18:1) has highest weight % (64%) in RSO composition. The chemical kinetic mechanism for Rapeseed oil combustion should therefore be described in terms of triglyceride consists of these three fatty acids.

The literature survey for Rapeseed oil combustion in chapter 2 (section 2.4.4) showed that most of the RSO combustion work has been done on commercial engines and not in chemical reactors like Jet Stirred Reactor. However Pederson et.al did RSO oxidation in a chemical reactor. Pederson [8.7] observed that oxidation of Rapeseed oil produced high amounts of reactive organic intermediates like Acrolein, 1-alkenes, dienes, and other aldehydes. Pederson also indicated that Rapeseed oil and RME fuel react in a similar way during oxidation with respect to formation of hydrocarbon products. Rapeseed oil and RME both contain the same building blocks of long unsaturated hydrocarbon chains in the fatty acids or fatty methyl ester respectively. Pederson observed that the higher contents of unsaturated organic compounds, in Rapeseed oil and RME promote formation of reactive intermediates like 1-alkenes, dienes and benzene during oxidation. The inherent carbonyl group (C=O) in rapeseed oil and RME promote formation of aldehydes.

The aim of this chapter is to develop chemical kinetic mechanism for Rapeseed oil oxidation. As there is no enough experimental data or kinetic data reported in the open literature for combustion or oxidation of Rapeseed oil in well stirred reactor like Jet-stirred reactor, the chemical kinetic mechanism developed here is based on similar carbon chain chemistry (in terms of long carbon (C_{17}) alkyl chain with unsaturation) between Rapeseed oil methyl ester (RME) and Rapeseed oil. In this mechanism, the chemistry for C_1-C_8 compounds is used from the n-hexadecane oxidation mechanism developed at CNRS [8.1]; the chemistry for C_8 to C_{17} compounds is based on a typical hydrocarbon oxidation mechanism and similar hydrocarbon chain chemistry between RME and Rapeseed oil.

Due to complex structure of Rapeseed oil (triglyceride consists of three fatty acid esters with unsaturation), it is very difficult to develop chemical kinetic mechanism for RSO oxidation including three fatty acid esters. As mentioned above decomposition or combustion of Rapeseed oil will produce oleic acid (C18:1), Linoleic acid (C18:2) and Linolenic acid (C18:3) along with Acrolein and ketene. So, the proposed chemical kinetic mechanism for RSO oxidation will be described in terms of:

- Decomposition of Triglycerides
- Oxidation Mechanism for Fatty Acid (Oleic Acid)

8.1.1 Decomposition of Triglycerides:

A lot of research has been done on decomposition of mono and triglyceride. Chia-Chu Chang and Shen-Wu Wan suggested a mechanism for thermal cracking of vegetable oil [8.3]. Alencar [8.2] and A.W.Schwab [8.4] developed a mechanism for decomposition of tropical oils and Soybean oil respectively. Kitamura [8.6] pyrolyzed triglycerides (trilaurin and tripalmitin) in an atmosphere of nitrogen at 300-700^{0}C and suggested the mechanism for pyrolysis of triglycerides. The pyrolysis products in his work consist of 45 to 55% fatty acids and 3.5 to 4 % that of Acrolein. The decomposition of triglyceride suggested by Chia-Chu Chang is described below:

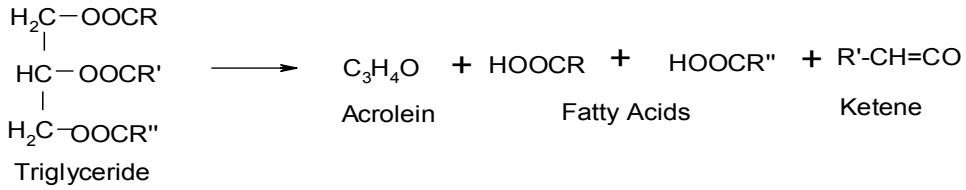

Figure 8.1: Decomposition of triglyceride

Figure 8.1 shows that triglyceride decomposes to give Acrolein (C_3H_4O), two fatty acids (R'COOH, R'''COOH) and Ketenes (R''CH=CO) [8.3]. Rapeseed oil decomposes to form two fatty acids namely; Oleic acid (C18:1), Linoleic acid (C18:2), along with Acrolein and Ketene.

As mentioned above the oxidation of Rapeseed oil produces high amounts of Acrolein [8.7]. This also confirms that oxidation of vegetable oil or triglyceride forms Acrolein and fatty acids. However chemical kinetic mechanism for oxidation or thermal decomposition of triglycerides is likely to be complex because of the many structures and multiplicity of possible reactions of mixed triglycerides. Due to lack of experimental data, bond energy values, and kinetic parameters, Rapeseed oil oxidation mechanism is presented in terms of triglyceride decomposition products i.e. Fatty acid, Acrolein and Ketene. As Oleic acid (C18:1), is dominating component in composition of Rapeseed oil, the chemical kinetic mechanism for RSO oxidation is developed in the form of Oleic acid ($C_{18}H_{34}O_2$) oxidation. Figure 8.2 represents structure of Oleic acid and figure 8.3 shows schematic diagram for development of chemical kinetic mechanism for Rapeseed oil oxidation.

8.1.2 Oleic Acid Oxidation Mechanism:

This section will describe the development of kinetic mechanism for oxidation of Oleic acid as a representative for Rapeseed oil (RSO). Alencar [8.2] observed that pyrolysis of triglycerides consist of Oleic acid, produced mainly straight-chain hydrocarbons as the major component and cyclo-paraffins, cyclo-olefins as minor intermediates [8.2]. Alencar also observed the absence of oxygenated compounds in pyrolysis volatiles, suggesting that elimination of CO_2 and CH_2=CO was dominant step. In 1983, Alencar published a mechanism for the decomposition of Oleic acid suggesting early removal of CO_2 and H from Oleic acid to form the Heptadecene ($C_{17}H_{34}$) radical.

Pederson [8.7] observed the alkanes up to C_8, 1-alkenes up to C_9, cyclo-paraffins up to C_9, cyclo-olefins up to C_8, aromatics up to C_{11} and oxygenated compounds up to C_6 as products formed from Rapeseed oil oxidation. The formation of these alkenes, aromatics and absence of long carbon chain oxygenated compounds indicate early removal of the carbonyl group (C=O) from Rapeseed oil. Schwab et.al [8.4] proposed a mechanism for decomposition of Oleic acid at 400^0C. This mechanism consists of breaking of carbon-carbon bond, β scission of double bond and removal CO_2.

So the chemical kinetic mechanism developed for oxidation of Oleic acid is also based on early removal of carbonyl group. The kinetic mechanism in this work is divided into two parts:

- Decomposition of Oleic acid to give CO_2 and Heptadecene($C_{17}H_{34}$)
- Detail mechanism for oxidation of Heptadecene($C_{17}H_{34}$)

The global formula for Oleic Acid is $C_{18}H_{34}O_2$. Oleic acid is presented as following with unsaturation typically at C9 position:

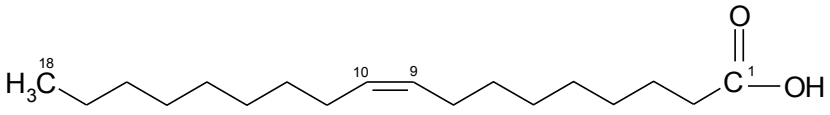

Figure 8.2: Structure of Oleic Acid with unsaturation at C9

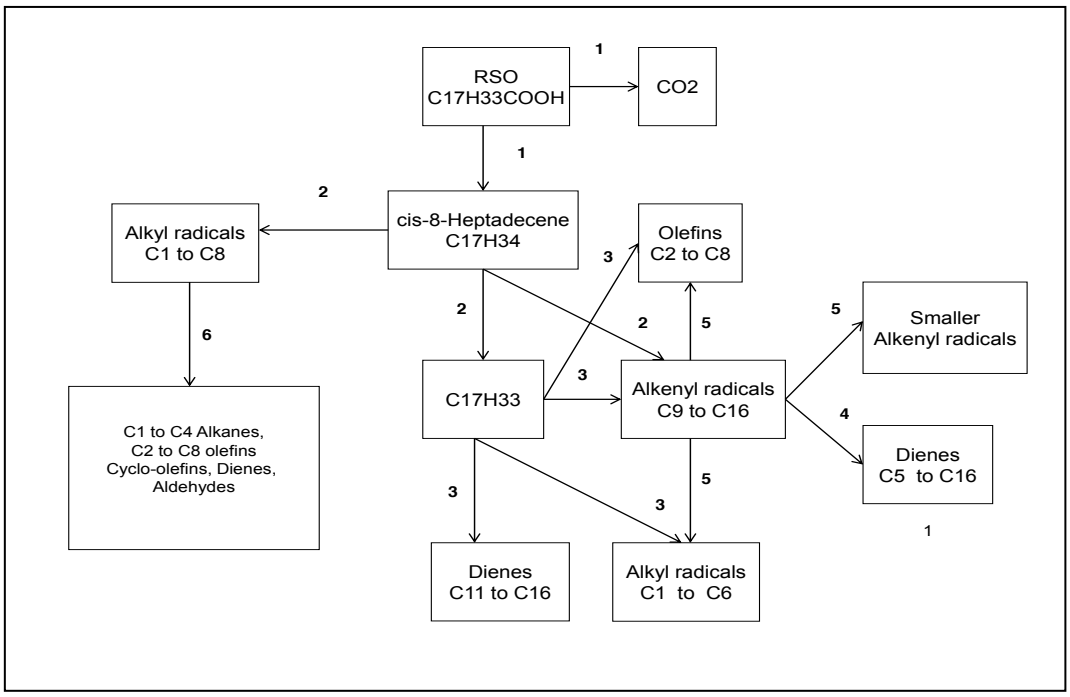

Figure 8.3: Flow diagram of kinetic mechanism for oxidation of Oleic acid

The oleic acid mechanism schematically represented in figure 8.3 was developed in following stages:

1. Decarboxylation of oleic acid giving cis-8-Heptadecene and CO_2
2. Metathesis reaction with O_2, O, OH, H, HO_2, CH_3 to C_2H_5 giving Heptadecyl ($C_{17}H_{33}$) radical, whereas initiation reactions (consist of C-C bond breaking)give alkenyl, alkyl radicalsfrom Heptadecene ($C_{17}H_{34}$)
3. Isomerization and β scission of Heptadecyl ($C_{17}H_{33}$)radical giving olefins, dienes, alkyl and alkenylradicals
4. Reaction of alkenyl radical with O_2, O, OH, H, HO_2, CH_3 to C_2H_5 giving dienes
5. Isomerization and β scission of alkenyl radicals giving olefins, dienes, alkyl (C_1 to C_8) and smaller alkenyl radicals
6. Metathesis, isomerization and β scission reactionswith alkyl radicals (C_1 to C_8) giving smalleralkanes, olefins, dienes, cyclo-olefins and aldehydes

The mechanism for oxidation of Oleic acid consists of:

- Initiation reactions including unimolecular decomposition and bimolecular reactions
- Metathesis Reactions
- Isomerization of radicals
- Decomposition of radicals by β scission

- Termination Reactions

In the following section, the statements added into the software are presented, alongside an explanation why each step has been included.

Initiation Reactions:

The mechanism begins with decomposition of oleic acid to give CO_2 and Heptadecene ($C_{17}H_{34}$).

1118. C17H33COOH=>C17H34+CO2

Initiation reactions include unimolecular decomposition and oxidation reactions with Heptadecene. The unimolecular decomposition consists of reactions for C-C bond breakage and reactions for thermal decomposition giving H radical and Heptadecene radicals. The unimolecular decomposition reactions give Alkyl and Alkenyl radicals.

1119. C17H34=>AC16H318+CH3

1122. C17H34=>AC13H255+PC4H9

1127. C17H34=>AC10H191+AC7H15

Thermal decomposition and oxidation of Heptadecene gives Heptadecene radicals, hydrogen and hydroperoxy radicals respectively.

1134. C17H34+O2=HO2+AC17H33

1164. C17H34+H=H2+AC17H33

Further on, all radicals formed from initiation are thermally decomposed and oxidized giving other radicals and dienes.

Metathesis Reactions:

Metathesis reactions consist of extracting H from long alkenyl chain forming Heptadecene radicals and other radicals, alkanes or olefins.

The metathesis reaction is represented as:

$$C_{17}H_{34} + X \longrightarrow C_{17}H_{33} + XH \qquad (8.1)$$

Where

X = O, OH , H , HO_2. CH_3, C_2H_3, C_2H_5

In a Heptadecenemolecule, there are total of 17 sites available for abstracting H by metathesis reaction.

Decomposition of Heptadecene radicals:

The Heptadecene radicals formed from initiation and metathesis reactions decompose by β scission reaction giving alkyl and alkenyl radicals, dienes and olefins.

1322. QC17H33=AC15H297+C2H4

1327. NC17H33=C15H2817+C2H5

1334. JC17H33=C11H2013+AC6H13

1341. DC17H33=AC12H233+AC5H10

Isomerization of radicals:

The isomerization reaction changes the position of the radical site on a molecule. In this mechanism, 1-4, 1-5 and 1-6 isomerizations are used. These include isomerization of primary to secondary, secondarytosecondary and secondary to primary isomerization.

1358. AC16H318=>DC16H318 (1-4 Isomerization)

1359. AC16H318=>EC16H318 (1-5 Isomerization)

1360. AC16H318=>FC16H318 (1-6 Isomerization)

Decomposition by β scission:

The reactions for decomposition by β scission are applicable to all the radicals formed, but types of radicals or products formed by β scission reactions depend on position of the radical site. These reactions are important as β scission of long carbon chain radicals form olefins and smaller radicals, which decompose further to give smaller radicals (C_1-C_3) and olefins.

In this mechanism alkyl, alkenyl and diene radicals are decomposed by β scission to give smaller, alkenyl, alkyl &diene radicals, and olefins.

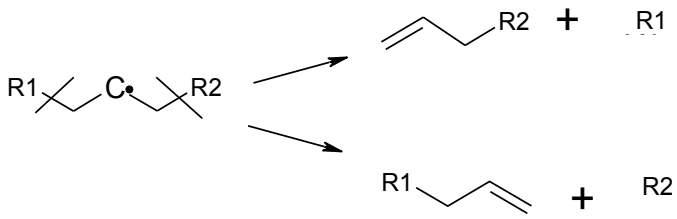

1367. DC16H318=C2H5+C14H2616 (Alkyl radical & Dienes)

1368. DC16H318=AC5H10+AC11H213 (Olefin & Alkenyl radical)

Termination Reactions:

The termination reactions are recombination of smaller alkyl as well as alkenyl radicals to give products like olefins, alkanes.

8.2 Rapeseed oil (RSO) oxidation

The chemical kinetic mechanism for Rapeseed oil was developed based on assumption that Rapeseed oil and Rapeseed oil methyl ester (RME) have similar hydrocarbon chain chemistry [8.7]. Rapeseed oil decomposes to give Acrolein (C_3H_4O), two fatty acids ($C_{17}H_{33}COOH$, $C_{17}H_{31}COOH$) and Ketenes (R''CH=CO). However, to simplify the combustion of Rapeseed oil only fatty acid amongst all Rapeseed oil decomposition products is considered for simulation work. As Oleic acid is main component of Rapeseed oil, the chemical kinetic mechanism for Oleic acid ($C_{18}H_{34}O_2$) oxidation is developed. The mechanism for oxidation of Oleic acid was based on early removal of CO_2 (Decarboxylation) and H from Oleic acid to form Heptadecene radical ($C_{17}H_{33}$). The reaction mechanism consists of 485 species and 2531 reversible reactions. The thermochemical data for Oleic acid and related compounds were computed using THERGAS code. The rate constants of all elementary reactions were calculated at the experimental temperature, using the modified Arrhenius equation:

$$k = A\,T^{b}\exp(-E/RT)$$

Where,

T = Absolute Temperature (°K), A = Pre-exponential factor,

E = Activation Energy, b = the temperature coefficient,

R = Universal Gas Constant.

Table 8.1 shows rate constants for some important reactions along with model fitting values. The values of pre-exponential factor (A) and activation energy (E) used for initiation reactions are taken from Methyl Oleate pyrolysis mechanism [8.12] and values for oxidation and metathesis reactions are used from n-Hexadecane mechanism [8.1]. The model fitting values are modified pre-exponential factor and activation energy values to fit the model as per experimental results. As initiation and thermal decomposition are important irreversible reactions, model fitting is done mainly for these reactions only. It was observed that initiation reactions were most influential reactions and values of pre-exponential factor (A) and activation energy (E) for these reaction have impact on chemical kinetics and simulation results.

Rate expressions for initiation reactions with RSO radicals (k= A Tb exp [-E/RT], (units: s, mole, cm3, cal, K)				Fitting Values	References
Reactions	A	b	E_a		
C17H33COOH= C17H34 +CO2	7.00 x 10^{+18}	0.0	74600	A*10, E -1400	8.12
Decomposition of Heptadecene					
C17H34 = R + R' (primary carbon)	2.51 x 10^{+16}	0.0	83000	E -2400	8.12
C17H34 = R + R'	2.51 x 10^{+16}	0.0	79000		8.12
C17H34 = R + R' (β position)	2.51 x 10^{+16}	0.0	85000	E -400	8.12
Oxidation and Metathesis reactions					
C17H34 + O2 = HO2 + AC17H33 & QC17H33	2.50 x 10^{+13}	0.0	49000		8.1
C17H34 + O2 = HO2 + BC17H33 TO PC17H33	4.00 x 10^{+13}	0.0	47600		8.1
C17H34 = H + A TO Q C17H33	1.00 x 10^{+15}	0.0	100000		8.1
C17H34 + H = H2 + AC17H33	5.60 x 10^{+07}	2.0	7700		8.1
C17H34 + H = H2 + BC17H33 TO QC17H33	1.20 x 10^{+07}	2.0	5000		8.1
C17H34 + O = OH + AC17H33	2.77 x 10^{+02}	3.5	3080		8.1
C17H34 + O = OH + BC17H33 TO QC17H33	1.28 x 10^{+03}	3.3	1653		8.1

C17H34 + OH = H2O + AC17H33 & QC17H33	1.41 x 10^{+07}	1.8	974		8.1
C17H34 + OH = H2O + BC17H33	2.00 x 10^{+06}	2.0	-596		8.1
C17H34 + OH = H2O + CC17H33 TO PC17H33	1.13 x 10^{+06}	2.0	-1391		8.1
C17H34 + HO2 = H2O2 + AC17H33	8.00 x 10^{+12}	0.0	19400		8.1
C17H34 + HO2 = H2O2 + BC17H33 TO QC17H33	4.88 x 10^{+12}	0.0	18500		8.1
C17H34 + CH3 = CH4 + AC17H33 & QC17H33	1.30 x 10^{+12}	0.0	11600		8.1
C17H34 + CH3 = CH4 + BC17H33 TO PC17H33	8.00 x 10^{+11}	0.0	9500		8.1
C17H34 + C2H3 = C2H4 + AC17H33 & QC17H33	1.00 x 10^{+12}	0.0	18000		8.1
C17H34 + C2H3 = C2H4 + BC17H33 TO PC17H33	8.00 x 10^{+11}	0.0	16800		8.1
C17H34 + C2H5 = C2H6 + AC17H33 & QC17H33	1.00 x 10^{+12}	6.0	13400		8.1
C17H34 + C2H5 = C2H6 + BC17H33 TO PC17H33	1.00 x 10^{+12}	0.0	10400		8.1
Decomposition of Heptadecyl radical					
QC17H33 = R' + R'''	2.51 x 10^{+13}	0.0	31800	A*100	8.12
OC17H33 = R + R''''	3.95 x 10^{+10}	0.0	31300	A/2	8.12
NC17H33 = AC12H234 + AC5H10	2.51 x 10^{+13}	0.0	33100	A*100, E +1000	8.12
EC17H33 = AC11H212 + AC6H12	3.31 x 10^{+11}	0.0	29500	E +1000,	8.12
CC17H33 = C16H3017 + CH3	3.97 x 10^{+12}	0.0	36000	A/2	8.12

Oxidation and metathesis reactions for alkenyl radicals				Fitting Values	References
R' + O2 = HO2 + R"	1.40 x 10^{+13}	0.0	39000		8.1
R' + O = OH + R"	1.00 x 10^{+13}	0.0	4000		8.1
R' + OH = H2O + R"	1.00 x 10^{+13}	0.0	1230		8.1
R' + HO2 = H2O2 + R"	1.00 x 10^{+11}	0.0	17000		8.1
R' + H = H2 + R"	1.00 x 10^{+13}	0.0	3900		8.1
R' + CH3= CH4 + R"	2.00 x 10^{+11}	0.0	7300		8.1
R' + C2H3 = C2H4 + R"	2.00 x 10^{+11}	0.0	7300		8.1
R' + C2H5 = C2H6 + R"	1.26 x 10^{+15}	0.0	10400		8.1
R' = H + R"	5.00 x 10^{+12}	0.0	40000		8.1
Decomposition of dienes					
R"= R + R"	2.51 x 10^{+11}	0.0	33100	E +1000	8.12
R"= R" + R"	2.51 x 10^{+11}	0.0	33100	E +1000	8.12

R= Alkyl radical R'= Alkenyl radical R"= Dienes R'"= Alkenes

Table 8.1: Rate expressions for some important reactions added to the model

The oleic acid chemical kinetic mechanism is used to simulate RME oxidation performed at 1 bar for stoichiometric conditions (φ = 1), and

temperature range of 900 to 1400K. The mole fractions of important oxygenated compounds, intermediate olefins (C_2 to C_6) and products are plotted against the temperature. The initial concentration (0.05 mole %) of Oleic acid was similar to RME concentration used in oxidation experiments mentioned in Chapter 3. The Oleic acid model results are compared with RME oxidation experimental results along with simulation results with RME as a model fuel in figure 8.4 and 8.5. As similar carbon chain chemistry was assumed between RME and RSO, RME simulation results are also plotted to compare with RSO i.e. oleic acid simulation results. The mole fractions of reactants, intermediates and products are plotted against the experimental working temperature. The mole fractions were obtained for Oxygen, Hydrogen, CarbonMonoxide (CO), Carbon Dioxide (CO_2), Formaldehyde (CH_2O), Methane(CH_4),Ethane (C_2H_6), Ethene (C_2H_4), Acetylene (C_2H_2), Propene (C_3H_6),1-Butene (1-C_4H_8),1-Pentene (1-C_5H_{10}), 1-Hexene (1-C_6H_{12}), 1-Heptene (C_7H_{14}) and 1,3-Butadiene (1,3-C_4H_6).

The comparison between RME modeling results and Oleic acid (RSO) modeling results (figure 8.4 and 8.5) shows that Oleic acid is producing similar results in terms of concentration profile trends for all compounds like RME. This comparison is based only on profile trends of intermediate hydrocarbons and oxygenated compounds. Oleic acid model is reproducing intermediates in exact manner like RME up to 1200 K, except it failed to reproduce early formation of CO_2 and CH_2O. It also under predicted formation of C_2H_6 compared to RME modeling results. However concentration profile trend few compounds like C_2H_4, C_3H_6 and 1-C_5H_{10} is very matching with RME simulation results in precise manner.

It can be seen from figure 8.4 and 8.5 that Oleic Acid model predicted similar intermediate species as measured in RME oxidation experiments. The model shows similar profile trends for all hydrocarbon intermediates, and CO, CO_2 with discrepancies. The model is able to reproduce emission of pollutants like CH_2O and 1, 3- Butadiene. The model is producing profile trends for all the compounds up to temperature range of 1200 K. After 1200 K reaction mechanism is too fast; thus consuming all the fuel and producing lesser concentration of intermediates. Figure 8.4 and 8.5 shows that there is sudden change in concentration of all compounds after 1200 K. Also, model under predicts molar

concentration of all intermediate compounds as well as O_2 and CO_2 after 1200 K, so to understand this phenomena Rate of Production analysis (ROP) was done for Heptadecene and intermediate hydrocarbons at different temperature values (1180 K, 1200K, 1220K and 1300K). As discrepancy in terms of sudden drop in concentration of all compounds is observed in results at 1200 K, 1180 K, 1200K and 1220 K along with 1300 K as a higher temperature are selected for ROP.

Reaction No	Reactions	1180 K	1200 K	1220 K	1300 K
C17H34					
1126	C17H34=>AC9H171+AC8H17	-0.415	-0.41	-0.279	-0.301
1127	C17H34=>AC10H191+AC7H15	-0.415	-0.41	-0.279	-0.301

Table 8.2: Normalized rate of production (ROP) for Heptadecene

Reaction No	Reactions	1220 K	1300 K
C17H34			
1149	C17H34<=>H+AC17H33	0.122	0.133
1150	C17H34<=>H+BC17H33 to PC17H33	0.077	0.077
1163	C17H34<=>H+QC17H33	0.115	0.122

Table 8.3: Normalized rate of production (ROP) for Heptadecene at 1220K and 1300 K

Table 8.2 to 8.4 shows the normalized rate of production analysis (ROP) for Heptadecene. Table 8.2 shows that at all temperature values, Heptadecene is mainly consumed in initiation reactions (reaction no 1126, 1127) consist of C-C bond breakage at β position (C-C bond next to double bond). Reaction 1126 and 1127 are most important reaction for Heptadecene consumption. Table 8.2 also shows that rate of consumption is reducing with increasing temperature. However it can be seen from table 8.4 that at 1220 K Heptadecene is also consumed in thermal decomposition reaction (reaction no 1164) producing Heptadecene radicals. This can be the reason for sudden change in concentration profiles of intermediate compounds. The accurate values of Arrhenius constant, activation energy are needed for these initiation and thermal decomposition reactions. Table 8.3 shows that Heptadecene is reproduced at 1220 K and 1300 K by reverse reaction of thermal decomposition (reaction no 1149 to 1163).

Reaction No	Reactions	Normalized ROP Coefficients
C17H34		
1164	C17H34+H<=>H2+AC17H33	-0.016
1165	C17H34+H<=>H2+BC17H33 to QC17H33	-0.011

Table 8.4: Normalized rate of production (ROP) for Heptadecene at 1220K

The rate of production analysis was also done for some important intermediates like CH_4 (table 8.5), CH_2O (table 8.6) and C_3H_6 (table 8.7). Table 8.5 shows that CH_4 is mainly consumed in metathesis reactions (reaction no 37, 38). However it is also consumed in reaction with H radical in reaction 39 at 1220 K and 1300 K. The same reaction (reaction 39) is responsible for reproducing CH_4 at 1180 and 1200 K. The higher normalized rate of consumption and change in route for CH_4 consumption at 1220 and 1300 K explains why model under predicted CH_4 concentration after 1200 K. At 1180 K and 1200 K CH_4 is reproduced by reaction 116,142 and 2496; whereas it is only reproduced by reaction 2496 at 1220 K and 1300 K.

Reaction No	Reactions	1180 K	1200 K	1220 K	1300 K
CH4					
37	CH4+OH<=>CH3+H2O	-0.83	-0.795	-0.329	-0.302
38	CH4+O<=>CH3+OH	-0.167	-0.204	-0.099	-0.102
39	CH4+H<=>CH3+H2	0.161	0.106	-0.571	-0.595
116	CH2O+CH3<=>HCO+CH4	0.161	0.146	-	-
142	C2H4+CH3<=>C2H3+CH4	0.335	0.329	-	-
2496	CH4(+M)<=>CH3+H(+M)	0.101	0.185	0.979	0.994

Table 8.5: Normalized rate of production (ROP) for CH_4 at various temperatures

Reaction No	Reactions	1180 K	1200 K	1220 K	1300 K
CH2O					
45	CH3+O<=>CH2O+H	-	-	0.533	0.617
98	CH3O+M<=>CH2O+H+M	0.122	0.108	0.071	0.064
112	CH2O+OH<=>HCO+H2O	-0.299	-0.289	-0.344	-0.35
114	CH2O+H<=>HCO+H2	-0.541	-0.571	-0.564	-0.555
245	CH2OH+O2<=>CH2O+HO2	0.115	0.125	0.15	0.099
305	C3H6+O<=>C2H4+CH2O	0.085	0.094	0.066	0.05
2525	C2H3+O2<=>CH2O+HCO	0.495	0.451	0.088	0.025

Table 8.6: Normalized rate of production (ROP) for CH_2O at various temperatures

The rate of production analysis (ROP) for CH_2O in table 8.6 shows that CH_2O is mainly consumed in metathesis reactions (reaction no 112 and 114). It is also reproduced in third body reaction (reaction no 98) with Methoxy radical (CH_3O) and oxidation reaction (reaction 2525) with Vinyl radical (C_2H_3). However it is mainly reproduced in metathesis reaction with methyl radical in reaction no 45 at 1220 and1300 K.

Reaction No	Reactions	1180 K	1200 K	1220 K	1300 K
C3H6					
300	C3H6+OH<=>AC3H5+H2O	-0.162	-0.15	-0.160	-0.164
303	C3H6+O<=>C2H5+HCO	-	-	-0.079	-0.076
305	C3H6+O<=>C2H4+CH2O	-	-	-0.118	-0.114
310	C3H6+H<=>AC3H5+H2	-0.406	-0.406	-0.359	-0.347
892	BC6H13<=>C3H6+NC3H7	0.081	0.074	0.074	0.094
2530	C3H6<=>AC3H5+H	0.548	0.61	0.668	0.648

Table 8.7: Normalized rate of production (ROP) for C_3H_6 at various temperatures

Table 8.7 shows that Propene (C_3H_6) is consumed in metathesis reaction with OH and H radical at 1180 and 1200 K (reaction no 300 and 305), whereas at 1220 K and 1300 K, it is consumed in metathesis reaction with O radical (reaction no 303 and 305) along with reaction no 300 and 310. Propane (C_3H_6) is reproduced in reaction no 892 and 2530 at all temperatures. The increase in rate of consumption at 1220 K again explains why model failed to reproduce formation of intermediate hydrocarbons after 1200 K.

The chemical kinetic mechanism was developed for Rapeseed oil oxidation in terms of Oleic acid oxidation mechanism. The model was used to simulate Rapeseed oil methyl ester (RME) oxidation in Jet stirred reactor. The comparison is based on intermediate hydrocarbons. The model is able to reproduce concentration profile trends for all intermediates up to 1200 K. After 1200 K, there is discrepancy in simulation results; model is under predicting concentration of intermediates. After 1300K concentration of O_2 and CO_2 is almost constant. The rate of production analysis (ROP) showed that Heptadecene is mainly consumed in C-C bond breakage at β position. The Arrhenius constant and activation energy values used for initiation reactions are taken from kinetic mechanism for Methyl Oleate pyrolysis [8.12]. The rate of production analysis in table 8.2 showed the important reactions responsible for Heptadecene consumption. It also showed that as temperature is increasing the rate of consumption for Heptadecene decreases indicating that model is predicting lower reactivity at higher temperature especially after 1200 K. The improvements in model will need accurate values of pre-exponential factor and activation energy for these initiation reactions (reaction no 1126 and 1127) and chain propagation reactions.

This simulation work is an attempt to simulate oxidation of vegetable oil using simple approach like considering chemistry associated with long carbon (C_{17}) alkyl chain with unsaturation. However the model is not validated for any vegetable oil or Rapeseed oil oxidation. The model needs to be validated against Rapeseed oil experimental results to confirm its efficiency. The current model is based on mono-glyceride and early removal of CO_2. The model does not include chemistry associated with carbonyl group (C=O) and triglycerides. The model needs to incorporate the reactions associated with oxidation of triglyceride instead of decomposition of triglyceride. Also reactions associated with triglycerides instead of monoglycerides need to be developed and considered for updated kinetic model. The experimental database for oxidation of vegetable oils in reactors like Jet stirred reactor or any other well stirred reactor is needed to verify developed chemical kinetic mechanism for Rapeseed oil oxidation.

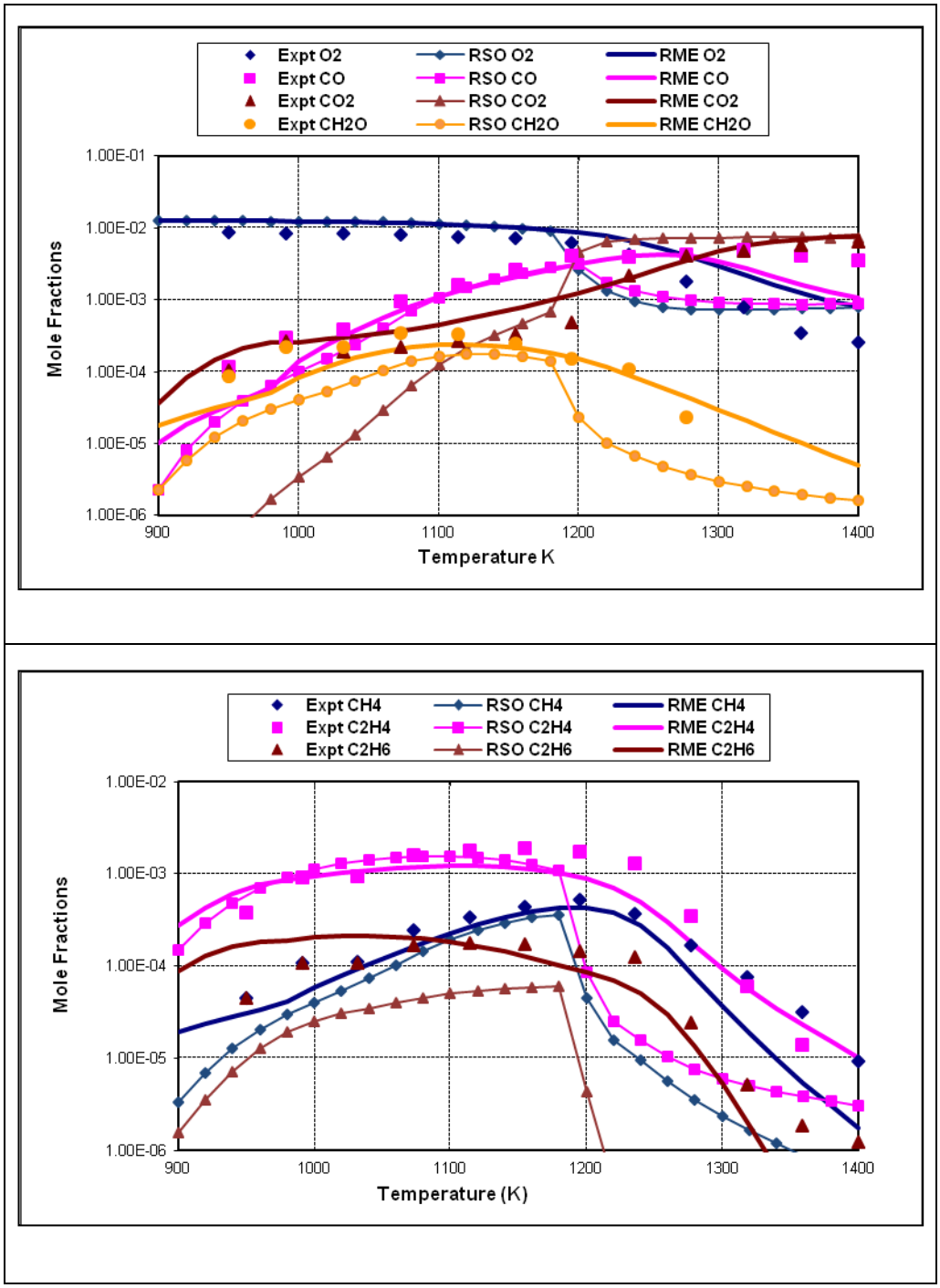

Figure 8.4: The oxidation of RME in a JSR (P = 1bar, φ = 1, τ = 0.1 s)
The experimental data (large symbols) are compared to the
(RSO model fuel: lines + symbols, RME model fuel: lines)

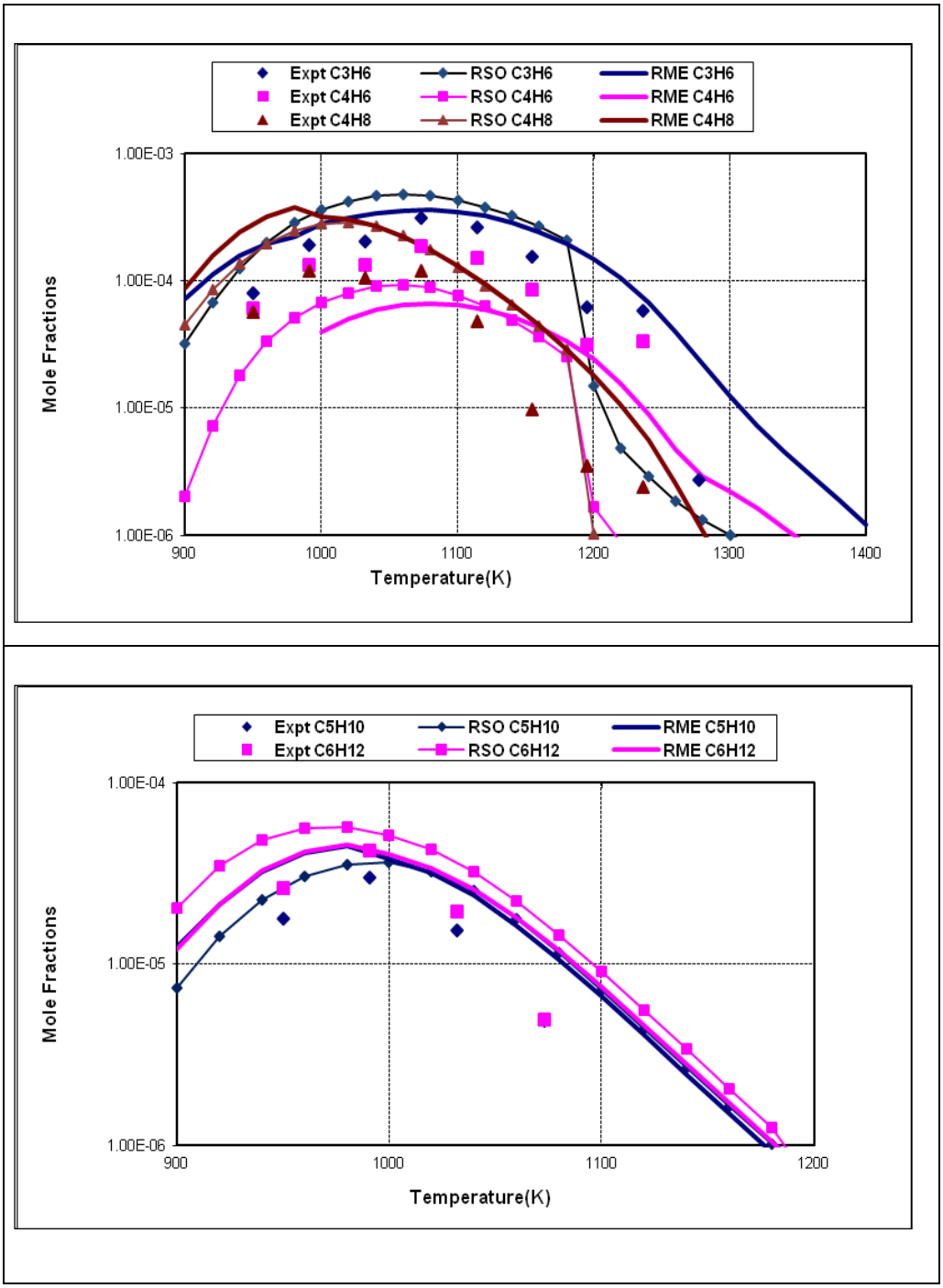

Figure 8.5: The oxidation of RME in a JSR (P = 1bar, φ = 1, τ = 0.1 s). The experimental data (large symbols) are compared to the (RSO model fuel: lines + symbols, RME model fuel: lines)

References

8.1 Dagaut.P, Ristori.A and Cathonnet.M, 2001, The*Oxidation of n-Hexadecane: Experimental and Detailed Kinetic Modeling*, Combustion and Flame, 125, 1128-1137

8.2 Alencar.J.W, Alves.P and Craveiro.A, 1983, *Pyrolysis of Tropical Vegetable Oils*, J.Agric.Food.Chem, 31, No.6, 1268-1270

8.3 Chang Chia-chu and Wan.Shen-wu, 1947, *China's Motor Fuels from Tung Oil*, Industrial and Engineering Chemistry, 39, Vol.12, 1543-1548

8.4 Schwab.W.A, Dykstra.J.G, Selke.E, Sorenson.C.S and Pryde.H.E, 1988, *Diesel Fuel from Thermal Decomposition of Soybean Oil*, JAOCS, 65, No.11, 1781-1786

8.5Bakhshi.N.Narendra, Katikaneni.R.P.Sai and Idem.O Raphael, 1996, *Thermal cracking of Canola oil: Reaction products in the presence and absence of Steam*, Energy & Fuels, 10, 1150-1162

8.6 Kitamura.Kazuo, 1971, *Studies of the Pyrolysis of Triglycerides*, Bulletin of the chemical society of Japan, Vol.44, No.6, 1606-1609

8.7 Pedersen.R.J, Ingemarsson.A and Olsson.O.J, 1999, *Oxidation of Rapeseed oil, Rapeseed Methyl Ester (RME) and diesel fuel studied with GC/MS*, Chemosphere, 38, 11, 2467-2474

8.8 Nwafor.O.M.I, 2004, *Emission characteristics of diesel engine operating on rapeseed methyl ester*,Renewable Energy,29, 119-129

8.9 Labeckas.G, Slavinskas.S, 2006, *The effect of rapeseed oil methyl ester on direct injection Diesel engine performance and exhaust emissions*, Energy Conversion and Management, 47, Issue 13-14, 1954-1967

8.10 Alonso Jose.San.J, Lopez.Sastre.A.J, Romero-Avila.C, Lopez.Romero.J.E, 2006, Combustion *of rapeseed oil and diesel oil mixtures for use in the production of heat energy*, Fuel Processing Technology, 87, 97-102

8.11 Lance.D.L and Anderson.J.D, 2004, *Emissions Performance of Pure Vegetable Oil in Two European, Light Duty Vehicles*, SAEngineers Paper No: 2005-01-1881

8.12 Billaud.F and Archambault.D, 1999, *Experimental and modeling study of methyl oleate pyrolysis between 500 and 650 ^{0}C*, J.Chim.Phys, 96, 778-796

CHAPTER 9

CONCLUSION

In this research work, the oxidation of RME was studied experimentally and a chemical kinetics reaction mechanism was developed. The RME oxidation was simulated first using a surrogate model fuel and then RME as model fuel. The chemical kinetics reaction mechanism for Rapeseed oil (RSO) was also developed. This chapter is divided into three parts

- Experimental conclusion
- Modeling Conclusion
- Recommendations for future work

9.1 Experimental work conclusion for RME combustion

The RME oxidation experiments were carried out at 1 and 10 bar for fuel-lean to fuel rich conditions (Φ= 0.25 to 1.5) in a Jet Stirred Reactor (chapter 3). The experimental conditions used were based on a compromise between conditions required to produce the reaction mechanism (conditions used in previous oxidation work done by Dagaut et.al) [9.1] and limitations of the experimental system used. The reactivity of RME was studied and compared at 1bar and 10 bar in terms of mole fraction profile trends of reactants, intermediate species and products. The effect of equivalence ratio and temperature on reactivity was observed keeping the total pressure constant.

Sections 4.1 and 4.2 in chapter 4 described the RME oxidation results. It was observed that, compared to lighter fuels, RME reacted immediately i.e. at initial experimental (working) temperature, RME yielded saturated, unsaturated hydrocarbon intermediates, saturated, unsaturated esters and oxygenated intermediates. The saturated and unsaturated hydrocarbons reach maximum concentration values at temperatures such as 1200 K as the equivalence ratio is increased. It was observed that RME reactivity increased with increasing temperature and pressure, but decreased with increasing equivalence ratio. The reactivity was higher in fuel-lean conditions (section 4.1 and 4.2). All intermediate species showed the same profile trends at 1 bar and at 10 bar. The level of saturated and unsaturated hydrocarbon compounds increased in fuel rich conditions. The maximum mole fraction value of intermediate species decreased

at high pressure indicating reactivity of RME was higher at high pressure than at low pressure (section 4.3 in chapter 4). The Carbon balance was done for each experiment and was within the range of -/+ 10%.

The RME emitted alkenes, pollutants like 1,3-Butadiene (C_4H_6), Formaldehyde (CH_2O) and Benzene (C_6H_6) in lower concentrations at high pressure, especially in fuel-lean and stoichiometric conditions. The formation of aromatics in lesser quantity and the increase in CO concentration with increasing Fuel/Air ratio was similar to observations made when RME and its blends were tested in different diesel engines [9.2] (section 4.2 in chapter 4). The emission profile of hydrocarbon intermediates and aldehydes is important as they are major contributor to atmospheric pollution, and global warming [9.3] (section 4.3 in chapter 4). It was also observed that the highest mole fractions of CO_2 were obtained in fuel-lean conditions. This shows that RME has higher combustion efficiency at high pressure and fuel-lean conditions. The reductions in intermediate hydrocarbon emission levels and increase in mole fractions of CO_2 shows that RME as a fuel has positive impact on environmental pollution.

It is known fact that lean mixtures are important in diesel engines especially at high pressure [9.4] (section 4.3, chapter 4). Table 4.3 in chapter 4 showed that RME gives better combustion performance at fuel-lean conditions and at higher temperatures, especially at higher pressure. This implies that fuel-lean condition or higher Air/Fuel ratio is more suitable for RME combustion.

The RME (Biodiesel) and commercial diesel oxidation at 10 bar and stoichiometric conditions ($\Phi = 1$) is compared and presented in section 5.1 of chapter 5. The results showed that the RME (Biodiesel) oxidation is similar to commercial diesel fuel oxidation and produces similar intermediate species. The concentration profile trends for all intermediates obtained in experiments are similar to that observed from diesel oxidation. It was observed that RME produces the same mole fractions and profile trends for regulated pollutant CO, CO_2 and lower quantities for pollutants like Acetylene (C_2H_2), Propane (C_3H_6), 1,3-Butadiene (C_4H_6) than that from Diesel, which indicated that RME gives efficient combustion performance. This also proved that RME is better than diesel as a fuel in terms of combustion performance.

9.2 Modeling work conclusion for RME combustion

The kinetic modeling work was carried out to validate and to understand the reaction pathways of RME combustion. The kinetic models were used and developed to validate RME oxidation. The modeling work was done in two parts namely: modeling using n-hexadecane ($C_{16}H_{34}$) and Methyl Acetate (CH_3COOCH_3) as a surrogate model fuel (section 5.2 and 5.3 in chapter 5) and the newly developed chemical kinetic mechanism using RME as a model fuel (chapter 7). The experimental results of RME oxidation showed strong similarity to that of n-large alkanes [9.5]. Therefore, the oxidation of RME was simulated using n-hexadecane ($C_{16}H_{34}$) as a surrogate model-fuel. The section 5.2.1 and 5.2.2 in chapter 5 describe the simulation results using n-Hexadecane as model fuel for 1 bar and 10 bar respectively.

The n-Hexadecane ($C_{16}H_{34}$) model reproduced experimental concentration profiles for reactants, all intermediates especially C_1-C_4 hydrocarbons and products. The mole fractions of reactants, intermediates and products are in agreement with experimentally measured. The model under predicted 1, 3-Butadiene, CH_2O and CO formation which is thought to be due to the absence of unsaturated and carbonyl groups in structure of n-Hexadecane. It also over-predicted the formation of intermediate olefins like 1-Pentene and 1-Hexene. As n-Hexadecane has only saturated alkyl chain in its structure, the model with n-Hexadecane is not able to reproduce these olefin products in a precise manner. The early formation of CO_2 in the experiments was not reproduced by the model. This early carbon dioxide production was may be due to the pyrolysis of the ester function, so RME oxidation was simulated using combined oxidation reaction mechanism of n-Hexadecane and Methyl Acetate (MA), which represents chemistry of the ester function.

The combined model of MA + $C_{16}H_{34}$ explained in section 5.3 of chapter 5, gave similar modeling results to that from n-hexadecane. The combined model gave a good description of C_1-C_4 hydrocarbons and CO formation in terms of profile trends. The early formation of CO_2 i.e. concentration of CO_2 at initial working temperature was not predicted satisfactory, whereas the concentration profile trend for 1, 3-Butadiene was improved compared to trend predicted by n-Hexadecane model. This modeling work confirmed the efficiency of using

surrogate model-fuels like n-Hexadecane and Methyl Acetate for modeling the combustion of commercial fuels. It also showed that oxidation of long carbon chain Biodiesel like RME can be simulated using surrogate model-fuels, but with some limitations and less accuracy.

The modeling with surrogate fuel showed that a model with long saturated carbon chain (C_{16}) and ester function ($COOCH_3$) is not sufficient to reproduce RME oxidation experimental results within reasonable degree of certainty. The above models lack the presence of unsaturation as well as ester groups associated with a long carbon chain in their structures. It was observed from the Methyl Acetate sub mechanism, that Methyl Acetate thermally decomposes to give an Acetyl radical (CH_3COO), which decomposes to give CO_2 and methyl radical [9.6] (reaction 5.7, section 5.3 of chapter 5). The major route for CO_2 formation is through decomposition of the acetyl radical only. So the early production of CO_2 in RME combustion was may be associated with pyrolysis of ester function as well as with chemistry associated with saturated and un-saturated ester compounds and intermediates formed from parent RME molecule.

So the model for RME oxidation has to be developed considering chemistry associated with unsaturation (carbon double bond) and ester function with long carbon chain (C_{18}) present in RME structure. The chemical kinetic mechanism for oxidation of RME was developed and explained in chapter 6. The RME oxidation mechanism was based on the n-Hexadecane oxidation mechanism and a typical high temperature hydrocarbon oxidation mechanism incorporating chemistry for all saturated & unsaturated esters, dienes and alkyl compounds. The mechanism consists of 2652 reactions and 496 species. The results were presented for 1 bar and 10 bar for fuel-lean to fuel-rich conditions (Φ = 0.25 to 1.5) in section 7.2 and 7.3 of chapter 7 respectively. The sensitivity analysis and rate of production analysis was done for 1 bar. The rate of production analysis was done for pollutants like CH_2O and 1-3 Butadiene for 1 bar to know the reaction path of their formation [9.7].

At 1 bar, the model confirmed that, compared to lighter fuels, RME reacted rapidly, yielding saturated, unsaturated hydrocarbon intermediates, and oxygenated intermediates. The model predicts the similar profile trends for all

combustion components as found in the experimental results. The model reproduced early formation of CO_2 especially at stoichiometric and fuel-rich conditions. The model reproduced formation of the pollutants such as CO, CH_2O and C_1-C_4 compounds reasonably well (in terms of profile trends) at all conditions, whereas it under predicted formation of 1,3-Butadiene at all conditions. The effect of an ester function ($COOCH_3$, i.e. fuel based oxygen) present in RME structure on the CO_2 formation was also evaluated. The formation path for important intermediates like 1-Pentene and 1-Hexene was also studied. It confirms the effect of a long carbon unsaturated chain present in the RME structure on formation of 1-alkenes. The model also confirmed the diesel engine combustion observation that RME has positive effect on intermediate hydrocarbon emission.

The sensitivity analyses explained in section 7.2.1 of chapter 7 showed that RME oxidation is more sensitive to initiation reactions of C-C bond breakage at the β position and unimolecular decomposition of unsaturated esters with small carbon chain of C_5-C_8. The rate of production analysis (section 7.2.2 of chapter 7) gave the reaction path for RME consumption during its combustion. It showed that RME was mostly consumed in initiation reactions i.e. decomposition and oxidation reactions, producing intermediate radicals and metathesis reactions producing RME radicals. The rate of production analysis (section 7.2.3 and 7.2.4 in chapter7) showed that pollutants like CH_2O are mainly produced from the Methoxy (CH_3O) and Vinyl radical (C_2H_3), whereas 1,3-Butadiene was mainly produced from Methyl Allyl radical (MEALL). This analysis confirmed the effect of unsaturation and ester function present in RME structure on formation of these pollutants.

Regarding the reactivity of RME, again, a good agreement between the data and the model in terms of profile trends of key oxidation products and reactants was obtained. The model also proves that RME reactivity decreases with increasing Fuel (RME) / Oxygen (O_2) ratio and increases with increasing temperature. The reactivity observed was highest at fuel lean conditions. As reactivity was higher at higher temperature and fuel-lean conditions especially at higher pressure, these conditions look favorable for RME combustion in diesel engine. The recommended fuel conditions for RME combustion in commercial

engines are fuel-lean conditions or RME in blends with diesel up to 50%.

At 10 bar the model under predicted reactivity at all equivalence ratios (section 7.4 in chapter 7). It was observed that intermediate species formed in a model are not consumed fast enough to allow fast oxidation of fuel. The disagreement with experimental results can be associated with inaccurate rate coefficients and pressure dependency considered or some missing reactions in the chemical kinetic model. The model reproduced early formation of CO_2 at stoichiometric and fuel-rich conditions and also gave good description of experimental results for C_2H_4 and 1,3-Butadiene (C_4H_6), especially in fuel-rich conditions. Overall model failed to predict reactivity and formation of major intermediate species like olefins and CO. The RME oxidation experiments were performed from 800 K to 1200 K. At this temperature range (800 K), some low temperature combustion chemistry may take place especially in case of reaction with molecular oxygen, however only high temperature combustion chemistry was considered in RME model. The model needs improvement, considering pressure dependency, suitable values of rate coefficients and incorporating effect of low temperature combustion chemistry.

9.3 Modeling work conclusion for RSO combustion

Chapter 8 explains development chemical kinetic mechanism for Rapeseed oil oxidation and simulation results. As experimental data for oxidation of RSO is not available, the chemical kinetic mechanism for Rapeseed oil (RSO) was developed based on assumption that Rapeseed oil and Rapeseed oil methyl ester (RME) have similar hydrocarbon chain chemistry. The Rapeseed oil decomposes to give Acrolein (C_3H_4O), two fatty acids (R'COOH, R'''COOH) and Ketenes (R''CH=CO) [9.8] (section 8.1.1 of chapter 8). However, to simplify the combustion of Rapeseed oil, only main component of Rapeseed oil, which is Oleic Acid, is considered for simulation work. So a chemical kinetic mechanism for Oleic acid ($C_{18}H_{34}O_2$) oxidation is developed to represent RSO oxidation (section 8.1.2 of chapter 8). The mechanism for oxidation of oleic acid was based on early removal of CO_2 (Decarboxylation) and H from Oleic acid to form Heptadecene radical ($C_{17}H_{33}$). The reaction mechanism consists of 485 species and 2531 reversible reactions.

The oleic acid oxidation mechanism was validated using experimental data of RME oxidation for 1 bar (section 8.2 of chapter 8). It was observed that oxidation of RSO also emits similar intermediate species like RME. The model is able to reproduce concentration profile trends for all intermediates up to 1200 K. After 1200 K, there is discrepancy in simulation results; model is under predicting concentration of intermediates. The model is able to reproduce emission of pollutants like CH_2O and 1,3- Butadiene. Though model is reproducing the profile trends in similar manner, it fails to reproduce early formation of CO_2. Also after 1300K concentration of O_2 and CO_2 is almost constant. The model needs improvements to remove those discrepancies. The rate of production analysis (ROP) showed that Heptadecene is mainly consumed in C-C bond breakage at β position. The future work can be improving this mechanism by including updated values of bond energies and kinetic parameters for these initiation reactions including thermal decomposition reactions. Also kinetic model needs to incorporate the reactions associated with oxidation of triglyceride instead of monoglyceride. The experimental database is needed to verify developed kinetic mechanism for Rapeseed oil oxidation.

9.4 Recommendation for future work

The oxidation of RME was carried out in Jet-stirred reactor at 1 bar and 10 bar. Due to experimental set up limitations, experiments were performed only up to 10 bar. The effect of pressure on combustion kinetics was evaluated at 10 bar only. The commercial diesel engines run at very high pressure (approximately 50-70 bar). So the combustion kinetics or fuel reactivity will be different at this pressure range. Though it is not possible to replicate these conditions at laboratory scale, the RME oxidation should be carried out at higher pressure like 40 or 50 bar in JSR to see the effect of pressure on fuel reactivity. The RME blends with commercial diesel were not evaluated in this research work. More experimental work should be carried out on different Biodiesel blends, to develop chemical kinetics of such blends.

RME oxidation was simulated using surrogate fuels (n-Hexadecane and Methyl Acetate) as model-fuel and RME as a model-fuel. It will be interesting to use more surrogate model fuels to simulate combustion of commercial long hydrocarbon chain Biodiesel. The modeling with RME as a model-fuel

reproduced experimental results in reasonably well manner in terms of mole fractions. However, model under-estimated reactivity of RME at 10 bar for all fuel conditions. The model needs improvements with more accurate values of activation energy, Arrhenius constants and considering pressure dependency. As fuel droplets were observed below 800 K, only high temperature chemistry is considered in this research work. It will be interesting to explore low temperature chemistry of commercial Biodiesel like RME.

The chemical kinetic mechanism was proposed for oxidation of Rapeseed oil. However there is no experimental data available for oxidation of rapeseed oil. It is important to generate experimental date for oxidation of rapeseed oil or any other vegetable oil. The kinetic model has to be improved considering accurate values of kinetic parameters. The chemical kinetic model for oxidation of vegetable oils needs to be developed considering chemistry associated with triglycerides instead of monoglyceride and oxidation of triglycerides. It will be interesting to simulate vegetable oil oxidation using surrogate fuel based models.

References

9.1 Dagaut.P, Cathonnet.M, Rouan.J-P, Foulatier.R, Quilgars.A, Boettner.J-C, Gaillard.F, James.H, 1986, *A jet-stirred reactor for kinetic studies of homogenous gas-phase reactions at pressures up to ten atmosphere (~1Mpa)*, *J*. Phys E: Instrum 19, 207-209.

9.2 Krahl.J, Munack.A, Bahadir.M, Schumacher.L and Elser.N, 1996, *Review: Utilization of Rapeseed oil, Rapeseed Oil Methyl Ester or Diesel Fuel: Exhaust Gas Emissions and Estimation of Environmental Effects,* SAE Technical Paper Series Paper no: 962096

9.3 Makareviciene.V, Sendzikiene.E, Janulis.P, 2006, *Influence of fuel oxygen content on diesel engine exhaust emissions*, Renewable Energy, 31, 2505-2512

9.4 Morin.C, Chauveau.C, Dagaut.P, Gokalp.I and Cathonnet.M, 2004, *Vaporization & Oxidation of liquid fuel droplets at high temperature and high pressure: Application to n-alkanes and vegetable oil methyl esters*, Combustion Science and Technology, 176, 499-529

9.5 Dagaut.P, Ristori.A and Cathonnet.M, 2001, *The Oxidation of n-Hexadecane: Experimental and Detailed Kinetic Modeling*, Combustion and Flame, 125, 1128-1137

9.6 Dagaut.P, Smoucovit.N and Cathonnet.M, 1997, *Methyl Acetate Oxidation in a JSR: Experimental and Detailed Kinetic Modeling Study*, Combustion Science and Technology, 127, 275-291

9.7 Labeckas.G, Slavinskas.S, 2006, *The effect of rapeseed oil methyl ester on direct injection Diesel engine performance and exhaust emissions*, Energy Conversion and Management, 47, Issue 13-14, 1954-1967

9.8 Chang Chia-chu and Wan.Shen-wu, 1947, *China's Motor Fuels from Tung Oil,* Industrial and Engineering Chemistry, 39, Vol.12, 1543-1548

APPENDIX A

Chemical Kinetic Mechanism for oxidation of RME

Arrhenius Constant : $k = A\ T^{b}\ exp(-E/RT))$

Units : A= mole-cm-sec T = K, E = cal/mole

Important Initiation reactions considered

		A	b	E
1107	C17:d9=>PC16:d9+CH3	2.51E+17	0	83000
1108	C17:d9=>OC15:d9+C2H5	2.51E+17	0	79000
1109	C17:d9=>NC14:d9+NC3H7	2.51E+17	0	79000
1110	C17:d9=>MC13:d9+PC4H9	2.51E+17	0	79000
1111	C17:d9=>LC12:d9+AC5H11	2.51E+17	0	79000
1112	C17:d9=>KC11:d9+AC6H13	2.51E+17	0	70800
1113	C17:d9=>AC10H192+GC7:0	2.51E+17	0	70800
1114	C17:d9=>AC11H213+FC6:0	2.51E+17	0	79000
1115	C17:d9=>AC12H234+EC5:0	2.51E+17	0	79000
1116	C17:d9=>AC13H255+DC4:0	2.51E+17	0	79000
1117	C17:d9=>AC14H276+CC3:0	2.51E+17	0	79000
1118	C17:d9=>AC15H297+BC2:0	2.51E+17	0	77000
1119	C17:d9=>AC16H318+COOCH3	2.51E+17	0	78000
1120	C17:d9=>AC16H31COO+CH3	2.51E+18	0	73000
1121	AC16H31COO=>AC16H318+CO2	2.51E+20	0	82000
1122	COOCH3=>CO2+CH3	1.50E+11	0	32700

Important RME oxidation reactions considered

		A	b	E
1123	C17:d9+O2=HO2+BC17:d9	4.00E+13	0	47600
1124	C17:d9+O2=HO2+CC17:d9	4.00E+13	0	47600
1125	C17:d9+O2=HO2+DC17:d9	4.00E+13	0	47600
1126	C17:d9+O2=HO2+EC17:d9	4.00E+13	0	47600
1127	C17:d9+O2=HO2+FC17:d9	4.00E+13	0	47600
1128	C17:d9+O2=HO2+GC17:d9	4.00E+13	0	47600
1129	C17:d9+O2=HO2+HC17:d9	4.00E+13	0	47600
1130	C17:d9+O2=HO2+KC17:d9	4.00E+13	0	47600
1131	C17:d9+O2=HO2+LC17:d9	4.00E+13	0	47600
1132	C17:d9+O2=HO2+MC17:d9	4.00E+13	0	47600
1133	C17:d9+O2=HO2+NC17:d9	4.00E+13	0	47600

1134	C17:d9+O2=HO2+OC17:d9	4.00E+13	0	47600
1135	C17:d9+O2=HO2+PC17:d9	4.00E+13	0	47600
1136	C17:d9+O2=HO2+QC17:d9	2.50E+13	0	49000

Important RME Metathesis reactions considered

		A	b	E
1151	C17:d9+H=H2+BC17:d9	1.20E+07	2	5000
1152	C17:d9+H=H2+CC17:d9	1.20E+07	2	5000
1153	C17:d9+H=H2+DC17:d9	1.20E+07	2	5000
1154	C17:d9+H=H2+EC17:d9	1.20E+07	2	5000
1155	C17:d9+H=H2+FC17:d9	1.20E+07	2	5000
1156	C17:d9+H=H2+GC17:d9	1.20E+07	2	5000
1157	C17:d9+H=H2+HC17:d9	1.20E+07	2	5000
1158	C17:d9+H=H2+KC17:d9	1.20E+07	2	5000
1159	C17:d9+H=H2+LC17:d9	1.20E+07	2	5000
1160	C17:d9+H=H2+MC17:d9	1.20E+07	2	5000
1161	C17:d9+H=H2+NC17:d9	1.20E+07	2	5000
1162	C17:d9+H=H2+OC17:d9	1.20E+07	2	5000
1163	C17:d9+H=H2+PC17:d9	1.20E+07	2	5000
1164	C17:d9+H=H2+QC17:d9	1.20E+07	2	5000
1165	C17:d9+O=OH+BC17:d9	1.13E+03	3.3	1653
1166	C17:d9+O=OH+CC17:d9	1.13E+03	3.3	1653
1167	C17:d9+O=OH+DC17:d9	1.13E+03	3.3	1653
1168	C17:d9+O=OH+EC17:d9	1.13E+03	3.3	1653
1169	C17:d9+O=OH+FC17:d9	1.13E+03	3.3	1653
1170	C17:d9+O=OH+GC17:d9	1.13E+03	3.3	1653
1171	C17:d9+O=OH+HC17:d9	1.13E+03	3.3	1653
1172	C17:d9+O=OH+KC17:d9	1.13E+03	3.3	1653
1173	C17:d9+O=OH+LC17:d9	1.13E+03	3.3	1653
1174	C17:d9+O=OH+MC17:d9	1.13E+03	3.3	1653
1175	C17:d9+O=OH+NC17:d9	1.13E+03	3.3	1653
1176	C17:d9+O=OH+OC17:d9	1.13E+03	3.3	1653
1177	C17:d9+O=OH+PC17:d9	1.13E+03	3.3	1653
1178	C17:d9+O=OH+QC17:d9	1.13E+03	3.3	1653
1179	C17:d9+OH=H2O+BC17:d9	1.13E+06	2	-1391
1180	C17:d9+OH=H2O+CC17:d9	1.13E+06	2	-1391
1181	C17:d9+OH=H2O+DC17:d9	1.13E+06	2	-1391

1182	C17:d9+OH=H2O+EC17:d9	1.13E+06	2	-1391
1183	C17:d9+OH=H2O+FC17:d9	1.13E+06	2	-1391
1184	C17:d9+OH=H2O+GC17:d9	1.13E+06	2	-1391
1185	C17:d9+OH=H2O+HC17:d9	1.13E+06	2	-1391
1186	C17:d9+OH=H2O+KC17:d9	1.13E+06	2	-1391
1187	C17:d9+OH=H2O+LC17:d9	1.13E+06	2	-1391
1188	C17:d9+OH=H2O+MC17:d9	1.13E+06	2	-1391
1189	C17:d9+OH=H2O+NC17:d9	1.13E+06	2	-1391
1190	C17:d9+OH=H2O+OC17:d9	1.13E+06	2	-1391
1191	C17:d9+OH=H2O+PC17:d9	1.13E+06	2	-1391
1192	C17:d9+OH=H2O+QC17:d9	1.41E+07	1.8	974
1193	C17:d9+HO2=H2O2+BC17:d9	4.88E+12	0	18500
1194	C17:d9+HO2=H2O2+CC17:d9	4.88E+12	0	18500
1195	C17:d9+HO2=H2O2+DC17:d9	4.88E+12	0	18500
1196	C17:d9+HO2=H2O2+EC17:d9	4.88E+12	0	18500
1197	C17:d9+HO2=H2O2+FC17:d9	4.88E+12	0	18500
1198	C17:d9+HO2=H2O2+GC17:d9	4.88E+12	0	18500
1199	C17:d9+HO2=H2O2+HC17:d9	4.88E+12	0	18500
1200	C17:d9+HO2=H2O2+KC17:d9	4.88E+12	0	18500
1201	C17:d9+HO2=H2O2+LC17:d9	4.88E+12	0	18500
1202	C17:d9+HO2=H2O2+MC17:d9	4.88E+12	0	18500
1203	C17:d9+HO2=H2O2+NC17:d9	4.88E+12	0	18500
1204	C17:d9+HO2=H2O2+OC17:d9	4.88E+12	0	18500
1205	C17:d9+HO2=H2O2+PC17:d9	4.88E+12	0	18500
1206	C17:d9+HO2=H2O2+QC17:d9	4.88E+12	0	18500
1207	C17:d9+CH3=CH4+BC17:d9	8.00E+11	0	9500
1208	C17:d9+CH3=CH4+DC17:d9	8.00E+11	0	9500
1209	C17:d9+CH3=CH4+EC17:d9	8.00E+11	0	9500
1210	C17:d9+CH3=CH4+FC17:d9	8.00E+11	0	9500
1211	C17:d9+CH3=CH4+GC17:d9	8.00E+11	0	9500
1212	C17:d9+CH3=CH4+HC17:d9	8.00E+11	0	9500
1213	C17:d9+CH3=CH4+KC17:d9	8.00E+11	0	9500
1214	C17:d9+CH3=CH4+LC17:d9	8.00E+11	0	9500
1215	C17:d9+CH3=CH4+MC17:d9	8.00E+11	0	9500
1216	C17:d9+CH3=CH4+NC17:d9	8.00E+11	0	9500

1217	C17:d9+CH3=CH4+OC17:d9	8.00E+11	0	9500
1218	C17:d9+CH3=CH4+PC17:d9	8.00E+11	0	9500
1219	C17:d9+CH3=CH4+QC17:d9	1.30E+12	0	11600
1220	C17:d9+C2H5=C2H6+BC17:d9	1.00E+15	0	8400
1221	C17:d9+C2H5=C2H6+CC17:d9	1.00E+15	0	8400
1222	C17:d9+C2H5=C2H6+DC17:d9	1.00E+15	0	8400
1223	C17:d9+C2H5=C2H6+EC17:d9	1.00E+15	0	8400
1224	C17:d9+C2H5=C2H6+FC17:d9	1.00E+15	0	8400
1225	C17:d9+C2H5=C2H6+GC17:d9	1.00E+15	0	8400
1226	C17:d9+C2H5=C2H6+HC17:d9	1.00E+15	0	8400
1227	C17:d9+C2H5=C2H6+KC17:d9	1.00E+15	0	8400
1228	C17:d9+C2H5=C2H6+LC17:d9	1.00E+15	0	8400
1229	C17:d9+C2H5=C2H6+MC17:d9	1.00E+15	0	8400
1230	C17:d9+C2H5=C2H6+NC17:d9	1.00E+15	0	8400
1231	C17:d9+C2H5=C2H6+OC17:d9	1.00E+15	0	8400
1232	C17:d9+C2H5=C2H6+PC17:d9	1.00E+15	0	8400
1233	C17:d9+C2H5=C2H6+QC17:d9	1.00E+15	0	13400
1234	C17:d9+C2H3=C2H4+BC17:d9	8.00E+12	0	16800
1235	C17:d9+C2H3=C2H4+CC17:d9	8.00E+12	0	16800
1236	C17:d9+C2H3=C2H4+DC17:d9	8.00E+12	0	16800
1237	C17:d9+C2H3=C2H4+EC17:d9	8.00E+12	0	16800
1238	C17:d9+C2H3=C2H4+FC17:d9	8.00E+12	0	16800
1239	C17:d9+C2H3=C2H4+GC17:d9	8.00E+12	0	16800
1240	C17:d9+C2H3=C2H4+HC17:d9	8.00E+12	0	16800
1241	C17:d9+C2H3=C2H4+KC17:d9	8.00E+12	0	16800
1242	C17:d9+C2H3=C2H4+LC17:d9	8.00E+12	0	16800
1243	C17:d9+C2H3=C2H4+MC17:d9	8.00E+12	0	16800
1244	C17:d9+C2H3=C2H4+NC17:d9	8.00E+12	0	16800
1245	C17:d9+C2H3=C2H4+OC17:d9	8.00E+12	0	16800
1246	C17:d9+C2H3=C2H4+PC17:d9	8.00E+12	0	16800
1247	C17:d9+C2H3=C2H4+QC17:d9	1.00E+12	0	18000

Important RME radical Isomerization reactions considered

		A	b	E
1248	BC17:d9=>EC17:d9	5.01E+11	0	17300
1249	BC17:d9=>FC17:d9	8.61E+10	0	12000
1250	BC17:d9=>GC17:d9	1.48E+10	0	17400

1251	CC17:d9=>FC17:d9	5.01E+11	0	17300
1252	CC17:d9=>GC17:d9	8.61E+10	0	12000
1253	CC17:d9=>HC17:d9	1.48E+10	0	17400
1254	DC17:d9=>GC17:d9	5.01E+11	0	17300
1255	DC17:d9=>HC17:d9	8.61E+10	0	12000
1256	EC17:d9=>HC17:d9	5.01E+11	0	17300
1257	FC17:d9=>KC17:d9	1.48E+10	0	17400
1258	GC17:d9=>KC17:d9	8.61E+10	0	12000
1259	GC17:d9=>LC17:d9	1.48E+10	0	17400
1260	HC17:d9=>KC17:d9	5.01E+11	0	17300
1261	HC17:d9=>LC17:d9	8.61E+10	0	12000
1262	HC17:d9=>MC17:d9	1.48E+10	0	17400
1263	KC17:d9=>NC17:d9	5.01E+11	0	17300
1264	KC17:d9=>OC17:d9	8.61E+10	0	12000
1265	KC17:d9=>PC17:d9	1.48E+10	0	17400
1266	LC17:d9=>OC17:d9	5.01E+11	0	17300
1267	LC17:d9=>PC17:d9	8.61E+10	0	12000
1268	LC17:d9=>QC17:d9	2.11E+10	0	19900
1269	MC17:d9=>PC17:d9	5.01E+11	0	17300
1270	MC17:d9=>QC17:d9	1.29E+11	0	14500
1271	NC17:d9=>QC17:d9	7.52E+11	0	19800
1272	EC17:d9=>BC17:d9	5.01E+11	0	17300
1273	FC17:d9=>BC17:d9	8.61E+10	0	12000
1274	GC17:d9=>BC17:d9	1.48E+10	0	17400
1275	FC17:d9=>CC17:d9	5.01E+11	0	17300
1276	GC17:d9=>CC17:d9	8.61E+10	0	12000
1277	HC17:d9=>CC17:d9	1.48E+10	0	17400
1278	DC17:d9=>DC17:d9	5.01E+11	0	17300
1279	HC17:d9=>DC17:d9	8.61E+10	0	12000
1280	HC17:d9=>EC17:d9	5.01E+11	0	17300
1281	KC17:d9=>FC17:d9	1.48E+10	0	17400
1282	KC17:d9=>GC17:d9	8.61E+10	0	12000
1283	LC17:d9=>GC17:d9	1.48E+10	0	17400
1284	KC17:d9=>HC17:d9	5.01E+11	0	17300
1285	LC17:d9=>HC17:d9	8.61E+10	0	12000

1286	MC17:d9=>HC17:d9	1.48E+10	0	17400
1287	NC17:d9=>KC17:d9	5.01E+11	0	17300
1288	OC17:d9=>KC17:d9	8.61E+10	0	12000
1289	PC17:d9=>KC17:d9	1.48E+10	0	17400
1290	OC17:d9=>LC17:d9	5.01E+11	0	17300
1291	PC17:d9=>LC17:d9	8.61E+10	0	12000
1292	QC17:d9=>LC17:d9	1.48E+10	0	17400
1293	PC17:d9=>MC17:d9	5.01E+11	0	17300
1294	QC17:d9=>MC17:d9	8.61E+10	0	12000
1295	QC17:d9=>NC17:d9	5.01E+11	0	17300

RME radicals decomposition reactions considered

		A	b	E
1296	BC17:d9=AC14H276+C3:1	2.51E+11	0	33100
1297	CC17:d9=AC13H255+C4:1	2.51E+11	0	33100
1298	CC17:d9=C16H3018+COOCH3	7.94E+10	0	36000
1299	DC17:d9=AC12H234+C5:1	2.51E+11	0	33100
1300	DC17:d9=C15H2817+BC2:0	2.51E+11	0	33100
1301	EC17:d9=AC11H213+C6:1	3.31E+12	0	29500
1302	EC17:d9=C14H2616+CC3:0	2.51E+11	0	33100
1303	FC17:d9=AC10H192+C7:1	3.31E+12	0	29500
1304	FC17:d9=C13H2415+DC4:0	2.51E+11	0	33100
1305	GC17:d9=AC9H171+C8:1	2.51E+11	0	29500
1306	GC17:d9=C12H2214+EC5:0	2.51E+11	0	29000
1307	HC17:d9=C11H2013+FC6:0	2.51E+11	0	29000
1308	KC17:d9=C12:d911+AC5H11	2.51E+11	0	29000
1309	LC17:d9=C13:d912+PC4H9	2.51E+11	0	33100
1310	LC17:d9=JC10:d9+AC7H14	3.31E+12	0	29500
1311	MC17:d9=C14:d913+NC3H7	2.51E+11	0	33100
1312	MC17:d9=KC11:d9+AC6H12	2.51E+11	0	33100
1313	NC17:d9=C15:d914+C2H5	2.51E+11	0	33100
1314	NC17:d9=LC12:d9+AC5H10	2.51E+11	0	33100
1315	OC17:d9=C16:d915+CH3	7.94E+10	0	36000
1316	OC17:d9=MC13:d9+C4H8	2.51E+11	0	33100
1317	PC17:d9=NC14:d9+C3H6	3.95E+10	0	29300
1318	QC17:d9=OC15:d9+C2H4	2.51E+11	0	31800

Example of Unsaturated Ester radical (C_{16}) reactions considered

		A	b	E
1319	PC16:d9+O2=HO2+C16:d915	1.40E+13	0	39000
1320	PC16:d9+O=OH+C16:d915	1.00E+13	0	4000
1321	PC16:d9+OH=H2O+C16:d915	1.00E+13	0	1230
1322	PC16:d9+HO2=H2O2+C16:d915	1.00E+11	0	17000
1323	PC16:d9+H=H2+C16:d915	1.00E+13	0	3900
1324	PC16:d9+CH3=CH4+C16:d915	2.00E+11	0	7300
1325	PC16:d9+C2H3=C2H4+C16:d915	2.00E+11	0	7300
1326	PC16:d9+C2H5=C2H6+C16:d915	1.26E+15	0	10400
1327	PC16:d9=H+C16:d915	1.15E+15	0	100000
1328	C16:d915=C2H3+NC14:d9	2.51E+11	0	33100
1329	C16:d915=C6H1151+JC10:d9	2.51E+11	0	33100
1330	C16:d915=AC8H1317+HC8:0	2.51E+11	0	33100
1331	PC16:d9=>MC16:d9	5.01E+11	0	17300
1332	PC16:d9=>LC16:d9	8.61E+10	0	12000
1333	PC16:d9=>KC16:d9	1.48E+10	0	17400
1334	MC16:d9=>HC16:d9	1.48E+10	0	17400
1335	LC16:d9=>HC16:d9	8.61E+10	0	12000
1336	LC16:d9=>GC16:d9	1.48E+10	0	17400
1337	KC16:d9=>HC16:d9	5.01E+11	0	17300
1338	KC16:d9=>GC16:d9	8.61E+10	0	12000
1339	KC16:d9=>FC16:d9	1.48E+10	0	17400
1340	HC16:d9=>EC16:d9	5.01E+11	0	17300
1341	HC16:d9=>DC16:d9	8.61E+10	0	18000
1342	HC16:d9=>CC16:d9	1.48E+10	0	17400
1343	GC16:d9=>DC16:d9	5.01E+11	0	17300
1344	GC16:d9=>CC16:d9	8.61E+10	0	12000
1345	GC16:d9=>BC16:d9	1.48E+10	0	17400
1346	FC16:d9=>CC16:d9	5.01E+11	0	17300
1347	FC16:d9=>BC16:d9	8.61E+10	0	12000
1348	EC16:d9=>BC16:d9	5.01E+11	0	17300
1349	MC16:d9=>PC16:d9	7.52E+11	0	19800
1350	LC16:d9=>PC16:d9	1.29E+11	0	14500
1351	KC16:d9=>PC16:d9	2.11E+10	0	19900

1352	HC16:d9=>MC16:d9	1.48E+10	0	17400
1353	HC16:d9=>LC16:d9	8.61E+10	0	12000
1354	GC16:d9=>LC16:d9	1.48E+10	0	17400
1355	HC16:d9=>KC16:d9	5.01E+11	0	17300
1356	GC16:d9=>KC16:d9	8.61E+10	0	12000
1357	FC16:d9=>KC16:d9	1.48E+10	0	17400
1358	EC16:d9=>HC16:d9	5.01E+11	0	17300
1359	DC16:d9=>HC16:d9	8.61E+10	0	18000
1360	CC16:d9=>HC16:d9	1.48E+10	0	17400
1361	DC16:d9=>GC16:d9	5.01E+11	0	17300
1362	CC16:d9=>GC16:d9	8.61E+10	0	12000
1363	BC16:d9=>GC16:d9	1.48E+10	0	17400
1364	CC16:d9=>FC16:d9	5.01E+11	0	17300
1365	BC16:d9=>FC16:d9	8.61E+10	0	12000
1366	BC16:d9=>EC16:d9	5.01E+11	0	17300
1367	BC16:d9=AC13H256+C3:1	2.51E+11	0	33100
1368	CC16:d9=AC12H235+C4:1	2.51E+11	0	33100
1369	CC16:d9=C15H2818+COOCH3	7.94E+10	0	36000
1370	DC16:d9=AC11H214+C5:1	2.51E+11	0	33100
1371	DC16:d9=C14H2617+BC2:0	2.51E+11	0	33100
1372	EC16:d9=AC10H193+C6:1	2.51E+11	0	33100
1373	EC16:d9=C13H2416+CC3:0	2.51E+11	0	33100
1374	FC16:d9=AC9H172+C7:1	3.31E+12	0	29500
1375	FC16:d9=C12H2215+DC4:0	2.51E+11	0	33100
1376	GC16:d9=C8H1511+C8:1	2.51E+11	0	33100
1377	GC16:d9=C11H2014+EC5:0	2.51E+11	0	33100
1378	HC16:d9=C10H1813+FC6:0	2.51E+11	0	29000
1379	KC16:d9=PC4H9+C12:d911	2.51E+11	0	29000
1380	LC16:d9=NC3H7+C13:d912	2.51E+11	0	33100
1381	LC16:d9=AC6H12+JC10:d9	2.51E+11	0	33100
1382	MC16:d9=C2H5+C14:d913	2.51E+11	0	33100
1383	MC16:d9=AC5H10+KC11:d9	2.51E+11	0	33100
1384	PC16:d9=C2H4+NC14:d9	2.51E+11	0	31800

Example of Unsaturated Ester radical (C_8) reactions considered

		A	b	E
1591	C8:1+O=OH+FC8:1	8.80E+10	0.7	3250
1592	C8:1+OH=H2O+FC8:1	3.00E+13	0	1230
1593	C8:1+HO2=H2O2+FC8:1	6.40E+03	2.6	12400
1594	C8:1+H=H2+FC8:1	1.00E+13	0	3900
1595	C8:1+CH3=CH4+FC8:1	2.00E+11	0	7300
1596	C8:1+C2H3=C2H4+FC8:1	2.00E+11	0	7300
1597	C8:1+C2H5=C2H6+FC8:1	1.26E+15	0	10400
1598	C8:1=H+FC8:1	5.40E+06	2.5	-1900
1599	C8:1+O=OH+EC8:1	8.80E+10	0.7	3250
1600	C8:1+OH=H2O+EC8:1	3.00E+13	0	1230
1601	C8:1+HO2=H2O2+EC8:1	6.40E+03	2.6	12400
1602	C8:1+H=H2+EC8:1	1.00E+13	0	3900
1606	C8:1=H+EC8:1	5.40E+06	2.5	-1900
1607	C8:1+O=OH+DC8:1	8.80E+10	0.7	3250
1608	C8:1+OH=H2O+DC8:1	3.00E+13	0	1230
1609	C8:1+HO2=H2O2+DC8:1	6.40E+03	2.6	12400
1610	C8:1+H=H2+DC8:1	1.00E+13	0	3900
1611	C8:1+CH3=CH4+DC8:1	2.00E+11	0	7300
1612	C8:1+C2H3=C2H4+DC8:1	2.00E+11	0	7300
1613	C8:1+C2H5=C2H6+DC8:1	1.26E+15	0	10400
1614	C8:1=H+DC8:1	5.40E+06	2.5	-1900
1615	C8:1+O=OH+CC8:1	8.80E+10	0.7	3250
1616	C8:1+OH=H2O+CC8:1	3.00E+13	0	1230
1617	C8:1+HO2=H2O2+CC8:1	6.40E+03	2.6	12400
1618	C8:1+H=H2+CC8:1	1.00E+13	0	3900
1619	C8:1+CH3=CH4+CC8:1	2.00E+11	0	7300
1620	C8:1+C2H3=C2H4+CC8:1	2.00E+11	0	7300
1621	C8:1+C2H5=C2H6+CC8:1	1.26E+15	0	10400
1622	C8:1=H+CC8:1	5.40E+06	2.5	-1900
1623	C8:1+O=OH+BC8:1	8.80E+10	0.7	3250
1624	C8:1+OH=H2O+BC8:1	3.00E+13	0	1230
1625	C8:1+HO2=H2O2+BC8:1	6.40E+03	2.6	12400
1626	C8:1+H=H2+BC8:1	1.00E+13	0	3900

1627	C8:1+CH3=CH4+BC8:1	2.00E+11	0	7300
1628	C8:1+C2H3=C2H4+BC8:1	2.00E+11	0	7300
1629	C8:1+C2H5=C2H6+BC8:1	1.26E+15	0	10400
1630	C8:1=H+BC8:1	5.40E+06	2.5	-1900
1631	FC8:1=C4H6+DC4:0	2.51E+10	0	33100
1632	EC8:1=C2H3+C6:1	2.50E+10	0	33100
1633	EC8:1=C5H814+CC3:0	2.50E+10	0	33100
1634	DC8:1=AC3H5+C5:1	2.50E+10	0	33100
1635	DC8:1=C6H10+BC2:0	2.50E+10	0	33100
1636	CC8:1=C4H73+C4:1	2.50E+10	0	33100
1637	CC8:1=C7H1216+COOCH3	3.97E+10	0	36000
1638	BC8:1=C5H941+C3:1	2.50E+10	0	33100

Example of Saturated Ester radical (C_8) reactions considered

		A	b	E
1726	HC8:0+O2=HO2+C8:1	1.00E+13	0	5030
1727	HC8:0+O=OH+C8:1	5.00E+12	0	1790
1728	HC8:0+OH=H2O+C8:1	2.69E+10	0.8	-340
1729	HC8:0+HO2=H2O2+C8:1	1.00E+11	0	17000
1730	HC8:0+H=H2+C8:1	1.00E+13	0	3900
1731	HC8:0+CH3=CH4+C8:1	2.00E+11	0	7300
1732	HC8:0+C2H3=C2H4+C8:1	2.00E+11	0	7300
1733	HC8:0+C2H5=C2H6+C8:1	1.26E+15	0	10400
1734	HC8:0=H+C8:1	3.00E+13	0	36000
1735	HC8:0=>EC8:0	5.01E+11	0	17300
1736	HC8:0=>DC8:0	8.61E+10	0	18000
1737	HC8:0=>CC8:0	1.48E+10	0	17400
1738	EC8:0=>BC8:0	5.01E+11	0	17300
1739	EC8:0=>HC8:0	7.52E+11	0	19800
1740	DC8:0=>HC8:0	1.29E+11	0	14500
1741	CC8:0=>HC8:0	2.11E+10	0	19900
1742	BC8:0=>EC8:0	5.01E+11	0	17300
1743	HC8:0=C2H4+FC6:0	2.50E+10	0	31800
1744	EC8:0=C2H5+C6:1	2.50E+10	0	33100
1745	EC8:0=AC5H10+CC3:0	2.50E+10	0	33100
1746	DC8:0=NC3H7+C5:1	2.50E+10	0	33100

1747	DC8:0=AC6H12+BC2:0	2.50E+10	0	33100
1748	CC8:0=PC4H9+C4:1	2.50E+10	0	33100
1749	CC8:0=AC7H14+COOCH3	3.97E+10	0	36000
1750	BC8:0=AC5H11+C3:1	2.50E+10	0	33100

Example of Intermediate Alkenyl radical (C_{16}) reactions considered

		A	b	E
1823	AC16H318+O2=HO2+C16H3018	1.40E+13	0	39000
1824	AC16H318+O=OH+C16H3018	1.00E+13	0	4000
1825	AC16H318+OH=H2O+C16H3018	1.00E+13	0	1230
1826	AC16H318+HO2=H2O2+C16H3018	1.00E+11	0	17000
1827	AC16H318+H=H2+C16H3018	1.00E+13	0	3900
1828	AC16H318+CH3=CH4+C16H3018	2.00E+11	0	7300
1829	AC16H318+C2H3=C2H4+C16H3018	2.00E+11	0	7300
1830	AC16H318+C2H5=C2H6+C16H3018	1.26E+15	0	10400
1831	AC16H318=H+C16H3018	1.15E+15	0	100000
1832	C16H3018=AC7H15+IC9H1518	2.51E+11	0	33100
1833	C16H3018=AC9H171+C7H1317	2.51E+11	0	33100
1834	C16H3018=C2H3+AC14H276	2.51E+11	0	33100
1835	AC16H318=>DC16H318	5.01E+11	0	17300
1836	AC16H318=>EC16H318	8.61E+10	0	18000
1837	AC16H318=>FC16H318	1.48E+10	0	17400
1838	DC16H318=>GC16H318	5.01E+11	0	17300
1839	DC16H318=>AC16H318	7.52E+10	0	19800
1840	EC16H318=>AC16H318	1.29E+11	0	14500
1841	FC16H318=>AC16H318	2.11E+10	0	19900
1842	GC16H318=>DC16H318	5.01E+11	0	17300
1843	AC16H318=C2H4+AC14H276	2.51E+11	0	31800
1844	DC16H318=C2H5+C14H2616	2.51E+11	0	33100
1845	DC16H318=AC5H10+AC11H213	2.51E+11	0	33100
1846	EC16H318=NC3H7+C13H2415	2.51E+11	0	33100
1847	EC16H318=AC6H12+AC10H192	3.31E+12	0	29500
1848	FC16H318=PC4H9+C12H2214	2.51E+11	0	33100
1849	FC16H318=AC9H171+AC7H14	2.51E+11	0	33100
1850	GC16H318=AC5H11+C11H2013	2.51E+11	0	29000

APPENDIX B

Chemical Kinetic Mechanism for oxidation of Oleic Acid (RSO)

Arrhenius Constant : $k = A\ T^{b}\ exp(-E/RT))$

Units : A= mole-cm-sec T = K, E = cal/mole

Important Initiation reactions considered

		A	b	E
1118	C17H33COOH=>C17H34+CO2	7.00E+15	0	74600
1119	C17H34=>AC16H318+CH3	2.51E+16	0	83000
1120	C17H34=>AC15H297+C2H5	2.51E+16	0	79000
1121	C17H34=>AC14H276+NC3H7	2.51E+16	0	79000
1122	C17H34=>AC13H255+PC4H9	2.51E+16	0	79000
1123	C17H34=>AC12H234+AC5H11	2.51E+16	0	79000
1124	C17H34=>AC11H213+AC6H13	2.51E+16	0	79000
1125	C17H34=>AC10H192+AC7H15	2.51E+16	0	76000
1126	C17H34=>AC9H171+AC8H17	2.51E+16	0	85000
1127	C17H34=>AC10H191+AC7H15	2.51E+16	0	85000
1128	C17H34=>AC11H212+AC6H13	2.51E+16	0	76000
1129	C17H34=>AC12H233+AC5H11	2.51E+16	0	79000
1130	C17H34=>AC13H254+PC4H9	2.51E+16	0	79000
1131	C17H34=>AC14H275+NC3H7	2.51E+16	0	79000
1132	C17H34=>AC15H296+C2H5	2.51E+16	0	79000
1133	C17H34=>AC16H317+CH3	2.51E+16	0	83000

Important Heptadecene oxidation reactions considered

		A	b	E
1134	C17H34+O2=HO2+AC17H33	2.50E+13	0	49000
1135	C17H34+O2=HO2+BC17H33	4.00E+13	0	47600
1136	C17H34+O2=HO2+CC17H33	4.00E+13	0	47600
1137	C17H34+O2=HO2+DC17H33	4.00E+13	0	47600
1138	C17H34+O2=HO2+EC17H33	4.00E+13	0	47600
1139	C17H34+O2=HO2+FC17H33	4.00E+13	0	47600
1140	C17H34+O2=HO2+GC17H33	4.00E+13	0	47600
1141	C17H34+O2=HO2+JC17H33	4.00E+13	0	47600
1142	C17H34+O2=HO2+KC17H33	4.00E+13	0	47600
1143	C17H34+O2=HO2+LC17H33	4.00E+13	0	47600
1144	C17H34+O2=HO2+MC17H33	4.00E+13	0	47600

1145	C17H34+O2=HO2+NC17H33	4.00E+13	0	47600
1146	C17H34+O2=HO2+OC17H33	4.00E+13	0	47600
1147	C17H34+O2=HO2+PC17H33	4.00E+13	0	47600
1148	C17H34+O2=HO2+QC17H33	2.50E+13	0	49000

Important Heptadecene Metathesis reactions considered

		A	b	E
1149	C17H34=H+AC17H33	1.00E+15	0	100000
1150	C17H34=H+BC17H33	1.00E+15	0	100000
1151	C17H34=H+CC17H33	1.00E+15	0	100000
1152	C17H34=H+DC17H33	1.00E+15	0	100000
1153	C17H34=H+EC17H33	1.00E+15	0	100000
1154	C17H34=H+FC17H33	1.00E+15	0	100000
1155	C17H34=H+GC17H33	1.00E+15	0	100000
1156	C17H34=H+JC17H33	1.00E+15	0	100000
1157	C17H34=H+KC17H33	1.00E+15	0	100000
1158	C17H34=H+LC17H33	1.00E+15	0	100000
1159	C17H34=H+MC17H33	1.00E+15	0	100000
1160	C17H34=H+NC17H33	1.00E+15	0	100000
1161	C17H34=H+OC17H33	1.00E+15	0	100000
1162	C17H34=H+PC17H33	1.00E+15	0	100000
1163	C17H34=H+QC17H33	1.00E+15	0	100000
1164	C17H34+H=H2+AC17H33	5.60E+07	2	7700
1165	C17H34+H=H2+BC17H33	1.20E+07	2	5000
1166	C17H34+H=H2+CC17H33	1.20E+07	2	5000
1167	C17H34+H=H2+DC17H33	1.20E+07	2	5000
1168	C17H34+H=H2+EC17H33	1.20E+07	2	5000
1169	C17H34+H=H2+FC17H33	1.20E+07	2	5000
1170	C17H34+H=H2+GC17H33	1.20E+07	2	5000
1171	C17H34+H=H2+JC17H33	1.20E+07	2	5000
1172	C17H34+H=H2+KC17H33	1.20E+07	2	5000
1173	C17H34+H=H2+LC17H33	1.20E+07	2	5000
1174	C17H34+H=H2+MC17H33	1.20E+07	2	5000
1175	C17H34+H=H2+NC17H33	1.20E+07	2	5000
1176	C17H34+H=H2+OC17H33	1.20E+07	2	5000
1177	C17H34+H=H2+PC17H33	1.20E+07	2	5000

1178	C17H34+H=H2+QC17H33	1.20E+07	2	5000
1179	C17H34+O=OH+AC17H33	2.77E+02	3.5	3080
1180	C17H34+O=OH+BC17H33	1.28E+03	3.3	1653
1181	C17H34+O=OH+CC17H33	1.28E+03	3.3	1653
1182	C17H34+O=OH+DC17H33	1.28E+03	3.3	1653
1183	C17H34+O=OH+EC17H33	1.28E+03	3.3	1653
1184	C17H34+O=OH+FC17H33	1.28E+03	3.3	1653
1185	C17H34+O=OH+GC17H33	1.28E+03	3.3	1653
1186	C17H34+O=OH+JC17H33	1.28E+03	3.3	1653
1187	C17H34+O=OH+KC17H33	1.28E+03	3.3	1653
1188	C17H34+O=OH+LC17H33	1.28E+03	3.3	1653
1189	C17H34+O=OH+MC17H33	1.28E+03	3.3	1653
1190	C17H34+O=OH+NC17H33	1.28E+03	3.3	1653
1191	C17H34+O=OH+OC17H33	1.28E+03	3.3	1653
1192	C17H34+O=OH+PC17H33	1.28E+03	3.3	1653
1193	C17H34+O=OH+QC17H33	1.28E+03	3.3	1653
1194	C17H34+OH=H2O+AC17H33	1.41E+07	1.8	974
1195	C17H34+OH=H2O+BC17H33	2.00E+06	2	-596
1196	C17H34+OH=H2O+CC17H33	1.13E+06	2	-1391
1197	C17H34+OH=H2O+DC17H33	1.13E+06	2	-1391
1198	C17H34+OH=H2O+EC17H33	1.13E+06	2	-1391
1199	C17H34+OH=H2O+FC17H33	1.13E+06	2	-1391
1200	C17H34+OH=H2O+GC17H33	1.13E+06	2	-1391
1201	C17H34+OH=H2O+JC17H33	1.13E+06	2	-1391
1202	C17H34+OH=H2O+KC17H33	1.13E+06	2	-1391
1203	C17H34+OH=H2O+LC17H33	1.13E+06	2	-1391
1204	C17H34+OH=H2O+MC17H33	1.13E+06	2	-1391
1205	C17H34+OH=H2O+NC17H33	1.13E+06	2	-1391
1206	C17H34+OH=H2O+OC17H33	1.13E+06	2	-1391
1207	C17H34+OH=H2O+PC17H33	1.13E+06	2	-1391
1208	C17H34+OH=H2O+QC17H33	1.41E+07	1.8	974
1209	C17H34+HO2=H2O2+AC17H33	8.00E+12	0	19400
1210	C17H34+HO2=H2O2+BC17H33	4.88E+12	0	18500
1211	C17H34+HO2=H2O2+CC17H33	4.88E+12	0	18500
1212	C17H34+HO2=H2O2+DC17H33	4.88E+12	0	18500

1213	C17H34+HO2=H2O2+EC17H33	4.88E+12	0	18500
1214	C17H34+HO2=H2O2+FC17H33	4.88E+12	0	18500
1215	C17H34+HO2=H2O2+GC17H33	4.88E+12	0	18500
1216	C17H34+HO2=H2O2+JC17H33	4.88E+12	0	18500
1217	C17H34+HO2=H2O2+KC17H33	4.88E+12	0	18500
1218	C17H34+HO2=H2O2+LC17H33	4.88E+12	0	18500
1219	C17H34+HO2=H2O2+MC17H33	4.88E+12	0	18500
1220	C17H34+HO2=H2O2+NC17H33	4.88E+12	0	18500
1221	C17H34+HO2=H2O2+OC17H33	4.88E+12	0	18500
1222	C17H34+HO2=H2O2+PC17H33	4.88E+12	0	18500
1223	C17H34+HO2=H2O2+QC17H33	4.88E+12	0	18500
1224	C17H34+CH3=CH4+AC17H33	1.30E+12	0	11600
1225	C17H34+CH3=CH4+BC17H33	8.00E+11	0	9500
1226	C17H34+CH3=CH4+DC17H33	8.00E+11	0	9500
1227	C17H34+CH3=CH4+EC17H33	8.00E+11	0	9500
1228	C17H34+CH3=CH4+FC17H33	8.00E+11	0	9500
1229	C17H34+CH3=CH4+GC17H33	8.00E+11	0	9500
1230	C17H34+CH3=CH4+JC17H33	8.00E+11	0	9500
1231	C17H34+CH3=CH4+KC17H33	8.00E+11	0	9500
1232	C17H34+CH3=CH4+LC17H33	8.00E+11	0	9500
1233	C17H34+CH3=CH4+MC17H33	8.00E+11	0	9500
1234	C17H34+CH3=CH4+NC17H33	8.00E+11	0	9500
1235	C17H34+CH3=CH4+OC17H33	8.00E+11	0	9500
1236	C17H34+CH3=CH4+PC17H33	8.00E+11	0	9500
1237	C17H34+CH3=CH4+QC17H33	1.30E+12	0	11600
1238	C17H34+C2H5=C2H6+AC17H33	1.00E+12	0	13400
1239	C17H34+C2H5=C2H6+BC17H33	1.00E+12	0	10400
1240	C17H34+C2H5=C2H6+CC17H33	1.00E+12	0	10400
1241	C17H34+C2H5=C2H6+DC17H33	1.00E+12	0	10400
1242	C17H34+C2H5=C2H6+EC17H33	1.00E+12	0	10400
1243	C17H34+C2H5=C2H6+FC17H33	1.00E+12	0	10400
1244	C17H34+C2H5=C2H6+GC17H33	1.00E+12	0	10400
1245	C17H34+C2H5=C2H6+JC17H33	1.00E+12	0	10400
1246	C17H34+C2H5=C2H6+KC17H33	1.00E+12	0	10400
1247	C17H34+C2H5=C2H6+LC17H33	1.00E+12	0	10400

1248	C17H34+C2H5=C2H6+MC17H33	1.00E+12	0	10400
1249	C17H34+C2H5=C2H6+NC17H33	1.00E+12	0	10400
1250	C17H34+C2H5=C2H6+OC17H33	1.00E+12	0	10400
1251	C17H34+C2H5=C2H6+PC17H33	1.00E+12	0	10400
1252	C17H34+C2H5=C2H6+QC17H33	1.00E+12	0	13400
1253	C17H34+C2H3=C2H4+AC17H33	1.00E+12	0	18000
1254	C17H34+C2H3=C2H4+BC17H33	8.00E+11	0	16800
1255	C17H34+C2H3=C2H4+CC17H33	8.00E+11	0	16800
1256	C17H34+C2H3=C2H4+DC17H33	8.00E+11	0	16800
1257	C17H34+C2H3=C2H4+EC17H33	8.00E+11	0	16800
1258	C17H34+C2H3=C2H4+FC17H33	8.00E+11	0	16800
1259	C17H34+C2H3=C2H4+GC17H33	8.00E+11	0	16800
1260	C17H34+C2H3=C2H4+JC17H33	8.00E+11	0	16800
1261	C17H34+C2H3=C2H4+KC17H33	8.00E+11	0	16800
1262	C17H34+C2H3=C2H4+LC17H33	8.00E+11	0	16800
1263	C17H34+C2H3=C2H4+MC17H33	8.00E+11	0	16800
1264	C17H34+C2H3=C2H4+NC17H33	8.00E+11	0	16800
1265	C17H34+C2H3=C2H4+OC17H33	8.00E+11	0	16800
1266	C17H34+C2H3=C2H4+PC17H33	8.00E+11	0	16800
1267	C17H34+C2H3=C2H4+QC17H33	1.00E+12	0	18000

Important Heptadecene radical Isomerization reactions considered

		A	b	E
1268	AC17H33=>DC17H33	5.01E+11	0	17300
1269	AC17H33=>EC17H33	8.61E+10	0	12000
1270	AC17H33=>FC17H33	1.48E+10	0	17400
1271	BC17H33=>EC17H33	5.01E+11	0	17300
1272	BC17H33=>FC17H33	8.61E+10	0	12000
1273	BC17H33=>GC17H33	1.48E+10	0	17400
1274	CC17H33=>FC17H33	5.01E+11	0	17300
1275	CC17H33=>GC17H33	8.61E+10	0	12000
1276	DC17H33=>GC17H33	5.01E+11	0	17300
1277	EC17H33=>JC17H33	1.48E+10	0	17400
1278	FC17H33=>JC17H33	8.61E+10	0	12000
1279	FC17H33=>KC17H33	1.48E+10	0	17400
1280	GC17H33=>JC17H33	5.01E+11	0	17300
1281	GC17H33=>KC17H33	8.61E+10	0	12000

1282	GC17H33=>LC17H33	1.48E+10	0	17400
1283	JC17H33=>MC17H33	5.01E+11	0	17300
1284	JC17H33=>NC17H33	8.61E+10	0	12000
1285	JC17H33=>OC17H33	1.48E+10	0	17400
1286	KC17H33=>NC17H33	5.01E+11	0	17300
1287	KC17H33=>OC17H33	8.61E+10	0	12000
1288	KC17H33=>PC17H33	1.48E+10	0	17400
1289	LC17H33=>OC17H33	5.01E+11	0	17300
1290	LC17H33=>PC17H33	8.61E+10	0	12000
1291	LC17H33=>QC17H33	2.11E+10	0	19900
1292	MC17H33=>PC17H33	5.01E+11	0	17300
1293	MC17H33=>QC17H33	1.29E+11	0	14500
1294	NC17H33=>QC17H33	7.52E+11	0	19800
1295	DC17H33=>AC17H33	7.52E+11	0	19800
1296	EC17H33=>AC17H33	1.29E+11	0	14500
1297	FC17H33=>AC17H33	2.11E+10	0	19900
1298	EC17H33=>BC17H33	5.01E+11	0	17300
1299	FC17H33=>BC17H33	8.61E+10	0	12000
1300	GC17H33=>BC17H33	1.48E+10	0	17400
1301	FC17H33=>CC17H33	5.01E+11	0	17300
1302	GC17H33=>CC17H33	8.61E+10	0	12000
1303	GC17H33=>DC17H33	5.01E+11	0	17300
1304	JC17H33=>EC17H33	1.48E+10	0	17400
1305	JC17H33=>FC17H33	8.61E+10	0	12000
1306	KC17H33=>FC17H33	1.48E+10	0	17400
1307	JC17H33=>GC17H33	5.01E+11	0	17300
1308	KC17H33=>GC17H33	8.61E+10	0	12000
1309	LC17H33=>GC17H33	1.48E+10	0	17400
1310	MC17H33=>JC17H33	5.01E+11	0	17300
1311	NC17H33=>JC17H33	8.61E+10	0	12000
1312	OC17H33=>JC17H33	1.48E+10	0	17400
1313	NC17H33=>KC17H33	5.01E+11	0	17300
1314	OC17H33=>KC17H33	8.61E+10	0	12000
1315	PC17H33=>KC17H33	1.48E+10	0	17400
1316	OC17H33=>LC17H33	5.01E+11	0	17300

1317	PC17H33=>LC17H33	8.61E+10	0	12000
1318	QC17H33=>LC17H33	1.48E+10	0	17400
1319	PC17H33=>MC17H33	5.01E+11	0	17300
1320	QC17H33=>MC17H33	8.61E+10	0	12000
1321	QC17H33=>NC17H33	5.01E+11	0	17300

Important Heptadecene radical decomposition reactions considered

		A	b	E
1322	QC17H33=AC15H297+C2H4	2.51E+13	0	31800
1323	PC17H33=AC14H276+C3H6	3.95E+10	0	29300
1324	OC17H33=AC13H255+C4H8	2.51E+13	0	33100
1325	OC17H33=C16H3018+CH3	3.97E+12	0	36000
1326	NC17H33=AC12H234+AC5H10	2.51E+13	0	33100
1327	NC17H33=C15H2817+C2H5	2.51E+13	0	33100
1328	MC17H33=AC11H213+AC6H12	2.51E+13	0	33100
1329	MC17H33=C14H2616+NC3H7	2.51E+13	0	33100
1330	LC17H33=AC10H192+AC7H14	3.31E+11	0	29500
1331	LC17H33=C13H2415+PC4H9	2.51E+13	0	33100
1332	KC17H33=AC9H171+AC8H16	3.31E+11	0	29500
1333	KC17H33=C12H2214+AC5H11	2.51E+13	0	33100
1334	JC17H33=C11H2013+AC6H13	2.51E+13	0	29000
1335	GC17H33=C12H2213+AC5H11	2.51E+13	0	29000
1336	FC17H33=C13H2414+PC4H9	2.51E+13	0	33100
1337	FC17H33=AC10H191+AC7H14	3.31E+11	0	29500
1338	EC17H33=C14H2615+NC3H7	2.51E+13	0	33100
1339	EC17H33=AC11H212+AC6H12	3.31E+11	0	29500
1340	DC17H33=C15H2816+C2H5	2.51E+13	0	33100
1341	DC17H33=AC12H233+AC5H10	2.51E+13	0	33100
1342	CC17H33=C16H3017+CH3	3.97E+12	0	36000
1343	CC17H33=AC13H254+C4H8	2.51E+13	0	33100
1344	BC17H33=AC14H275+C3H6	3.95E+10	0	29300
1345	AC17H33=AC15H296+C2H4	2.51E+13	0	31800

Example of Intermediate Alkenyl radical (C_{16}) reactions considered

		A	b	E
1346	AC16H318+O2=HO2+C16H3018	1.40E+13	0	39000
1347	AC16H318+O=OH+C16H3018	1.00E+13	0	4000
1348	AC16H318+OH=H2O+C16H3018	1.00E+13	0	1230

1349	AC16H318+HO2=H2O2+C16H3018	1.00E+11	0	17000
1350	AC16H318+H=H2+C16H3018	1.00E+13	0	3900
1351	AC16H318+CH3=CH4+C16H3018	2.00E+11	0	7300
1352	AC16H318+C2H3=C2H4+C16H3018	2.00E+11	0	7300
1353	AC16H318+C2H5=C2H6+C16H3018	1.26E+15	0	10400
1354	AC16H318=H+C16H3018	1.15E+15	0	100000
1355	C16H3018=AC7H15+IC9H1518	2.51E+13	0	33100
1356	C16H3018=AC9H171+C7H1317	2.51E+13	0	33100
1357	C16H3018=C2H3+AC14H276	2.51E+13	0	33100
1358	AC16H318=>DC16H318	5.01E+11	0	17300
1359	AC16H318=>EC16H318	8.61E+10	0	18000
1360	AC16H318=>FC16H318	1.48E+10	0	17400
1361	DC16H318=>GC16H318	5.01E+11	0	17300
1362	DC16H318=>AC16H318	7.52E+10	0	19800
1363	EC16H318=>AC16H318	1.29E+11	0	14500
1364	FC16H318=>AC16H318	2.11E+10	0	19900
1365	GC16H318=>DC16H318	5.01E+11	0	17300
1366	AC16H318=C2H4+AC14H276	2.51E+13	0	31800
1367	DC16H318=C2H5+C14H2616	2.51E+13	0	33100
1368	DC16H318=AC5H10+AC11H213	2.51E+13	0	33100
1369	EC16H318=NC3H7+C13H2415	2.51E+13	0	33100
1370	EC16H318=AC6H12+AC10H192	3.31E+11	0	29500
1371	FC16H318=PC4H9+C12H2214	2.51E+13	0	33100
1372	FC16H318=AC9H171+AC7H14	2.51E+13	0	33100
1373	GC16H318=AC5H11+C11H2013	2.51E+13	0	29000
1374	AC16H317+O2=HO2+C16H3017	1.40E+13	0	39000
1375	AC16H317+O=OH+C16H3017	1.00E+13	0	4000
1376	AC16H317+OH=H2O+C16H3017	1.00E+13	0	1230
1377	AC16H317+HO2=H2O2+C16H3017	1.00E+11	0	17000
1378	AC16H317+H=H2+C16H3017	1.00E+13	0	3900
1379	AC16H317+CH3=CH4+C16H3017	2.00E+11	0	7300
1380	AC16H317+C2H3=C2H4+C16H3017	2.00E+11	0	7300
1381	AC16H317+C2H5=C2H6+C16H3017	1.26E+12	0	10400
1382	AC16H317=H+C16H3017	1.15E+15	0	100000
1383	C16H3017=AC8H17+HC8H1317	2.51E+11	0	33100

1384	C16H3017=AC10H191+C6H1116	2.51E+11	0	33100
1385	C16H3017=C2H3+AC14H275	2.51E+11	0	33100
1386	AC16H317=>DC16H317	5.01E+11	0	17300
1387	AC16H317=>EC16H317	8.61E+10	0	12000
1388	AC16H317=>FC16H317	1.48E+10	0	23400
1389	DC16H317=>IC16H317	1.48E+10	0	17400
1390	EC16H317=>IC16H317	8.61E+10	0	12000
1391	EC16H317=>JC16H317	1.48E+10	0	17400
1392	FC16H317=>IC16H317	5.01E+11	0	17300
1393	FC16H317=>JC16H317	8.61E+10	0	12000
1394	FC16H317=>KC16H317	1.48E+10	0	17400
1395	IC16H317=>LC16H317	5.01E+11	0	17300
1396	IC16H317=>MC16H317	8.61E+10	0	12000
1397	IC16H317=>NC16H317	1.48E+10	0	23400
1398	JC16H317=>MC16H317	5.01E+11	0	17300
1399	JC16H317=>NC16H317	8.61E+10	0	12000
1400	JC16H317=>OC16H317	1.48E+10	0	17400
1401	KC16H317=>NC16H317	5.01E+11	0	17300
1402	KC16H317=>OC16H317	8.61E+10	0	12000
1403	KC16H317=>PC16H317	2.11E+11	0	19900
1404	LC16H317=>OC16H317	5.01E+11	0	14500
1405	MC16H317=>PC16H317	7.52E+10	0	19800
1406	DC16H317=>AC16H317	7.52E+10	0	19800
1407	EC16H317=>AC16H317	1.29E+11	0	14500
1408	FC16H317=>AC16H317	2.11E+11	0	19900
1409	IC16H317=>DC16H317	1.48E+10	0	17400
1410	IC16H317=>EC16H317	8.61E+10	0	12000
1411	JC16H317=>EC16H317	1.48E+10	0	17400
1412	IC16H317=>FC16H317	5.01E+11	0	17300
1413	JC16H317=>FC16H317	8.61E+10	0	12000
1414	KC16H317=>FC16H317	1.48E+10	0	17400
1415	LC16H317=>IC16H317	5.01E+11	0	17300
1416	MC16H317=>IC16H317	8.61E+10	0	12000
1417	NC16H317=>IC16H317	1.48E+10	0	23400
1418	MC16H317=>JC16H317	5.01E+11	0	17300

1419	NC16H317=>JC16H317	8.61E+10	0	12000
1420	OC16H317=>JC16H317	1.48E+10	0	17400
1421	NC16H317=>KC16H317	5.01E+11	0	17300
1422	OC16H317=>KC16H317	8.61E+10	0	12000
1423	PC16H317=>KC16H317	1.48E+10	0	17400
1424	OC16H317=>LC16H317	5.01E+11	0	14500
1425	PC16H317=>MC16H317	5.01E+11	0	14500
1426	AC16H317=C2H4+AC14H275	2.51E+11	0	31800
1427	BC16H317=C3H6+AC13H254	3.95E+10	0	29300
1428	CC16H317=C4H8+AC12H233	2.51E+11	0	33100
1429	CC16H317=CH3+C15H2816	3.97E+12	0	36000
1430	DC16H317=AC5H10+AC11H212	3.31E+11	0	29500
1431	DC16H317=C2H5+C14H2615	2.51E+11	0	33100
1432	EC16H317=AC6H12+AC10H191	3.31E+11	0	29500
1433	EC16H317=NC3H7+C13H2414	2.51E+11	0	33100
1434	FC16H317=PC4H9+C12H2213	2.51E+11	0	29000
1435	IC16H317=AC6H13+C10H1813	2.51E+11	0	29000
1436	JC16H317=AC5H11+C11H2014	2.51E+11	0	33100
1437	JC16H317=AC8H16+C8H1511	2.51E+11	0	33100
1438	KC16H317=PC4H9+C12H2215	2.51E+11	0	33100
1439	KC16H317=AC9H172+AC7H14	2.51E+11	0	33100
1440	LC16H317=NC3H7+C13H2416	2.51E+11	0	33100
1441	LC16H317=AC10H193+AC6H12	2.51E+11	0	33100
1442	MC16H317=C2H5+C14H2617	2.51E+11	0	33100
1443	MC16H317=AC11H214+AC5H10	3.31E+11	0	29500
1444	NC16H317=AC12H235+C4H8	2.51E+11	0	33100
1445	OC16H317=AC13H256+C3H6	3.95E+10	0	29300
1446	PC16H317=AC14H277+C2H4	2.51E+11	0	31800

APPENDIX C- NOMENCLATURE

C17:d9 RME $C_{18}H_{34}O_2$	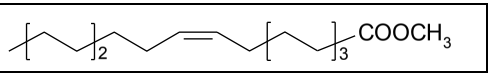
BC17:d9 $C_{18}H_{33}O_2$	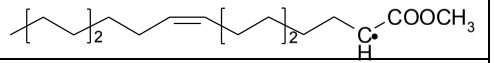
CC17:d9	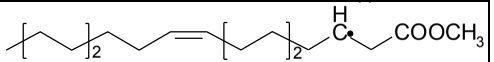
DC17:d9	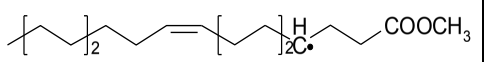
EC17:d9	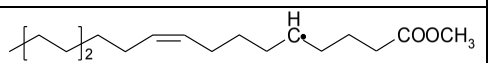
FC17:d9	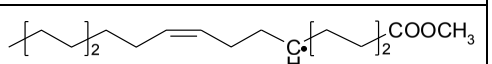
GC17:d9	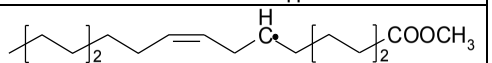
HC17:d9	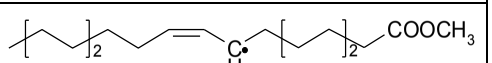
KC17:d9	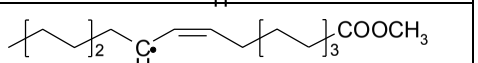
LC17:d9	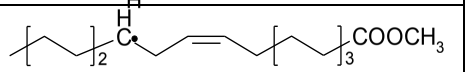
MC17:d9	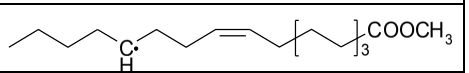
NC17:d9	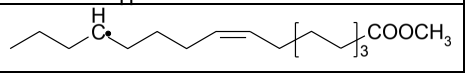
OC17:d9	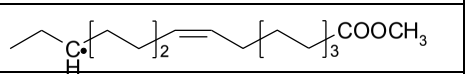
PC17:d9	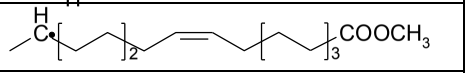
QC17:d9	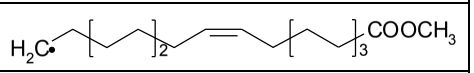
C17:d916 $C1_8H_{32}O_2$	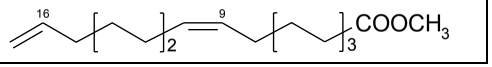

C17:d915	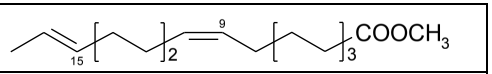
C17:d914	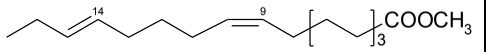
C17:d913	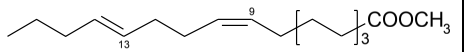
C17:d912	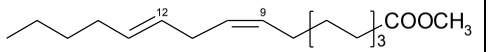
C17:d911	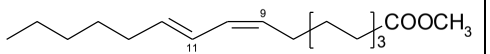
C17:d69	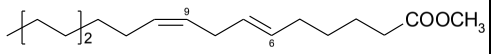
C17:d59	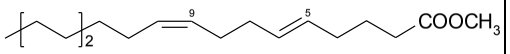
C17:d49	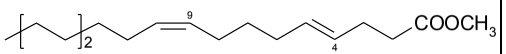
C17:d39	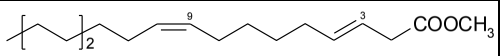
C17:d29	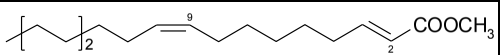

All C16 Species

C16:d9 $C_{17}H_{32}O_2$	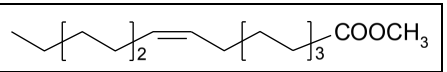
BC16:d9 $C_{17}H_{31}O_2$	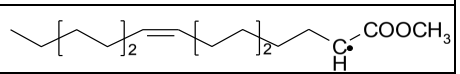
CC16:d9	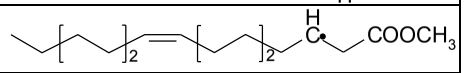
DC16:d9	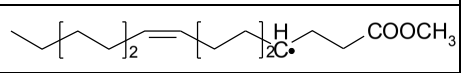
EC16:d9	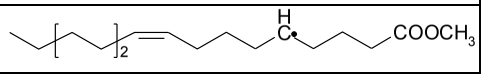

FC16:d9	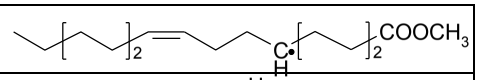
GC16:d9	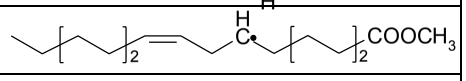
HC16:d9	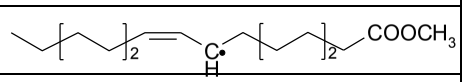
KC16:d9	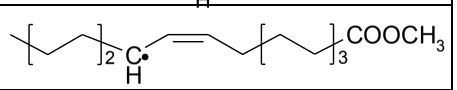
LC16:d9	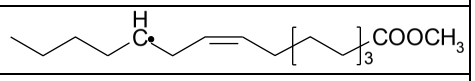
MC16:d9	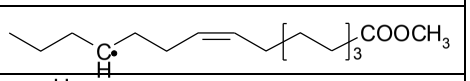
NC16:d9	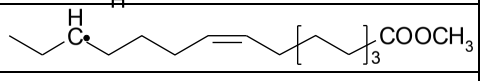
OC16:d9	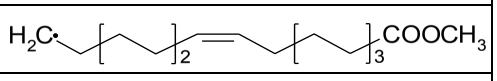
PC16:d9	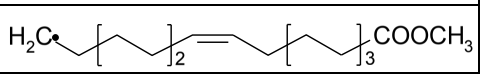

C16:d915 $C_{17}H_{30}O_2$	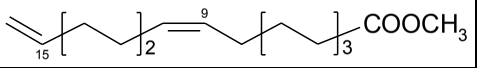
C16:d911	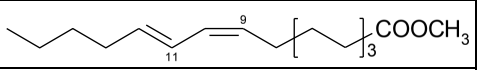
C16:d79	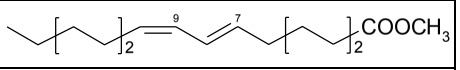
C16:d29	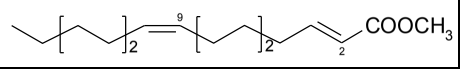

AC16H318	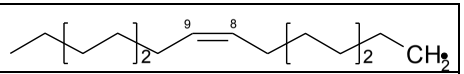
BC16H318	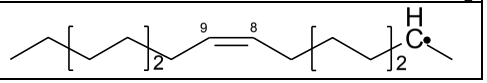

CC16H318	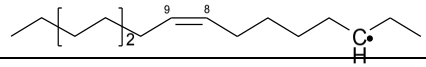
DC16H318	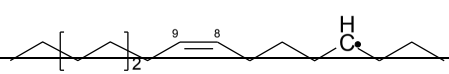
EC16H318	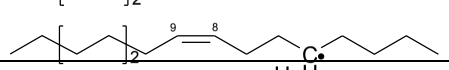
FC16H318	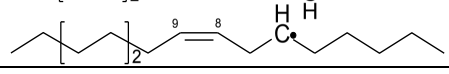
GC16H318	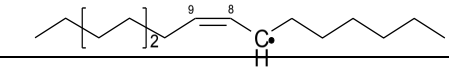
PC16H318	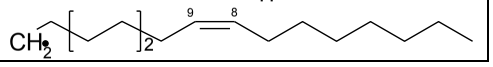

C16H3018	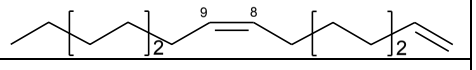
AC16H2918	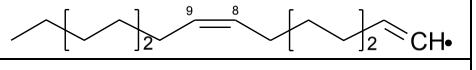
AC16H31COO	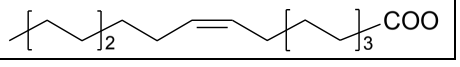

All C15 species

C15:d9 $C_{16}H_{30}O_2$	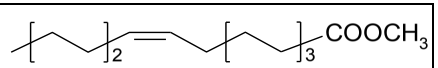
BC15:d9 $C_{16}H_{29}O_2$	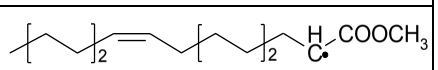
CC15:d9	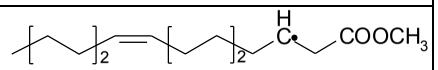
DC15:d9	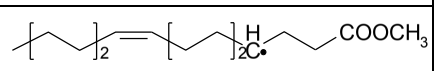
EC15:d9	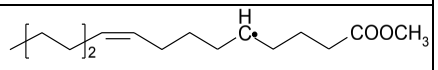
FC15:d9	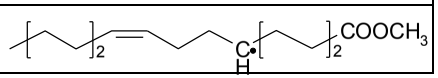

GC15:d9	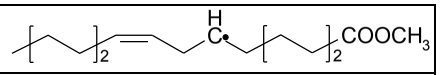
HC15:d9	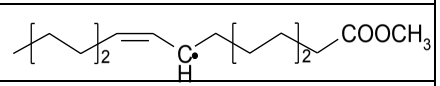
KC15:d9	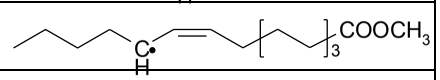
LC15:d9	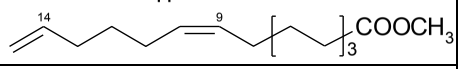
OC15:d9	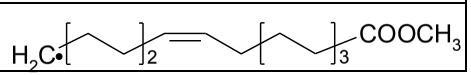

C15:d914 $C_{16}H_{28}O_2$	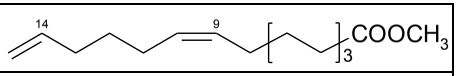
C15:d911	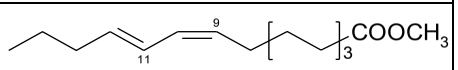
C15:d79	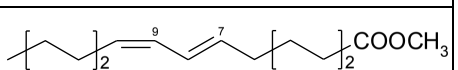
C15:d29	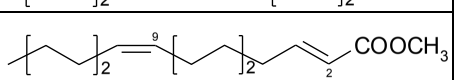
AC15H297	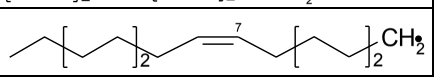
BC15H297	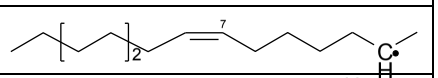
CC15H297	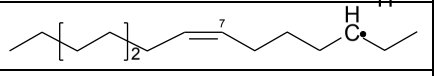
DC15H297	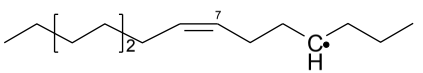
EC15H297	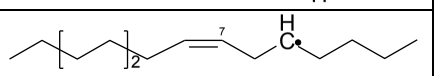
FC15H297	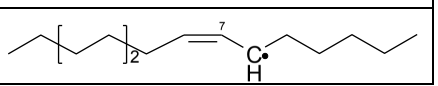

IC15H297	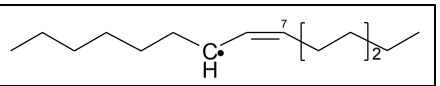
JC15H297	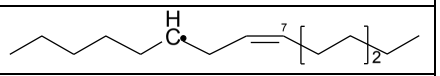
KC15H297	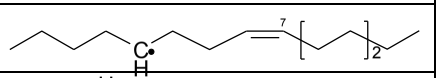
LC15H297	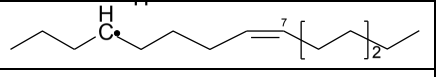
MC15H297	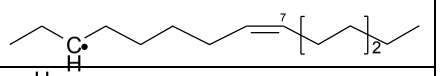
NC15H297	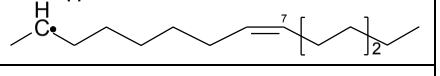
OC15H297	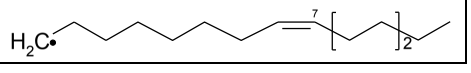

C15H2816	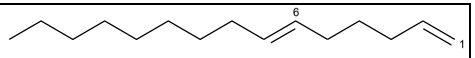
C15H2817	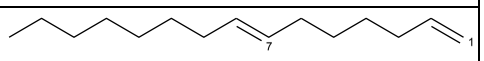
C15H2818	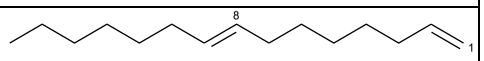
C15H2819	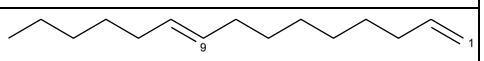

All C14 species

C14:d9 $C_{15}H_{28}O_2$	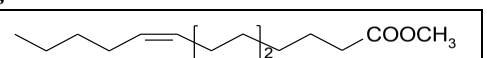
BC14:d9 $C_{15}H_{27}O_2$	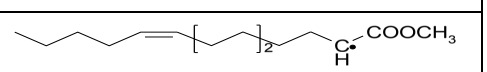

CC14:d9	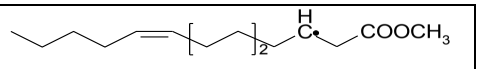
DC14:d9	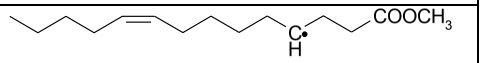
EC14:d9	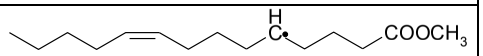
FC14:d9	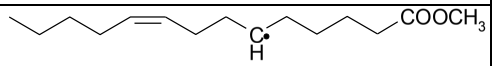
GC14:d9	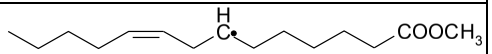
HC14:d9	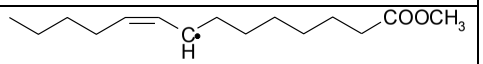
KC14:d9	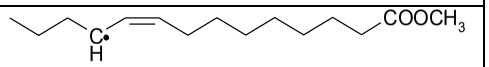
NC14:d9	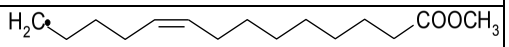

C14:d913 $C_{15}H_{26}O_2$	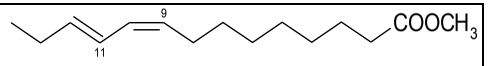
C14:d911	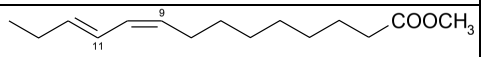
C14:d79	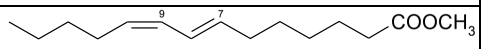
C14:d29	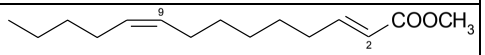

AC14H276	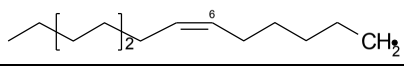

DC14H276	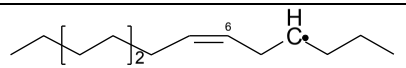
EC14H276	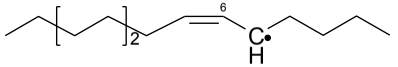
HC14H276	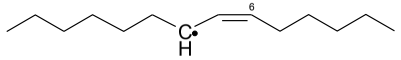
IC14H276	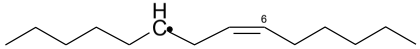
JC14H276	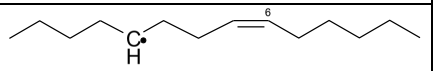
KC14H276	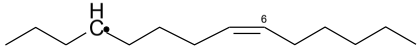
LC14H276	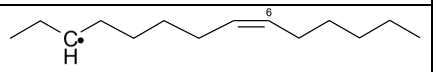
MC14H276	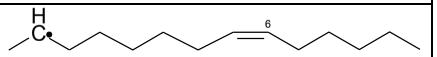
NC14H276	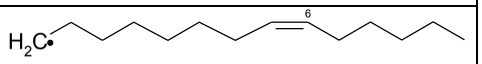

C14H2614	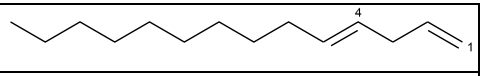
C14H2615	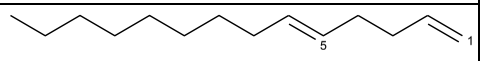
C14H2616	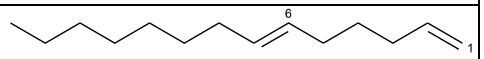
C14H2617	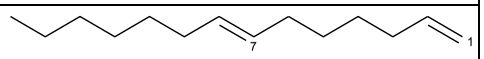
C14H2618	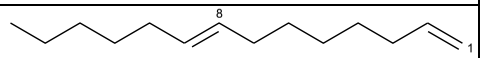
C14H2619	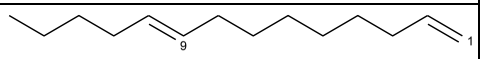

All C13 species

C13:d9 $C_{14}H_{26}O_2$	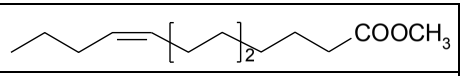
BC13:d9 $C_{14}H_{25}O_2$	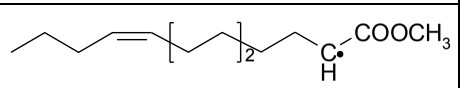
CC13:d9	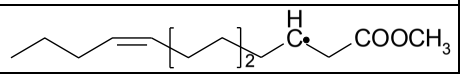
DC13:d9	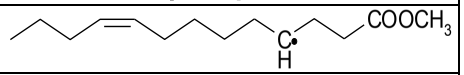
EC13:d9	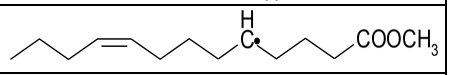
FC13:d9	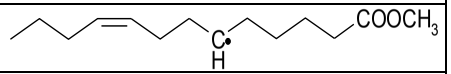
GC13:d9	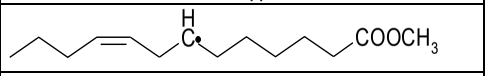
HC13:d9	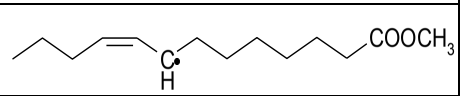
MC13:d9	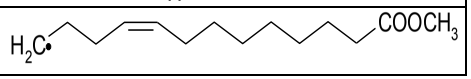

C13:d912 $C_{14}H_{24}O_2$	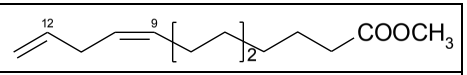
C13:d29 $C_{14}H_{24}O_2$	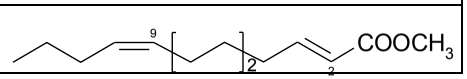

AC13H256	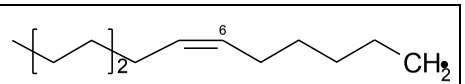
BC13H256	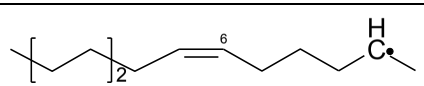

DC13H256	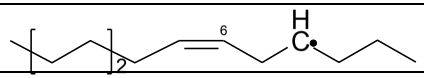
EC13H256	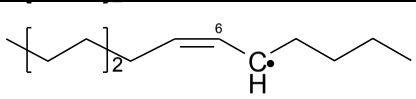
HC13H256	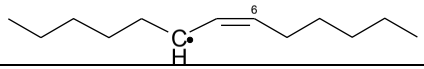
IC13H256	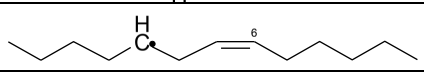
JC13H256	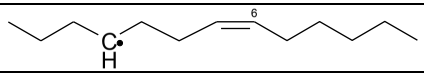
KC13H256	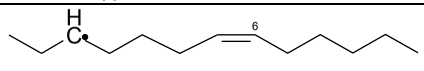
LC13H256	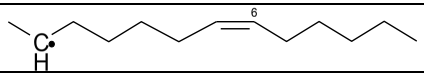
MC13H256	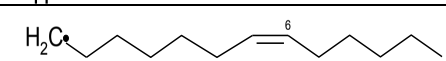

AC13H255	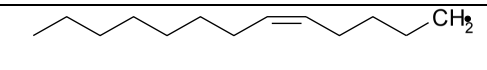
DC13H255	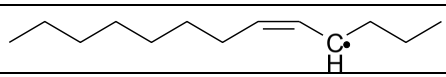
GC13H255	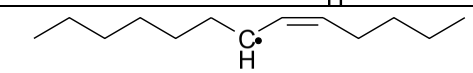
HC13H255	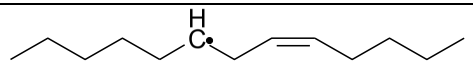
IC13H255	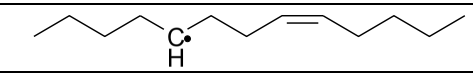
JC13H255	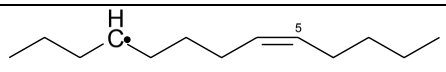
KC13H255	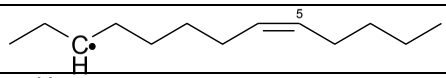
LC13H255	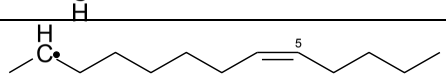

MC13H255	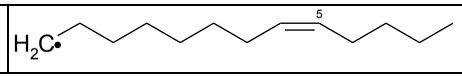

C13H2413	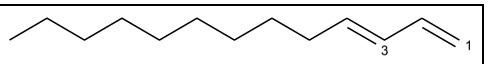
C13H2414	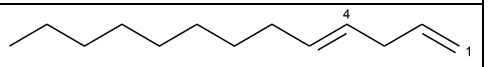
C13H2415	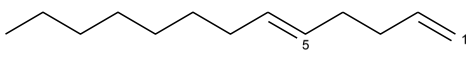
C13H2416	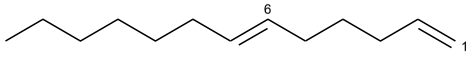
C13H2417	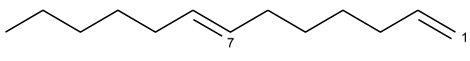
C13H2418	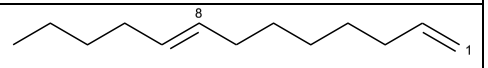
C13H2419	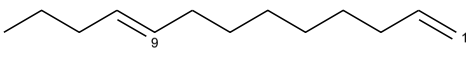

All C12 species

C12:d9 $C_{13}H_{24}O_2$	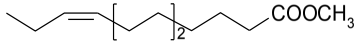
BC12:d9 $C_{13}H_{23}O_2$	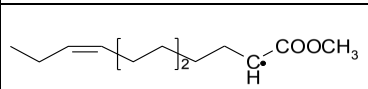
CC12:d9	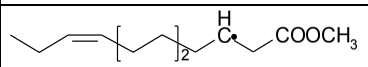
DC12:d9	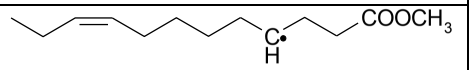
EC12:d9	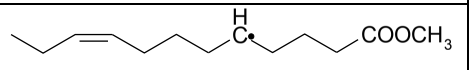
FC12:d9	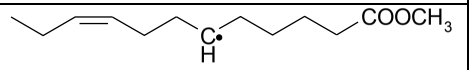
GC12:d9	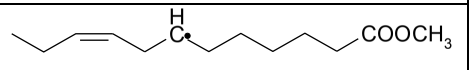

LC12:d9	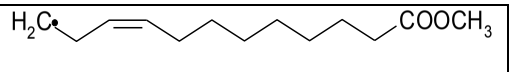

C12:d911 $C_{13}H_{22}O_2$	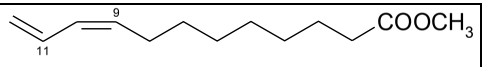
C12:d79 $C_{13}H_{22}O_2$	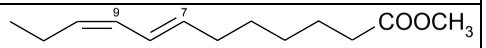
C12:d29 $C_{13}H_{22}O_2$	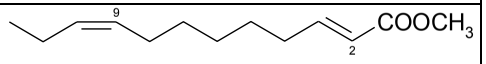

AC12H236	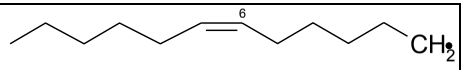
DC12H236	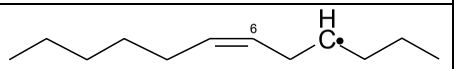
EC12H236	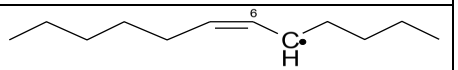
HC12H236	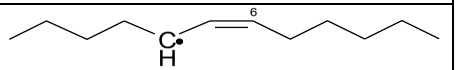
IC12H236	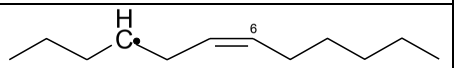
JC12H236	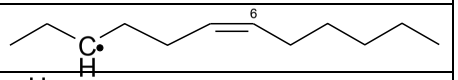
KC12H236	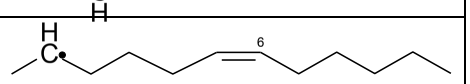
LC12H236	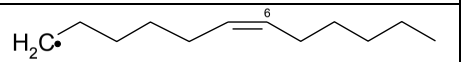

AC12H235	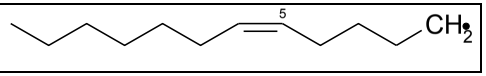

BC12H235	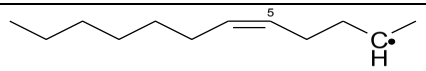
DC12H235	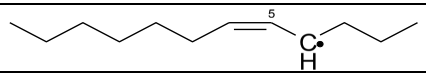
GC12H235	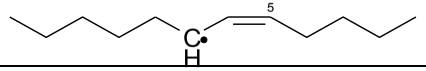
HC12H235	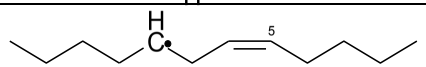
IC12H235	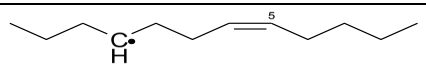
JC12H235	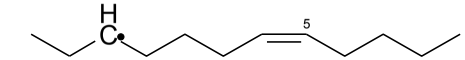
KC12H235	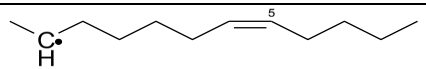
LC12H235	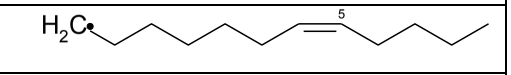
AC12H234	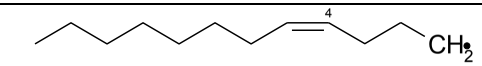
FC12H234	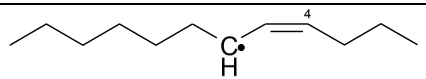
IC12H234	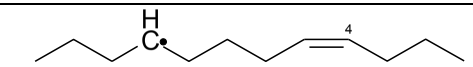
JC12H234	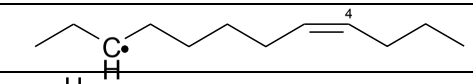
KC12H234	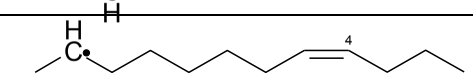
LC12H234	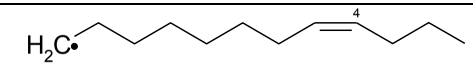

C12H2213	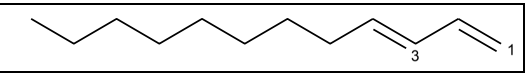

C12H2214	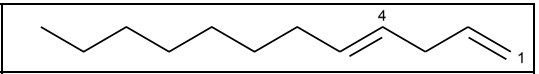
C12H2215	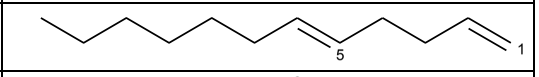
C12H2216	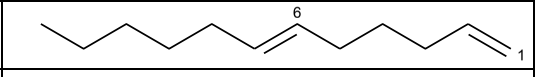
C12H2217	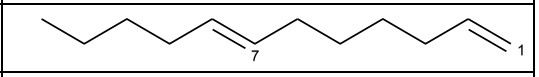
C12H2218	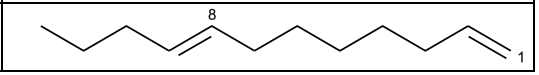

All C11 species

C11:d9 $C_{12}H_{22}O_2$	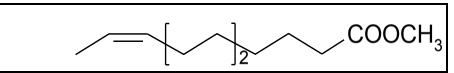
BC11:d9 $C_{12}H_{21}O_2$	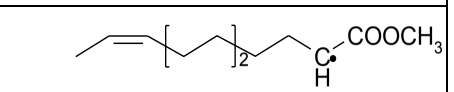
CC11:d9	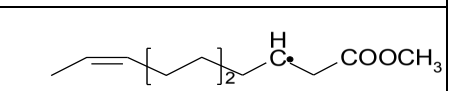
DC11:d9	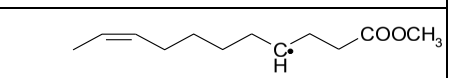
FC11:d9	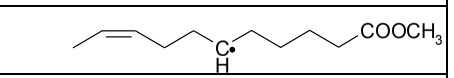
GC11:d9	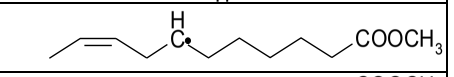
KC11:d9	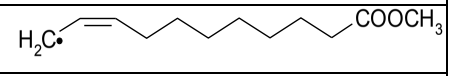
C11:d29 $C_{12}H_{20}O_2$	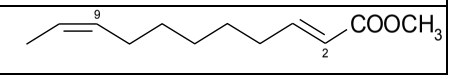

AC11H216	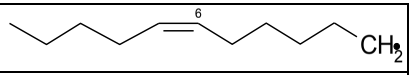
BC11H216	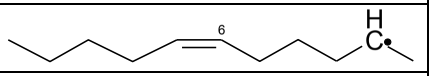
CC11H216	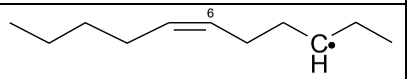
DC11H216	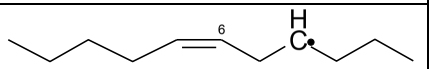
EC11H216	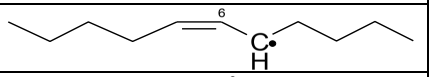
HC11H216	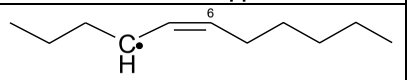
KC11H216	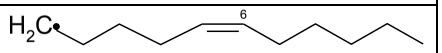
AC11H215	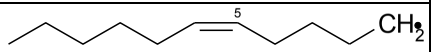
DC11H215	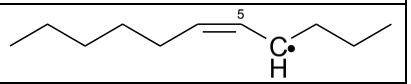
GC11H215	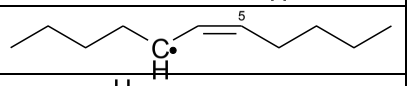
HC11H215	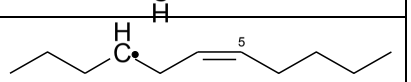
IC11H215	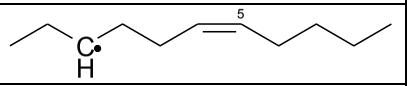
JC11H215	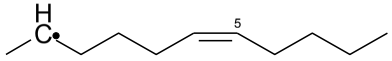
KC11H215	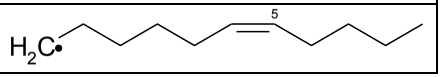

AC11H214	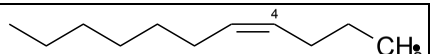

FC11H214	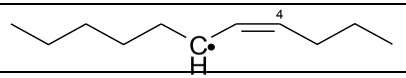
GC11H214	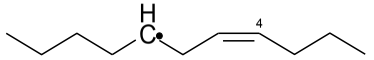
HC11H214	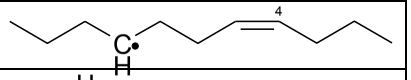
IC11H214	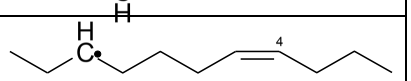
JC11H214	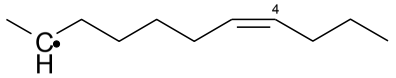
KC11H214	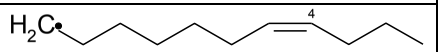

AC11H213	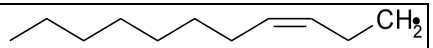
EC11H213	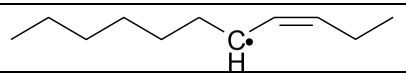
FC11H213	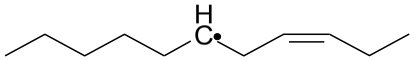
GC11H213	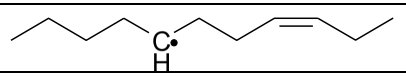
HC11H213	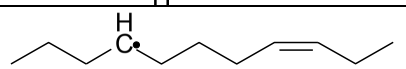
IC11H213	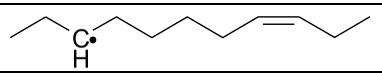
JC11H213	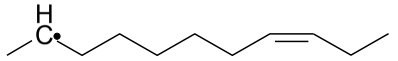
KC11H213	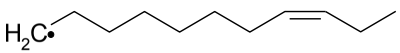

C11H2013	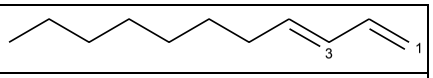
C11H2014	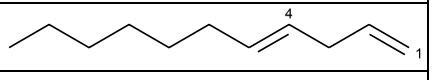
C11H2015	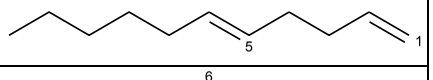
C11H2016	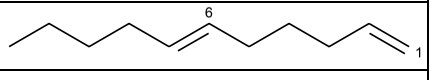
C11H2017	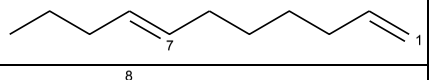
C11H2018	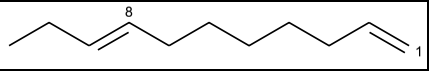

All C10 species

C10:d9 $C_{11}H_{20}O_2$	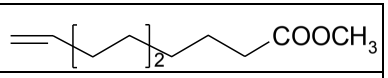
BC10:d9 $C_{11}H_{19}O_2$	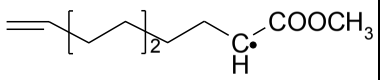
CC10:d9	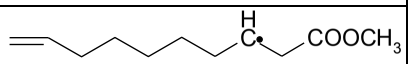
DC10:d9	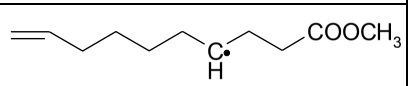
EC10:d9	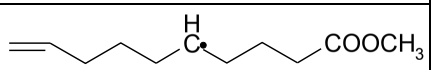
FC10:d9	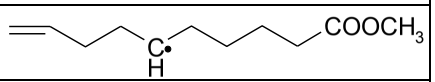
GC10:d9	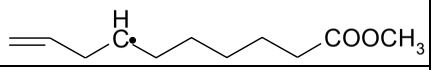
JC10:d9	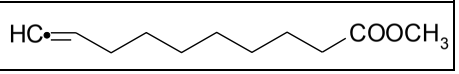

C10:d79 $C_{11}H_{18}O_2$	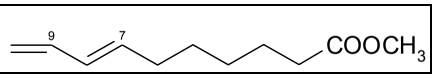
C10:d29 $C_{11}H_{18}O_2$	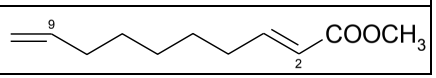

AC10H196	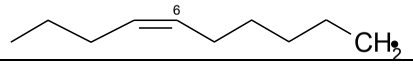
BC10H196	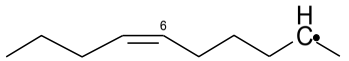
EC10H196	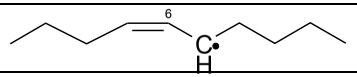
JC10H196	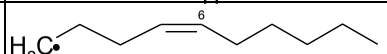

AC10H195	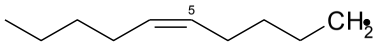
BC10H195	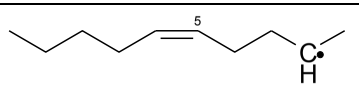
CC10H195	
DC10H195	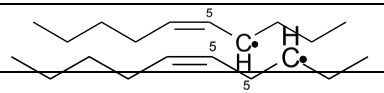
GC10H195	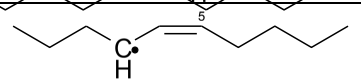
JC10H195	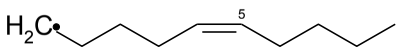

AC10H194	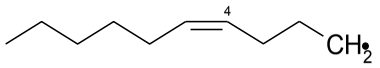
FC10H194	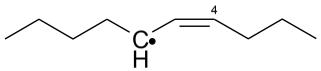
IC10H194	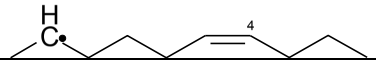
JC10H194	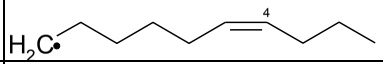
C10H1813	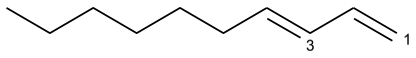
C10H1814	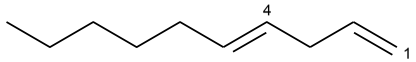
C10H1815	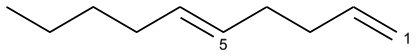
C10H1816	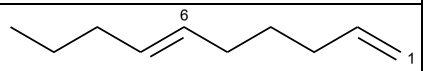
C10H1817	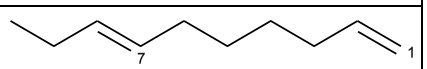
C10H1818	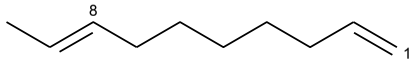
C10H1819	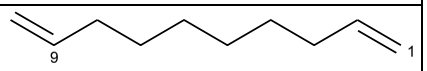

AC10H193	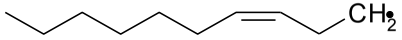
EC10H193	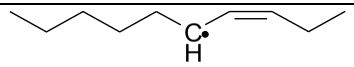
FC10H193	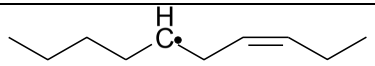

GC10H193	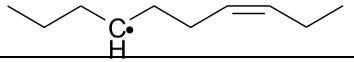
HC10H193	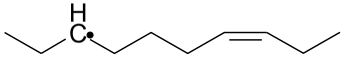
IC10H193	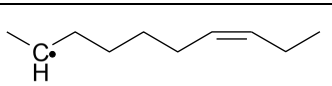
JC10H193	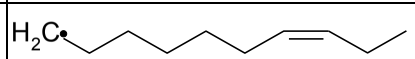

AC10H192	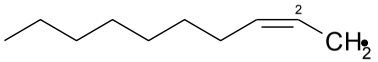
DC10H192	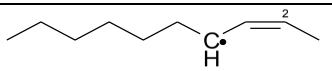
EC10H192	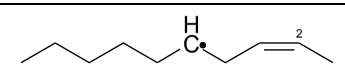
FC10H192	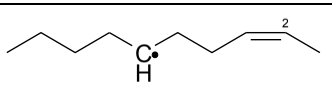
GC10H192	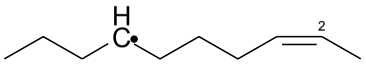
HC10H192	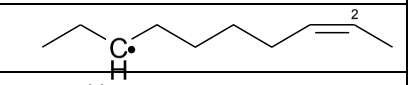
IC10H192	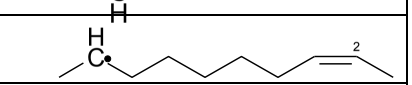
JC10H192	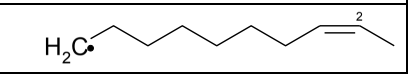

All C9 species

C9:d8 $C_{10}H_{18}O_2$	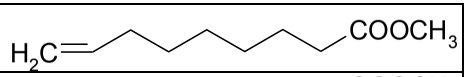
BC9:d8 $C_{10}H_{17}O_2$	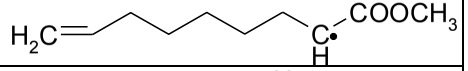
CC9:d8	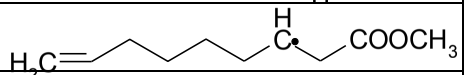
DC9:d8	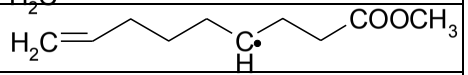
EC9:d8	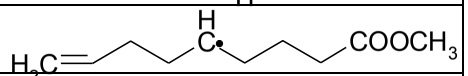
FC9:d8	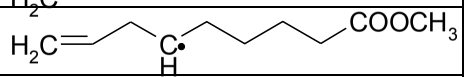
IC9:d8	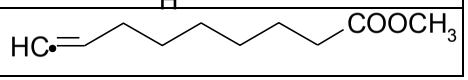

IC9H176	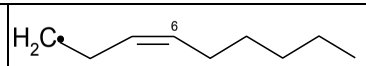
IC9H175	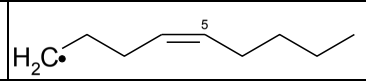

AC9H174	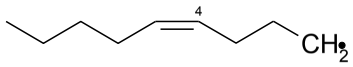
FC9H174	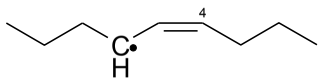

IC9H174	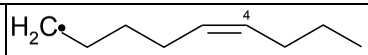

AC9H173	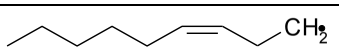
EC9H173	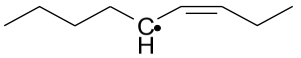
FC9H173	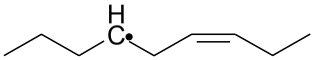
HC9H173	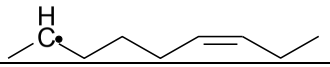
IC9H173	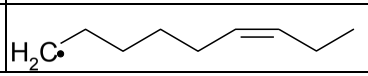

AC9H172	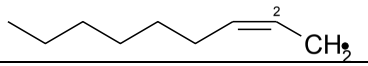
DC9H172	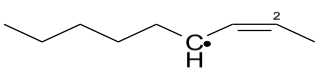
EC9H172	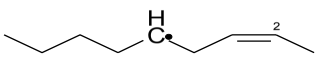
FC9H172	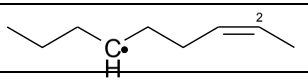
GC9H172	
HC9H172	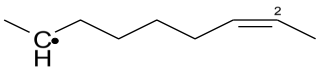
IC9H172	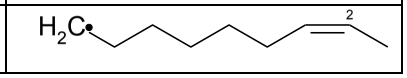

AC9H171	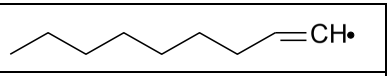
DC9H171	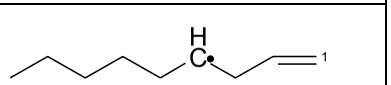
EC9H171	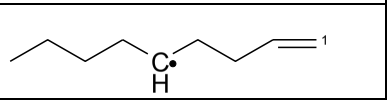
FC9H171	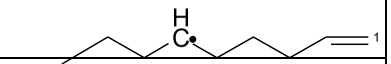
GC9H171	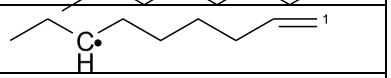
HC9H171	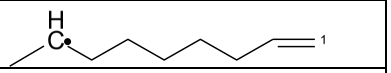
IC9H171	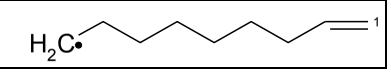

C9H1613	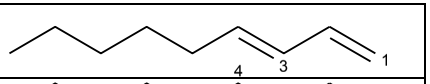
C9H1614	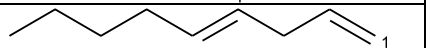
C9H1615	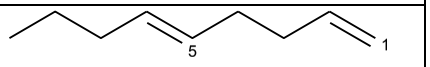
C9H1616	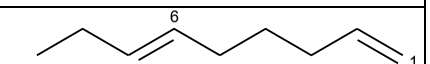
C9H1617	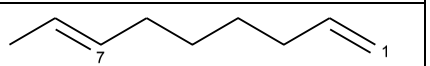
C9H1618	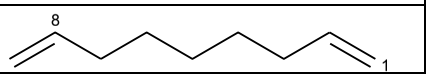

All C8 to C2 species

C8H1413	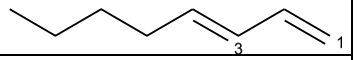
C8H1414	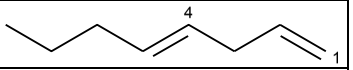
C8H1415	
C8H1416	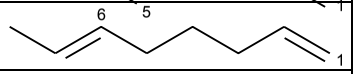
C8H1417	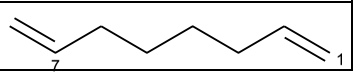

C7H1214	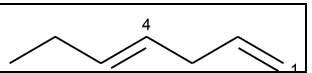
C7H1215	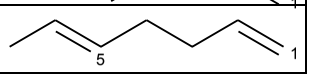

C6H1013	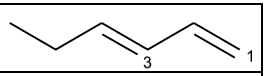
C6H1014	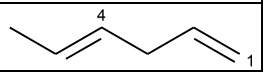
C6H1015	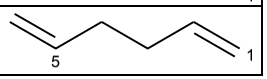

C5H814	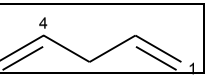

C8:1 $C_9H_{16}O_2$	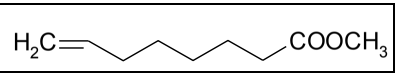

C7:1 $C_8H_{14}O_2$	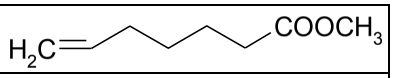
C6:1 $C_7H_{12}O_2$	
C5:1 $C_6H_{10}O_2$	
C4:1 $C_5H_8O_2$	
C3:1 $C_4H_6O_2$	
CC3:1 $C_4H_5O_2$	

Saturated Esters

C9:0 $C_{10}H_{20}O_2$	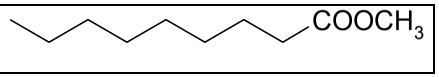

C8:0 $C_9H_{18}O_2$	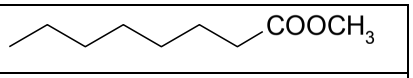
BC8:0 $C_9H_{17}O_2$	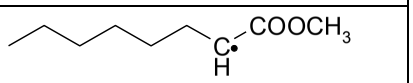
CC8:0	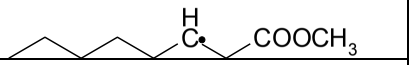
DC8:0	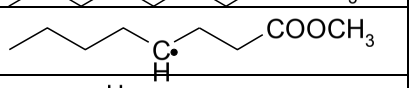
EC8:0	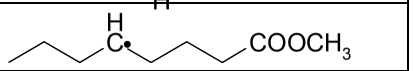
HC8:0	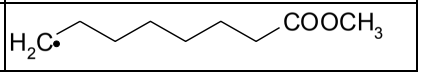

C7:0 $C_8H_{16}O_2$	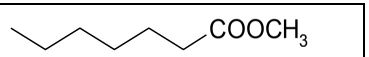
BC7:0 $C_8H_{15}O_2$	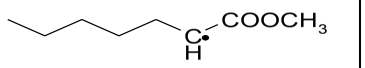
CC7:0	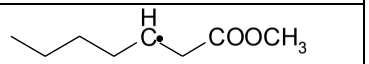
DC7:0	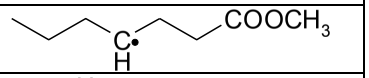
EC7:0	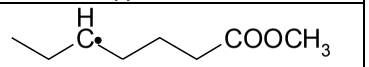
FC7:0	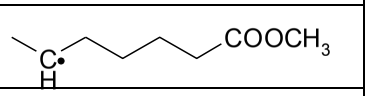
GC7:0	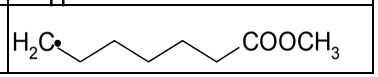

C6:0 $C_7H_{14}O_2$	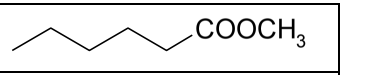
BC6:0 $C_7H_{13}O_2$	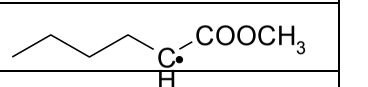
CC6:0	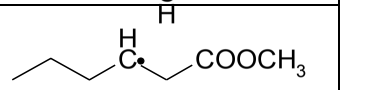
EC6:0	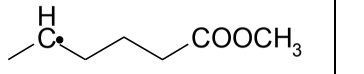
FC6:0	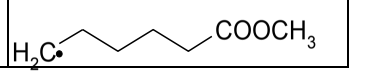

C5:0 $C_6H_{12}O_2$	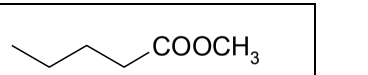

BC5:0 $C_6H_{11}O_2$	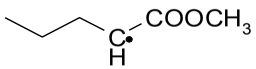
EC5:0	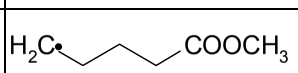

C4:0 $C_5H_{10}O_2$	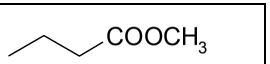
DC4:0 $C_5H_9O_2$	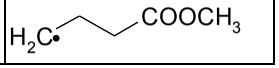

C3:0 $C_4H_8O_2$	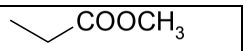
CC3:0 $C_4H_7O_2$	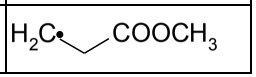

C2:0 $C_3H_6O_2$	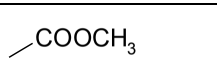
BC2:0 $C_3H_5O_2$	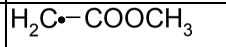
C10H1859	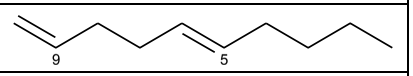
C10H1869	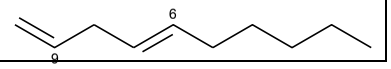

AC9H1518	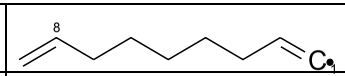
IC9H1518	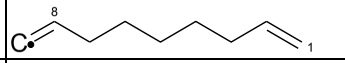
AC9H1517	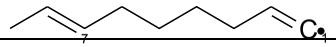

AC9H1513	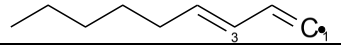
AC8H1317	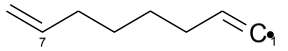
HC8H1317	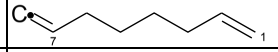
AC7H1116	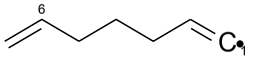
GC7H1116	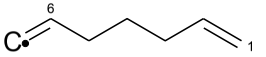

AC6H915	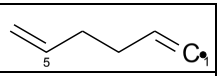
FC6H915	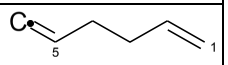
AC5H714	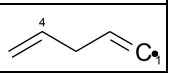
EC5H714	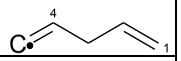
AC4H513	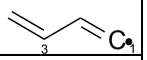
DC4H513	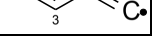

AC6H115	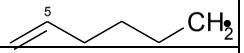
AC6H113	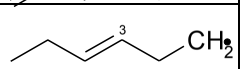
AC6H112	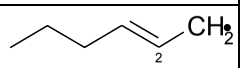
FC6H112	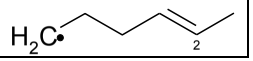

AC6H111	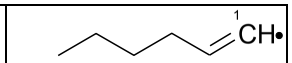
FC6H111	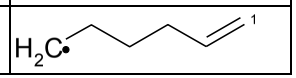

AC5H94	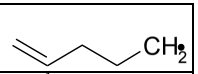
C5H92	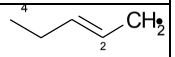
EC5H92	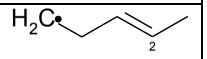
AC5H91	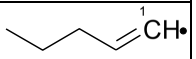
EC5H91	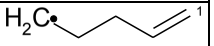

AC4H71	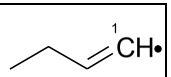
AC4H72	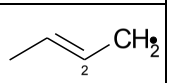
AC4H73	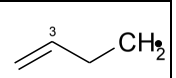

Species with 1 Carbon atom

C, CH4, CO, CO2, CH3, CH2, SCH2, CH

HCO	
CH2O	
CH3OH	
CH2OH	
CH3O	
CH3O2	
CH3O2H	

Species with 2 Carbon atoms

C2H6, C2H5, C2H4, C2H2, C2H3

CH3HCO	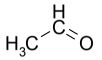
CH2CO	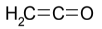
C2H4O2H	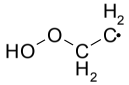
CH2HCO	
C2H	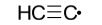
C2H4O	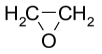
HCCO	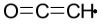
HCCOH	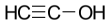
C2	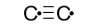
CHOCHO	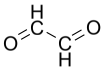
CHOCO	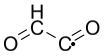
C2H3O	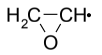
CH3CO	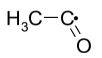

C2H2OH 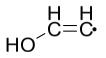

C2O 

C2H5O2 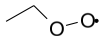

C2H5O2H 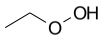

C2H5O 

Species with C3 carbon chain

NC3H7 

IC3H7 

AC3H5 

SC3H5 

TC3H5 

AC3H4 

PC3H4 

C3H3 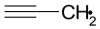

C3H2 

C3H3O 

C3H6O 

C3H5O 

C3H4O2H 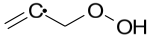

C3H4O 

C2H3CO 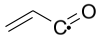

C3H4OH 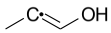

ETHCO 

ACROL 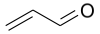

ACETON 

CH2COCH3 

C2H5CO 

Species with C4 Carbon Chain

C4H4 

C4H6 

C4H2 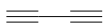

BUTYNE 

C2C4H8 

C4H8 

T2C4H8 

IC4H8 

C4H8O 

C4H612 

BUTYN2 

HOC4H6 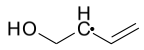

IC4H3 

IC4H7 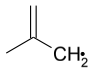

NC4H3 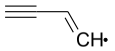

MEALL 

SC4H9 

PC4H9 

NC4H5 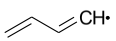

IC4H5 

H2C4O 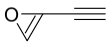

C4H 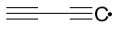

OC4H6 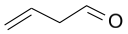

C4H5O 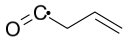

C4H6O2H 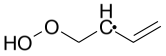

C4H73 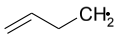

C3H5CO 

IC4H9 

TC4H9 

C4H7O 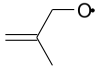

METACROL 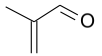

NC4H10 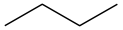

BMEPRAL 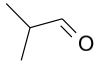

BMEPRYL 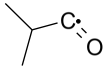

CH3CCCH2 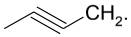

CH3CHCCH 

H2CCCCH2 

Species with C5 carbon chain

AC5H10 

T2C5H10 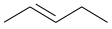

C2C5H10 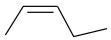

C5H813 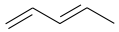

CPD 

BME1BU 

BME2BU 

ISOPE 

CYC5H8 

AC5H11 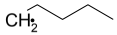

BC5H11 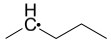

CC5H11 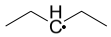

C5H913 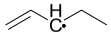

C5H924 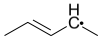

C5H5 

C5H4OH 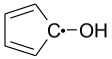

C5H4O 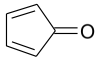

C5H5O13 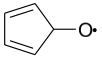

BME2B1 

CME2B1 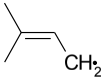

ISOPY 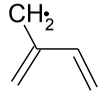

NEC5H11 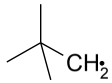

C5H7 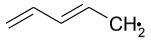

CYC5H7 

C5H915 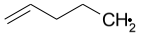

C5H911 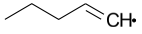

Species with C6 carbon chain

C6H6 

AC6H12 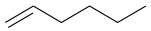

C6H10 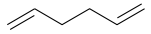

C6H5OH 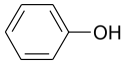

CHD13 

CYC6H12 

CYC6H10 

HEX1245 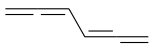

MC6H6 

FULVENE 

C6H615 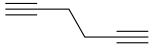

AC6H13 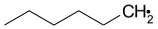

BC6H13 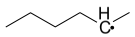

CC6H13 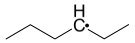

C6H1113 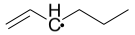

C6H1116 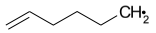

C6H5 

C6H5O 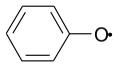

C6H9 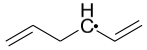

C6H9CY2 

C6H7C 

BME2PE4 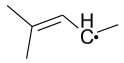

CYC6H11 

C6H1112 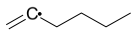

C6H1115 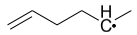

C6H1111 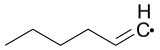

C6H2 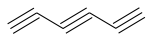

C6H4O2 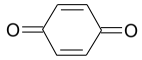

C-2*4C6H6O 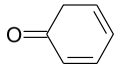

U-C6H5 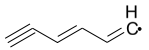

Species with C7 carbon chain

AC7H14 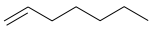

BC7H14 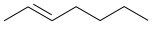

CC7H14 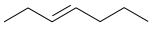

C6H5CH3 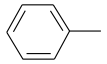

C6H5CH2 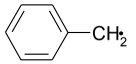

C6H5CH2OH 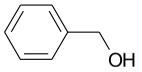

C6H5CH2O 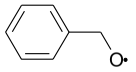

C6H5HCO 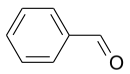

C6H5CO 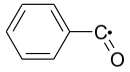

BDDM2PE 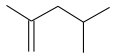

BDDM2PE 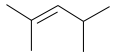

DDDM1PE 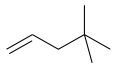

DDDM2PE 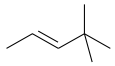

BDDMPE2 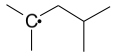

MHD 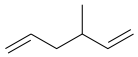

CYC7H12 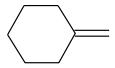

P2C4H513 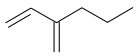

C7H1213 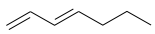

C7H1216 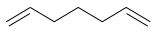

AC7H15 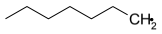

BC7H15 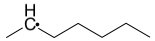

CC7H15 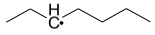

DC7H15 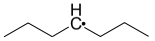

C7H1313 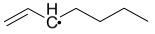

C7H1331 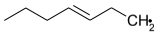

C7H1324 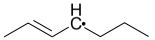

C7H1335 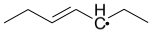

BDDM3PE2 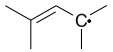

DDDMPE2 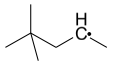

DDDM2PE1 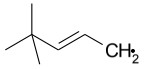

BDDM1PE3 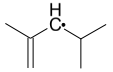

BDDM2PE3 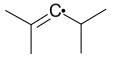

DDDM2PE2 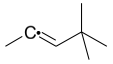

DM2MY1PE 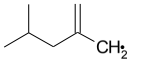

DDDM1PE3 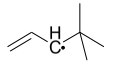

BDDM2PE1 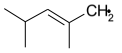

DDDM1PE2 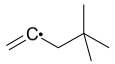

BDDM1PE1 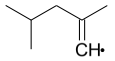

C7H1314 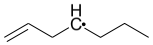

AC7H13C 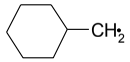

P2C4H614 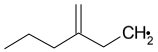

HOC6H4CH3 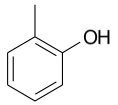

OC6H4CH3 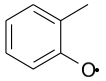

C6H5C2H* 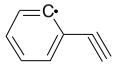

Species with C8 carbon chain

AC8H16 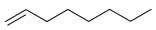

C6H5C2H5 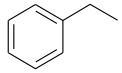

AC6H5C2H4 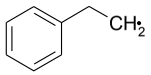

BC6H5C2H4 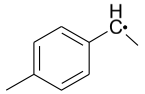

C6H5C2H3 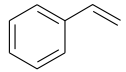

ASTYRYL 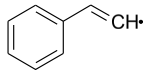

BSTYRYL 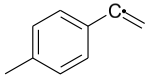

C6H5C2H 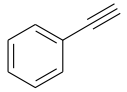

IC8H18 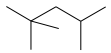

BBDTMPE1 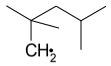

CYC8H14 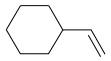

I1C8H16 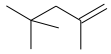

I2C8H16 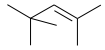

AC8H17 

BC8H17 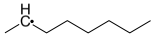

CC8H17 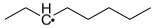

DC8H17 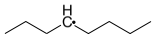

C8H1513 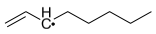

C8H1514 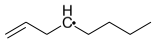

C8H1515 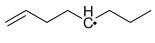

C8H1516 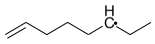

C8H1517 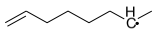

C8H1518 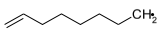

BBDTMPE3 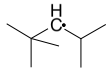

BDDTMPE2 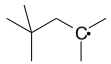

BDDTMPE1 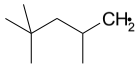

AC8H15C 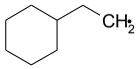

C6H4C2H3 

CH3C6H4CH3 

CH3C6H4CH2 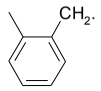

C6H5CCO 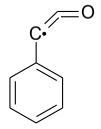

C6H5CCH2